EFFECT OF LUBRICATING OIL CHARACTERISTICS

ON

GEAR VIBRATIONS

by

P. A. B. A. R. PERERA

A thesis submitted to the
University of Newcastle upon Tyne
for the Degree of Doctor of Philosophy

NEWCASTLE UNIVERSITY LIBRARY
086 11702 2
Thesis L3103

Department of Marine Engineering

October 1986

CONTENTS

ACKNOWLEDGEMENTS

Sincere thanks are due to my supervisor, Professor R. V. Thompson, Professor in Marine Engineereing, for his constant encouragement and active guidance throughout the period of this research.

My appreciation is also due to Mr. John Smith, Senior Technician in the Marine Engineeering Laboratory, and his assistants for their help in the construction of the test rig.

I wish to thank Mr. D. Glennie, Senior Research Associate in the Department of Marine Engineering, for his valuable suggestions and assistance in the preparation of the instrumentation for the experiments.

I would like to acknowledge the financial support provided by the Association of Commonwealth Universities and the University of Newcastle upon Tyne.

Finally, a warm thank you to my wife for her continuous support and hard work during the course of this research.

ABSTRACT

An extensive literature survey of the subject of gear dynamics is undertaken and the increasing recognition of the role of the lubricating oil film in this field, especially as a damping source, is highlighted.

The oil film separating the mating surfaces of involute spur gears is analysed assuming hydrodynamic conditions, rigid teeth (as far as the film shape is concerned) and pressure dependent viscosity.

Gear tooth mesh stiffness is expressed as a function of the dynamic load and the position of contact.

A simple model of a pair of spur gears is subjected to a transient response analysis and the behaviour of the lubricating oil film observed. According to the motions of equivalent masses of the gears under these transient conditions damping due to the oil film is determined. The numerical solutions obtained at various operating conditions are combined to form an approximate formula to predict the damping ratio in terms of the dynamic tooth load, rolling speed of the tooth surfaces and the viscosity of the lubricating oil.

A digital computer simulation of the dynamic motion of the pair of gears is carried out incorporating the above damping ratio formula. The actual load sharing between the pairs of teeth (when more than

one pair of teeth are in mesh), considering the tooth deflections, pitch errors, oil film thicknesses and the differences in mesh stiffnesses, is taken into account.

The variations of the total maximum dynamic load and the maximum tooth load are studied under different nominal loads, contact ratios, oil viscosities and pitch errors over a wide range of speeds covering the resonance area. The variations of the dynamic load, individual tooth load, mesh stiffness and the oil film thickness during complete mesh cycles are also analysed under different operating conditions to identify particular areas where high loads and minimum film thicknesses occur.

Theoretical results are compared with the experimental results obtained on a back-to-back gear test rig.

NOMENCLATURE

2b	Width of Hertz contact zone
Cd	Centre distance
E	Elastic modulus of gear material
F	Force on gear teeth
FO	Force at the line of action due to external load
F_p	Force due to oil pressure
F_s	Force due to shear stress
G	Bulk modulus of gear material
G_a, G_b	Tooth thickness (circular) of gears A and B, respectively
HO	Minimum oil film thickness
$\dot{HO}$	d(HO)/dt
K	Stiffness of an individual tooth
K_{eq}	Total tooth mesh stiffness
KO	Mesh stiffness of a pair of gear teeth
m	Speed ratio
M_a, M_b	Equivalent masses of gears A and B, respectively
M_{ab}	$= 1 + M_a/M_b$
N	Speed in rpm of gears
p	Pressure
PE	Pitch error
PO	Base pitch
q	$(1 - e^{-\alpha p})/\alpha$ reduced pressure
R	Radius
R_b	Base circle radius
R_r	Root circle radius
R_y	Radius at which force is acting

u, v, w	Fluid velocities in x, y and z directions
u_a, u_b	Tooth surface velocities of gears A and B, respectively, in x directions
x, y, z	Coordinates
x_{po}	Position at which the pressure is zero
x_{max}	Extreme position of the oil film on the inlet side
y_a, y_b	Distance from the x axis to the tooth surfaces of gears A and B, respectively
y_{ao}	$= y_a$ when $x = 0$
$\dot{y}_{ao}$	$= d\frac{(y_{ao})}{dt}$
Y_{ao}, Y_{bo}	Distance from the origin to the tooth surfaces of the gears A and B, respectively, measured along the y axis
Y_{ar}	Distance from the x axis to the reference axis XA - XA
Z	Deformation of gear teeth
α	Viscosity/pressure coefficient
β	Viscosity/temperature coefficient
δ	Total mesh compression
ζ	Damping ratio
μ_o	Viscosity of oil at atmospheric temperature
μ_t	Viscosity at inlet to the gear mesh
ν	Poisson's ratio
ρ	Density of oil
τ	Shear stress
ψ	Pressure angle
ω	Angular velocity of gears

Subscripts:

a,b	Driving (A) and Driven (B) gear respectively
1,2,3	First, second and third pair of teeth respectively

CHAPTER 1

INTRODUCTION

Gears have a large number of possible modes of failure; more than many other machine components have. These failure types can be categorised under the two headings: tooth breakage and surface failure. As a result of the development of tougher gear materials and more accurate manufacturing techniques, tooth strength can no longer be considered as the major design obstacle, even though gears are nowadays designed to run heavily loaded. Tooth surface failures form the boundary over a large region in the operating domain of such gears, with pitting and scuffing taking the front line. This has led the lubricating oil, which was initially inended to reduce friction and wear at the point of contact, to change its role to that of a barrier which separates the tooth surfaces, thereby reducing the risk of surface failure. In addition to the above function, lubricating oil also has an indirect effect on almost all modes of gear failure. This is due to its active involvement in the dynamic process of the gears. It is the intention of this research to study this role of the lubricating oil in the dynamic process of gears and its resulting effects which could have some influence on the design of gears.

Gears, by the nature of their mode of power transmission, are natural sources of vibration. This effect is more pronounced in

spur gears. The study here is therefore confined to a dynamic analysis of straight spur gears.

It is practically impossible to produce a pair of gears that could transmit power absolutely smoothly at all loads and speeds. The smooth transmission which is expected while designing the gears will usually be disturbed by manufacturing and mounting errors, and further errors will be introduced due to tooth deflection and deformation when operating away from the design load. These interruptions to the smooth transmission cause the gears and their connected inertias to accelerate and decelerate causing the instantaneous load on the gears to deviate from the mean transmitted value. The difference between the maximum value of this load and the nominal load being transmitted is generally referred to as the 'dynamic component of the load'.

A pair of gears is only a small sub-system of the main transmission system. Any analysis of the gear pair should therefore include the effect of the main system on the sub-system. Except for certain special cases, this effectively means analysing the torsional characteristics of the whole transmission network as a single system. But since the idea of this research is to study the behaviour of the lubricating oil at the tooth mesh, it seems reasonable to isolate the pair of gears from the main system in order to carry out a dynamic analysis.

A pair of gears can usually be modelled by two masses with the tooth flexibility represented by a spring of equivalent stiffness. But the difficulty has always been in representing the properties of the tooth mesh sufficiently accurately (for the results to be of any use) and in a reasonably simple manner (to make an analytical solution possible). There are two major obstacles to this. These are:

(i) Nonlinear nature of the mesh stiffness.

In addition to the variation of the mesh stiffness of a single pair of teeth along the path of contact and also with the tooth load, the total mesh stiffness varies as the number of pairs of teeth in mesh varies.

(ii) The extent of damping at the tooth mesh.

This is the least known characteristic of the gear tooth mesh and is the main focal point of this study.

The problem can, therefore, be classified as the vibration of a highly nonlinear system. But the achievement of a satisfactory solution is further hindered by the randomness of the exciting function which is governed by gear manufacturing and mounting errors, tooth deflections and deformations, etc.

The exact nature of the dynamic characteristics of the system depends on a large number of factors. These can be basically

categorised under three headings: sources, system parameters and running conditions.

Sources

The factors that ultimately generate dynamic loads are the accelerations and decelerations of the moving masses. The magnitudes of these dynamic loads depend on the rates of the accelerations and decelerations which in turn depend, among other things, on the type, magnitude and location of the original sources of excitation. These sources in a normal gear transmission system could be:

(i) Manufacturing errors of gears.

Even though manufacturing methods and quality of machines have improved vastly in the past decades, errors in various forms and sizes are unavoidable though their magnitudes are much smaller now. But these errors, when subjected to the extremely high loads and speeds to which gears are designed these days, could produce dynamic loads of a similar scale if not of a higher than those found in the early days. These errors usually take the form of tooth profile errors, relative pitch errors or purely random errors such as high or low spots on tooth surfaces. Errors of this nature could creep in as a result of wear and tear of the tools and machines used in the production of gears, inaccurate mounting or positioning of the gear blank relative to the cutter or

due to errors in the transmission system of the gear cutting machine which itself consists of gears.

(ii) Elastic deflection of gears due to the load being transmitted.

The total deflection of each gear relative to the point of contact consists of the beam deflection of individual teeth as a result of the bending moment of tooth load, shear deflection due to the tangential component of the above force, deflection due to the normal component, deformation of the tooth surface at the point of contact and the adjoining area, and in the case of gears with a thin rim and a web, the deflection of the rim and the web.

(iii) Elastic deflections of supporting members of the gears.

These are mainly the deflections of the shafts carrying the gears, the bearings on which they are mounted and the gear housing.

(iv) Gear mounting errors.

Even though classified as mounting errors these are, in fact, manufacturing errors of individual components of the gear unit (housing, gear blanks, shafts, etc.) resulting in eccentric mounting of gears and errors in shaft alignment.

(v) Pitch errors due to tooth deflection.

If the gears are made so that they have true tooth profiles at no-load or at a particular load, when they operate at a different load a new pair of teeth coming into contact will engage prematurely (or late if the operating load is lower than the above design value) as a result of the change in tooth pitch due to the deformation (or insufficient deformation) of the loaded pair of teeth.

Usually all the above mentioned errors are present in a gear transmission system in varying amounts depending on the accuracy to which the components are manufactured and also depending on the skill of the workmen involved. Although the actual amounts are unknown before the gears are produced, some of those errors are limited by design tolerances; hence, their maximum values can be predicted according to the class of the gears. But elastic deflections depend on running conditions and are thus themselves dependent on dynamic load.

System Parameters

These are basically the inertias of the rotating elements and stiffnesses of their connecting members including that of the tooth mesh. Of these the mesh stiffness is time dependent. In addition to this the change from single to double tooth contact and vice versa adds further nonlinearity into mesh stiffness function. In fact, this sudden change in mesh stiffness itself is considered to be another source of excitation for the creation of dynamic loads.

The contact ratio of the pair of gears, though it does not change appreciably during transmission, governs the pattern of the above excitation.

Another system parameter of which little is known at present is the damping in the system. There are several sources which could offer damping. These are the oil film between mating tooth surfaces, bearings, friction at various rubbing surfaces and the gear material. But the damping due to the oil film is considered to have a far greater effect on the dynamic load than any of the others. Hence, damping could also be classified under the sub-heading 'running conditions'.

Running Conditions

Load and speed are the two main parameters that come under this category. The effective viscosity of the lubricating oil also could be considered important when considering the role of the oil film in the dynamic process of gears. But this viscosity is not entirely controllable and depends on a number of other parameters as well. This aspect will be discussed in detail later.

The speed of rotation of gears primarily determines the frequency of the excitation function. This frequency is important in that the approach to the problem of dynamic load depends on it. If this excitation frequency is very low compared to the natural frequency of the pair of gears then the problem is similar to that of a system subjected to a step or an impulse disturbance. A transient response

analysis would solve it in that case. Whereas, if the frequencies are of the same order then a dynamic analysis and a frequency analysis are required since the question of resonance comes into the picture.

The main role of a lubricating oil in a dynamic situation is regarded as that of maintaining an oil film between the two sliding surfaces. Apart from keeping the mating teeth separate in a gear drive thereby reducing friction and wear, the lubricating oil film offers resistance against almost all other modes of surface failure; scuffing and abrasion are two of the most common types. In addition to reducing the amount of heat generated by reducing friction, lubricating oil also takes away most of the generated heat, thereby keeping the operating temperatures down. The oil film helps to distribute the load being transmitted over a wider area than it would act if there was no lubricating oil, although it has not been proved conclusively that the maximum stress the gear tooth is subjected to is reduced as a result.

The notable difference between dynamic loads predicted by theory and those measured experimentally under similar conditions has led investigators to believe that there is a significant amount of damping at the tooth mesh. At low loads film thickness is a function of load and a considerable amount of damping can be expected due to squeeze film effect. But at high loads the oil film thickness is almost independent of the tooth load. Hence, in the absence of squeeze action the possible sources of damping at the

tooth mesh are the damping of the material and that due to friction, which are very small in the case of gears. Therefore, one cannot expect much damping at high loads.

Probably, due to this reason, most investigators when modelling such highly loaded gear systems have either completely neglected damping or assumed an arbitrary constant value. Some have used values so that the maximum dynamic loads predicted by their theories agree with experimental results. An analysis showed that there is a vast variation in the values used for damping by different investigators. Damping ratios as far apart as 0.005 and 0.3 times critical have been used.

It can be shown that, irrespective of the nominal load being transmitted, individual tooth loads oscillate and as a result reach low values (some have observed even momentary tooth separation taking place) during the mesh cycle. It thus seems appropriate to represent damping also as close as possible to its true nonlinear form in order to obtain a realistic dynamic simulation of the system. This is further supported by the fact that when a new pair of teeth come into mesh the tooth load of that pair has to increase from zero. High damping at the initial stages of tooth engagement have a cushioning effect on the sudden tooth impact. Zero damping or a mean damping coefficient would have in such a case predicted a very high dynamic load especially if the tooth engagement is premature due to tooth deflection or pitch errors.

To observe the behaviour of the oil film under dynamic conditions, especially its damping characteristics, an equivalent linear mass-spring model of a pair of gears was used. The stiffness of the spring representing the variable mesh stiffness was found using true positions of gears. It was assumed that a hydrodynamic oil film was maintained at all times between the teeth, and the properties of the oil film were expressed accordingly.

This model was then subjected to a transient response analysis where a small step change in the load was imposed while keeping the theoretical position of contact fixed, though the tooth surfaces were given their normal rolling and sliding velocities. The subsequent motions of the gear masses were used to calculate the damping ratio of the system. The unique feature of this method was that it enabled us to observe the dynamic behaviour of the system at any fixed angular position of the gears while retaining all the dynamic properties. Such an analysis is not possible in practice since a fixed point of contact means zero speed and, of course, no oil film. The closest practical situation one can achieve as far as the oil film is concerned is by using a disk machine. But it does not have dynamic properties similar to those of the gears.

By this arrangement each of the principal parameters that affect the oil film, namely the nominal load, the speed, the effective radius of curvature of the tooth faces at the point of contact, and the viscosity of the oil at the entry to the oil film, could be varied independently. It was then possible to find the influence of each

of these variables on the damping ratio.

The relationships of individual parameters were then combined to form an empirical formula so that the damping ratio could be found for any given set of operating conditions.

A digital computer simulation of the dynamic process of the pair of gears was then carried out incorporating the above damping ratio formula. The variation of the dynamic load, loads on individual pairs of teeth, their minimum film thicknesses and the mesh stiffness were studied under different operating conditions.

The above analysis should also be able to answer the following questions.

(a) What is the maximum dynamic factor that could be expected in a pair of spur gears?

(b) What are the factors that contribute to the increase of the dynamic load?

(c) Does the maximum dynamic load, tooth load and the minimum film thickness occur at any particular phase in the tooth mesh cycle?

CHAPTER 2

LITERATURE REVIEW

The importance of dynamic load as a design parameter is widely accepted now and it is in the process of being introduced into standard gear design methods. The role of the lubricating oil in the dynamic process of gears is also considered to be important and investigators believe that the selection of the lubricating oil should be a part of the gear design process rather than a thing which is decided at the end.

The role of the lubricating oil in gear dynamics was first considered to be limited to that of reducing friction and wear. It was not until the 1940's that people started to believe that the development of a hydrodynamic oil film was possible between loaded gear teeth. This was mainly because of the failure of earlier attempts to prove it by classical theory.

While the existence of dynamic loads in gears was accepted as far back as in the late 19th Century, with the hydrodynamic oil film not entering into the picture, oil film damping was not even mentioned in the earlier reports on the analysis of dynamic loads. Gradually as the knowledge of the process of gear lubrication and dynamic load widened, the importance of the role of the lubricating oil in gear dynamics became clear.

When we look back into the history of dynamic load and lubrication of gears, we can see that they have followed two separate paths which became closer as time went by until at present they stand almost overlapping each other. Thus the topic, 'influence of lubricating oil on gear dynamics', will be divided into the two subjects, 'gear dynamics' and 'gear lubrication' for the purpose of reviewing their progress during the past few decades.

Gear dynamics

Any load on a gear in excess of that corresponding to the load being driven can be termed as a 'dynamic load'. Naturally it is the maximum value of this load that is important from the design point of view. But equally important is the pattern with which it occurs.

The opinion as to the cause of this dynamic load initially centred around manufacturing errors of the gears. This can be clearly seen from the fact that most of the early research on the subject was concentrated on analysing the dynamic load due to isolated high spots or pitch errors. Also, it is very likely that at loads and speeds the gears operated those days, which were comparatively low, these errors could have been the only significant source responsible for the generation of dynamic loads.

Very little was done to investigate this phenomenon until the 1920's and, when looking at the bulky gears employed in the early days, it looks as though the gear manufacturers were content to 'take care' of this unwanted load by 'increasing the safety factor'.

But as the requirement for high power to weight ratio gears increased, so did the competition between rival gear manufacturers to come up with better designs, and it thus became aware that more research into the aspect of dynamic loading was needed urgently.

The report of Franklin and Smith (16) in 1924 was the outcome of one such research where they presented the results of experiments carried out to test the effect of pitch errors on the strength of spur gear teeth. Cast iron gears with different pitch errors ranging from 0.00005 in. to 0.006 in. were run on a gear test rig. The load was increased from zero until the destruction of the gear teeth. They have observed a reduction in the load carrying capacity with the increase of the tooth spacing error, especially at high speeds.

As the manufacturing techniques and the quality of machines and tools improved, it was realised that there were other factors which also interrupted the smooth rotation of gears to cause dynamic loads. These included the deflections of the gear teeth and shafts under load and inaccurate mounting of shafts and gears.

During the same period the American Society of Mechanical Engineers (ASME) formed a special committee to study about the strength of gears. The committee chaired by Mr. Wilfred Lewis carried out extensive tests over a period of several years, on the Lewis gear testing machine. Based on experimental results and analytical work they developed formulae to calculate dynamic loads. These with

further improvements were then presented by Buckingham (6) in 1949. In this analysis they have assumed the motion of the two gears to be equivalent to two masses initially forced together by the applied load, then suddenly forced apart by the tooth error (or a high spot on the tooth surface or a foreign body) and finally colliding with each other. Thus the load cycle on the gears was divided into two phases:

(i) the acceleration load - the load on the gears as they are forced apart by the discontinuity;

(ii) the dynamic load - the load caused as a result of the subsequent impact.

Assuming the above acceleration load to be constant and neglecting the time parameter, equations were derived to calculate the dynamic load by equating the kinetic energy of the two gears before impact to the work done in deforming the gear teeth during impact. The influence of other connected masses was also taken into account in the analysis by using an effective mass acting at the pitch line of gears. One interesting suggestion was the existence of a critical speed when the dynamic load would be maximum and further increase in speed cause it to come down. This was attributed to the fact that the high speed of rotation of the gears decreases the time of the mesh cycle which cuts down the time left for the second part of the load cycle (i.e. the dynamic load) thereby decreasing the maximum load reached.

Reswick (42) also analysed the dynamic load due to both tooth deformation under load and manufacturing errors. He separated the effects due to the above two causes by assuming that:

(i) profile errors are negligible compared to tooth deflection when the load is very high; and

(ii) tooth deflection is negligible compared to manufacturing errors when the load is low.

This left only two situations to be analysed. One where there are only tooth deflection errors and one where there are only manufacturing errors. Reswick, too, used a linear model consisting of two masses in his analysis (Figure 2.1) where one mass (representing one gear) had a short rigid tooth of uniform cross-section and a vertically movable tooth one pitch away which had a varying cross-section of the form of a parabolic cam. The second mass had two flexible teeth of constant cross-section one pitch apart.

The beginning of mesh of a pair of teeth was analysed by inserting the 'cam' (the movable tooth) vertically downwards at a speed equivalent to the pitch line speed of the gears. By solving the equations of motion of the transient tooth engagement process and the subsequent oscillation of the whole system, evaluation of the dynamic load took place. According to these calculations, for heavily loaded gears total dynamic load increases from eK/2 to a

maximum of eK (e - tooth error; K - tooth stiffness) and for lightly loaded gears also the maximum was eK.

In this he had assumed the introduction of the error to be at constant acceleration which he justified by claiming that since the full load had to be shared by the second pair of teeth in a very short time, the corners of interference get worn off during running in to form cams. As inertia forces are proportional to acceleration he assumed that high spots would be worn off in such a way to produce cams of constant acceleration. Also a constant tooth stiffness had been assumed while neglecting viscous damping. In conclusion he stated that the total dynamic load may be less than the static load determined from the transmitted power in heavily loaded gears since the full static load can be taken up by one pair of teeth for contact ratios between 1 and 2. Thus static load could be used as the design load for heavily loaded gears. This claim was further substantiated by saying that initial wear failures usually commence near the centre of the tooth surface.

Even though the argument that the dynamic load due to pitch error or tooth deflection is usually shared by two teeth compared to a single tooth carrying the full static load is true, one has to approach the situation with caution since:

(i) The exact nature of load sharing between the two pairs of teeth carrying the load is unknown which obviously depends on individual tooth stiffness and errors;

(ii) The variation of load when the load is transferred from two teeth to one, which obviously change the mesh stiffness and hence the loading pattern could lead to a situation where the single tooth has to carry a load higher than the static load.

The International Conference on Gearing in 1958 of the Institution of Mechanical Engineers produced several papers on the aspect of dynamic loading. Johnson (26) considered the problem to fall into two categories:

(i) slow and medium speed gears for which high tooth spacing errors are tolerable;

(ii) high speed gears where tooth spacing errors are very small and thus under high load the tooth deflection errors predominate.

In the first category, he said, the excitations due to a tooth spacing error could be assumed to be a single disturbance as its effects are damped out before the next excitation, whereas in the second category the excitations occur so frequently that they merge together to form a continuous error curve. This being a periodic function of time he suggested that it should first be analysed to find its harmonic components so that the response of the system to each of those harmonic components could be studied to find which are the critical ones. Assuming continuous tooth contact and constant tooth flexibility during the mesh cycle and neglecting all other nonlinearities in the system, he predicted that for precision gears

the largest component of excitation will be at the tooth mesh frequency and multiples of it.

The main difficulty in such an analysis is to obtain the true error curve. Even though it is possible to obtain the static error curve (at slow speed), the true error curve will be different since the errors themselves are functions of the dynamic load.

Tuplin (53c) presented a more up-to-date version of his equations to calculate the dynamic load using the wedge analogy (53a and b). In this analysis Tuplin assumed that errors in pitch and form of teeth cause a change in the relative angular position of gears, similar to those caused by the insertion of thin wedges between the loaded teeth of non-rotating gears. The subsequent motion of gears and the maximum loads reached thus depend on the shape and size of the wedge, time of insertion and the elasticity and inertia of the elements. Tuplin, too, used the energy principle to calculate the dynamic load, which seems appropriate for single impulse type disturbances. On possible resonances of the system, he commented that large simple harmonic forces cannot be present since the exciting function is a non-harmonic displacement, and that any harmonic load variation of amplitude greater than the mean load would cause tooth separation with consequent detuning.

Niemann and Rettig (38), using a practical approach to the problem, tested a number of gears with purposely introduced errors on a gear testing machine. Tooth deflections were measured under various

loads and speeds and together with tooth stiffnesses obtained from static deflection measurements and Hertzian formulae calculated the corresponding dynamic loads of the gears. Commenting on these results they have stated that after the initial impact the deflection patterns show vibrations superimposed on static deflections. For the rate of decay observed in these vibrations they have estimated a damping ratio in the range of 0.13 to 0.15. Some of the main conclusions drawn are that the dynamic load is linearly proportional to the pitch line velocity, the slope of the above lines increase with static load and effective tooth error and that the dynamic load is proportional to the fourth root of the equivalent mass at the pitch line.

Harris (21) in a theoretical analysis of the dynamic load considered three sources of vibration in a pair of precision gears:

(i) periodic variation in the velocity ratio due to tooth deflection or manufacturing errors;

(ii) mesh stiffness fluctuations mainly due to the change between single and double tooth contact;

(iii) nonlinearity in tooth stiffness as a result of loss of contact between teeth.

According to him the amplitude of vibration caused by (i) depend on damping while those due to (ii) and (iii) will be significant if

damping is below the limiting value of about 0.02 of critical.

He has also shown how profile modification could be used to achieve a constant velocity ratio at the designed load. He discussed the effects of the following possible modes of vibration.

(a) Due to a periodic error:

Unless teeth lose contact, the vibrational amplitudes are only limited by damping, especially when occurring with a frequency near a natural frequency of the gears. He predicted that amplitudes as high as five times the magnitude of errors could be present even when the damping coefficient is 0.1 of critical, but there is only one band of speed within which this type of vibration could occur.

(b) Due to sudden changes in mesh stiffness:

Vibrations could start due to this even without any tooth errors when the damping is low and there are many bands of speed within which vibrations of this mode could set up.

(c) High class gears running at loads other than the designed load:

Here the small error due to the difference in load, and the stiffness variations mentioned in (b) may start vibrations which, according to him, could give greater amplitudes of vibration than either of the excitations acting separately.

(d) Due to nonlinearity of the tooth mesh stiffness function as a result of tooth separation:

This could result in tooth contact being made every third or fourth teeth. He pointed out the fact that tooth separation, though acted as a limiter to vibrations in cases (b) and c), could itself act as the source in (d).

According to his calculations, the greatest load is twice the load which gives zero error in velocity ratio provided the applied load is less than the design load.

Attia (2) measured the deflection of gear teeth under dynamic conditions by attaching strain gauges to gear teeth and observing the output of the strain gauge bridges on a C.R.O. From the tooth deflection patterns obtained at various loads and speeds in the above test, he observed that the maximum dynamic load on the tooth does not occur at any fixed phase in the mesh cycle and that the dynamic effect is quite different from the simple case of a smooth gear with an isolated pitch error disturbing the constant speed rotation of gears. According to him to evaluate the position and magnitude of the maximum dynamic load precisely one has to study the motion and vibration of gears as a continuous process interrupted by the initial interference between the teeth at the start of contact due to pitch error or tooth deflection under load or both, which cause a forced vibratory motion and a subsequent free motion. The free motion is then interrupted by machining errors and other nonlinearities in the mesh stiffness. This, of course, is a more

general case whereas most of the previously mentioned investigators used extreme cases where only one type of error predominated. Comparing his results with those of Buckingham's (6) and Tuplin's (53), he said that Buckingham's equations predict very high dynamic loads while Tuplin's equations give nearer values.

The report of Gregory, Harris and Munro (18), based on results of tests related to nonlinear oscillations of lightly damped spur gears near to and above resonance speed, was one of the first to deal with the dynamic behaviour of gears near resonance. The importance of damping, especially when operating gears near resonance conditions, was highlighted. Tests have been carried out on a back-to-back gear test rig equipped with instruments to measure the transmission error. Static transmission errors recorded at very low speeds have been found to agree well with the theoretical curves, despite the presence of small manufacturing errors. Tests have also been carried out at speeds below primary resonance where the vibratory motions were found to be small. The authors hence arrived at the conclusion that the nonlinear terms in the equation of motion could be neglected. Using the above assumption, and that the damping is primarily viscous, they suggested a figure of 0.02 of critical for the damping ratio.

Another conclusion they arrived at was that when running at speeds near primary resonance the gears always vibrated at the tooth contact frequency while running at speeds near twice the resonance speed they vibrated at their natural frequency.

They too have stated that backlash helps to limit the amplitudes of oscillations. It has also been observed that the amplitudes at resonance have been less than what the theoretical single degree of freedom model predicted, which the authors attributed to probable higher damping in the test rig than assumed, and to the effect of random manufacturing errors to force the periodic oscillations to breakdown at lower amplitudes.

The authors have also pointed out the effect of the flexibility of bearings which according to them is considerable, even with very stiff bearings, suggesting that bearing deflections may have an important influence on the dynamic behaviour of practical geared systems. The authors seemed to agree with many of the previous investigators in stating that the maximum dynamic load never exceeds twice the design load for applied loads less than the design load.

Houser and Seireg (23) carried out tests using spur and helical gears to study the effect of the variation of the area of contact from one pair of teeth to the other and also the effect of the pitch error. For these tests they have used gears with purposely introduced (i) facewidth variations and (ii) pitch errors. Using strain gauges mounted at the root of teeth the tooth strain histories at various loads and speeds have been obtained. It had been found that the average of maximum tooth strains obtained at the point when the facewidth change suddenly did not vary appreciably when the speed was increased. On the other hand, with gears having pitch errors the dynamic increment seemed to increase approximately

linearly with speed, while the tooth strains developed for positive pitch errors were larger than the tooth strains due to negative pitch errors for the same test conditions. The linear proportionality between the speed and the dynamic increment had been found to exist at all loads.

In the subsequent theoretical analysis of the dynamic increment in gears with pitch errors, the authors have presented formulae for the dynamic factor of gears operating at speeds away from resonance. Unlike many of the previous investigators who considered the dynamic factor to be a function of only the pitch line velocity, the authors have included the effect of the tooth error, mesh stiffness and the effective mass of the gears on the dynamic factor.

Kohler, Pratt and Thompson (29) used a frequency analysis of the noise generated by the meshing gears to identify the frequencies at which vibrations occur. The transmission error of the gear pair under load had been identified as the main source of excitation for these vibrations. Though unique for a particular pair of gears, once manufactured and installed, this transmission error had been found to consist of two primary frequencies; one corresponding to the period for any given mesh condition to recur, and the other the tooth contact frequency. The former had been considered as the basic frequency since the latter, though similar for each mesh cycle, is not identical. The frequency analysis of the noise had revealed the presence of peak components at almost all the harmonics of the basic frequency which they said gives the frequency spectrum

"a sideband structure, which is characteristic of gear noise". They have also found that this sideband structure is not caused by random errors but by regular periodic errors similar to those caused by mounting eccentricities.

Commenting on modelling a gear system, the authors have said that the commonly represented single degree of freedom model is not sufficient, since the bearings and shafts have stiffnesses which could be of the same order as that of the gear teeth. Hence they have used a six degree of freedom model to represent the gear system. The tooth mesh stiffness had been treated as a linear one, considering the effect of variation of the tooth stiffness to be negligible compared to the effect due to the transmission error. The natural frequencies calculated using the above model had been found to agree reasonably well with the natural frequencies of the actual system obtained experimentally. Due to the presence of a large number of natural frequencies and their harmonics in the system, and the nature of the transmission error curve, it was stated that resonance could be found at almost any speed between some natural frequency of the system and some component of the excitation function, with major resonances occurring at several speeds. It has also been stated that for lightly loaded gears with large errors, tooth separation could occur giving dynamic loads considerably higher than the nominal load, whereas for highly loaded precision gears the dynamic responses are smaller.

A similar model with no damping was used by Remmers (41) in his investigations where he considered the transmission error curve to consist of a large number of harmonic components, mainly of tooth contact frequency. He then analysed the response of the model to sinusoidal exciting functions in order to study the effect of each of the above harmonic components on the system. The dynamic bearing forces and tooth loads thus calculated for various exciting frequencies were reported to agree with the results obtained experimentally, except near resonance frequencies which is understandable, since damping was not taken into account in the theoretical analysis.

Wang and Morse (57) showed how the transfer matrix technique could be used to analyse the dynamic response of a gear train. In this method the shafts and gears were assumed to consist of a series of spans each of which could be described by a lumped mass system. Then characteristic equations were written for each span and state vectors of adjacent spans were then linked by 'transfer matrices'. In this way the state vectors at two ends could be linked together by successive matrix multiplications.

This method, unlike normal torsional analysis techniques, can be used to take into account all the items in the transmission system, most of which are usually neglected (these include keys, gear webs). But the inclusion of damping terms complicates the operations considerably.

Mahalingam and Bishop (31) outlined an analytical technique to calculate the dynamic response of a linear, n-degree of freedom torsional system with two branches coupled by a pair of gears. According to this method the natural frequencies and mode shapes of the two branches are first found and then the transmission error is introduced into the system as an internal displacement which increases the strain energy of the system. The strain energy and kinetic energy then could be used to find the torque at any rotor. Here, too, a linear system with no damping had been used for simplicity but the general nature in which the transmission error is introduced into the system facilitates any type of error, either periodic or random, to be considered in the analysis.

The analog computer, too, proved to be a very useful tool in the struggle to gain further knowledge on the subject of dynamic load. Its capability to simulate dynamic systems and the ease with which the influence of various parameters on the performance of a geared system could be analysed was first made use of by Kasuba (27). He pointed out that in critical applications the entire transmission system should be studied as a whole, which he illustrated by using an n-degree of freedom rotary system. But he accepted that it was not possible to use the results of such an analysis in general due to individual characteristics of different systems. He then selected four simple gear models which could be described as sub-systems of a major transmission system and the analysis of which could provide useful information for the solution of complex problems. The four simple gear system models he suggested were:

(i) The inertia of the driving gear infinite: thus it rotates at a constant velocity while the gear teeth, the driven gear, and its connected members absorb all the changes in the kinetic energy of the system due to dynamic loading.

(ii) Stiffness of the shafts connecting the gears to the rest of the system is very low compared to the stiffness of the gear teeth in mesh. In such a case the pair of gears could be analysed separate from the rest of the system.

(iii) Same as (ii) but the inertia of both gears finite.

(iv) Tooth mesh stiffness and the stiffnesses of connecting shafts comparable. In this case it is not possible to have a simple model.

In the subsequent analog simulation of the above models, the author used a sinusoidal function of the tooth contact frequency to represent the error which provided the excitation, while damping at the tooth mesh was represented by a viscous damping element. It was shown that with insufficient damping, the time varying parameters such as tooth stiffnesses could cause instabilities in the system at certain frequency ranges independent of the applied load, thus highlighting the importance of damping. But he said that in practice backlash causes the teeth to separate which eventually results in limiting the amplitudes of vibration. A table giving the minimum critical damping ratios required to prevent this self-

excited vibration was presented for gears with contact ratios between 1.1 and 1.9. The effects of velocity, magnitude, shape and frequency of error, load, elasticity of gear teeth, contact ratio and damping on dynamic factor had been analysed. The results obtained were found to agree well with those obtained experimentally. He had emphasised the importance of contact ratio which could be used to change the dynamic characteristics of a system. Stating that the AGMA formulae for dynamic factors yield figures which are too conservative, especially when applied to heavily loaded precision gears at high speed, he suggested the possibility of deriving dynamic factor lines with the inclusion of the AGMA quality numbers, transmitted loads and various contact ratios over certain frequency ranges.

Azar and Crossley (3) used a digital computer simulation to study the dynamics of a lightly loaded pair of gears. The gears were modelled by an 'impact pair' which consisted of four inertias, each representing the driving element, the two gears and the load respectively. This model had been chosen so that gear motion, when tooth separation and impact occur, could be studied. Instead of the commonly used linear force approach law of $c\dot{x} + kx$, the authors have used a law of the form $(\lambda x^n)\dot{x} + kx^n$ for impacting bodies where n, the nonlinearity index, had been assigned values between 1.0 and 1.5 to agree with experimental results. It has to be noted that the damping force indicated above contains only the damping offered by the deforming material and does not include the oil film damping which most of the previous investigators considered to be the main

component of damping in a gear pair. The simulation results with various backlash values have shown that under no load the output shaft oscillated at its own natural frequency and the amplitude of oscillations were strongly influenced by backlash. When a constant load was applied the principal oscillations of the output shaft were found to occur at a frequency equal to the tooth contact frequency with a smaller harmonic component at twice this frequency. The amount of backlash was observed to have very little effect when the gears were vibrating in this mode.

Benton and Seireg (5), like many of the previous investigators, isolated the pair of gears from its surroundings for the purpose of dynamic analysis, pointing out that the connecting shaft stiffnesses are most of the times much lower than the tooth mesh stiffness. But they nevertheless took the influence of the rest of the system on the gear pair by considering the external load to be a time varying one. This was illustrated by first considering a double reduction geared torsional system in their analysis which was subsequently broken into two single degree of freedom systems. Using these single d.o.f. systems, the effects of external excitations (external torques and their frequencies), system inertias, variation in mesh stiffness, contact ratio, and damping on the stability of the system were analysed. The mesh stiffness had been assumed to be a periodic function of frequency equal to the tooth contact frequency and two types of functions have been considered. One was a sinusoidal function and the other a rectangular one which, according to the authors, are the two extreme forms of stiffness variations expected

to occur in practical gear drives. The above analysis had shown the unstable regions and possible resonance conditions. According to these following factors affect the stability.

(a) The ratio of tooth mesh frequency (ωm) to the natural frequency of the system (ωn)

$\omega m/\omega n = 2, 1, 1/2, 1/3 \ldots$ for square wave stiffness

and $\omega m/\omega n = 2, 1, 1/2$ for sinusoidal stiffness variation

(b) Contact ratio. According to the report there is a particular contact ratio which requires less damping for stability than others at a particular $\omega m/\omega n$ value.

(c) The form and magnitude of stiffness variation.

(d) Damping ratio. It was reported that a damping ratio of 0.03 will eliminate all instability regions except for the one near $\omega m/\omega n = 2$, which also became stable when the damping ratio was above 0.11.

High oscillatory tooth loads have been predicted near the unstable $\omega m/\omega n$ regions even under steady load conditions, and also when the excitation frequencies are equal to the sum and difference frequencies [$(\omega m-\omega n)$, $(2\omega m-\omega n)$, $(\omega n-\omega m)$, $(\omega n-2\omega m)$] and the primary resonance frequency.

Kasuba and Evans (28) pointed out that most of the previous investigators on gear dynamics have either used a constant value for the tooth mesh stiffness or a variable one which depended only on the theoretical position of contact, whereas in actual practice the tooth stiffness and contact ratio are affected by factors such as the transmitted load, load sharing between teeth in mesh, gear tooth profile modifications, tooth deflections and the position of contact. The authors have taken the above aspects into account to form a mesh stiffness termed as the 'variable - variable mesh stiffness'. A four inertia model representing a geared system has been used in a digital computer simulation. Gear tooth profiles were defined by one to two hundred digitized points which have been established by superimposing the profile modifications and predefined errors on the true involute profiles. Once the tooth profiles were defined the position of contact, number of pairs of teeth in contact, sliding velocity vectors, the stiffness of individual pairs of teeth as well as the mesh stiffness, dynamic loads and dynamic factors at each mesh point were calculated using iterative processes. Gear tooth deflections due to load have been considered as equivalent positive profile errors. It has been found that the load has a considerable effect on the contact ratio while the profile errors and pitting affect the mesh stiffness characteristics to varying degrees, depending on their positions and amplitudes. The change in contact ratio due to tooth deflections which cause the point of contact to deviate from the theoretical has been found to reach values as high as 5% for high tooth loads. The dynamic load has been found to be affected by the inertia of all

elements, shaft stiffnesses, transmitted loads, gear mesh stiffness characteristics, damping in the system, amount of backlash and speed. The results according to the authors showed that geared transmission systems could be designed to limit the dynamic loads to within acceptable levels by selecting the masses, gear mesh and shaft stiffnesses and damping properly. It was also reported that the type of the profile error considerably affects the harmonic content in the mesh stiffness function which could excite any of the system's natural frequencies. But it has been found that the main source of excitation is the variable mesh stiffness and its interruptions.

Gear Lubrication

Load carrying capacity has been the main criterion for characterising the performance of lubricating oils. This meant that for satisfactory performance an oil film of sufficient thickness had to be maintained at all times beteween the mating surfaces. It was then argued that, for such an oil film to exist between gear teeth, hydrodynamic conditions have to prevail at the meshing zone, which was later proved to be true. But what puzzled the scientists was how these gears transmitted extremely high loads without failure when classical hydrodynamic theory predicted the oil films to break down at much lower loads.

The first published article where an attempt had been made to predict the oil film thickness between loaded gear teeth, using the hydrodynamic theory, was that by Martin (32) in 1916. Assuming the

conditions at the meshing point to be similar to those between a rotating rigid cylinder and a plane, he used Reynolds' equation to derive a formula for the thickness of the oil film. According to this, film thickness is directly proportional to the relative velocity between the surfaces and inversely proportional to the load.

It was soon realised that this yielded film thicknesses which were far too small, when compared with surface irregularities, for the gears to operate without severe metal to metal contact, while in practice they operated with no metal to metal contact. Several investigators tried to find an explanation for the above. Some of them analysed the effect of high pressure on tooth surface, i.e. elastic deflection, but could not come up with a satisfactory answer.

It was not until 1945 that a valid argument was brought forward to account for the high load carrying capacity of gears found in practice. Gatcombe (17a) suggested that the above could be due to the increase in the oil viscosity at high pressure. Assuming a viscosity/pressure relationship of the form $\mu = \mu_o (10)^{p\delta}$ (where p = pressure and δ = constant) he solved the equation of motion of a viscous fluid element. Even though his equations did not produce film thicknesses observed in practice, they were nevertheless higher than those predicted by previous formulae, thus indicating one aspect that has to be included in a lubricating oil film thickness analysis of gears.

Later in 1951 (17b) he carried out experiments using two rollers in which one of the roller assemblies was made to vibrate in the transverse sense at moderate frequencies (about 425 Hz). He found that the load capacities in this unsteady state to be much higher than the load capacities predicted by the steady state formula. He used this phenomenon to explain why high load capacities are obtained in gears where the conditions at the tooth mesh are definitely unsteady. Under these forced vibration conditions Gatcombe estimated a damping coefficient of about 0.005 of critical.

Cameron (7) used a disk machine to test the frictional losses and scuffing failures of gears in the presence of hydrodynamic oil films. Instead of a normal disk machine with two disks mounted on parallel shafts representing the gears, Cameron used a variable slide/roll test machine. In this a rotating disk forced against the flat surface of a plate which has an axis of rotation perpendicular to that of the disk, represents the gear tooth mesh. By swinging the plate about the point of contact he could obtain any desired slide/roll ratio which was more realistic of the conditions at the gear mesh than a simple rolling contact. The experiments have revealed that the coefficient of friction is virtually independent of the load while scuffing follows a law of the form:

$$\text{Load} \times (\text{Speed})^{n} = \text{Constant}$$

Scuffing load was found to be increasing approximately with the square root of the viscosity.

In addition to an isoviscous analysis of the problem which predicted loads lower than those found by experiment, he reviewed the analysis using a pressure dependent viscosity. This suggested that the maximum pressure within the oil film could approach infinity while the total load is still finite. This, he reported, indicated that under such conditions the effects of variation of temperature within the oil film, deformation of disk surfaces and surface roughnesses which were neglected previously should be taken into consideration.

Meanwhile in 1949 Grubin (19) had published an important report on the subject of gear lubrication; the main outcome of which was the development of an approximate equation to calculate the film thickness in highly loaded gear tooth contacts. Grubin included the variation of viscosity with pressure and the elastic deformation of gear teeth in his analysis. Instead of trying to obtain a solution that would satisfy both the equations for elastic deformation and pressure distribution, he assumed that for highly loaded tooth contacts the surfaces deform in the same way they would do under dry contact conditions. This proved to be very successful and the film thicknesses predicted by his formula were higher than those obtained by others and consistent with experimental observations.

McEwan (34) tackled the problem of increasing viscosity with pressure using a pressure/viscosity relationship of the form:

$$\mu = \mu_o(1 + p/k)^n$$

μ_o - viscosity at zero pressure

p - pressure

k,n - constants.

His analysis was based on the Reynolds boundary conditions (i.e. at some point in the divergent section of the film both the pressure (p) and the pressure gradient (dp/dx) are zero) whereas Gatcombe used the Sommerfeld boundary condition (i.e. no load is carried by the divergent part of the oil film) which McEwan considered to be incorrect. He, too, assumed the contact surfaces to be rigid and then used the point at which the pressure within the oil film reached infinity as the limiting point. The minimum film thickness, or alternatively the limiting load for hydrodynamic lubrication, was calculated based upon the conditions at this point. He suggested that formulae to calculate load capacities should be based on two failure criteria. They are scuffing, which occurs as a result of the breakdown of the oil film in the boundary lubrication regime, and pitting, which is the fatigue failure of the surface material occurring in the fluid film lubrication regime.

Crook (10) carried out a series of tests on a disk machine basically to find the properties of the oil film. Even though his initial attempt to measure the thickness of the oil film accurately using its electrical resistance was not successful due to the variation of the resistivity of the oil with the surface temperature of the

disks, Crook managed to prove that a hydrodynamic film existed between the rollers even at very high loads. Subsequently he used the capacitance across the oil film to measure its thickness. He found that at low loads film thickness was inversely proportional to load and directly proportional to speed, which agreed with those predicted by simple theory (constant viscosity, rigid disks, etc.) such as Martin's. At relatively high loads film thicknesses were found to be increasing with speed while decreasing slightly with the increase in load, which agreed well with film thicknesses predicted by Grubin's formula. This decrease of the film thickness with load was observed to be more rapid when there was rolling and sliding compared to when there was only rolling. This he attributed to the frictional heating due to sliding. The viscosity of the oil at the surface temperature of the disks has been found to have the greatest influence on film thickness.

MacConochie and Cameron (30) employed what was described as the discharge voltage method to measure the thickness of the oil film between gear teeth. It has been found that if an electric current is passed across a thin oil film, when this current exceeds about 0.5 amps it ceases to obey Ohm's law and the voltage drop across the film reaches a constant value independent of the current. This voltage drop termed as the discharge voltage was said to be dependent on the film thickness for rotating disks. The film thicknesses thus measured were found to be proportional to $\mu^{0.15}$ whereas according to Grubin's theory it was $\mu^{0.73}$. The huge difference in this relationship was attributed to the relaxation

time, the adiabatic frictional heating of the oil and the variation of viscosity across the oil film, the effects of which were not taken into account in the theoretical analysis. The variation of the film thickness with load on the other hand was found to be much higher than that predicted by Grubin's theory.

The usual approach to the numerical solution of the elasto-hydrodynamic problem is to first assume the film shape and then determine the corresponding pressure distribution. The film shape is then corrected according to this pressure and a new pressure curve obtained. The process is repeated until a stable pressure curve and a film shape is reached. Dowson and Higginson (14) in 1959 reported what was described as the solution of the inverse hydrodynamic lubrication problem where the numerical calculations are carried out in the reverse order, i.e. the pressure distribution is assumed first and the film shape corresponding to that is then calculated. According to them a stable solution is reached in this method much faster than in the conventional method. The initial film shape for medium - high load and low - medium speed cases, considered as near - Hertzian cases, was assumed to be parallel over most of the contact zone. The usual pressure/viscosity relationship was used in their analysis, but thermal effects were not taken into account as they were considered to be not important according to experimental results obtained for pure rolling. Minimum film thicknesses thus obtained were found to agree with experimental results reported by other investigators.

Later in a separate paper (14) in 1961 they presented a film thickness formula, based on the results of the above analysis, similar to that of Grubin's, using non-dimensional parameters.

Even though Grubin and Dowson-Higginson type formulae are meant for highly loaded gear tooth contacts, Cheng (8) in a paper pointed out that the prediction of oil film thicknesses using such formulae was not adequate in high load and speed situations. He said that investigations using X-ray techniques have shown that film thicknesses dependend on load to a greater extent than predicted by those fomulae for such cases. Discussing the possible reasons for this he commented that even though the heating effect at the inlet region can be responsible for the loss of film generating capacity at high speeds, it cannot account for the higher load dependence of the film thickness. Another suggestion he brought forward was that though the pressure/viscosity coefficient is high at static conditions, at very high speeds there is insufficient time available for the viscosity of the oil to rise to the value predicted by the assumed relationship.

Adkins and Radzimovsky (1) investigated the variation of the oil film thickness between lightly loaded spur gear teeth as the meshing point moved along the path of contact. Rolling, sliding and squeezing motions of the tooth surfaces were considered in this analysis where hydrodynamic lubrication conditions were assumed. But the variation of the lubricant viscosity with pressure and temperature were not taken into account. The authors, however,

included the effect of the variation of the number of pairs of teeth in contact at one time and hence the load supported by each film, in calculating the oil film thickness, although rigid teeth and a constant load were assumed. This was perhaps the first attempt ever to be made to study the variation of the oil film thickness between gear teeth in a dynamic situation even though true dynamic behaviour of the gears was not included. A similar approach, but including the variation of oil viscosity with pressure and true gear dynamics, was used in the present analysis. Some of the conclusions drawn by the authors based on the results of the analysis were:

(i) The minimum film thickness in a cycle occurred when the point of contact was near the pitch point.

(ii) Squeeze motion plays an important role in developing the pressure in the oil film.

(iii) A load-carrying film is built up considerably before the theoretical beginning of contact.

Radzimovsky and Vathayanon (40) in 1966 published a report in which they extended the previously described theory of Adkins and Radzimovsky to include the elastic deformation of the gear teeth. Numerical solutions were obtained to satisfy both the pressure distribution and the elastic deformation at each point as the position of contact moved along. Comparing these results with those obtained for rigid teeth they stated that the difference between the

two results was large only in situations having small film thicknesses.

Wang and Cheng (56) were probably the first to investigate the variation of dynamic load and the lubricating oil film thickness between gear teeth together as a continuous process affected by other parameters. They have also concentrated heavily on the contact temperature at the mesh, saying that scuffing at the root and the tip of tooth surfaces, which was a main source of gear failure, was to a great extent dependent on the film thickness and the surface temperature. For the analysis a simple, two inertia, single degree of freedom model had been chosen. Using a finite element method, first a set of results for the tooth deflection for a fixed load in non-dimensional form have been generated for different positions of contact as a function of the number of teeth. This, although assuming that the tooth stiffness is independent of the load which is not exactly true, simplifies subsequent calculations. A constant viscous damping coefficient of values ranging from 0.1 to 0.2 was also assumed. The assumed main excitation to the system has been the periodic variation of the mesh stiffness as a result of the change of contact between one and two pairs of teeth.

The dynamic load has been found to depend greatly on the operating speed, which eventually reaches very high values, as one would expect, near resonance, and then once again comes down to normal levels as the speed is increased beyond the resonance speed. The

contact ratio too has been found to have a considerable effect on the dynamic load with higher contact ratios, giving lower dynamic loads. But it has to be taken into account that in the above test the contact ratios were varied by changing the diametral pitch which could have affected the dynamic load in other ways as well, such as by altering the stiffness variation patterns of individual teeth and radius of curvature of tooth surfaces at the point of contact. It has been found that gears with finer pitches have lower surface temperatures and lower total flash temperatures compared to gears with coarser pitches under similar conditions. It was also reported that, except for a short period after tooth engagement, the squeeze film does not have a significant effect on the minimum film thickness, while the viscosity of the oil and the pitch line velocity were found to have a marked influence on the minimum film thickness.

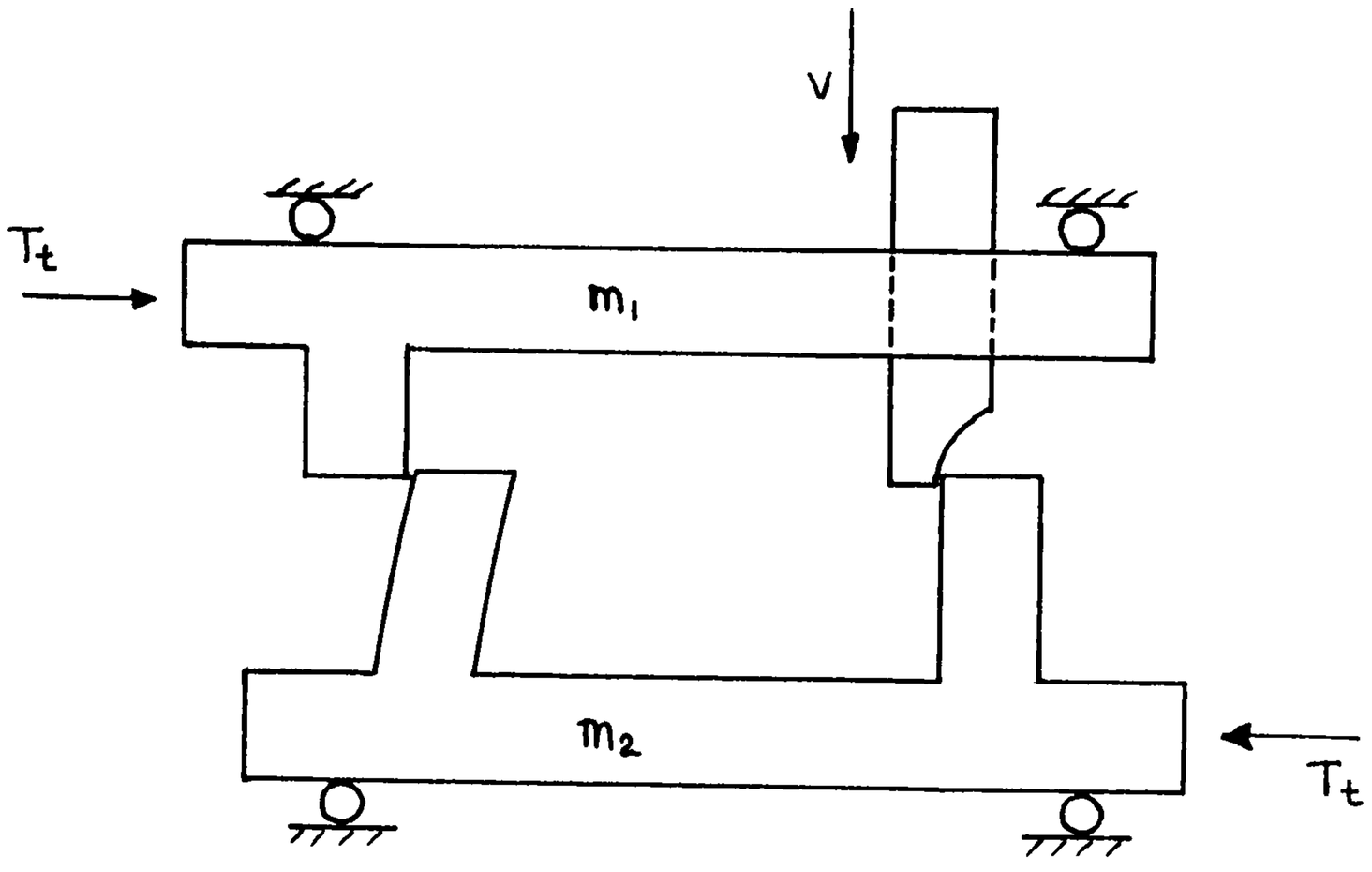

FIGURE 2.1

CHAPTER 3

DYNAMIC CHARACTERISTICS OF THE GEARED SYSTEM

3.1. Introduction

Dynamic factor is a convenient way of expressing the magnitude of the maximum dynamic load that could be expected in a pair of gears. From the days the existence of the dynamic load was realised, investigators from time to time have come up with various formulae to calculate the dynamic factor. Initially, this was expressed only as a function of speed, but in more recent works the influence of various other parameters of the system have also been included. Yet the application of dynamic factors to predict dynamic loads sufficiently accurately is limited due to individual properties of different transmission systems. This could be a crucial point in precision gears running at high speed with high loads. In such cases it could prove to be worthwhile to carry out a dynamic analysis of the complete system. Even a simulation on an analog or a digital computer would help very much in the design of the system, especially if it is required to operate under a variety of conditions. Such an analysis would obviously be costly and time consuming and, for many of the systems, may not prove to be worthwhile. For such systems a reliable but simple dynamic factor estimation would be sufficient. This aspect could be better illustrated by dividing geared systems into four categories.

For simplicity the sections of the transmission system on the driving side and the driven side are represented by two simple inertias as shown in Figure 3.1. The four categories are:

(i) Equivalent stiffnesses of the connecting shafts (K1 and K2) very low compared to the average tooth mesh stiffness, while the inertias of the gears are considerably higher than those of the shafts they are mounted on. This indirectly ensures that the natural frequency of the gears is much higher than those of the two branches calculated separately. Under these conditions the relatively slow torsional response of the system has negligible effect on the much faster vibratory motions of the gears, especially at high speeds when the mesh cycles too are of high frequency. In this case it seems perfectly reasonable to analyse the dynamics of the gears separate from the rest of the system and the use of a dynamic factor could give very good results.

(ii) Natural frequencies of the branches relatively low compared to that of the pair of gears, but not low enough to be neglected altogether. In this case also the gears can be treated separate from the rest of the system. But a dynamic analysis of the complete system should also be carried out, perhaps neglecting the tooth mesh effect (either assuming the teeth to be rigid or the mesh stiffness to be a constant) to establish the nature of the load cycle, especially its maximum value, imposed on the gears. The results of this

could be used in the dynamic load calculation of the pair of gears.

(iii) Natural frequencies of the branches and gears comparable. In this situation we cannot isolate the gears from the surroundings since it plays an active part in the dynamic behaviour of the system. Under these conditions any attempt to predict the dynamic loads using a dynamic factor is meaningless. For such a case there is no alternative to find the dynamic loads but to carry out a thorough dynamic analysis of the whole system.

(iv) Natural frequencies of the system high compared to the natural frequency of the pair of gears. These types of systems are very rare. A careful analysis is needed here too, due to the periodic nature of tooth contact cycle and its strong harmonic content, any one of which could resonate with any of the system's natural frequencies. In this case it is the rest of the system that requires a thorough analysis and the exact nature of the tooth mesh is not critical.

In categories (i) and (ii) it is necessary to ensure that the torsional characteristics of both branches of the system are properly investigated. This is particularly important in situations such as when a small load is driven from the power taken off a main transmission system (or when a load is disconnected in a branched

system by disengaging the clutch) which has a high inertia and a low natural frequency. Here, even though the natural frequency of the pair of gears calculated using standard formulae is much higher than that of the rest of the transmission system, due to the low inertia of the load part of the inertia of the shafts on the driven side will be added to the driven gear, bringing the natural frequency of the gears down as well as increasing the dynamic load considerably. Very high dynamic factors can be expected in such situations despite the low nominal load. The case of relatively small gears connected to heavy shafts should also be treated carefully, since the effective inertia of the gears could be quite different from their actual inertias due to the influence of the shafting.

Under these circumstances it can thus be seen that a fixed 'dynamic factor' formula can be applied usefully only for certain types of geared systems. Whether to find the dynamic factor of a single pair of gears or to analyse the dynamic characteristics of a whole transmission system it is necessary to know the properties of the gear tooth mesh. Even after making a number of assumptions these can usually be expressed with very complicated formulae, the application of which is restricted to a very limited area. One of the aims of this research is to study the behaviour of the tooth mesh in detail under different conditions in an effort to identify the role each parameter plays. To look into these properties it seems appropriate to treat the gears separately, independent of the system to which it is connected. Thus the system that will be analysed here will consist of only two gears.

3.2. The Analytical Model

The three basic parameters which determine the characteristics of any vibrational system are the inertias, stiffnesses and damping. With the inertias of gears fixed, stiffness and damping are responsible for the nonlinear behaviour of the system, and thus need special attention. If one looks at the way power is transmitted from one gear to the other, it can be seen that there are three imortant links:

(a) the driving gear;

(b) the oil film between the tooth surfaces;

(c) the driven gear.

All three of the above are affected by the force they transmit. Gear teeth and body deform under load and the work done by the force in deforming will be stored as strain energy. In addition to this work a further amount of work has to be done to overcome friction, both inside the gear material as well as on the outside, on tooth surfaces. Frictional forces can usually be represented by viscous damping forces, although in the case of gears it is a very nonlinear function. The strain energy in the gear can be represented by an equivalent spring compressed by an amount equal to the deformation of the gear. In this case the spring is capable of exerting only compressive forces. A discontinuity occurs beyond this point unless it is assumed that there is no backlash in the gear system. Thus,

each of the two links (a) and (c) can be represented by equivalent nonlinear springs and dashpots.

The action of the oil film between the tooth surfaces is much more complicated. This is due to the fact that the thickness of this oil film depends on a larger number of parameters which are interdependent. If we consider a simple situation where an oil film is subjected to the tooth load, assuming all the other variables to remain constant, the forces at the boundary of the oil film are:

(i) The force due to the oil pressure.

(ii) The shear force due to the relative velocity between the tooth surface and oil in a direction parallel to the tooth surface.

(iii) The force in the direction normal to the tooth surface due to the relative velocity between the tooth surfaces in the same direction.

If it is assumed that the oil is incompressible and that the thickness of the oil film is very small compared to the other dimensions, then the oil pressure across the depth of the film will remain constant, making the force on the tooth surfaces on either side of the film equal. Thus this force can be represented by a spring having nonlinear characteristics. Forces (ii) and (iii) both depend on relative velocities, which are the feature of viscous

damping forces. This makes it possible for the oil film also to be represented by a nonlinear spring and damper combination.

Thus the three links in the transmission chain can each be represented by a spring and a damper combination, all of them nonlinear, and if the inertia of the oil is neglected then the rotary gear system (Figure 3.2) can be modelled by an equivalent linear mass-spring-damper system (Figure 3.3).

Generally, the internal damping in the material is low. Azar and Crossley (3) have found it to be of the order of 0.015 of critical. Thus it will be neglected in the analysis. This leaves the oil film as the only source of damping in the system. But since the exact nature of the properties of the oil film are not yet known, i.e. since we cannot express mathematically the behaviour of the spring and the damper representing the oil film, it seems appropriate to represent the effect of the oil film by a single force instead of the spring and damper, to avoid confusion at early stages.

The load due to 'reverse contact' is neglected for the sake of simplicity and clarity.

Usually the transmission efficiency of a pair of spur gears is over 98%. Hence in the analysis, as far as dynamic equilibrium is concerned, we can assume it to be 100%, thereby neglecting the losses at the tooth mesh.

This will yield:

$$F_{a1} = FO_{a1} = FO_{b1} = F_{b1} = \text{Say } F_1$$

$$F_{a2} = FO_{a2} = FO_{b2} = F_{b2} = \text{Say } F_2$$

$$F_{ao} = F_{bo} = \text{Say FO.}$$

This assumption simplifies computations considerably. Even though it is possible to calculate the forces on individual tooth surfaces giving due regard to losses, the improvement in the results is not considered to be worthwhile.

The resulting simplified model will be as shown in Figure 3.4.

3.3. Dynamics of the System

Y_{ma} is the distance of M_a from a reference axis XA - XA on gear 'A' and Y_{mb} is the distance of M_b from a similar reference axis on gear 'B'. The distance of XA - XA from a fixed axis is denoted by Y_{ar}, which determines the theoretical angular position of gear 'A'.

Thus the equations of motion for the two masses will be:

$$M_a \frac{d^2(Y_{ma})}{dt^2} = FO - F_1 - F_2 \qquad (1)$$

$$M_b \frac{d^2(Y_{mb})}{dt^2} = - FO + F_1 + F_2 \qquad (2)$$

which yields

$$\frac{d^2(Y_{mb})}{dt^2} = - \frac{M_a}{M_b} \cdot \frac{d^2(Y_{ma})}{dt^2} \qquad (3)$$

Axes XA - XA and XB - XB can be selected in such a way that

$Y_{mb} = 0$ when $Y_{ma} = 0$, and

with the forces on the tooth surfaces on either side of the oil film assumed equal, this becomes a single degree of freedom system for which

$$\frac{d(Y_{mb})}{dt} = 0 \quad \text{when} \quad \frac{d(Y_{ma})}{dt} = 0 .$$

Then equation (3) can be integrated to yield:

$$\frac{d(Y_{mb})}{dt} = - \frac{M_a}{M_b} \frac{d(Y_{ma})}{dt} \qquad (4)$$

and

$$Y_{mb} = - \frac{M_a}{M_b} Y_{ma} \qquad (5)$$

Forces F_1 and F_2 are the tooth forces of the first and the second pairs of teeth respectively. For dynamic equilibrium these forces should be equal to the forces offered by the respective oil films on each tooth surface at any instant.

With true involute teeth, contact always occurs along the tangent line to the base circles of the gears. Thus theoretically the minimum oil film thickness occurs along this line. The positions of the tooth surfaces of gears 'A' and 'B' from the fixed OX axis, measured along the Y axis, are given by Y_{ao} and Y_{bo} respectively (Figure 3.5). The minimum oil film thickness will therefore be:

$$HO = Y_{bo} - Y_{ao} \qquad (6)$$

For convenience XA - XA, the reference axis of gear 'A' is chosen so that it coincides with the position of the surface of the first tooth of gear 'A' when the gears are not loaded and there is no oil film between the teeth (Figure 3.6).

Referring to Figure 3.7, which is the linear equivalent of Figure 3.6:

The combined stiffness of the gear teeth in mesh

$$KO = \frac{K_a K_b}{K_a + K_b} \qquad (7)$$

$$Y_b = - Y_a \frac{M_a}{M_b} \qquad (8)$$

Total compression of the springs:

$$\delta = \frac{F}{KO} \tag{9}$$

$$Y_a - Y_b = \frac{F}{KO} = \delta$$

$$Y_a\left(1 + \frac{M_a}{M_b}\right) = \delta$$

$$\text{Let } M_{ab} = 1 + \frac{M_a}{M_b} \tag{10}$$

$$\therefore Y_a = \frac{\delta}{M_{ab}} \tag{11}$$

By a similar argument we can write:

$$HO_a = \frac{HO}{M_{ab}} \tag{12}$$

The deflection of gear 'A':

$$Y_a - DY = \frac{F}{K_a}$$

$$DY = Y_a - \frac{F}{K_a}$$

$$DY = \frac{\delta}{M_{ab}} - \frac{F}{K_a} \qquad (13)$$

$$Y_{ao} = Y + DY - HO_a$$

$$Y = Y_{ar} \quad \text{(Figure 3.6)}$$

$$\therefore \quad Y_{ao} = Y_{ar} + \frac{\delta}{M_{ab}} - \frac{F}{K_a} - \frac{HO}{M_{ab}}$$

$$\text{But} \quad \delta = Y_{ma} M_{ab} + HO \qquad (14)$$

$$\text{or} \quad Y_{ma} = \frac{(\delta - HO)}{M_{ab}} \qquad (15)$$

$$\therefore \quad Y_{ao} = Y_{ar} + Y_{ma} - \frac{F}{K_a} \qquad (16)$$

$$\frac{d(Y_{ao})}{dt} = \frac{d}{dt}(Y_{ar}) + \frac{d}{dt}(Y_{ma}) - \frac{d}{dt}\left(\frac{F}{K_a}\right)$$

$$\text{But} \quad \frac{F}{K_a} = \frac{Y_a M_{ab} KO}{K_a}$$

$$\frac{F}{K_a} = \left(Y_{ma} + \frac{HO}{M_{ab}}\right) M_{ab} \frac{KO}{K_a} \quad .$$

It can be assumed that $\frac{d}{dt}\left(\frac{KO}{K_a}\right)$ is small compared to the other derivatives.

$$\therefore \frac{d}{dt}\left(\frac{F}{K_a}\right) = \left(\frac{d}{dt}(Y_{ma}) + \frac{1}{M_{ab}}\frac{d}{dt}(HO)\right) M_{ab}\frac{KO}{K_a}$$

$$\therefore \frac{d}{dt}(Y_{ao}) = \frac{d}{dt}(Y_{ar}) + \frac{KO}{K_a}\left(\frac{K_a}{K_b} - \frac{M_a}{M_b}\right)\frac{d}{dt}(Y_{ma})$$

$$- \frac{KO}{K_a}\frac{d}{dt}(HO) \qquad (17)$$

When two pairs of teeth are in mesh, equations (3.14) and (3.16) can be written as:

$$\delta_1 = Y_{ma} M_{ab} + HO_1 \qquad (18)$$

$$\delta_2 = Y_{ma} M_{ab} + HO_2 + PE_{a2} - PE_{b2} \qquad (19)$$

$$Y_{ao1} = Y_{ar} + Y_{ma} - \frac{F_1}{K_{a1}}$$

$$Y_{ao2} = Y_{ar} - PO + PE_{a2} + Y_{ma} - \frac{F_2}{K_{a2}} \qquad (20)$$

and also

$$F_1 = KO_1 (Y_{ma} M_{ab} + HO_1) \qquad (21)$$

$$F_2 = KO_2 (Y_{ma} M_{ab} + HO_2 + PE_{a2} - PE_{b2}) \qquad (22)$$

The equation of motion of the model (equation 1) can thus be written as:

$$\frac{d^2}{dt^2}(Y_{ma}) = \frac{1}{M_a}[FO - KO_1\, HO_1 - KO_2\,(HO_2 + PE_{a2} - PE_{b2}) - Y_{ma}\,(KO_1 + KO_2)\, M_{ab}] \quad (23)$$

Where PE_{a2} and PE_{b2} are the pitch errors of the second pair of teeth of gears A and B respectively, relative to the first pair of teeth. PE_a and PE_b are taken as positive when material projects beyond the theoretical tooth profile. Pitch errors of the first pair of teeth (PE_{a1} and PE_{b1}) are not important since the calculations can be started with the first pair of teeth meshing at the pitch point (hence only one pair in contact) which eliminates the influence of the pitch errors of the neighbouring teeth.

3.4. Gear Mesh Stiffness

The best method available at the moment in finding the behaviour of a gear under load is the Finite Element Method. Though this could be applied to gear teeth of any shape, size or type, the individual nature of the approach of the method tends to make it difficult for the results to be generalised. Besides, the computer time required to obtain a set of results could be prohibitive in a dynamic application where repetitive calculations involving iterative solutions are needed. In such a situation a much more straightforward, simpler and a generalised method would be preferred, though at the expense of accuracy. Thus it was decided to calculate tooth deflections and stiffnesses assuming the gear teeth to be cantilevers on elastic foundations.

For a gear tooth considered to be a cantilevered beam under load, there are a number of deflection modes. These are:

(i) Hertz contact deformation as a result of the curvatures of the contact surfaces;

(ii) bending of the tooth;

(iii) shear deformation at the base of the tooth;

(iv) deformation due to the normal component of the load;

(v) deformation of the adjacent parts of the body;

(vi) deflection due to load acting on neighbouring teeth;

(vii) torsional deformation of the web or the body;

(viii) deformation of the gear rim.

Of the above deflections, the contribution of the web or body deflection is not included in the dynamic system. This is because, generally, in gears with webs the major contribution to its inertia comes from the weight of the material at the rim. Thus, when the system under consideration is only the pair of gears which is modelled by two inertias, the bulk of which coming from the rims, connected by the tooth mesh, the gear webs can be considered to be parts virtually 'outside' the above system. Hence its deformation has negligible effect on the tooth mesh deflection. On the other hand, for solid gears with no webs the deflection of the body is small enough, compared to other deflections, to be neglected.

The deformation of the rim can be caused in two ways. The first is the torsional deformation due to the tangential component of the load. This type of deformation is very small and can easily be neglected since the width of the rim is usually high compared to that of the web. But in gears where the thickness of the rim in the radial direction is small the rim may get deformed in such a way that it loses its normal circular shape. This will cause all the affected teeth to be deformed. Yet for the gear shapes found normally, this deformation is also very small compared with total tooth deflections and hence will be neglected from stiffness calculations.

The remaining tooth deformations are calculated according to the formulae suggested by Weber (59).

It is assumed here that the total tooth deflection is equal to the sum of the deflections due to each of the causes mentioned earlier, and also that the change in the position and direction of the tooth load as a result of the above deflections is negligible.

Equations suggested by Weber are:

(i) Hertz deformation (Figures 3.8 and 3.9)

$$\text{Gear 'A'} \quad ZH_a = \frac{2F}{\pi} \frac{(1 - \nu_a^2)}{Ea} \left[\ln\left(\frac{2h_a}{b}\right) - \frac{\nu_a}{2(1 - 2\nu_a)}\right] \qquad (24)$$

$$\text{Gear 'B'} \quad ZH_b = \frac{2F}{\pi} \frac{(1 - \nu_b^2)}{E_b} \left[\ln\left(\frac{2h_b}{b}\right) - \frac{\nu_b}{2(1 - 2\nu_b)}\right] \tag{25}$$

$$\text{where } b = \left[\frac{4F}{\pi} R\left\{\frac{(1 - \nu_a^2)}{E_a} + \frac{(1 - \nu_b^2)}{E_b}\right\}\right]^{1/2} \tag{26}$$

$$R = \frac{Y_{ao}(Cd \sin(\psi) - Y_{bo})}{Y_{ao} + Cd \sin(\psi) - Y_{bo}} \tag{27}$$

$$h_a = Y_{ao} - R_{ba} \tan(\theta) \tag{28}$$

$$\theta = \frac{(Y_{ao} - G_{ab/2.0})}{R_{ba}} \tag{29}$$

$$h_b = C_d \sin(\psi) - Y_{bo} - R_{bb} \tan(\gamma) \tag{30}$$

$$\gamma = \frac{(C_d \sin(\psi) - Y_{bo} - G_{bb/2.0})}{R_{bb}} \tag{31}$$

The deflections of the gear teeth due to the bending moment, shear force and the normal force are found by equating the respective stress energy to the work done in deforming the material in each case.

Thus for gear 'A' (Figure 3.10):

(a) Bending

$$\frac{1}{2} F.ZB_a = \frac{1}{2} \int_{R_{ra}}^{R_{ya}} \frac{BM_a^2}{Ea.I_{ya}} dR_a \qquad (32)$$

$$BM_a = F \cos\theta (R_{ya} - R_a) \qquad (33)$$

$$I_{ya} = \frac{1}{12} G_a^3 \qquad (34)$$

per mm face width of the gears.

(b) Shear

$$\frac{1}{2} F.ZS_a = \frac{1}{2} \int_{R_{ra}}^{R_{ya}} \frac{1,2\ SF^2}{G\ G_a} dR_a \qquad (35)$$

$$SF = F \cos\theta \qquad (36)$$

(c) Normal

$$\frac{1}{2} F.ZN_a = \frac{1}{2} \int_{R_{ra}}^{R_{ya}} \frac{NF^2}{E_a\ G_a} dR_a \qquad (37)$$

$$NF = F \sin\theta \qquad (38)$$

A similar set of equations can be written for the deflections of the tooth on gear 'B' also.

In order to simplify the above integrations it was decided to approximate the tooth profile by a square root function of the height (Figure 3.11). Thus the tooth thickness at any point could be expressed by the formula:

$$H = H_r \left(\frac{x}{LO}\right)^{1/2} \qquad (39)$$

H_r is the tooth thickness at the root circle radius or the base circle radius, whichever is larger. The effect of root radius is neglected in calculating the thickness and an uninterrupted involute profile is assumed up to the root circle.

To make the assumed tooth shape as close as possible to the actual, the height LO is calculated in such a way that the thickness of the assumed shape at the outside radius (tip radius) is equal to the thickness of the actual tooth at tip radius. With this approximation it was found that the assumed tooth thickness was never more than 6.0% away from the true involute thickness for gears with the number of teeth above 25. Figures 3.15(a) to (d) show typical examples of the assumed tooth profiles against true involute profiles.

The above approximate tooth profile was used only in the calculation of the tooth deflections due to bending, shear and normal forces. For all other calculations the actual profile was used. Tooth deflections were calculated for the assumed ones and for the true

involute teeth and the results (Appendix I) showed that even though the differences are high when the number of teeth are low, for gears with the number of teeth above 40 the errors are negligible.

Using the above tooth thickness approximation, Equations (2), (5) and (7) could be integrated (Appendix II) to yield:

$$ZB = \frac{F}{E} \cos^2\theta \; 8 \frac{LO}{H_r} [8\, LC^{3/2}\, LO^{1/2} - 3LC^2 - 6\, LC\, LO + LO^2] \quad (40)$$

$$ZS = 2.4 \; F \cos^2\theta \; \frac{LO^{1/2}}{G \; Hr} [LO^{1/2} - LC^{1/2}] \quad (41)$$

$$ZN = 2.0 \; F \sin^2\theta \; \frac{LO^{1/2}}{E \; Hr} [LO^{1/2} - LC^{1/2}] \quad (42)$$

where

$$LC = R_r + LO - RF \quad (43)$$

R_r = Root radius

LO = Total height of the assumed tooth profile (Figure 3.11)

RF = Radius at which the force is acting.

(iii) Deformation of the adjacent part of the body of the gear.

According to Weber this is:

$$ZD = 2 F \cos^2\theta \left[C_{11}(RF - R_r) + 2C_{12}(RF - R_r) + C_{22}\left(1 + \frac{\tan^2\theta}{3.1}\right)\right] \quad (44)$$

where

$$C_{11} = \frac{9}{\pi}\left(\frac{1 - \nu^2}{E}\right)\frac{1}{H_r^2}$$

$$C_{12} = \frac{(1 + \nu)(1 - 2\nu)}{2E}\frac{1}{H_r}$$

$$C_{22} = \frac{2.4}{\pi E}(1 - \nu^2)$$

The total deflection of the point of contact of a gear tooth is therefore:

$$Z = ZH + ZB + ZS + ZN + ZD \quad (45)$$

3.5. Lubricating Oil Film

The reactive force of the oil film on gear teeth consists of two main components. These are the normal force which is primarily due to the oil pressure and the tangential force which is the shear force (Figure 3.13). Thus the total force of the oil film will be:

$$F_{oil} = \int p.ds + \int \tau (\lambda + \epsilon) \, ds \qquad (46)$$

Navier-Stokes equation (equation (47)) which could be regarded as the most general mathematical description of the flow of a viscous fluid is a sensible starting point for any hydrodynamic analysis. Reynolds equation, which too has been used widely as the starting point for the analysis of thin lubricating oil films, is also derived from equation (47) in conjunction with the continuity equation with suitable assumptions.

$$F_{in} = F_{pr} + F_{gr} + F_{vi} \qquad (47)$$

where

$F_{in} = \rho \left\{ \frac{\partial u_i}{\partial t} + (u_i \bar{\nabla}) \, u_i \right\}$ = Inertia force

$F_{pr} = - \bar{\nabla} p$ = Pressure force

$F_{gr} = - \rho \bar{\nabla} \phi$ = Gravity/Body force

$F_{vi} = \mu \nabla^2 u_i + (\mu + \mu') \bar{\nabla} (\bar{\nabla} u_i)$ = Viscous force

u_i = Velocity of a fluid particle in x,y and z directions (u,v and w respectively)

$\bar{\nabla} = \left(\frac{\partial}{\partial x} , \frac{\partial}{\partial y} , \frac{\partial}{\partial z} \right)$ = Nabla operator

$$\nabla^2 = \left(\frac{\partial^2}{\partial x^2} + \frac{\partial^2}{\partial y^2} + \frac{\partial^2}{\partial z^2}\right) = \text{Laplace operator}$$

ϕ = Force potential per unit mass

$$\mu' = -\frac{2}{3}\mu$$

The assumptions we can make with respect to thin lubricating oil films between gear teeth, which include Reynolds' assumptions are:

(i) Inertia and body forces are negligible compared to pressure and viscous forces

$$\frac{\partial u_i}{\partial t} + (u_i \bar{\nabla})\, u_i = 0$$

$$\bar{\nabla}\phi = 0 .$$

(ii) Thickness of the oil film is much smaller than other dimensions. Therefore,

(a) The variation of pressure across the film (in the y-direction) can be neglected

$$\frac{\partial p}{\partial y} = 0$$

(b) The derivatives of velocity components u and w with respect to y can be assumed to be large compared with all other derivatives of velocities. Thus the latter can be neglected.

(iii) The effects due to side leakage are negligible

$$\frac{\partial p}{\partial z} = 0$$

(iv) No surface tension effects.

(v) Zero slip at liquid - solid boundaries.

With the above assumptions the flow equation reduces to:

$$\frac{\partial p}{\partial x} = \frac{\partial}{\partial y}\left[\mu\left(\frac{\partial u}{\partial y}\right)\right] \tag{48}$$

This can be integrated twice with respect to y to yield,

$$u = \frac{1}{\mu}\frac{\partial p}{\partial x}\frac{y^2}{2} + \frac{A}{\mu}(x,z)\, y + B(x,z) \tag{49}$$

which assumes that pressure and viscosity do not vary in the y-direction.

Using the boundary conditions

$$u = u_a \quad \text{when} \quad y = y_a$$

and $u = u_b$ when $y = y_b$

A(x,z) and B(x,z) can be found.

$$A(x,z) = \mu \frac{(u_a - u_b)}{(y_a - y_b)} - \frac{1}{2} \frac{\partial p}{\partial x} (y_a + y_b) \tag{50}$$

$$B(x,z) = \frac{1}{2\mu} \frac{\partial p}{\partial x} y_a y_b - \frac{(u_a y_b - u_b y_a)}{y_a - y_b} \tag{51}$$

and

$$u = \frac{1}{2\mu} \frac{\partial p}{\partial x} [y^2 - y(y_a + y_b) + y_a y_b] +$$

$$\frac{1}{y_a - y_b} [y (u_a - u_b) - (u_a y_b - u_b y_a)] . \tag{52}$$

At this point it is assumed that the oil is incompressible even though at extremely high pressures the oil gets compressed by a considerable amount. This, together with the other assumptions made earlier regarding the oil film, reduces the equation of continuity which is normally written as:

$$\frac{\partial \rho}{\partial t} + \frac{\partial (\rho u)}{\partial x} + \frac{\partial (\rho v)}{\partial y} + \frac{\partial (\rho w)}{\partial z} = 0 \tag{53}$$

$$\text{to} \quad \frac{\partial(\rho u)}{\partial x} + \frac{\partial(\rho v)}{\partial y} = 0 \qquad (54)$$

This can be integrated with respect to y across the oil film with the limits $y = y_a$ and $y = y_b$.

$$\int_{y_a}^{y_b} \frac{\partial(\rho u)}{\partial x}\, dy + [\rho v]_{y_a}^{y_b} = 0 \qquad (55)$$

Substituting for u (equation (52)),

$$\frac{\partial}{\partial x}\left[\frac{\rho}{12\mu}\frac{\partial p}{\partial x}(y_a - y_b)^3 - \frac{1}{2}\rho(u_a + u_b)(y_a - y_b)\right] -$$

$$\rho u_b \frac{\partial y_b}{\partial x} - \rho u_a \frac{\partial y_a}{\partial x} + \rho(v_b - v_a) = 0 \qquad (56)$$

Referring to Figure 3.14

$$u_a = -y_a \omega_a$$

$$u_b = -(C_d \sin\psi - y_b)\omega_b$$

$$v_a = (R_{ba} + x)\omega_a$$

$$v_b = (R_{bb} - x)\omega_b$$

Where ω_a and ω_b are the angular velocities of the two gears A and B respectively with ω_a - anti-clockwise and ω_b - clockwise.

It can be shown that:

$$u_a \frac{\partial y_a}{\partial x} = -\frac{1}{2}\omega_a \frac{\partial (y_a^2)}{\partial x}$$

and $$u_b \frac{\partial y_b}{\partial x} = -\omega_b C_d \sin\psi \frac{\partial y_b}{\partial x} + \frac{1}{2}\omega_b \frac{\partial (y_b^2)}{\partial x} \qquad (57)$$

Substituting these in equation (56) and integrating with respect to x,

$$\frac{1}{12\mu}\frac{\partial p}{\partial x}(y_a - y_b)^3 + \frac{\omega_b}{2} C_d \sin\psi (y_a + y_b) -$$

$$\frac{1}{2} y_a y_b (\omega_a + \omega_b) + (R_{bb}\omega_b - R_{ba}\omega_a) x -$$

$$\frac{1}{2}(\omega_a + \omega_b) x^2 + C_1 = 0 \qquad (58)$$

But $$\omega_a = \frac{V_a|_{x=0}}{R_{ba}} = \frac{1}{R_{ba}} \frac{d(y_{ao})}{dt}$$

$$\omega_a = \frac{\dot{y}_{ao}}{R_{ba}} \qquad (59)$$

$$\text{and} \quad V_b\big|_{x=0} = V_a\big|_{x=0} + \frac{d(HO)}{dt}$$

$$\omega_b = \frac{V_b\big|_{x=0}}{R_{bb}} = \frac{1}{R_{bb}} \left(\frac{d(y_{ao})}{dt} + \frac{d(HO)}{dt}\right)$$

$$\omega_b = \frac{1}{R_{bb}} (\dot{y}_{ao} + \dot{HO}) \tag{60}$$

$$\text{Let} \quad m = \frac{R_{ba}}{R_{bb}}$$

$$\text{then} \quad C_d \sin\psi = R_{ba} \left(1 + \frac{1}{m}\right) \tan\psi \tag{61}$$

Thus, equation (58) can be written as:

$$\frac{1}{12\mu}\frac{\partial p}{\partial x} = \frac{1}{(y_b - y_a)^3} \frac{\dot{y}_{ao}}{2R_{ba}} (1 + m) [R_{ba} \tan\psi (y_a + y_b) - y_a y_b - x^2]$$

$$+ \frac{\dot{HO}}{2R_{ba}} [R_{ba} (1 + m) \tan\psi (y_a + y_b) - m (y_a y_b + x^2)$$

$$+ 2 R_{ba} x] + C \tag{62}$$

Viscosity of the oil is a function of both the pressure and temperature. It has been found that these can be expressed satisfactorily using exponential functions. Thus the following relations between the viscosity and pressure and temperature will be used here.

$$\mu = \mu_t \, e^{\alpha p}$$

p - pressure (N/m^2)

α - pressure/viscosity coefficient (m^2/N)

$$\text{and} \quad \mu_t = \mu_o \, e^{(1/T - 1/T_o)\beta}$$

$\mu_o (NS/m^2)$ - viscosity at temperature T_o (^oK)

β - temperature/viscosity coefficient ($1/^oK$)

With the viscosity considered to be a function of pressure it is not possible to integrate equation (62) to find the pressure distribution within the oil film. To overcome this difficulty a new variable 'q' is introduced so that

$$\partial q = e^{-\alpha p} \, \partial p$$

$$\text{and} \quad q = 0 \quad \text{when } p = 0$$

$$\text{Then} \quad q = \frac{1}{\alpha} (1 - e^{-\alpha p})$$

and $$p = -\frac{1}{\alpha} \ln (1 - \alpha q)$$

q is generally referred to as the reduced pressure. With this substitution equation (62) becomes,

$$\frac{\partial q}{\partial x} = \frac{6\mu_t}{R_{ba}(y_b - y_a)^3} \left\{ \dot{y}_{ao} (m + 1) [R_{ba} \tan\psi (y_a + y_b) - y_a y_b - x^2] \right.$$

$$+ \dot{H}O [R_{ba} (1 + m) \tan\psi (y_a + y_b) - m(y_a y_b + x^2)$$

$$\left. + 2R_{ba} x] + C \right\} \qquad (63)$$

The two boundary conditions required to solve the above equation are:

(i) $p = 0$ and thus $q = 0$ at the inlet to the convergent section, i.e. when $x = x_{max}$.

(ii) Cavitation occurs at some point in the divergent section of the film ($x = x_{po}$) so that, at that point

$$p = 0 \quad \text{and} \quad \frac{\partial p}{\partial x} = 0$$

which leads to $q = 0$ and $\frac{\partial q}{\partial x} = 0$

With the first boundary condition the reduced pressure at any point x can be written as:

$$q = \int_{x_{max}}^{x} \frac{\partial q}{\partial x}\, dx \qquad (64)$$

and the force on the gear tooth due to the oil pressure acting on it is:

$$F_p = \int_{x_{po}}^{x_{max}} \frac{p}{\cos\epsilon}\, dx \qquad (65)$$

Assuming the oil to behave like a Newtonian fluid, the shear stress on the surface of the tooth of gear 'A' can be written as (Figure 3.15):

$$\tau = \mu \frac{\partial u_i}{\partial j}\Big|_{y=y_a} \qquad (66)$$

$$\tau = \mu\left[\frac{\partial u_i}{\partial x}\frac{\partial x}{\partial j} + \frac{\partial u_i}{\partial y}\frac{\partial y}{\partial j}\right]_{y=y_a} \qquad (67)$$

With the initial assumption $\frac{\partial u}{\partial y}$ >> other derivates of velocities and that

$$u_i = u \cos\epsilon$$

$$\tau = \mu \cos^2\epsilon \left.\frac{\partial u}{\partial y}\right|_{y=y_a}$$

From equation (52)

$$\left.\frac{\partial u}{\partial y}\right|_{y=y_a} = \frac{1}{2\mu}\frac{\partial p}{\partial x}(y_a - y_b) - \frac{1}{R_{ba}(y_a-y_b)}\left\{\dot{y}_{ao}\,[y_a + R_{ba}\,(1+m)\tan\psi - m\,y_b] + \dot{H}O\,[R_{ba}\,(1+m)\tan\psi - m\,y_b]\right\} \quad (68)$$

and with $\partial q = e^{-\alpha p}\,\partial p$

the shear stress becomes:

$$\tau = \mu_t\, e^{\alpha p} \cos^2\epsilon \left\{\frac{1}{2\mu_t}\frac{\partial q}{\partial x}(y_a - y_b) - \frac{1}{2R_{ba}(y_a-y_b)}\right.$$

$$[\dot{y}_{ao}\,(y_a + R_{ba}\,(1+m)\tan\psi - m y_b) + \dot{H}O\,(R_{ba}\,(1+m)$$

$$\left.\tan\psi - m y_b)]\right\} \quad (69)$$

The force due to shear on the tooth of gear 'A', in the direction of the line of contact is:

$$F_s = \int_{x_{po}}^{x_{max}} \frac{\tau(\lambda+\epsilon)}{\cos\epsilon} \cdot dx \qquad (70)$$

And the total force on gear 'A' along the line of contact is:

$$F = F_p + F_s = \int_{x_{po}}^{x_{max}} \frac{p}{\cos\epsilon}\, dx + \int_{x_{po}}^{x_{max}} \frac{\tau(\lambda+\epsilon)}{\cos\epsilon}\, dx \qquad (71)$$

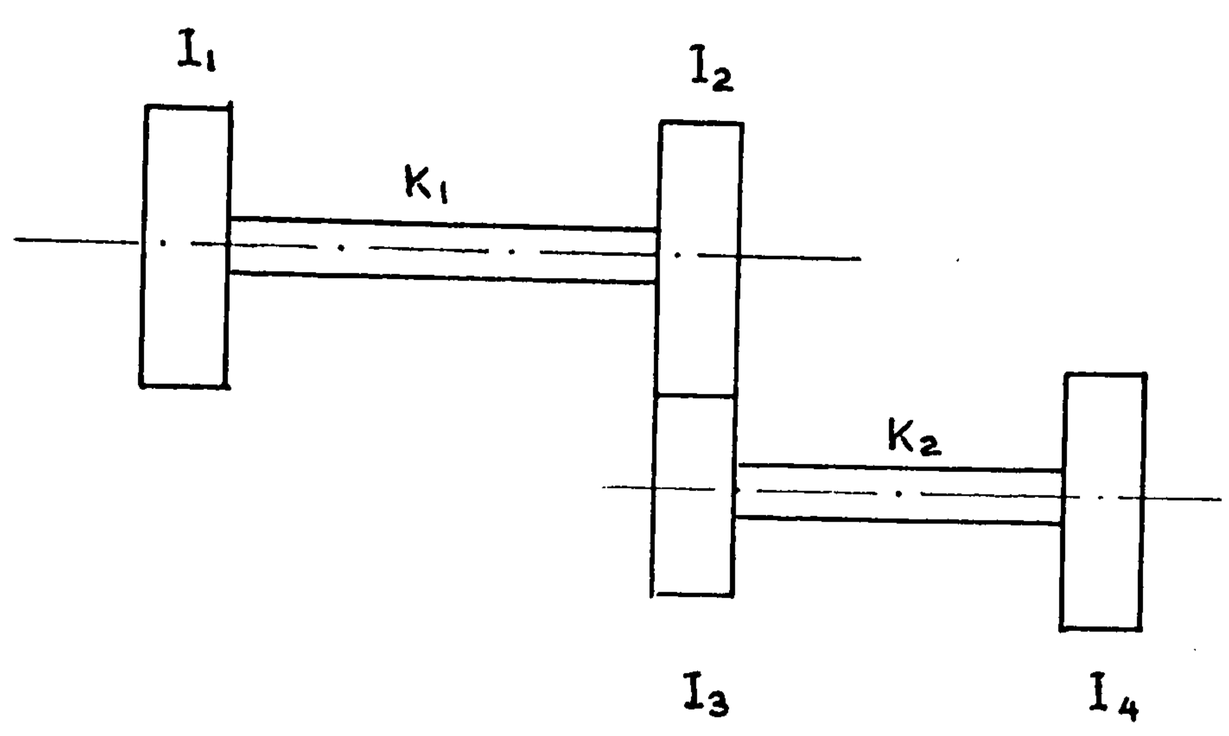

FIGURE 3.1

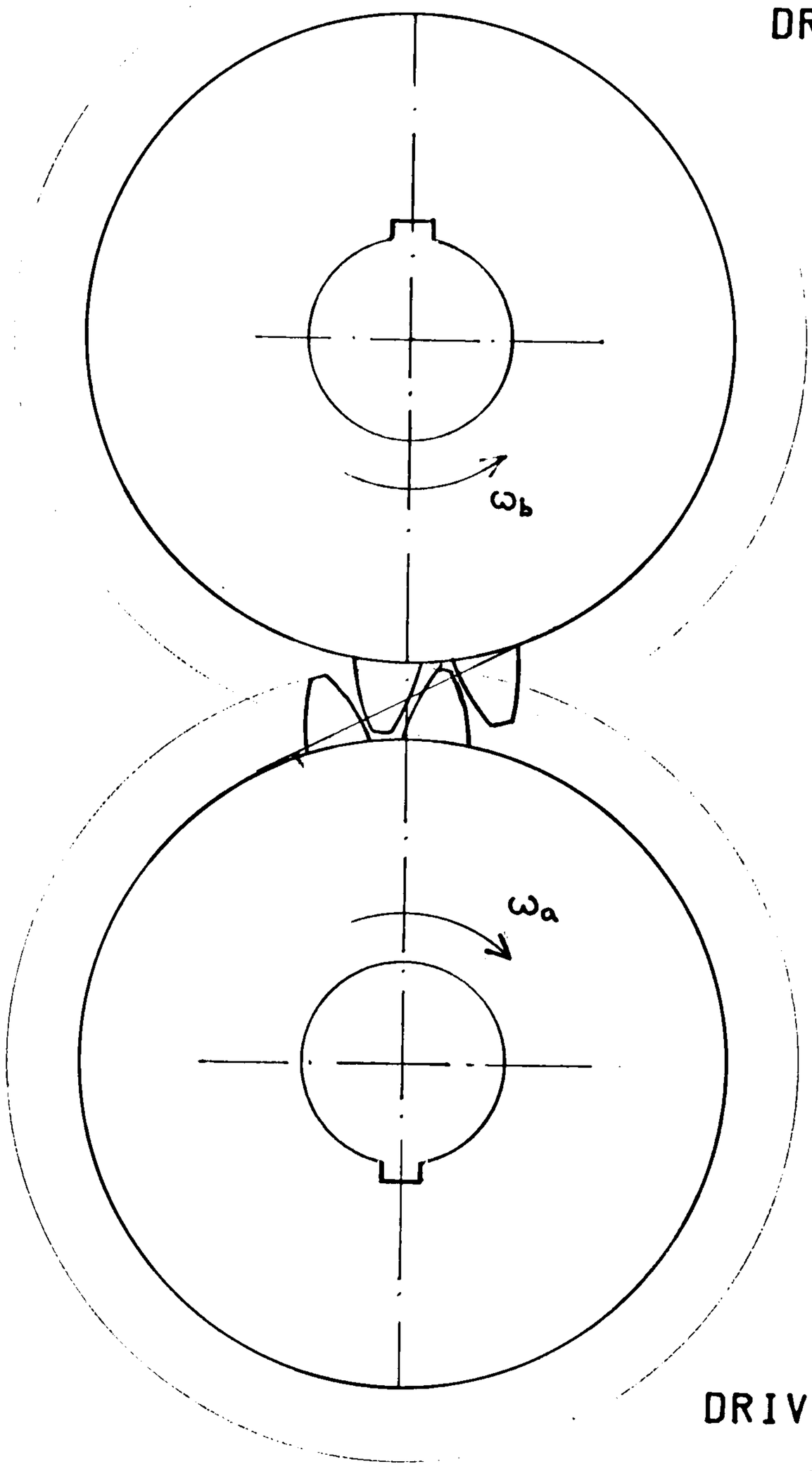

FIGURE 3.2

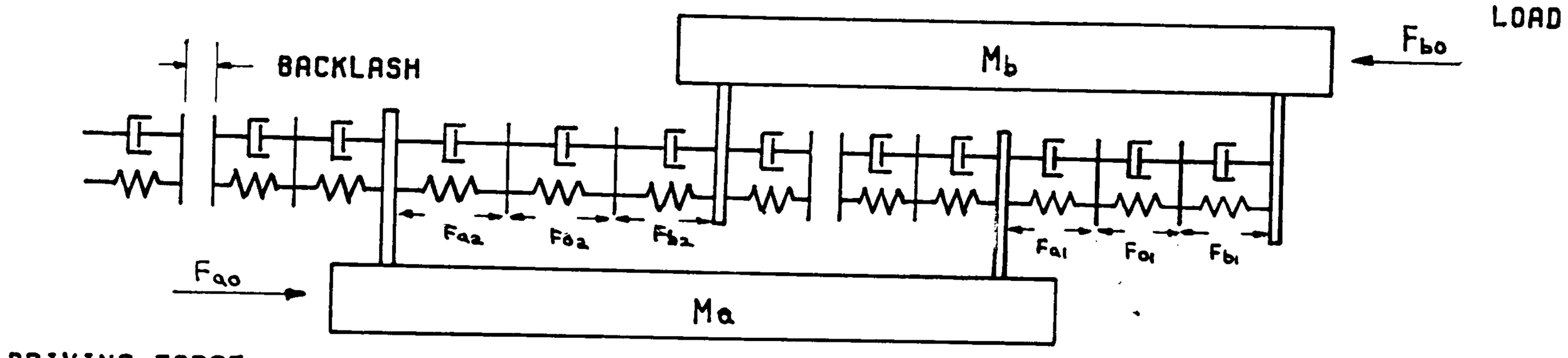
BACKLASH
M_b
F_{bo}
LOAD
F_{a2}
F_{o2}
F_{b2}
F_{a1}
F_{o1}
F_{b1}
F_{ao}
M_a
DRIVING FORCE

FIGURE 3.3

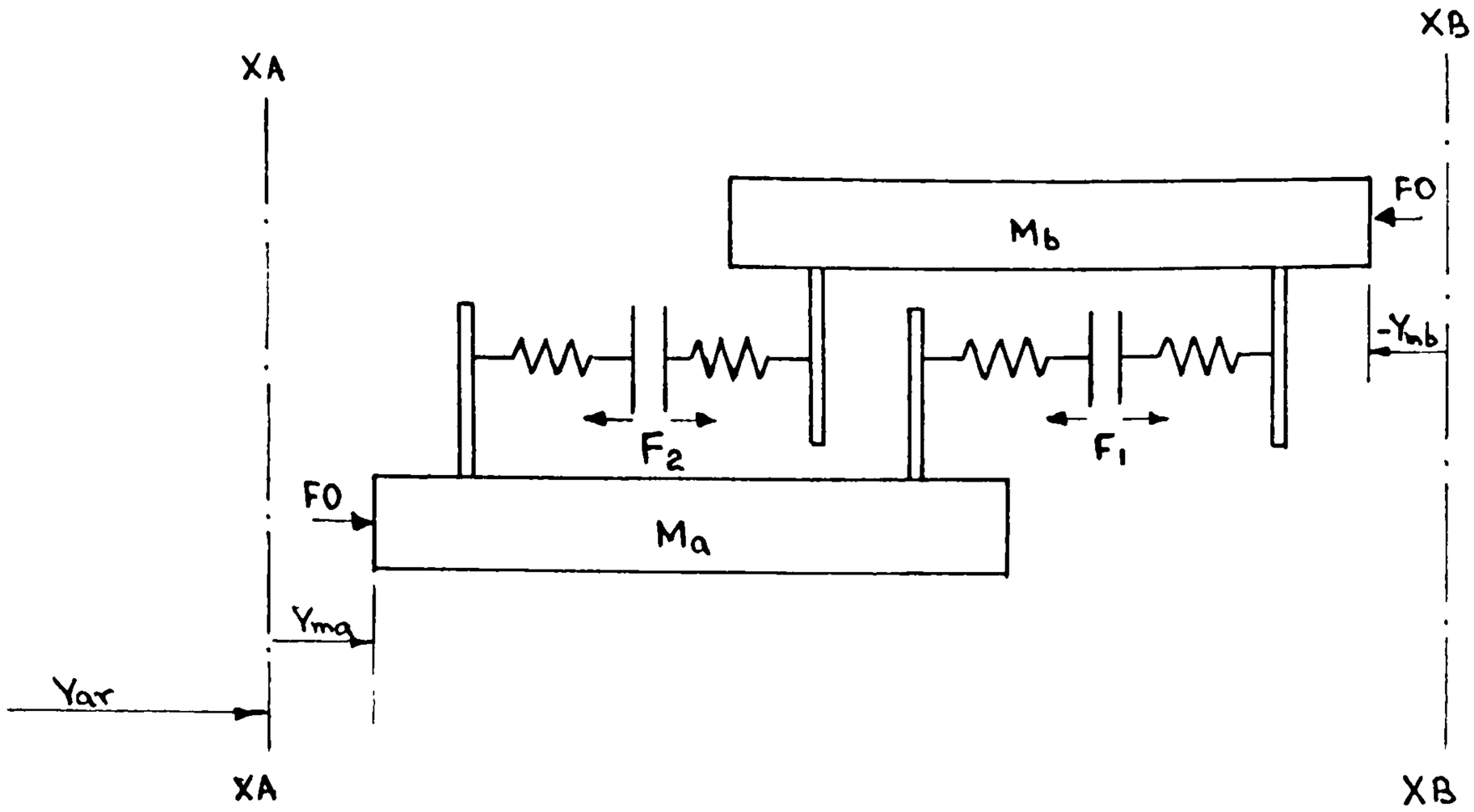

FIGURE 3.4

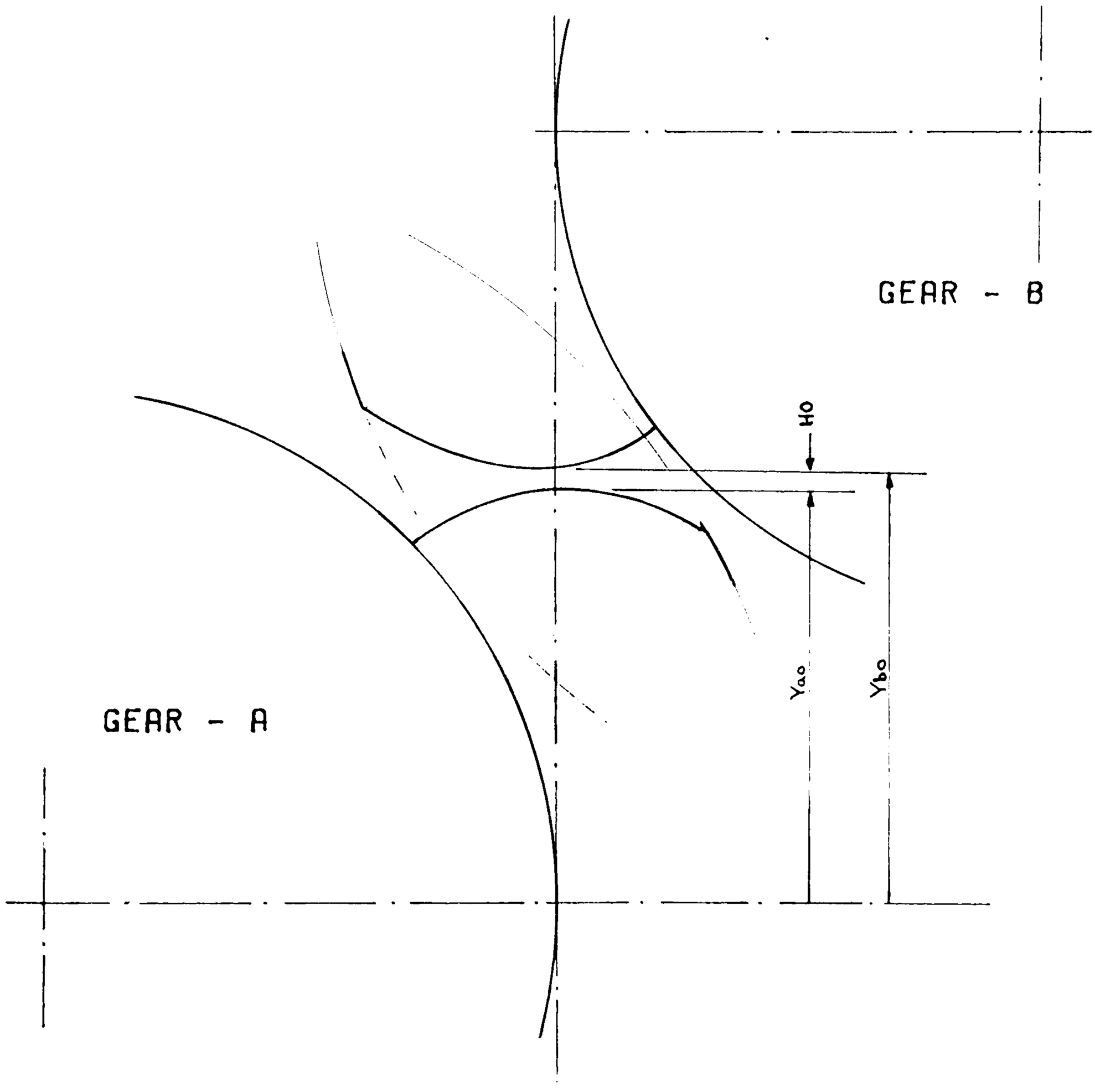

FIGURE 3.5

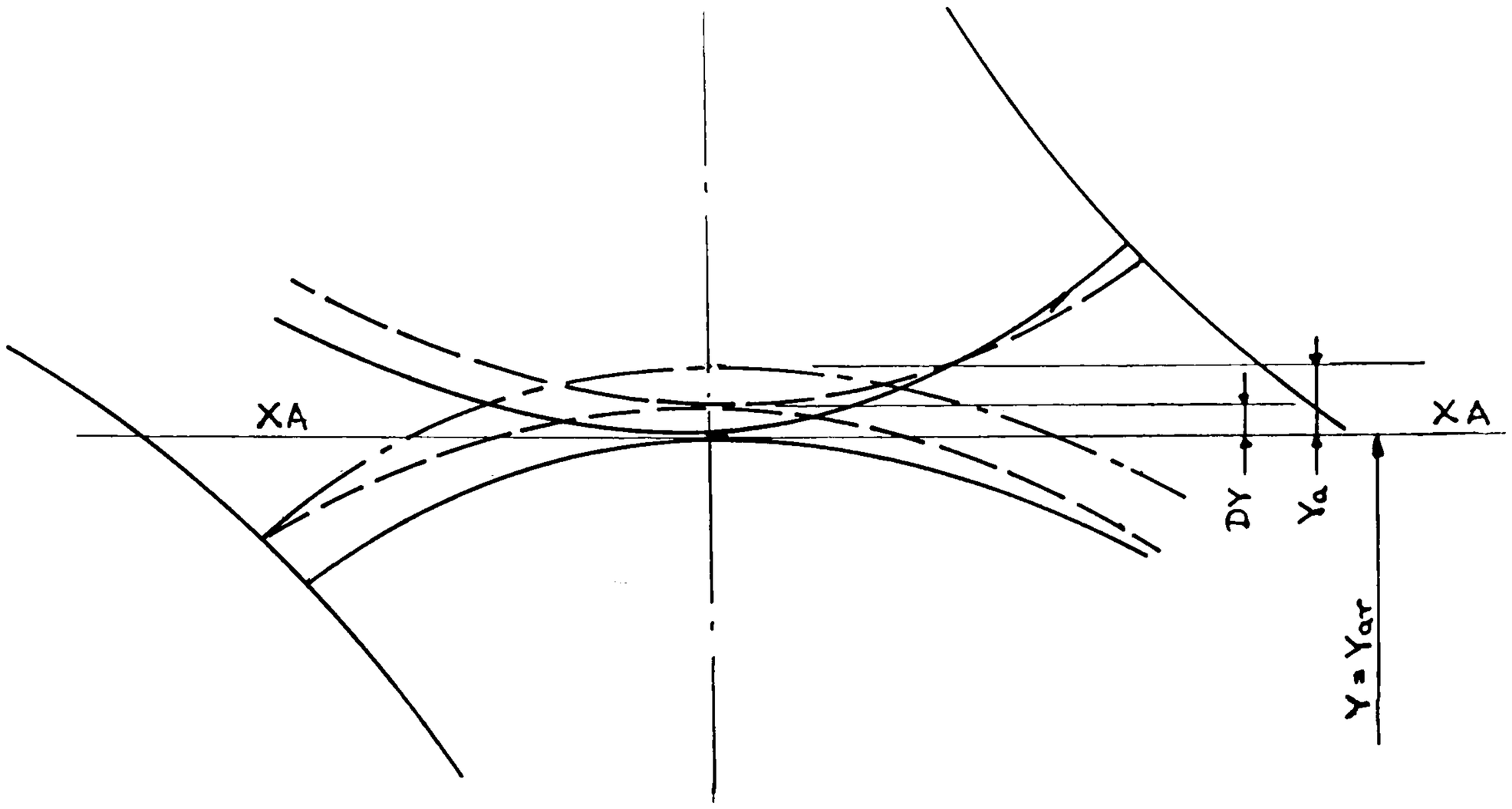

FIGURE 3.6

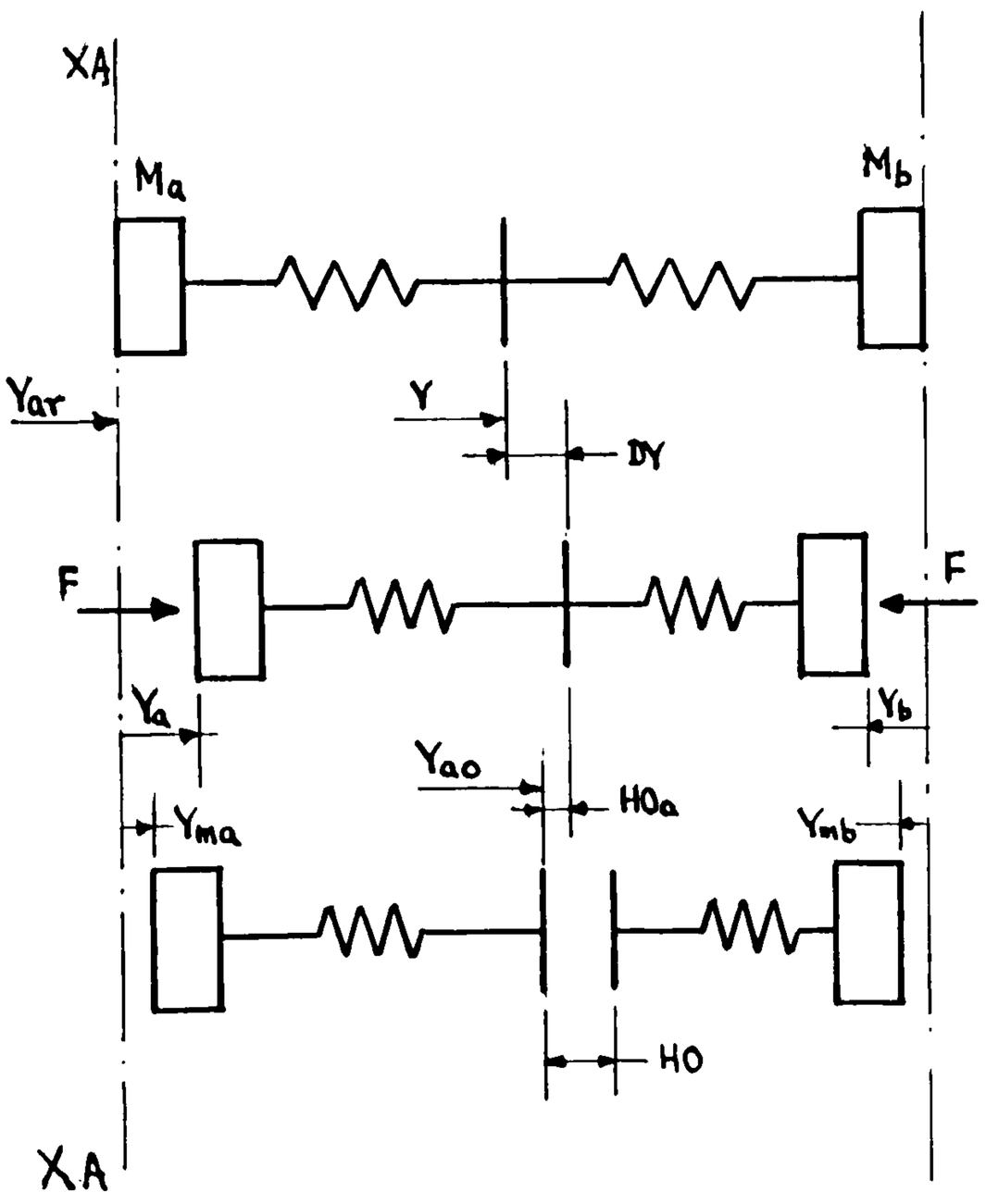

FIGURE 3.7

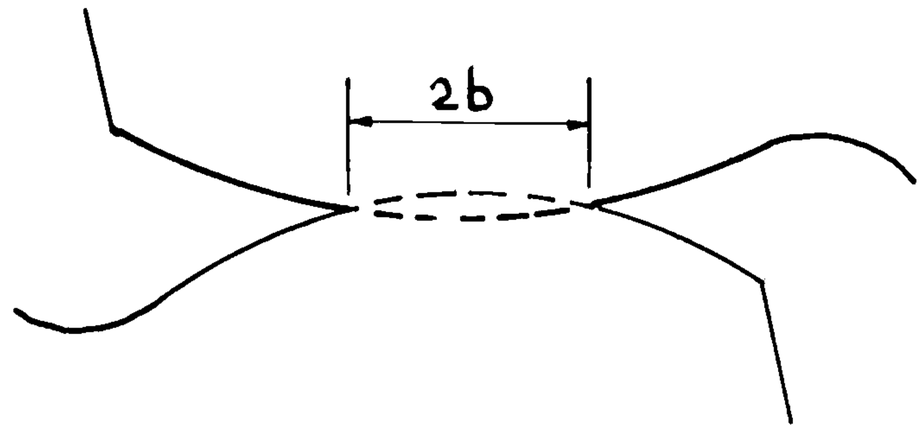

FIGURE 3.8

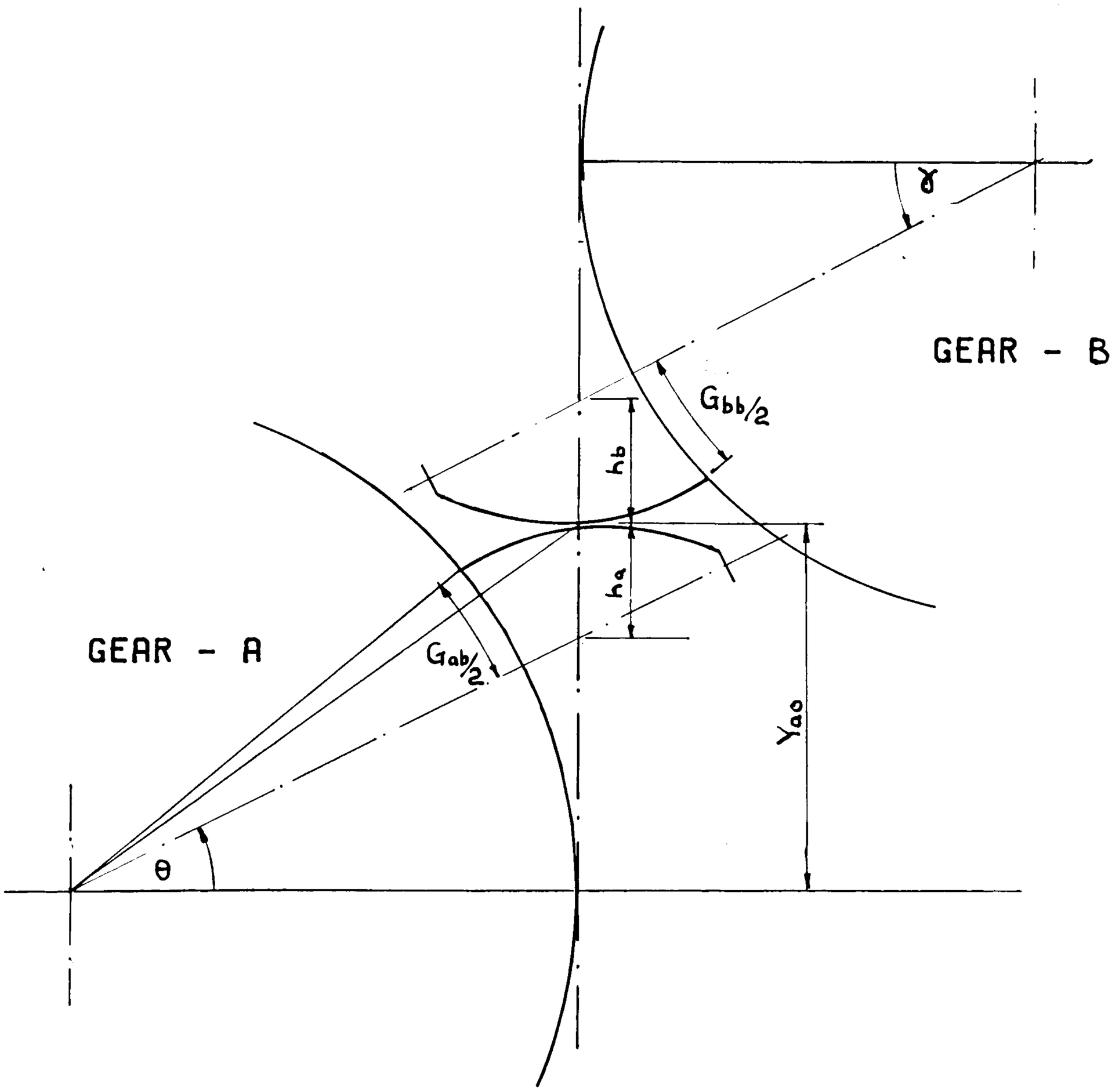

FIGURE 3.9

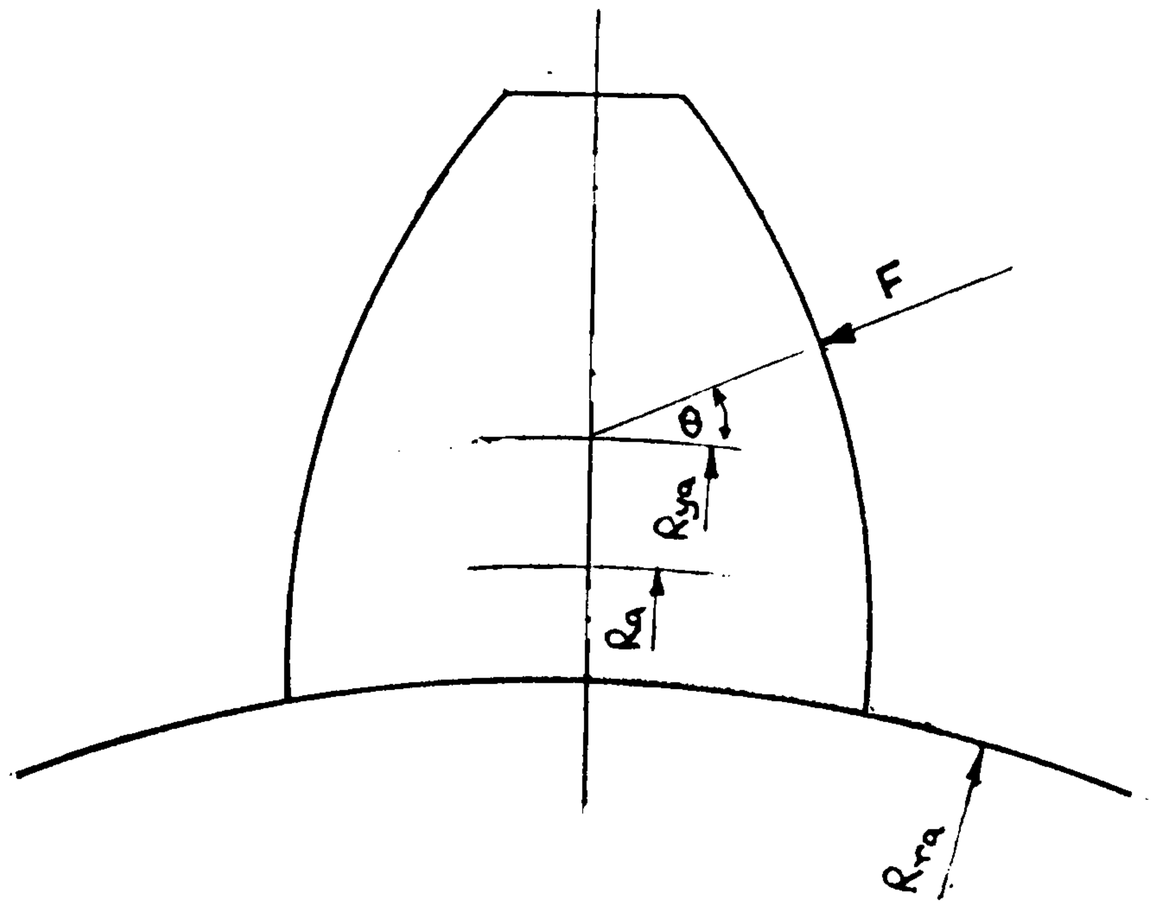

FIGURE 3.10

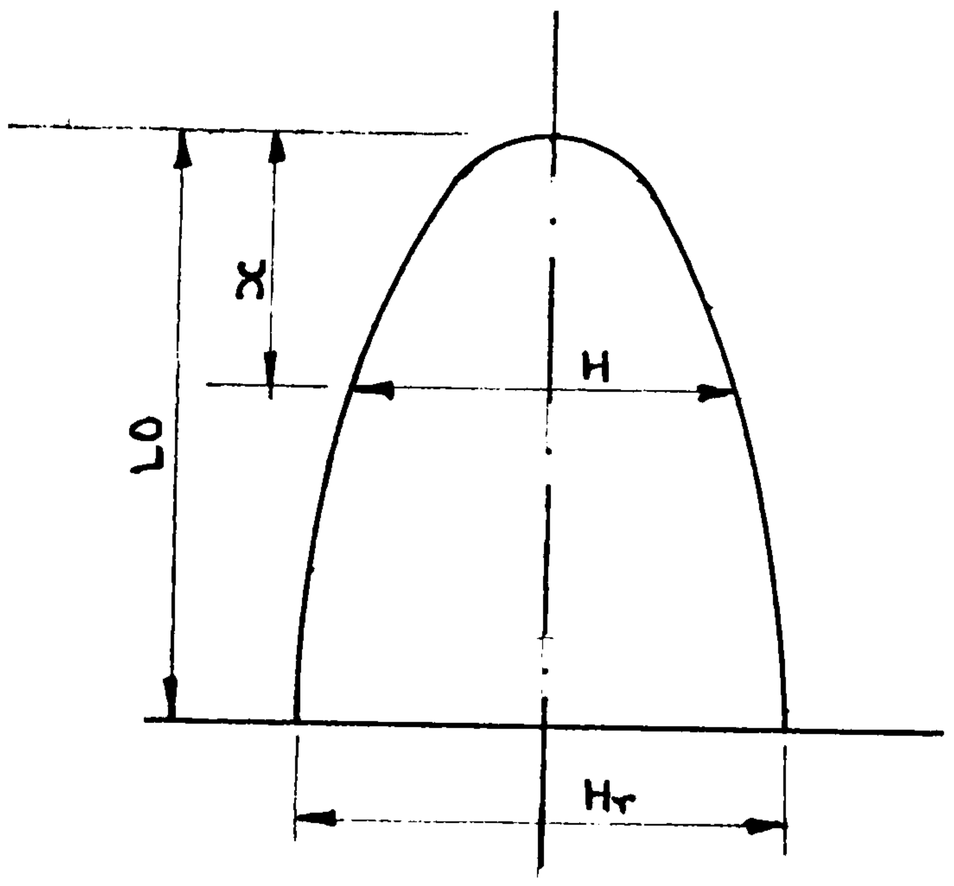

FIGURE 3.11

———— INVOLUTE TOOTH PROFILE

– – – – – – – ASSUMED TOOTH PROFILE

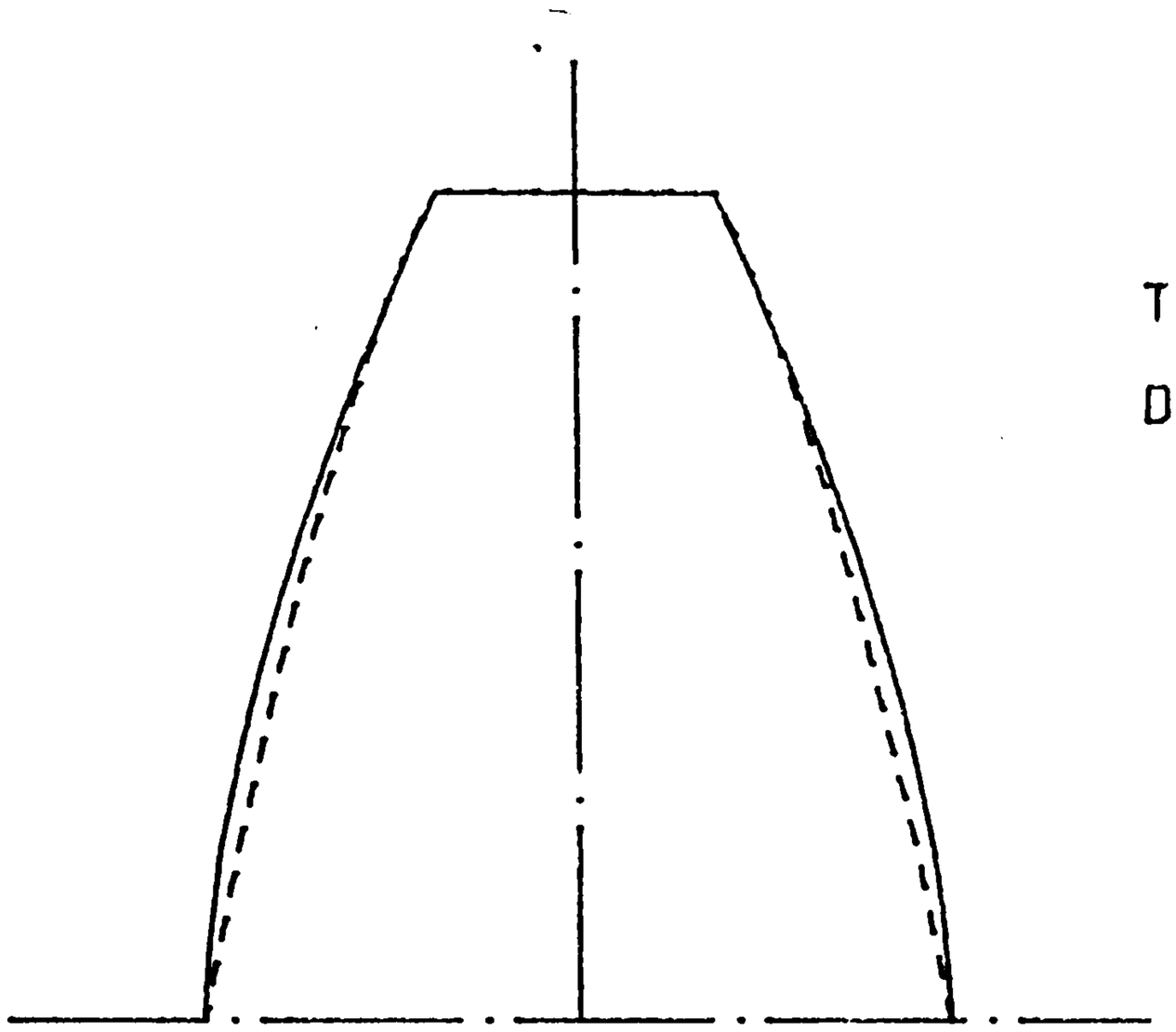

T = 42

DP = 16

FIGURE 3.12(a)

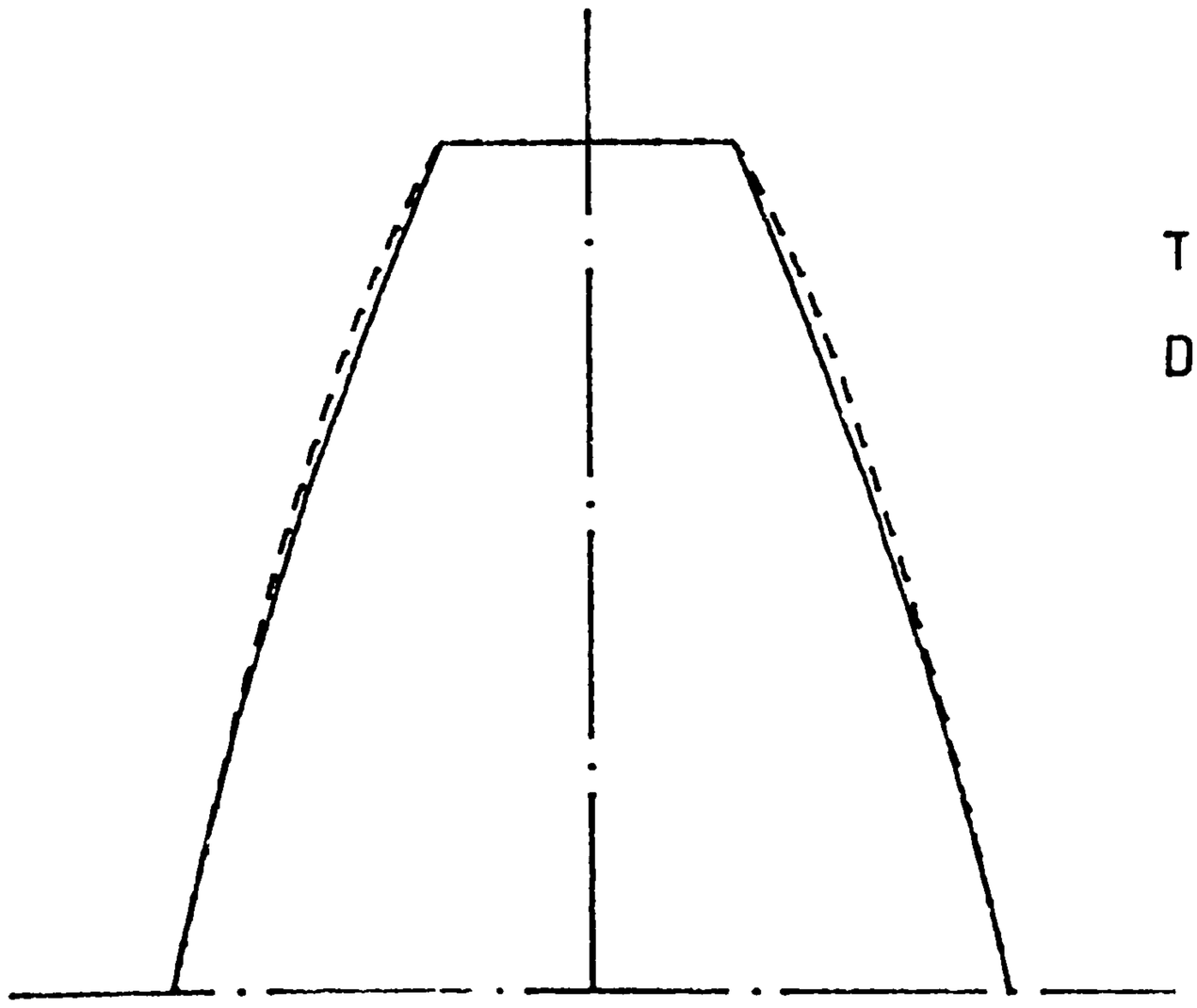

T = 73

DP = 16

FIGURE 3.12(b)

———— INVOLUTE TOOTH PROFILE

– – – – – – ASSUMED TOOTH PROFILE

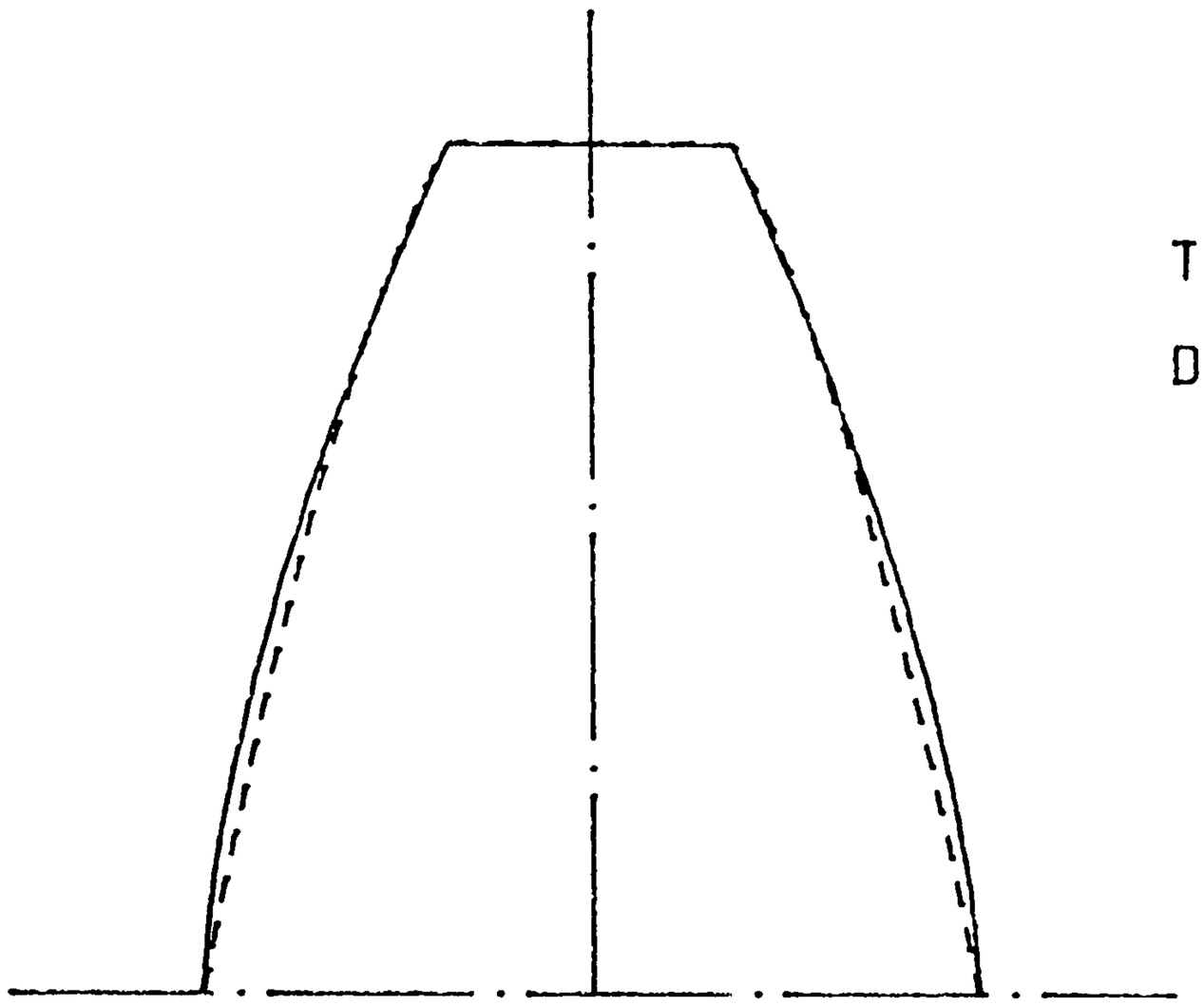

T = 45

DP = 8

FIGURE 3.12(c)

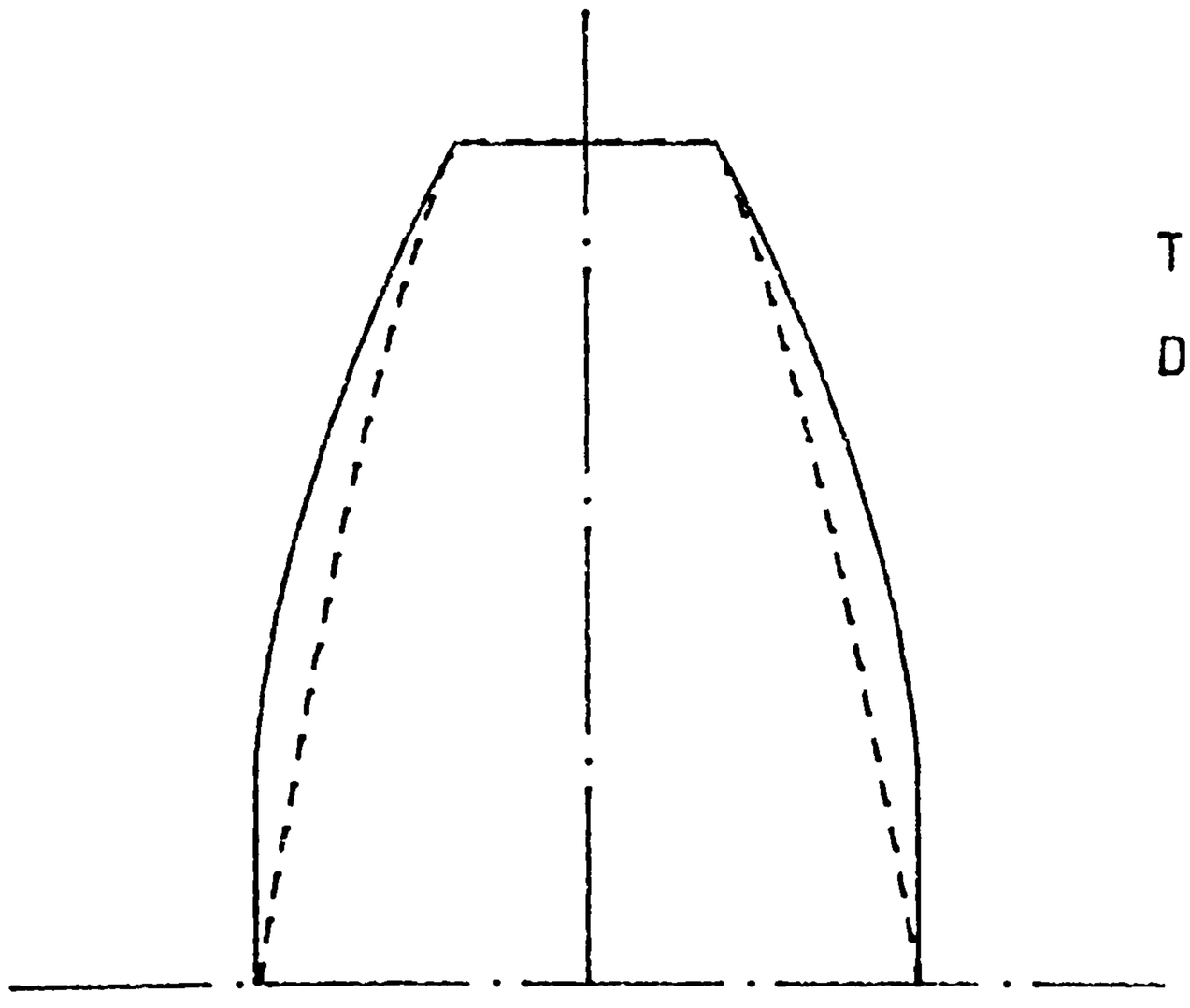

T = 25

DP = 8

FIGURE 3.12(d)

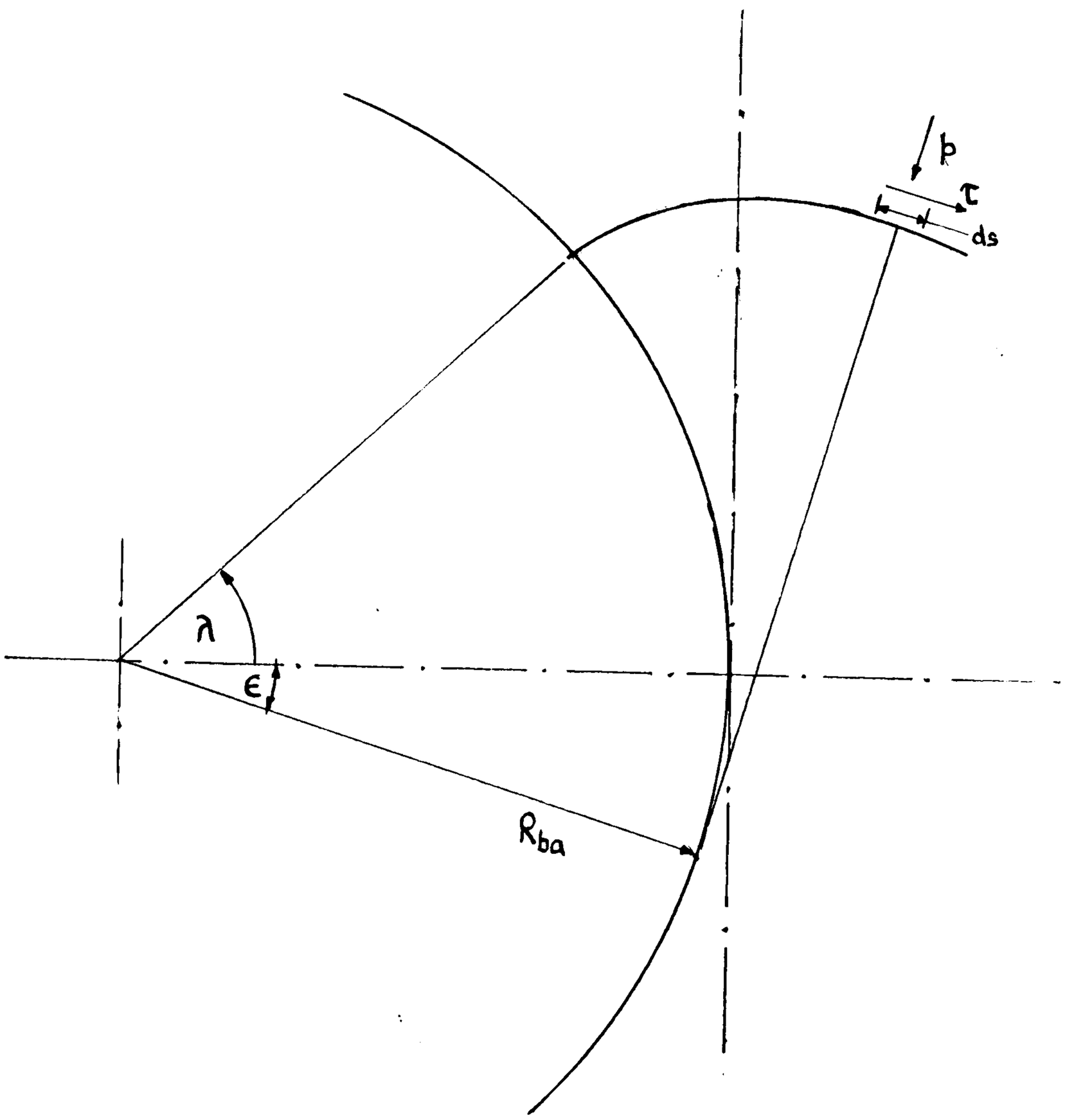

FIGURE 3.13

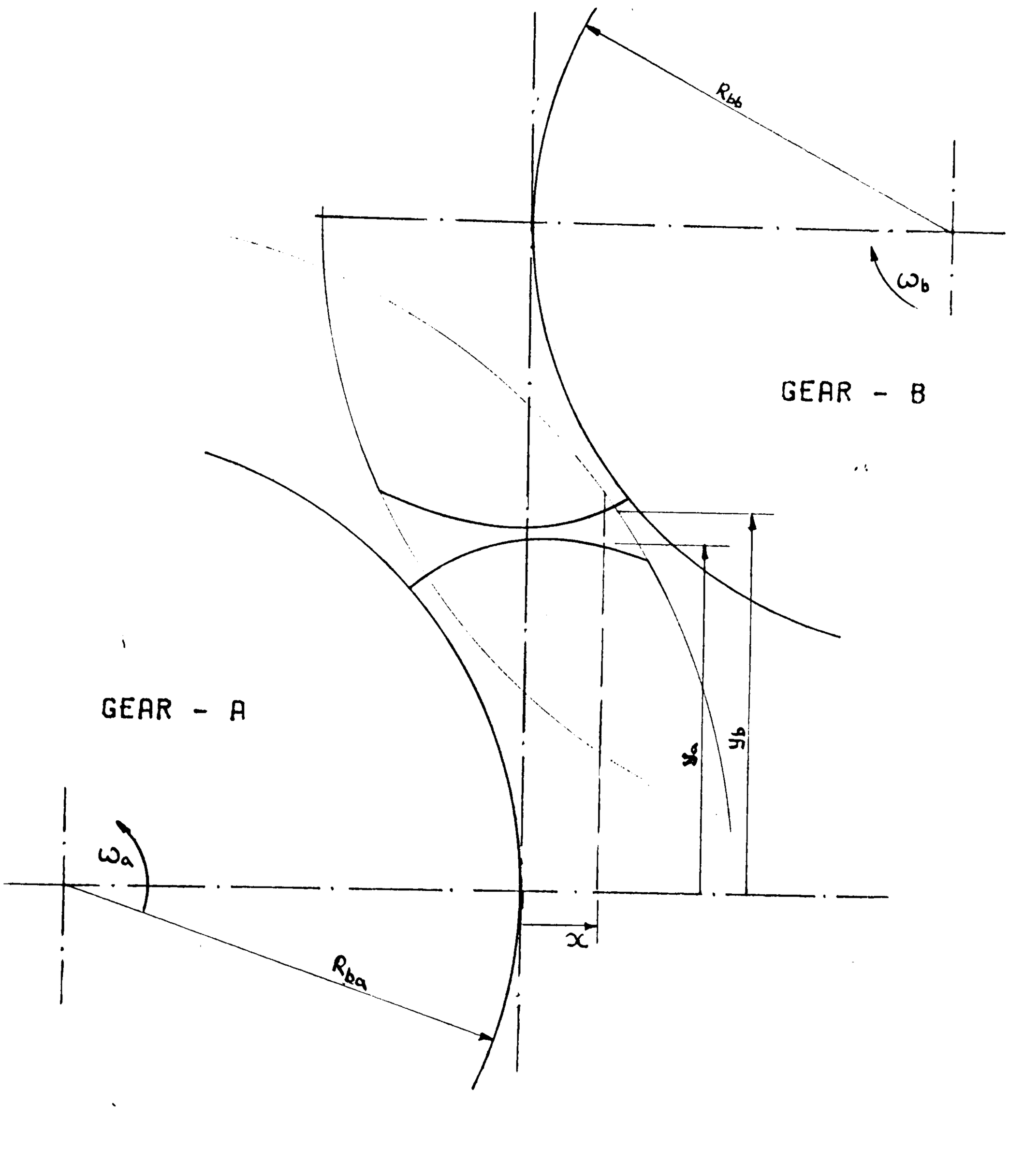

FIGURE 3.14

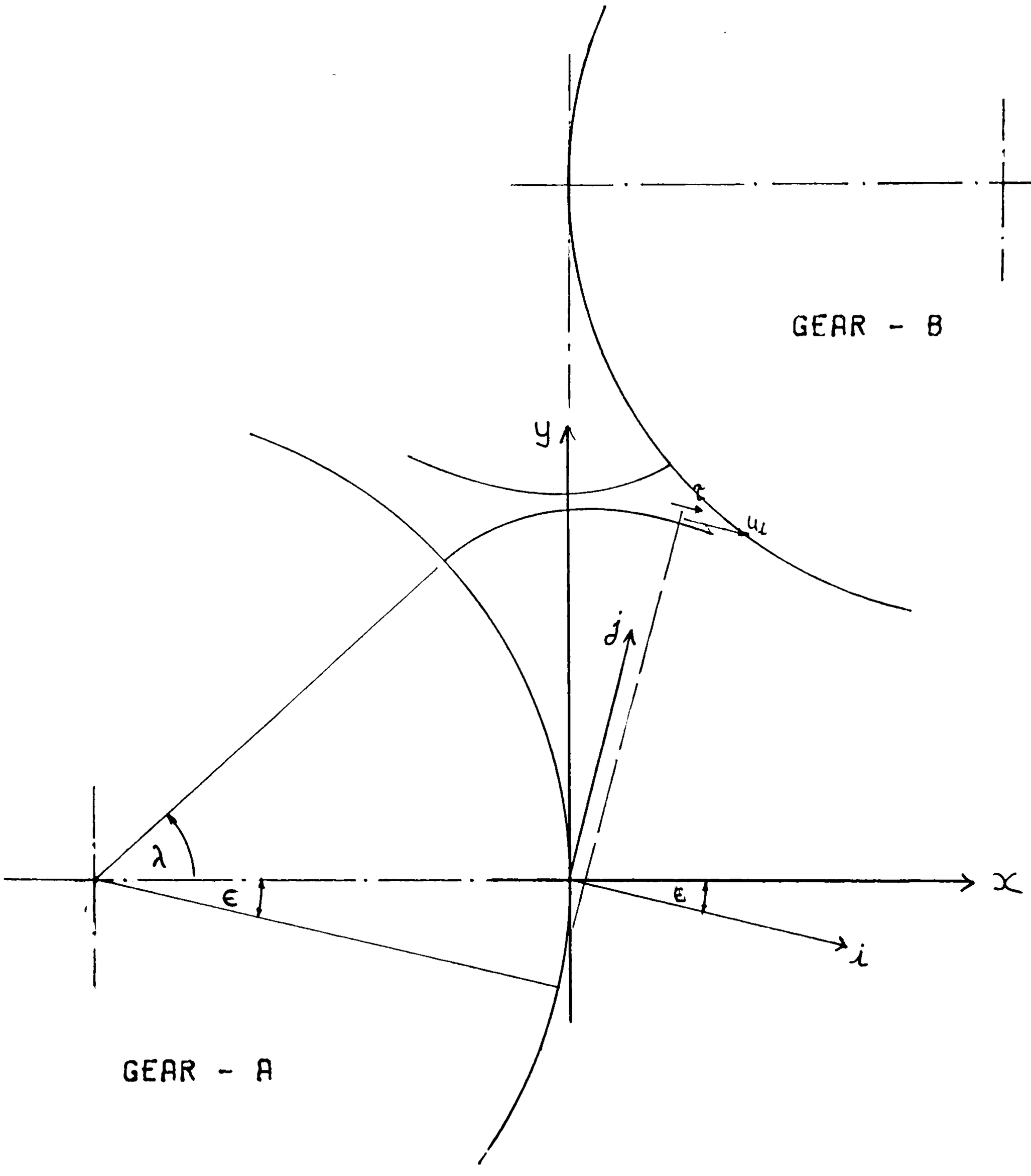

FIGURE 3.15

CHAPTER 4

DIGITAL COMPUTER ANALYSIS

The computer analysis of the model of the gear pair was divided into three main sections. They were the calculation of the minimum film thickness, analysis of the transient response characteristics of the oil film and the dynamic simulation of the pair of gears.

4.1. Minimum Oil Film Thickness

Minimum oil film thicknesses between gear teeth were calculated based on steady state operating conditions for a range of loads, speeds, oil viscosities and effective radii (Table 4.1 gives the values of the above variables used in the numerical calculations). To achieve a steady state, all the parameters involved were held constant at the values corresponding to those at the point of contact selected. The main assumption made was that the force due to the pressure of the oil and the shear force was equal to the external load applied.

Gear teeth were considered to be rigid in the calculation of the shape of the oil film. If very high tooth loads are involved then the effect of the deformation of the contact surfaces on the film shape and hence on the minimum thickness is considerable. Under such conditions to obtain a true equilibrium state both hydrodynamic and elastic deformation formulae need to be solved simultaneously. But for the low loads considered here it was thought that the effect of elastic deformation on minimum film thickness was not significant enough to warrant such an analysis.

The procedure used for the calculation of the oil film thickness for a given tooth load was as follows.

Initially an approximate minimum film thickness was assumed. The Grubin formula was used for this purpose.

Corresponding to this thickness the total force offered by the oil film was then calculated which required the integration of equation (71) numerically over its length. To carry this out the pressure distribution within the oil film had to be found first. To determine the pressure at any point within the oil film equation (63) had to be integrated between the limits x_{max} and the point at which it was required. Typical pressure distribution curves indicated that high pressures were concentrated on a small region close to the theoretical point of contact. Therefore it was thought that the pressure should be found at closer intervals in this area for more accuracy. Hence the length of the film from x_{po} to x_{max} was divided into three segments (a) from x_{po} to $5|x_{po}|$, (b) from $5|x_{po}|$ to $15|x_{po}|$ and (c) from $15|x_{po}|$ to x_{max}. Segment (a) was further divided into 120 equal lengths, (b) into 20 equal lengths and (c) into 10 equal lengths and pressures were calculated at each of these points of division by integrating equation (63).

But it was first required to determine the value of the constant C in equation (63). The remaining boundary conditions were utilised for this, which were:

$$p = 0 \quad \text{and} \quad \frac{\partial p}{\partial x} = 0 \qquad \text{and hence}$$

$$q = 0 \quad \text{and} \quad \frac{\partial q}{\partial x} = 0$$

at $x = x_{po}$ where cavitation was assumed to occur.

Using an assumed x_{po} first in equation (63) and the boundary condition $\partial q/\partial x = 0$ the corresponding value of C was obtained which was used again to integrate the same equation between the limits x_{max} and x_{po} to find the value of the reduced pressure at the assumed point x_{po}. If the assumption was correct then the integration should have yielded a zero pressure at this point. On the other hand, if the magnitude of the pressure was not below a specified limit, a new approximate for x_{po} was found using an interpolation process and the corresponding pressure calculated again. The cycle was repeated until a satisfactory solution was reached.

Once 'C' and 'x_{po}' were determined, the pressures at each point dividing the length of the film were found which were then used to integrate equation (71) numerically to yield the total force. This force was then compared with the applied force and if not within the set limit of 0.1% of it, a correction was made to the film thickness assumed initially and the whole process was repeated until the required accuracy was attained.

Figure 4 shows the flow chart of the calculation procedure used and the Fortran computer programme used is listed in Appendix III.

Some of the results obtained are presented in graphical form in Figures 4.1 to 4.4. The complete set of results showed that at low loads (relative to the values used here) the oil film thickness increased linearly with the speed, viscosity and the effective radius. This agrees with the earlier theories based on rigid teeth and isoviscous lubricating oil, such as those of Martin's (32) and McEwen's (34). The rate of increase of the film thickness with the above variables, however, tended to slow down with the increase of the load. Martin's and McEwen's formulae predicted very low film thicknesses at high loads, since they considered it to be inversely proportional to the load. The results of the analysis, however, showed that the dependence of the film thickness on the load, though high at very low loads, diminished rapidly with the increase of the load. This agrees well with the elasto-hydrodynamic theory which predicts the oil film thickness to be only slightly dependent on the load.

It has to be noted that the film thicknesses calculated here are for steady state conditions only. In a practical situation, in addition to the usual change of all the parameters as the gears rotate, there will be rapid fluctuations in the tooth load due to the vibration of the gears. If these fluctuations are high, so that the load reaches low values, they will produce corresponding variations in the film thickness as well, creating an additional force within the oil film due to the squeeze action. This will result in a higher film thickness in order to maintain dynamic equilibrium.

Damping at the tooth mesh is thought to be mainly due to this squeeze film effect. Hence, according to the results of the

analysis, which showed the film thickness to be very sensitive to the change in the load when the nominal load is low, high damping could be expected at these loads. When the load was high, film thickness was found to be almost independent of the load. This should result in very low damping forces at high loads.

4.2. Transient Response of the Oil Film

The main object of this test was to subject the mathematical model of the pair of gears discussed in the previous chapter to a transient response analysis in order to analyse its damping characteristics. By using a mathematical model the main problem in carrying out such an analysis experimentally, i.e. keeping the nominal values of the leading parameters constant, was avoided.

The mathematical model, while maintaining all the dynamic properties and characteristics of the pair of gears and the lubricating oil film, allowed us to study the behaviour of the system by changing one parameter at a time. In a practical situation it is not possible to achieve this, since the change in the point of contact as the gears rotate changes most of the parameters which govern the behaviour of the system, such as the mesh stiffness, effective radius of curvature at the point of contact, sliding and rolling speeds and nominal load on a single pair of teeth. This makes it impossible to study the influence of each of those parameters on the dynamic characteristics of the system; especially damping which is the focal point of our analysis here. But in the test using the model, the point of contact was held stationary, thereby keeping the nominal values of the above parameters constant. As far as the

lubricating oil was concerned, gear tooth surfaces were allowed to move at the chosen speed, though the radius of curvature of them were held constant corresponding to the values at the selected point of contact. This enabled a steady hydrodynamic oil film to be created subjected to a set of constant system parameters, which in a practical gear drive would have been only a momentary situation in a continuously varying process.

The procedure for the analysis was as follows:

- The equilibrium state was first established corresponding to the nominal values of the parameters, except the tooth load which was 1.1 times the nominal value, at the selected point of contact.

- The force was then reduced suddenly to the nominal value causing a step change in load.

- The subsequent transient motion of the gears was then obtained by solving the formulae related to the dynamics of the gears and the lubricating oil film simultaneously.

In establishing the initial equilibrium state the same process used to calculate the oil film thickness in the previous section was used. Once the equilibrium was disturbed the equation of motion (equation (23)) was integrated using a fourth-order Runge-Kutta formula to predict the new positions of the gear masses and their velocities. The methods of determination of the other relevant parameters will be described in the next section (dynamic simulation) which used the same procedures.

The basic structure of the computer programme used is illustrated in Figure 4.5 and the programme itself is listed in Appendix IV.

Since the level of excitation used was very small, the response of the system was very similar to that of a linear system. The small excitation level also helped to minimise the effect of the variation of the load on damping. For a linear, single degree of freedom system with viscous damping, the damping ratio can be expressed by the fomula:

$$\zeta \approx \frac{1}{2\pi j} \ln \left(\frac{x_{mi}}{x_{m(i+j)}}\right) \qquad (72)$$

x_{mi} - Maximum displacement of the equivalent mass, from the equilibrium position, in the ith cycle

$x_{m(i+j)}$ - Maximum displacement of the equivalent mass, from the equilibrium position, after j cycles from the above point.

The rate of decay of the displacement of the gear masses from the above tests were then used to calculate the equivalent damping ratio.

A 1:1 ratio spur gear pair with both gears having 45 teeth each was used in the mathematical analysis. The gears were assumed to be standard ones without any modifications and a pressure angle of 20^{o} was used in the calculations. The centre distance of the pair of gears was taken to be equal to the sum of the pitch circle radii of

the two gears. Gear teeth were considered to have perfect involute profiles and tip relief was not taken into account.

For the transient analysis of the pair of gears also, the values given in Table 4.1 for different parameters were used.

The tooth load is the component of the force on the gear tooth considered in a direction tangential to its base circle, which is also the line of action as well as the Y-axis of the co-ordinate system employed.

The lubricating oil viscosities given in the table are those at atmospheric pressure and at $30^{o}C$. The temperature of the oil at the entry to the gear mesh was taken as $90^{o}C$. Since the latter was more important, results were presented against the viscosity of the oil corresponding to $90^{o}C$ (and atmospheric pressure).

Mean speed (u) refers to the mean rolling speed of the two surfaces at the point of contact given by the equation:

$$u = \frac{1}{2}(u_a + u_b) \qquad (73)$$

where $u_a = y_{ao}\,\omega_a$

and $u_b = (C_d \sin\psi - y_{bo})\,\omega_b$

The effective radius of curvature of the contact surfaces was changed using two different methods:

(i) by varying the diametral pitch of the gears and

(ii) by changing the position of contact.

In the first method a large variation in the radius of curvature was obtained by having diametral pitches between 4 and 12 while the second method yielded the usual variation that occurs within one mesh cycle. In both cases the speed of rotation of the gears was adjusted according to the radius of curvature so that the mean rolling speed was kept constant. One noteworthy difference between the two methods was that when the diametral pitch was changed the sliding speed of the two surfaces remained unchanged (equal to zero since contact was assumed to take place at the pitch point) whereas when the position of contact was changed there was a corresponding change in the sliding speed too. Hence the numerical results obtained from this method include the effects of the change in sliding speed.

Gear motions were determined for a minimum of two complete cycles. This produced two values for the damping ratio. One when the maximum values of the cycles were used for x_i and x_{i+j} and one when the minimum values were used. The mean of the two was taken as the damping ratio corresponding to the values of the parameters used. At certain loads and speeds it was found that the damping ratios, calculated using the maximum displacements above the steady state value, were slightly different from those calculated using the displacements below the steady state value. This could be considered as an indication of the level of sensitivity of the damping ratio on load. Another reason for this could have been the

errors in the steady state position of the mass of gear 'A' used in calculating the damping ratio. This position was determined according to the deformation of the gears and the minimum thickness of the oil film between the gear teeth. It is very likely that the oil film thickness calculated at steady state was slightly different from (smaller than) the thickness that should have been when the gears were vibrating, since an additional damping force was present in the latter case. But generally, transient displacement of the gear masses plotted against time showed that they followed closely a sinusoidal pattern with exponential decay. This supported the initial assumption that the system was linear and the damping was viscous for the low excitation levels considered.

Figures 4.6 through 4.10 show a selected set of displacement patterns of the gear mass with time during the initial cycles following the step change in load.

Figure 4.6 shows the transient motion of the gears at different loads with the speed, viscosity and the radius of curvature held constant at 2.56 m/s, 0.0048 Ns/m^2 and 12.22 mm respectively. Since the step change in load at the start was taken as 10% of the nominal load, higher loads had a higher excitation level. This is the reason for larger amplitudes of vibration at higher loads. Apart from the amplitudes the frequency of vibration also shows an increase with the nominal load. There are two reasons for this: they are, the increase in the mesh stiffness and the decrease in the amount of damping with the increase in load. The high level of

damping at lower loads can also be seen from the rapid decrease in the maximum amplitude with time.

Transient vibration pattern of the gears at different speeds (Figure 4.7) shows an interesting feature of the system. Even though evidence of high damping can be seen at low speeds it was the lower speeds that produced higher natural frequencies. The inertia of the gears, mesh stiffness and the damping constant are the parameters that determine the natural frequency of vibration of the system. With the effective inertia remaining unchanged and damping forces helping to reduce the frequency, mesh stiffness was the only parameter that could have caused the frequency of vibration to increase with the decrease of the speed. The most probable reason that could account for this is the influence of the oil film on the mesh stiffness. It is possible that, as the speed was increased, the hydrodynamic oil film developed became stiffer and therefore more dependent on the load. This phenomenon can be seen more clearly in the film thickness against force graphs (Figure 4.1) which shows an increase in steepness of the above graphs as the speed increases. The amplitude of vibration also showed a marked difference at different speeds: it increased with the speed. The oil film can be considered responsible for this too, since at higher speeds the film thickness was also higher, which allowed a larger displacement of the mass to take place. The difference in the steady state position at different speeds is also due to this variation in the oil film thickness with speed.

Transient displacement at different viscosities (Figure 4.8) (force = 5.0 N/mm; speed = 2.56 m/s; radius = 12.22 mm) yielded a set of

curves representative of a perfectly linear, single degree of freedom system with viscous damping. The effect of increase of viscosity, and hence damping, is clearly demonstrated in these graphs. That is an exponential type decay in the maximum (and minimum) displacements in successive cycles. The rate of this decay in the amplitude increased with viscosity accompanied by a slight decrease in the frequency of vibration; both apparently due to the increase in damping.

Transient response curves at different diametral pitches (Figure 4.9), as expected, displayed a large variation in the frequency of vibration due to the variation in the inertia of the gears. Calculations based on the theory described in Chapter 3 showed that the mesh stiffness was almost independent of the diametral pitch, despite the fact that the size of the gear teeth increased with the decrease in the diametral pitch. In fact, the mesh stiffness showed a slight decrease with the decrease in the diametral pitch, but not large enough to influence the behaviour of the system. A slight increase in the mean position of the gears was also observed with the increase in the radius of curvature (decrease in the diametral pitch) as a result of the direct influence of the radius on the oil film thickness.

There was very little change in the transient response curves when the position of contact was varied (Figure 4.10). The frequency of vibration and the steady state position of the gears showed a slight increase with the radius. This variation, of course, has to be

compared with the change in the radius of curvature, which was also very small, at the different positions of contact.

Damping Ratio vs. Load (Figure 4.11)

As expected, damping ratio was found to increase with the reduction in the applied load. But this trend did not continue up to zero load. Instead, it reached a maximum at a load slightly above zero and started to decrease for lower loads. The load at which the maximum damping ratio occurred, as well as the value of this maximum value, were determined by the other parameters, mainly the speed and the viscosity. It was found that for a fixed viscosity, lower speeds (within the range used in the test) produced higher maximum damping ratios. The load at which this maximum damping ratio occurred increased with the speed.

Increasing the viscosity produced a corresponding increase in the damping ratio which was prominent at low loads at low speeds, and at higher loads at higher speeds. The load at which the maximum damping ratio occurred also increased slightly with the increase of the viscosity. At very high speeds and low loads it appeared that increasing the oil viscosity actually reduced the damping ratio. This is explicable, since at very low loads and high speeds the influence of the speed on the film thickness was more than that of the load, and increasing the oil viscosity further strengthened the influence of speed, thereby reducing the squeeze effect of the load.

When the speed and oil viscosity were constant, higher effective radii yielded higher damping ratios at high loads, while at low loads it produced the reverse result. The effect of the radius on

damping was found to be greater at low speeds than at high speeds. The maximum damping ratio for a particular speed and viscosity decreased with the increase of the radius accompanied by a slight increase in the load at which the maximum occurred.

Damping Ratio vs. Speed (Figure 4.12)

These graphs showed that damping was greatest when the speed and the load were both low. The damping ratio/speed relationship displayed the same trend at all loads, viscosities and radii, which consisted of an initial increase with speed, eventual reaching of a maximum value, followed by a gradual decrease with further increase in speed. At very high speeds damping ratio seemed to reach a constant value; at least the graphs at low loads indicated so. At high loads the graphs, in fact, still showed an increasing trend, apparently yet to reach their peak values.

The influence of other parameters on the damping ratio also could be seen clearly from these graphs. For a fixed load, increasing oil viscosity seemed to increase the damping ratio at all speeds (except at very high speeds and low loads when the relationship was different, as explained earlier), accompanied by a slight decrease in the speed at which the maximum damping ratio occurred.

The effect of load on the damping ratio/speed relationship was the greatest. The magnitude of the maximum value dropped sharply while the speed at which it occurred increased with the increase of the applied load.

The radius of curvature had only a negligible effect on this set of curves. In the few areas it did have some effect, the damping ratio increased slightly with the increase of the radius.

Damping Ratio vs. Viscosity (Figure 4.13)

Damping ratio was found to increase with the viscosity at almost all speeds and loads, as has already been observed from previous results. However, these graphs showed that the high damping ratios obtained when the speed and the load were low, rose to still higher values as the viscosity was increased.

The role of speed on damping ratio/viscosity relationship changed with load. At low loads lower speeds produced higher damping ratios, while at high loads higher speeds yielded higher damping ratios.

Increasing the load brought the damping ratio down at all viscosities with the greater effect shown near the low viscosity area.

Damping Ratio vs. Effective Radius of Curvature (Figure 4.14)

(i) Diametral pitch varied:

A linear relationship between damping ratio and radius was observed at most speeds and loads, though the change in damping ratio resulted was relatively small considering the large variation of the radius used in the test.

For constant speeds damping ratio decreased with the increase of the radius at very low loads and increased at high loads.

When the load was held constant, damping ratio decreased with the increase of the radius at high speeds and increased at slow speeds.

(ii) Position of contact varied:

A linear variation in damping ratio was observed when the radius was changed by changing the position of contact too. But in this case the damping ratio increased with the radius at all speeds and loads used in the analysis.

The above analysis of the variation of the damping ratio with the four parameters separately has indicated that the combined effect of them could prove to be very complex. The relationship between the damping ratio and any one of the variables was determined by the values of the rest of the variables.

On the other hand, it is not only the instantaneous values of the parameters that govern the characteristics of a dynamic system. The rates of change of them also have a certain amount of influence which is absent in this analysis. It is not possible to conduct this type of an analysis, i.e. observe the change in the system's behaviour with one parameter at a time, which includes the effect of the rates of changes of the parameters. When one considers a practical situation, apart from the tooth load, the other parameters (speed, viscosity and radius of curvature) undergo only slight variations during each mesh cycle. This means that the small rates of change of these parameters usually encountered in practice cannot be expected to affect the characteristics of the system very

much. The elimination of their influence from the analysis can hence be assumed to make only a negligible effect on the numerical solutions obtained.

Tooth load is the only parameter that suffers a large variation during the mesh cycle. The analysis allowed the variation in the load to take place even though it was limited to a small amount. Besides it is this variation in load which is mainly responsible for the variation in the thickness of the oil film and consequently the generation of the damping force.

One special feature that was noted was that when three of the four parameters concerned were fixed, there was a particular value of the fourth one (except the radius of curvature) which produced a maximum damping ratio. When the damping ratio was plotted against the load with speed, viscosity and the radius of curvature held constant, the normal pattern was a rapid rise initially which reached a maximum, and as the load was increased further the damping ratio decreased gradually. This type of variation in the damping ratio can be expressed by a formula of the form:

$$\zeta = Ae^{-B(C-F)^2} \qquad (74)$$

where A, B and C are functions of the other three parameters.

The effective radius of curvature did not prove to be critical in determining the value of the damping ratio. Thus, A, B and C in the above equation were considered to be functions of only the speed and

the viscosity. Approximate functions were then determined to suit the numerical solutions obtained previously. This resulted in the following:

$$A = 18.24 \frac{\mu_t}{u^{1.09}} + \ln \left[\frac{1.1193}{u^{0.027}}\right] \qquad (75)$$

$$B = \frac{0.1535}{u} \qquad (76)$$

$$C = 39.08\, u\, \mu_t + 57.0\, \mu_t + 1.15 \qquad (77)$$

4.3. Dynamic Simulation of the Pair of Gears

Numerical solutions obtained so far involved a fixed position of contact which enabled the dynamic behaviour of the gear system to be studied under steady conditions. In practice there are no such steady conditions during the mesh cycle of a pair of gears, since all the parameters vary continuously. This section of the analysis is primarily concerned with the development of a numerical solution to the dynamic tooth load variation in a pair of spur gears.

The same linear, two inertia, single degree of freedom model, representing a system consisting of only two gears of 45 teeth each and 8 diametral pitch, used in the previous analysis, was used here. But there was one basic difference between the two models. In the previously used one the role of the lubricating oil was represented using fundamental properties of hydrodynamic oil films. This resulted in a model as shown in Figure 4.15 where the characteristics of the oil film were governed entirely by the

conditions prevailing at the tooth surfaces (such as the force, rolling, sliding and normal speeds, and the shape of the oil film). The study of the above model enabled an empirical formula to be developed to express the instantaneous damping force offered by the oil film in terms of the relative velocities of the two gear masses. When the damping force at the mesh is expressed this way, the analytical model takes the form as shown in Figure 4.16. The equation of motion for this system can then be written as:

$$M_a \frac{d^2(Y_{ma})}{dt^2} = -KO\,(Y_{ma} - Y_{mb} + HO) - C\left[\frac{d(Y_{ma})}{dt} - \frac{d(Y_{mb})}{dt}\right] + FO \qquad (78)$$

$$\text{and} \quad M_b \frac{d^2(Y_{mb})}{dt^2} = -KO\,(Y_{mb} - Y_{ma} - HO) - C\left[\frac{d(Y_{mb})}{dt} - \frac{d(Y_{ma})}{dt}\right] - FO \qquad (79)$$

which could eventually be reduced to:

$$\frac{d^2(Y_{ma})}{dt^2} = -\frac{C}{M_{eq}}\frac{d(Y_{ma})}{dt} - \frac{KO}{M_{eq}}Y_{ma} - \frac{KO}{M_a}HO + \frac{FO}{M_a} \qquad (80)$$

where $M_{eq} = \dfrac{M_a M_b}{(M_a + M_b)}$

When two pairs of teeth are in contact the above equation could be written as:

$$\frac{d^2(Y_{ma})}{dt^2} = - \frac{(C_1 + C_2)}{M_{eq}} \frac{d(Y_{ma})}{dt} - \frac{(KO_1 + KO_2)}{M_{eq}} Y_{ma}$$

$$- \frac{KO_1}{M_a} (HO_1 - PE_{a1} + PE_{b1}) - \frac{KO_2}{M_a} (HO_2 - PE_{a2} + PE_{b2}) + \frac{FO}{M_a} \quad (81)$$

C_1 and C_2 the damping constants of the two pairs of teeth are calculated as follows:

Generally the damping constant can be written as:

$$C = \zeta C_{cr} \quad (82)$$

where C_{cr} = Critical damping constant

For a single degree of freedom system

$$C_{cr} = 2\sqrt{KM} \quad (83)$$

K - stiffness

M - inertia

When there are two pairs of teeth in mesh the total inertia of the system is divided between the two pairs. For the purpose of calculating the damping ratio, the effective inertias on each pair of teeth in contact were calculated using the following equations:

$$M_{ei} = M_{eq} \frac{KO_i}{K_{eq}} \qquad (84)$$

$i = 1,2,...$ - number of the pair of teeth considered

$K_{eq} = KO_i + KO_{(i\mp1)}$ - the equivalent mesh stiffness.

This is based on the assumption that the kinetic energy of the whole system can be divided between the two pairs of teeth according to the proportion of the stress energies each pair is capable of storing for the same amount of deformation.

ζ - the instantaneous damping ratio was calculated separately for each pair of teeth according to equation (74)

Although an empirical formula could have been developed based on the steady state results obtained to predict the oil film thickness under dynamic conditions, this was left out in favour of the Grubin formula. Even though the film thicknesses it predicted at low loads were too small, the Grubin formula was expected to give more accurate film thicknesses at high loads. This did not affect the analysis to any significant extent, since the damping ratio was calculated independently based on the operating conditions at the tooth mesh, while the minimum film thickness that mattered most was that at high load which the Grubin formula predicted more accurately.

A digital simulation programme in Fortran was written to obtain simultaneous solutions to the equation of motion, the elastic

deformation and the oil film thickness formulae (flow chart, Figure 4.17, and a listing of the programme in Appendix V). A fourth-order Runge-Kutta formula was used to integrate the equation of motion and the integration interval was automatically selected to ensure that there were at least 250 steps in one mesh cycle in order to obtain the desired level of accuracy.

The first pair of teeth was assumed to be at the pitch point at the start of the simulation programme, and stable equilibrium conditions were assumed with the tooth load equal to that corresponding to the applied torque. Taking the pitch point as the starting point also made certain that only one pair of teeth was in contact which made the calculation of the initial conditions slightly simpler.

The initial excitation of the system occurred when the second pair of teeth came into mesh. The smooth rotation of the gears was disturbed due to the deformation of the gear teeth already in mesh under the imposed load, which resulted in a change in the relative pitch of the gears. Provision was made to incorporate a further pitch error to represent manufacturing errors. Similar excitations occurred when subsequent pairs of teeth came into mesh and also when teeth already in mesh moved out. These were also accompanied by corresponding variations in the mesh stiffness which added a further disturbance to the system.

As far as determining the position of contact was concerned, gear tooth faces were assumed to have perfect involute profiles even under load, so that contact always took place along the line tangent

to the base circles of the gears, which is generally referred to as the line of action.

When 'full contact' occurred, i.e. when the positions of contact of the pairs of teeth in mesh were within the theoretical limits (starting and ending) of the line of action, mesh stiffnesses were calculated separately according to the formulae described in Chapter 3. Since the mesh stiffness itself was dependent on the load, an iteration process was incorporated into the programme to ensure that the difference between the forces used in calculating the mesh stiffnesses and the resulting forces were within the required limit, which was taken as 0.1% of the tooth load corresponding to the applied torque. This whole process was within another iteration routine which ensured that the forces calculated in the above process agreed with the forces supported by the respective lubricating oil films.

When gear teeth come into mesh prematurely as a result of pitch errors, either due to the deformation of teeth under load, or due to manufacturing errors, contact occurs away from the line of action. The oil film between the teeth of the incoming pair causes this to take place even earlier and further away from the theoretical line. It is not possible to use the normal method to calculate the mesh stiffness and the thickness of the oil film, since the full involute profile of the gear teeth are not involved. An approximate method was used to calculate the above two variables. This assumed the involute profiles of the gear teeth to extend without any limit and the mesh stiffness was calculated based on the dimensions of the gear teeth at the corresponding positions along the line of action.

The minimum distance between the two teeth coming into contact, calculated using their true positions and dimensions, was used as the effective minimum thickness of the oil film, while the normal equation (Grubin formula with the force written as a function of the other variables) was used to calculate the force supported by it.

There was a basic difference between this procedure and that used for full contact. When full contact took place the tooth mesh stiffness, deflection and force were found using the iteration process mentioned earlier, and the oil film thickness calculated according to this force using the Grubin formula; whereas when 'partial contact' took place the mesh force was first calculated using the transposed form of the Grubin formula and, corresponding to this force, the mesh stiffness and deflection were determined, which was a straightforward calculation.

A similar procedure was adopted to calculate mesh stiffnesses, oil film thicknesses and forces when a pair of teeth was about to move out of mesh. Here, too, 'partial contact' was assumed to take place when the actual point of contact has moved past the theoretical end point of contact.

The simulation process was allowed to continue uninterrupted by equating the values of all the parameters pertaining to the third pair of teeth to those of the first pair of teeth. This was done at the point the second pair of teeth completes its mesh cycle, thereby re-starting the whole cycle again. It was found that generally after two cycles all the influences of the transient effects

diminished, and a near steady state was reached when there were no pitch errors. Hence, data were collected during the third cycle, and when pitch errors were to be introduced this was done when the second pair of teeth came into mesh in the third cycle.

Table 4.2 gives some of the data used in the dynamic simulation test. The same pair of gears modelled in the oil film thickness and the transient response analyses were used as the basic test gear pair. Initially the programme was run at speeds ranging from 1000 rpm to 6000 rpm at increments of 200 rpm. The maximum dynamic load and the load on a single pair of teeth during one complete mesh cycle was recorded at each speed.

Figures 4.18 to 4.21 show some of the graphs of the variation of the maximum total load and the maximum individual tooth load with speed. The forces are represented in non-dimensional form by dividing them from the nominal load. Hence the maximum dynamic load graphs can also be read as dynamic factor/speed graphs.

All graphs show high dynamic factors at resonance speed. When there were no pitch errors, dynamic factors around 4-5 were predicted. Minor resonances with dynamic factors around 2.5 were predicted at one-half the above speed. At speeds away from resonance the dynamic factor was generally around 1.8.

The programme was run with different contact ratios which was achieved by varying the centre distance between the two gears. These graphs (Figure 4.18) showed that there is a particular contact ratio that produced the maximum dynamic load at resonance.

For the pair of gears used in the analysis it was found to be about 1.4. But dynamic loads at other speeds with different contact ratios did not show any significant difference. Higher contact ratios produced higher resonance frequencies since at high contact ratios two pairs of teeth are in mesh for a longer time. But this difference in the resonance frequencies was not significant at lower contact ratios. For example, at 4000.0 Nm/m load torque and 0.15 Ns/m^2 oil viscosity, the resonance frequencies for contact ratios 1.2 to 1.4 were almost equal. High dynamic factors were predicted even when the speed was well above resonance, especially when the contact ratio was high.

Individual tooth loads, too, showed a similar pattern to the total load curves with the maximum load at resonance reaching about 2.0 to 2.5 times the nominal load. But the highest individual tooth loads seemed to occur at speeds slightly less than those at which the corresponding maximum total loads occurred.

Computer results at different loads (Figure 4.19), as expected, predicted resonance frequencies that increased with the load. The above increase was more distinct at higher contact ratios. The magnitude of the dynamic factor at resonance did not seem to depend on the applied load. Even the ratio of the maximum individual tooth load to the nominal load was nearly equal at different loads. The system tended to become unstable at low speeds, at about 1/4 of the resonance speed, when the load was very high.

At relatively high speeds lower oil viscosities resulted in only slightly higher maximum loads (both total and individual) even at resonance. But at slow speeds, low viscosities produced unstable regions at moderate loads also similar to those predicted for high loads at higher viscosities. This could thus be considered as a result of insufficient damping as well as the decreasing trend of the damping force with decrease of load. The low film thickness which allows the load to change rapidly for very slight variations in film thickness might also have contributed to the creation of the unsteady state.

In practice, such unstable situations - where the maximum load continues to increase up to extremely high levels - do not arise. The limited backlash clearance does not allow the harmonic motion of the gears to continue freely. Although this interrrupted cycle could again have its own resonance frequency, the maximum dynamic load will be restricted due to the discontinuities in the cycle. In addition to this, there will be an additional damping force due to the oil film between the non-load carrying faces of the gear teeth when reverse contact occurs. When these faces come into contact this damping force, and the discontinuity mentioned, not only prevent instabilities in the system but they will also reduce the maximum dynamic load at other speeds too, especially at resonance where it was found that teeth lose contact.

Inclusion of a pitch error in one of the gears seemed to generate higher dynamic loads at all operating conditions when compared with the corresponding dynamic loads without pitch errors (Figure 4.21). Apart from this higher dynamic load, pitch errors did not cause any

additional instabilities in the system. The increase in the dynamic load with pitch error appeared to be more when the contact ratio was high. It may be that at lower contact ratios the period over which two pairs of teeth are in mesh is smaller, and hence the influence of the pitch error is less, although it can be argued that the greatest effect of the pitch error occurs at the beginning when a new pair of teeth comes into contact, hence the value of the actual contact ratio is of very little consequence. It has to be remembered that the tooth deflections which caused the dynamic loads when there were no pitch errors, were in fact functioning as pitch errors, though as a function of dynamic load itself, at least at the beginning of contact. Hence the purposely introduced errors were merely increasing the effective pitch error.

Variation of the dynamic load and individual tooth loads over the mesh cycle (Figure 4.22) showed that loss of contact was inevitable when the speed was near the resonance speed. At and above resonance maximum tooth load was recorded at the beginning of contact, whereas at speeds below resonance the maximum tooth load occurred near the pitch point. This suggests that at high speeds the major tooth load is caused by the initial impact due to the premature contact of the gear teeth, whereas at slower speeds the sudden change in mesh stiffness as one pair of teeth leaves contact, is responsible for the maximum tooth load.

Tooth mesh stiffness increased with load as expected, and at the same time the contact ratio was also found to increase significantly since tooth deflections caused the incoming pair of teeth to engage

earlier. It can be said that these two factors jointly contributed to the increase in the natural frequency of the pair of gears with load.

The variation of mesh stiffness as a result of the change in the position of contact when the gears rotated did not prove to be significant, whereas the amount it varied with the fluctuating load was greater, especially at high loads when the total fluctuation was very high.

The minimum film thickness was calculated using the Grubin formula, and hence produced the expected results. That is, it showed a general increase with the increase of speed and a slight variation with the load, thereby yielding the smallest film thickness at the point the load is highest.

TABLE 4.1

	VARIABLE	1	2	3	4	5
A	Tooth load (N/mm)	2.5	5.0	10.0	15.0	20.0
B	Mean speed (m/sec)	1.28	2.56	5.12	7.67	10.23
C	Diametral pitch	4	6	8	10	12
D	Viscosity of oil at atmospheric conditions (Ns/m^2)	0.04	0.075	0.10	0.125	0.15
E	Position of contact	E1	E2	E3	E4	E5

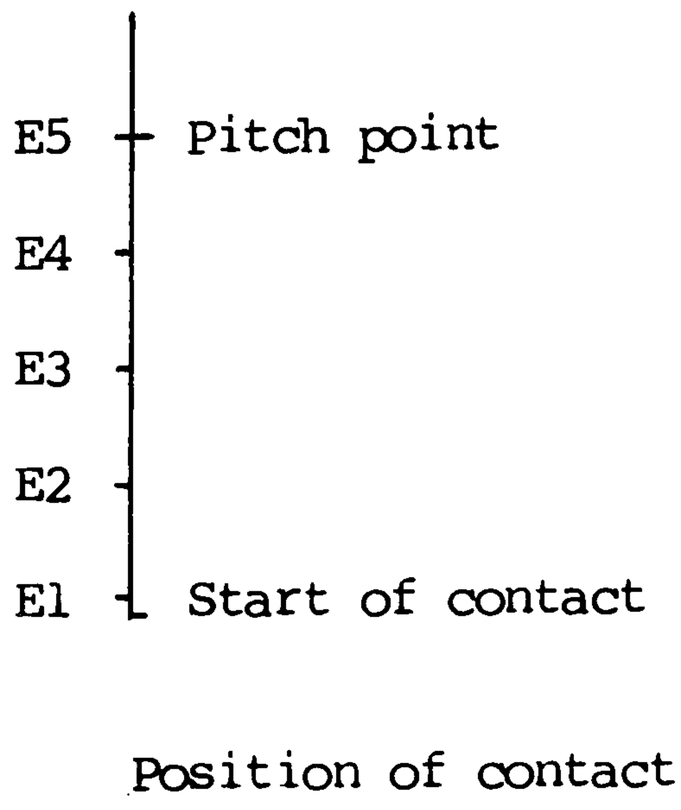

TABLE 4.2

Data used in the dynamic simulation test:

Number of teeth of gear 'A'	= 45
Number of teeth of gear 'B'	= 45
Diametral pitch	= 8
Flank angle of pitch radius	= 20^{o}
Addendum modification (both gears)	= zero

Load torque (Nm):	1000.0, 4000.0, 8000.0, 12,000.0
Speed of rotation (rpm):	1000.0 to 6000.0 in steps of 200.0
Oil viscosity (Ns/m^2):	0.05, 0.10, 0.15
Contact ratio:	1.20 to 1.60 in steps of 0.10
Pitch error (mm):	0.001 and 0.0025

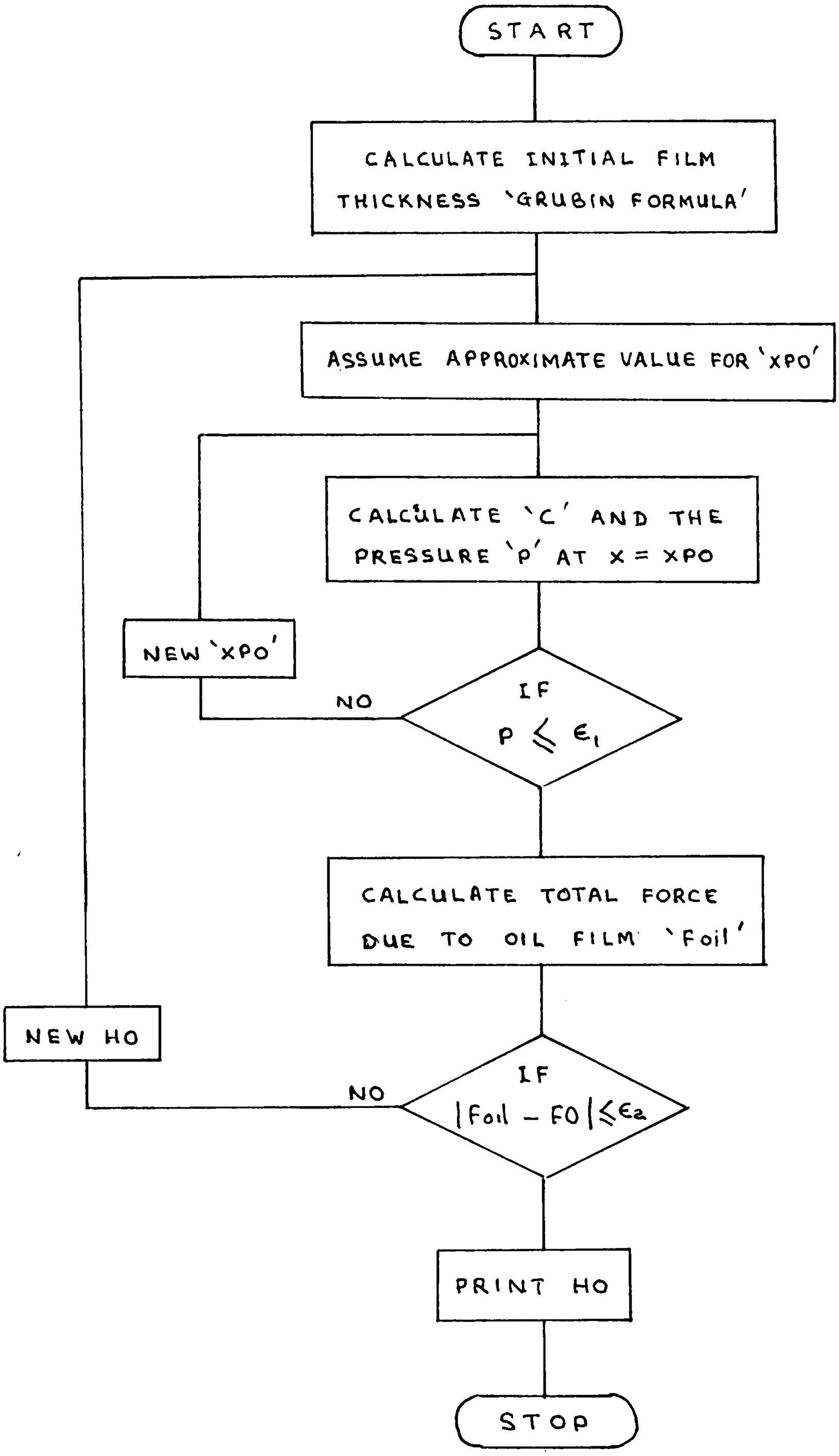

FLOW CHART OF THE PROGRAMME TO CALCULATE THE OIL FILM THICKNESS

FIGURE 4

OIL FILM THICKNESS (HO) Vs FORCE (FO)

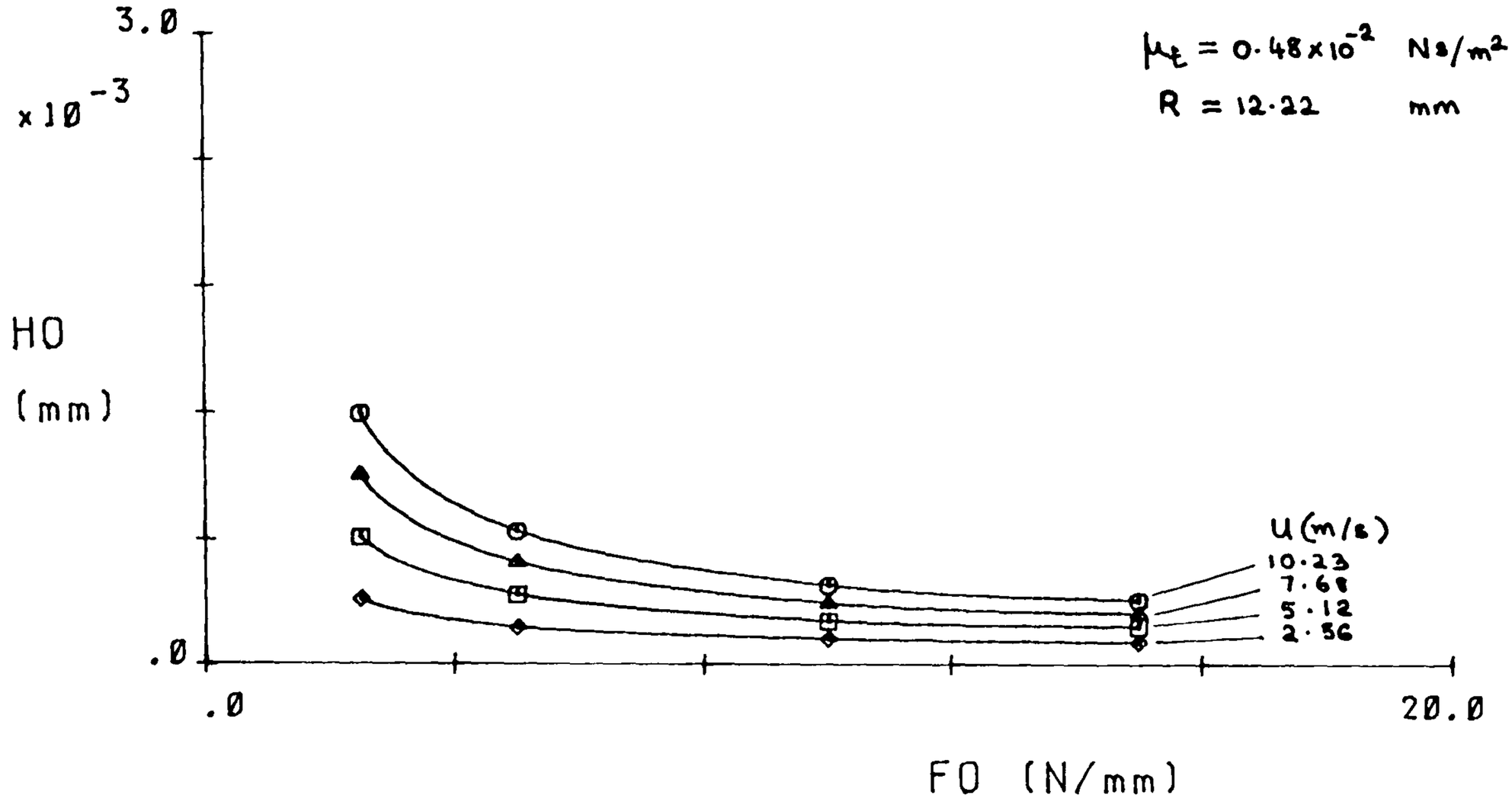

FIGURE 4.1(a)

OIL FILM THICKNESS (HO) Vs FORCE (FO)

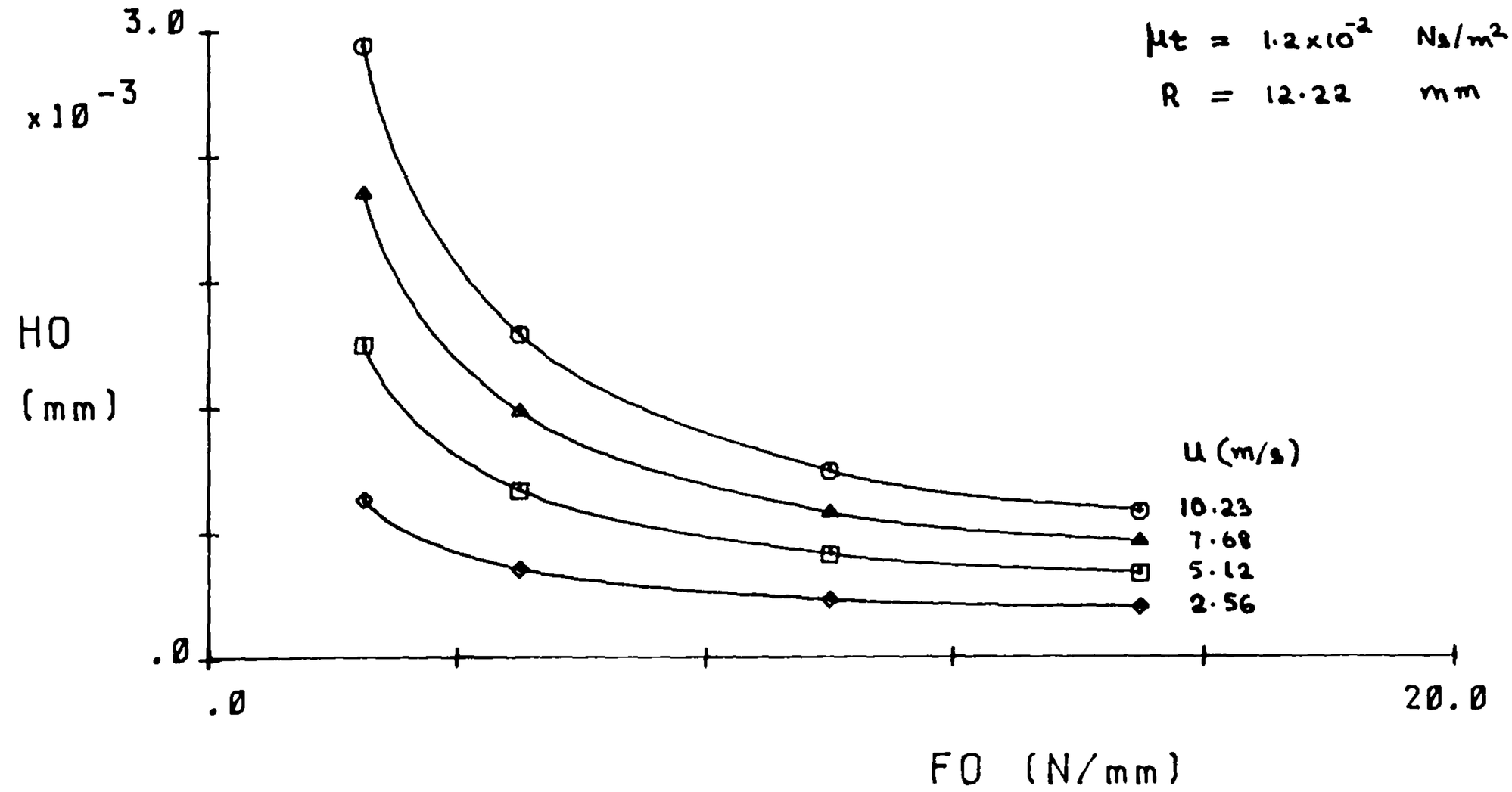

FIGURE 4.1(b)

OIL FILM THICKNESS (HO) Vs VELOCITY (U)

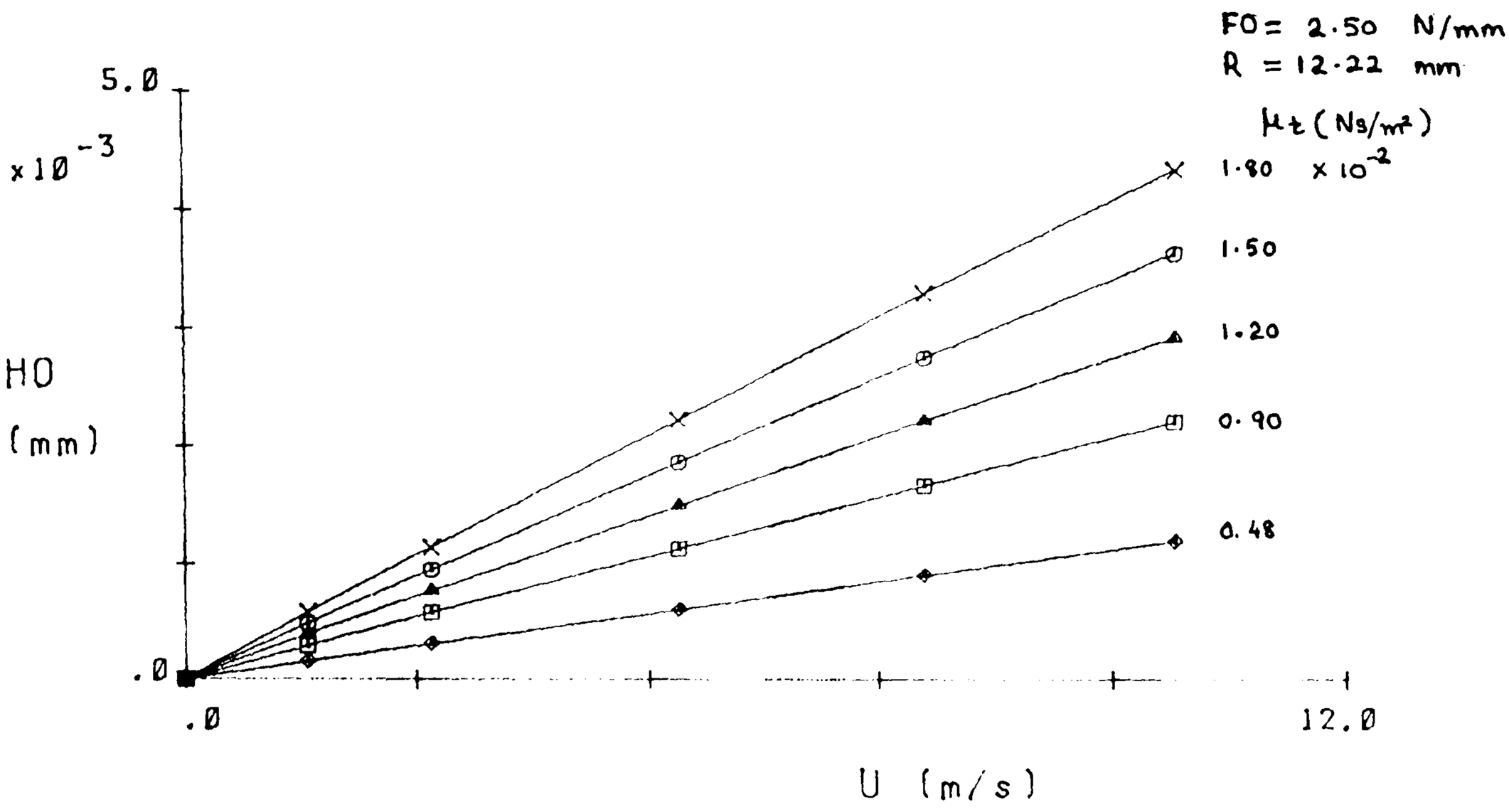

FIGURE 4.2(a)

OIL FILM THICKNESS (HO) Vs VELOCITY (U)

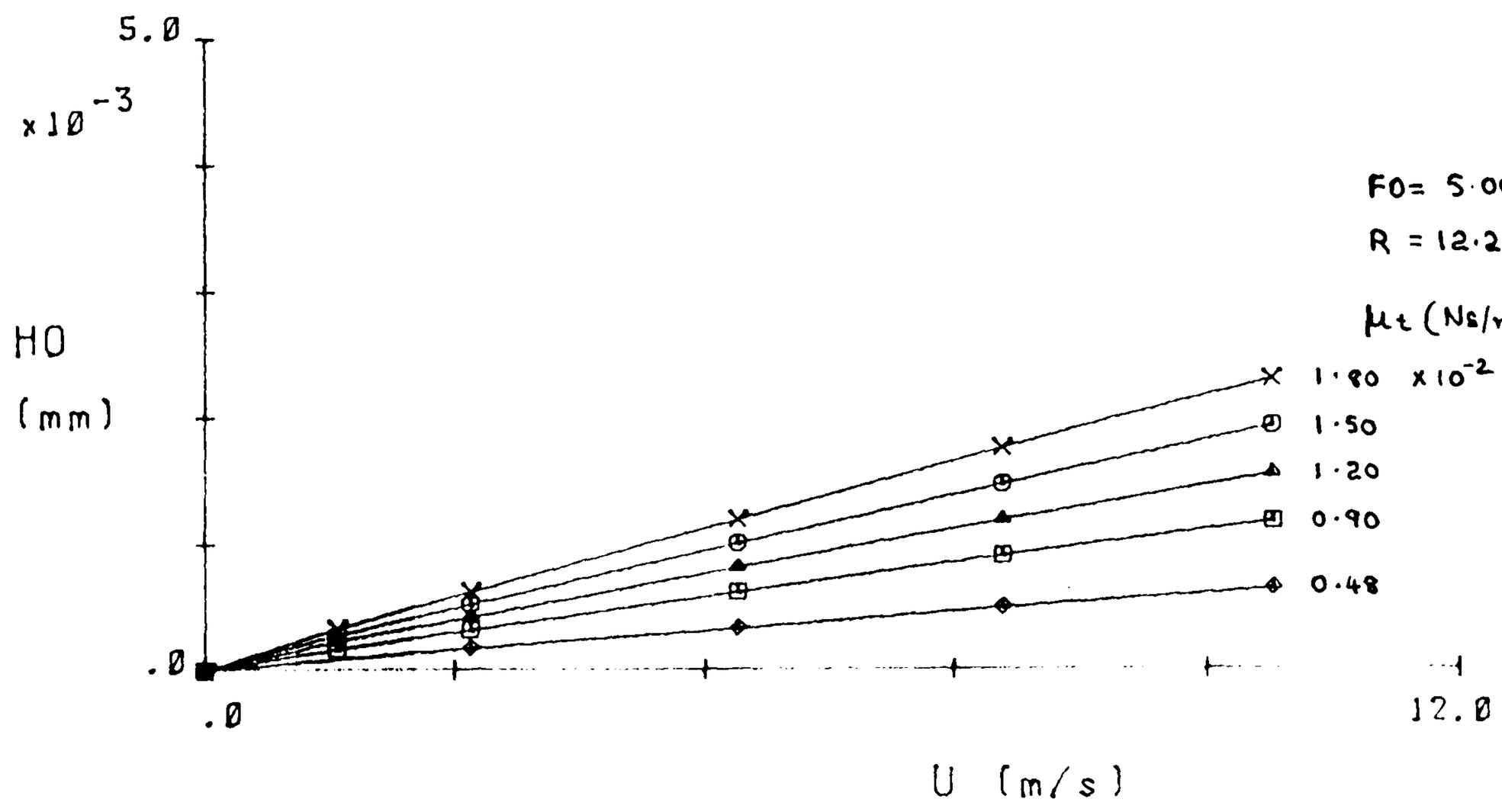

FIGURE 4.2(b)

OIL FILM THICKNESS (HO) Vs VISCOSITY (μ_t)

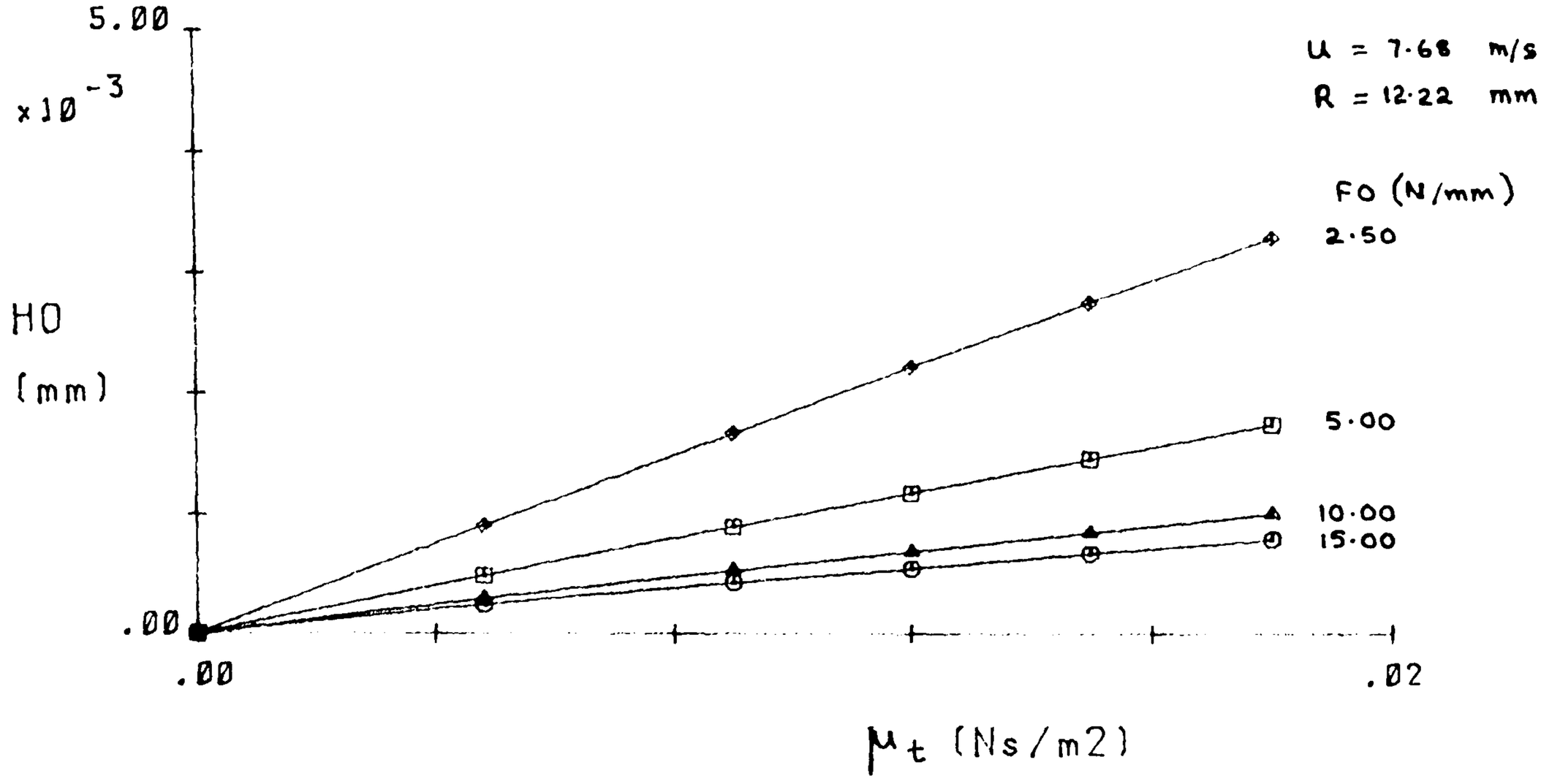

FIGURE 4.3(a)

OIL FILM THICKNESS (HO) Vs VISCOSITY (μ_t)

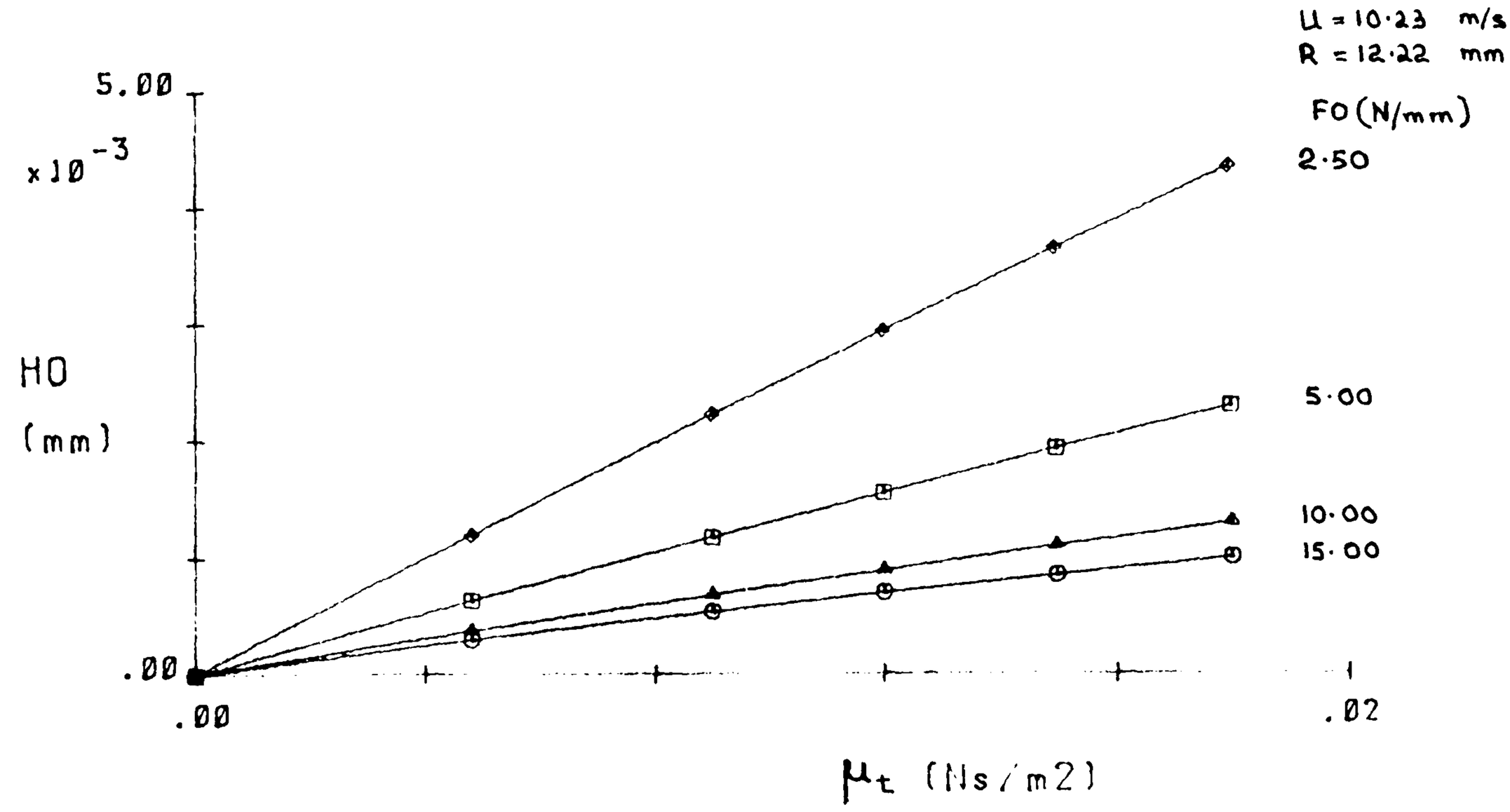

FIGURE 4.3(b)

OIL FILM THICKNESS (HO) Vs VISCOSITY (μ_t)

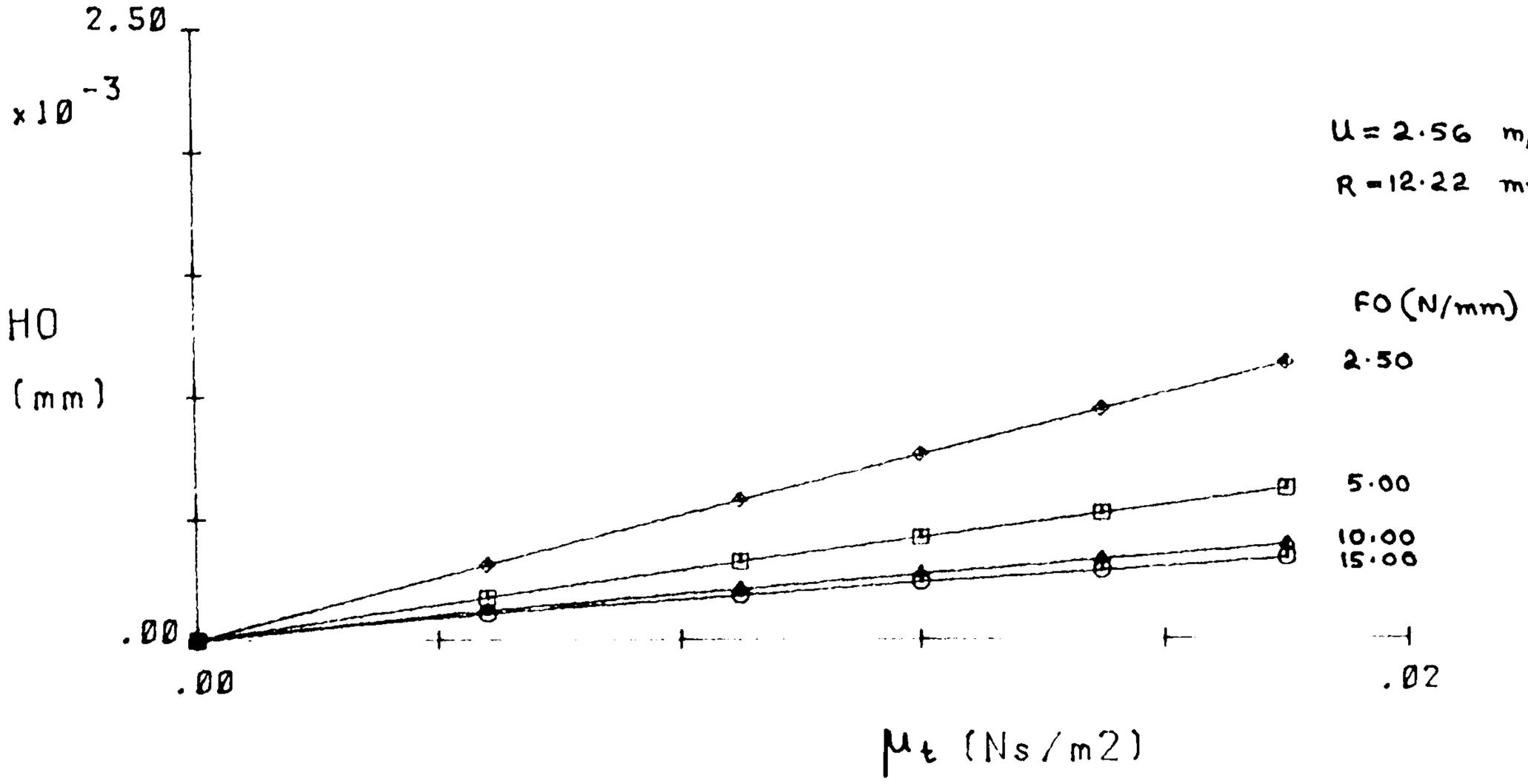

FIGURE 4.3(c)

OIL FILM THICKNESS (HO) Vs VISCOSITY (μ_t)

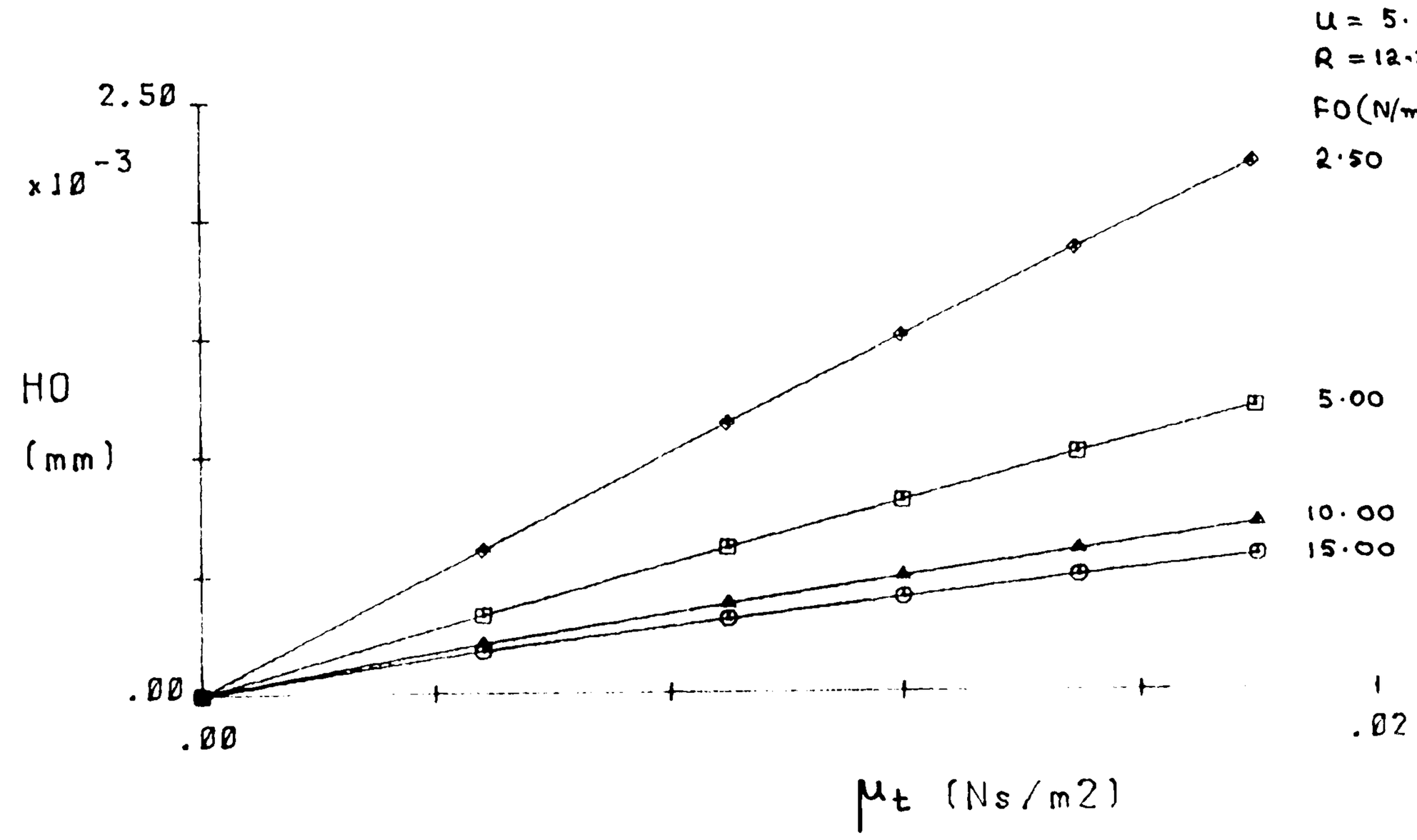

FIGURE 4.3(d)

OIL FILM THICKNESS (HO) Vs RADIUS (R)

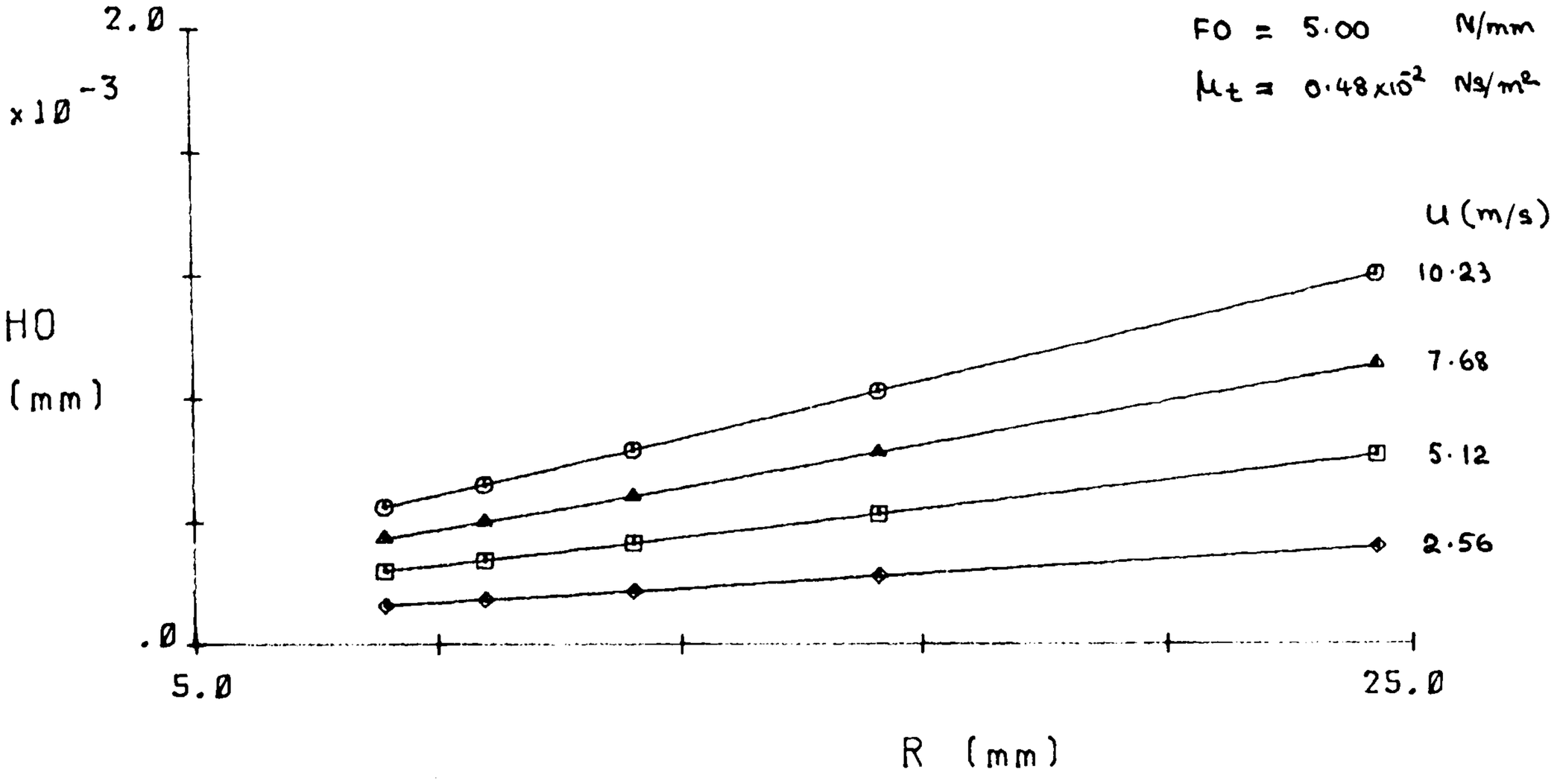

FIGURE 4.4(a)

OIL FILM THICKNESS (HO) Vs RADIUS (R)

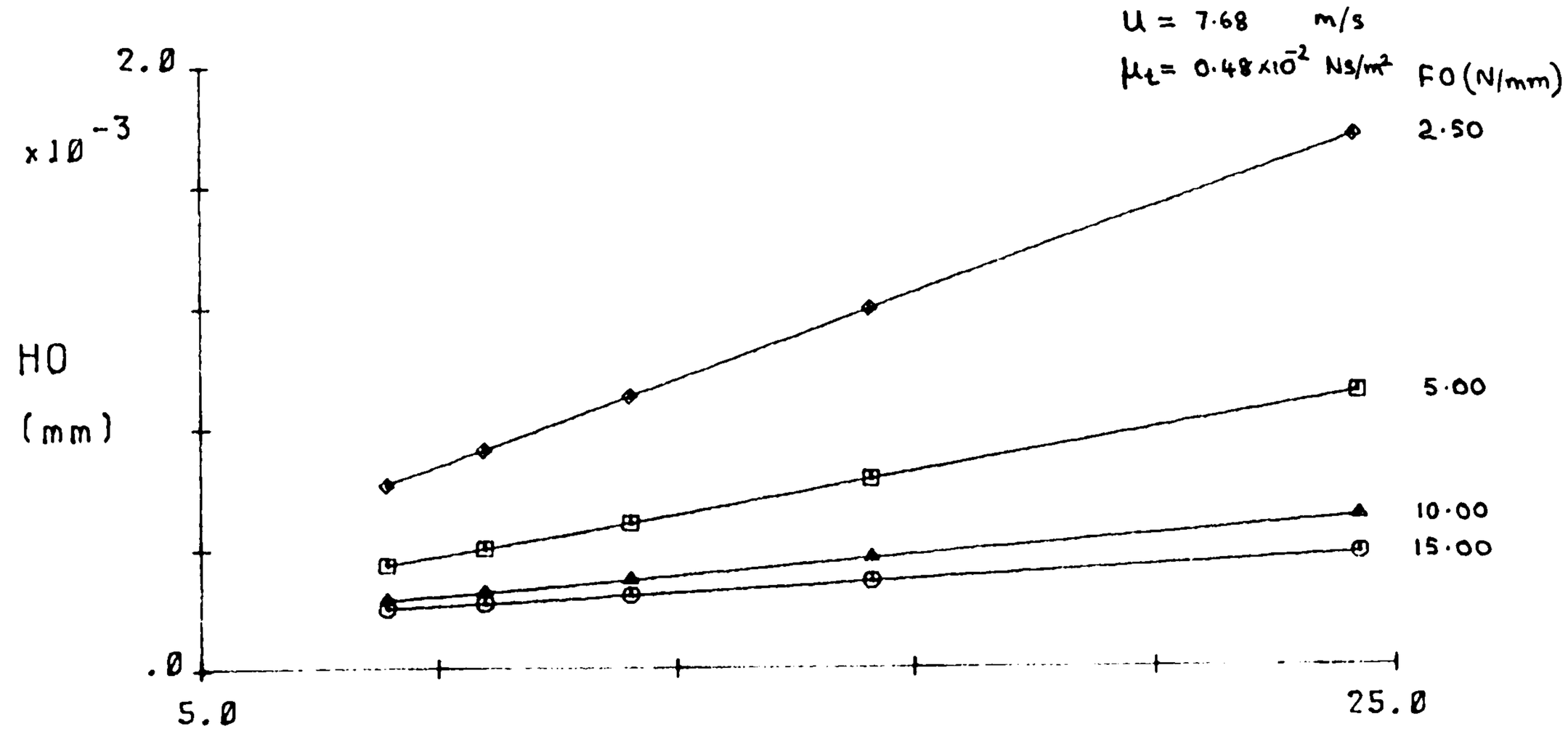

FIGURE 4.4(b)

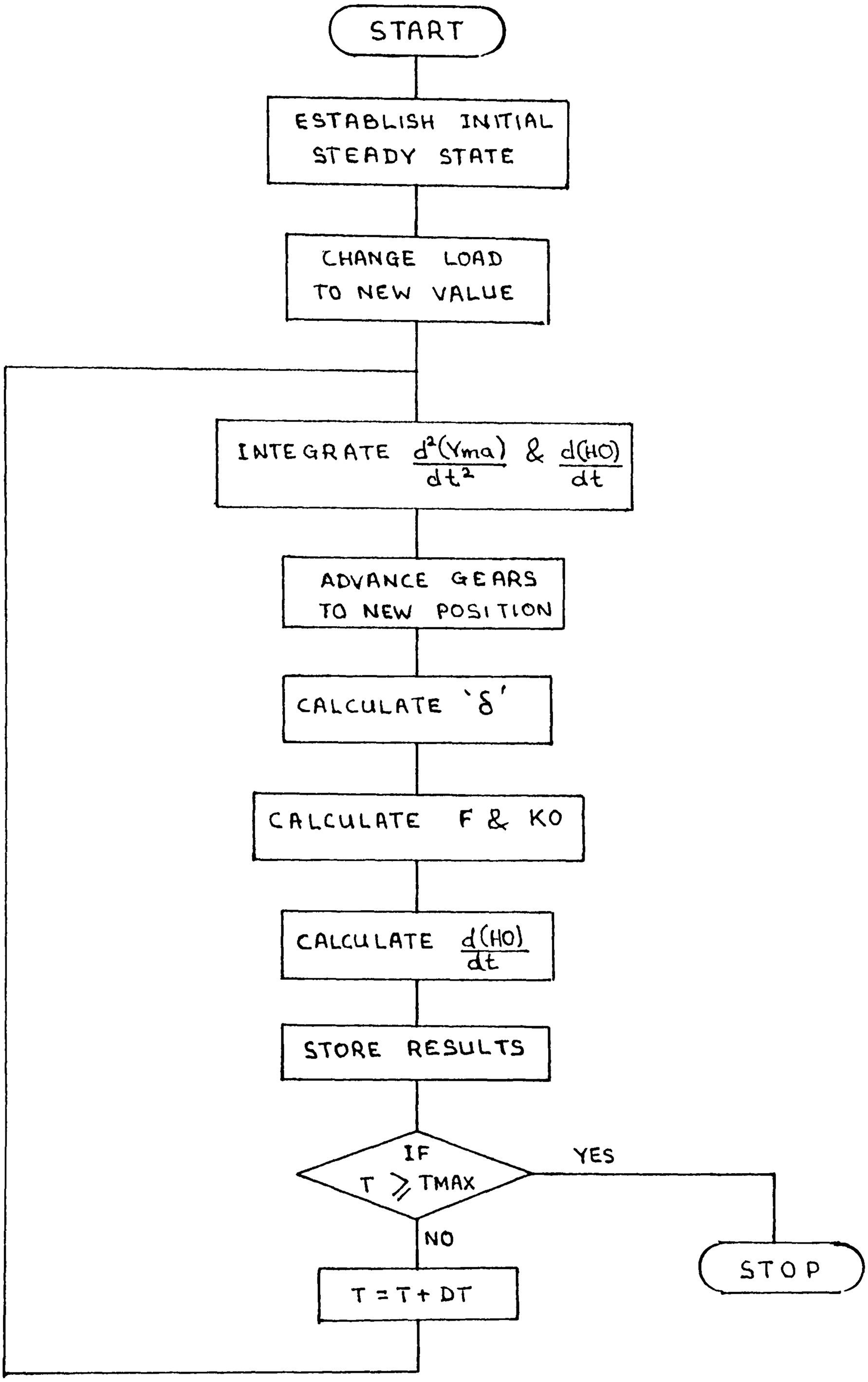

FLOW CHART OF THE TRANSIENT RESPONSE ANALYSIS PROGRAMME

FIGURE 4.5

Data relevant to Figures 4.6 to 4.10, unless otherwise stated, are:

Nominal tooth force (FO) = 5.0 N/mm

Speed (u) = 2.56 m/s

Viscosity of oil (μ_t) = 0.48×10^{-2} Ns/m^2

Effective radius (R) = 12.22 mm

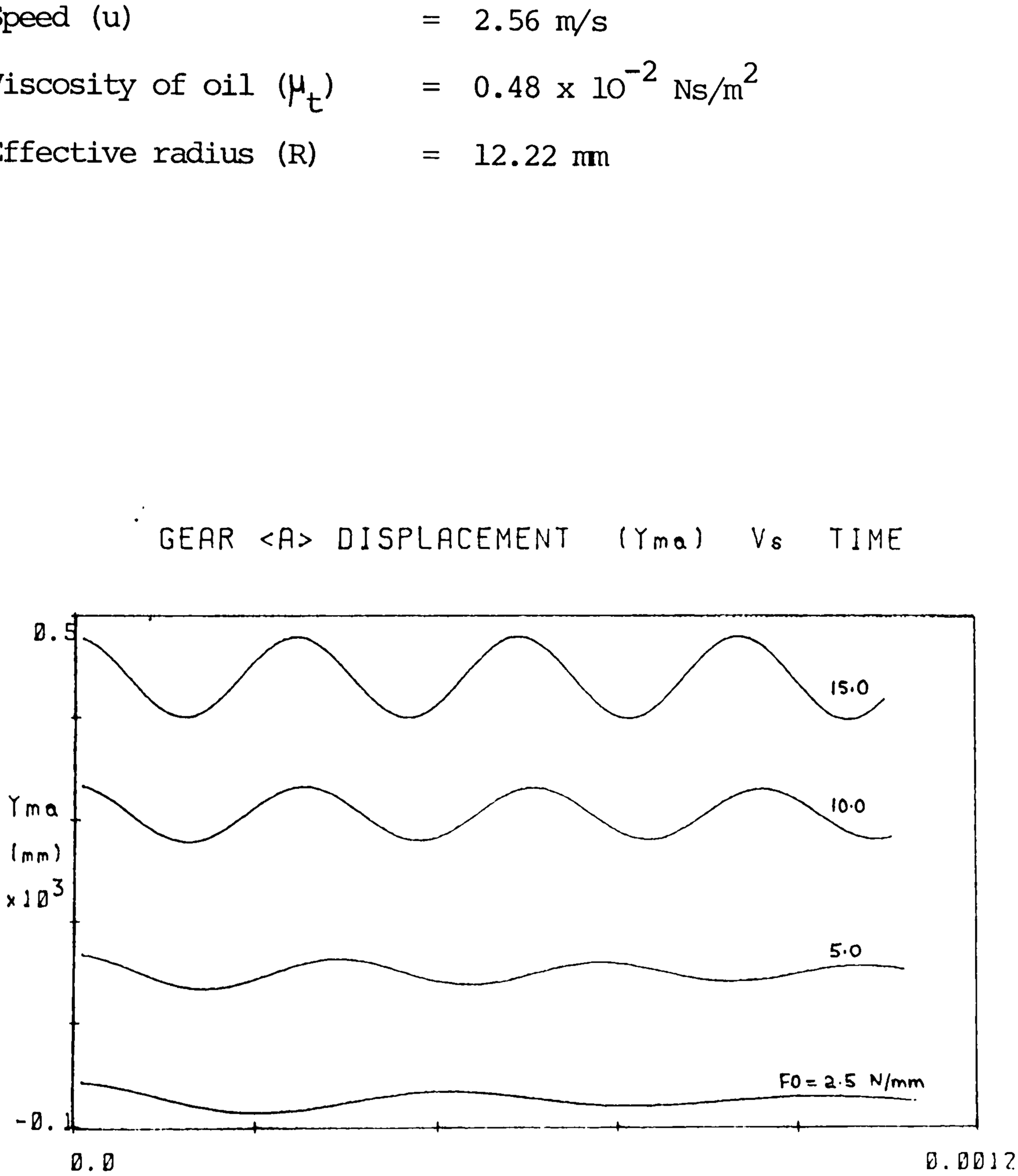

FIGURE 4.6

GEAR <A> DISPLACEMENT (Yma) Vs TIME

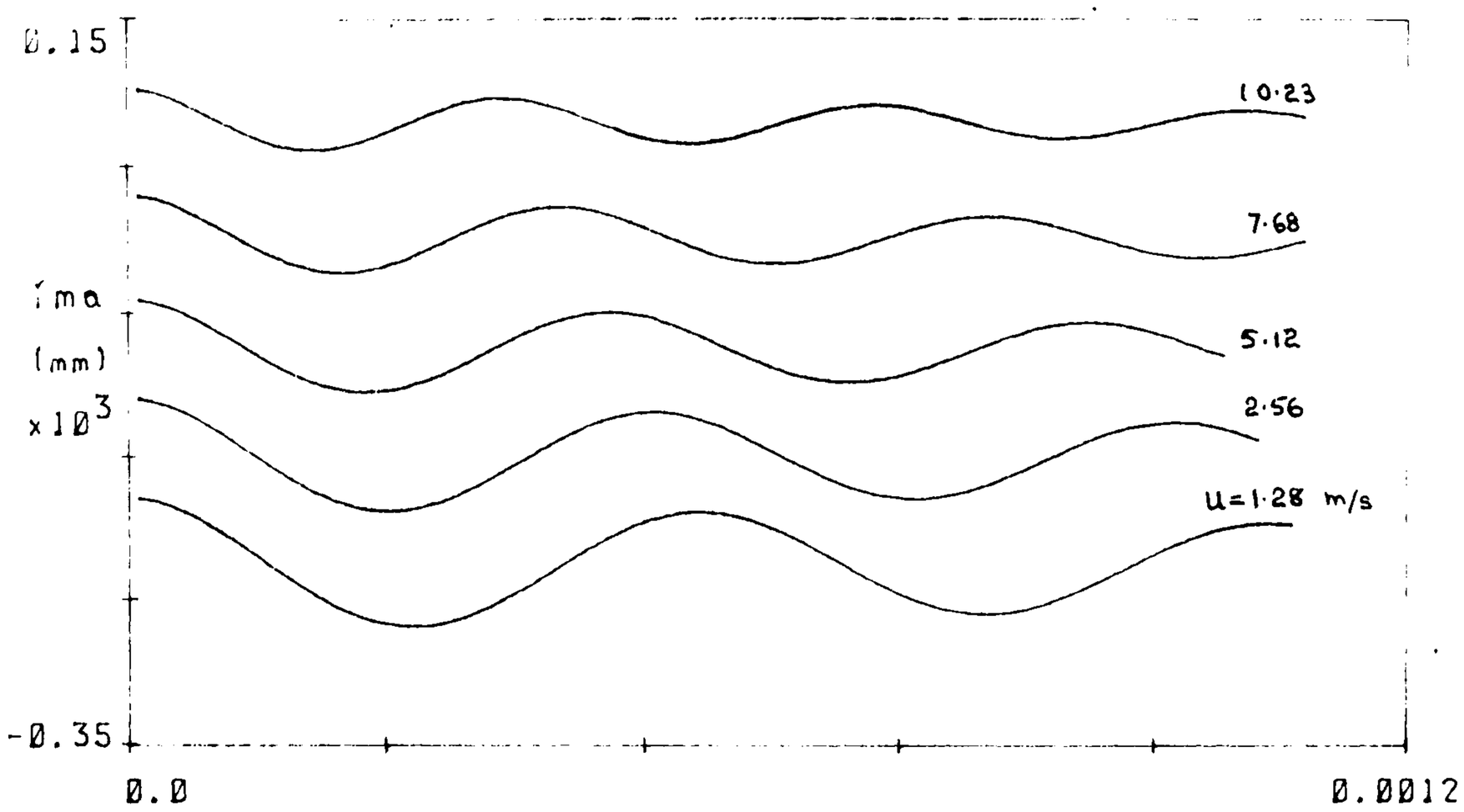

FIGURE 4.7

GEAR <A> DISPLACEMENT (Yma) Vs TIME

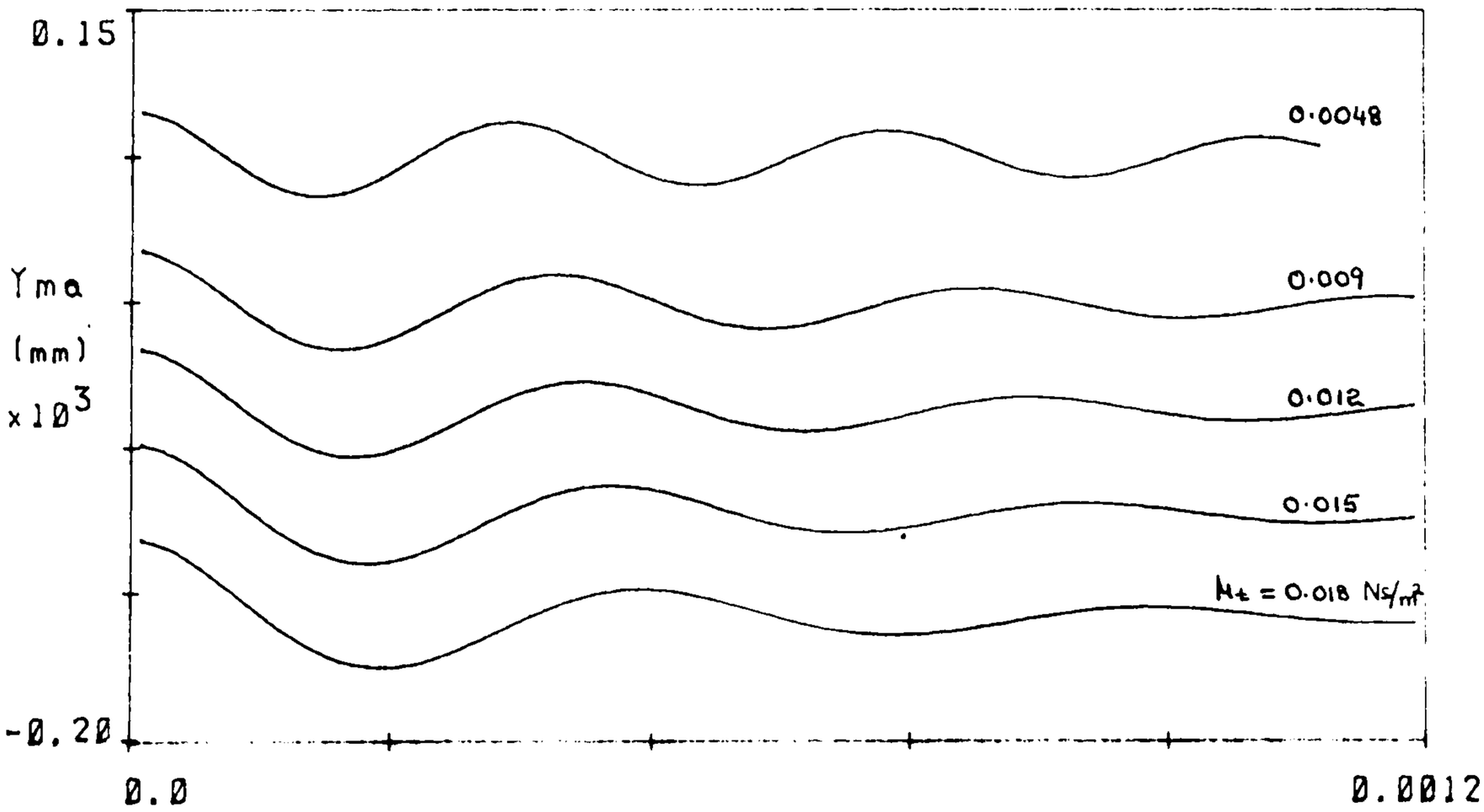

FIGURE 4.8

GEAR <A> DISPLACEMENT (Yma) Vs TIME

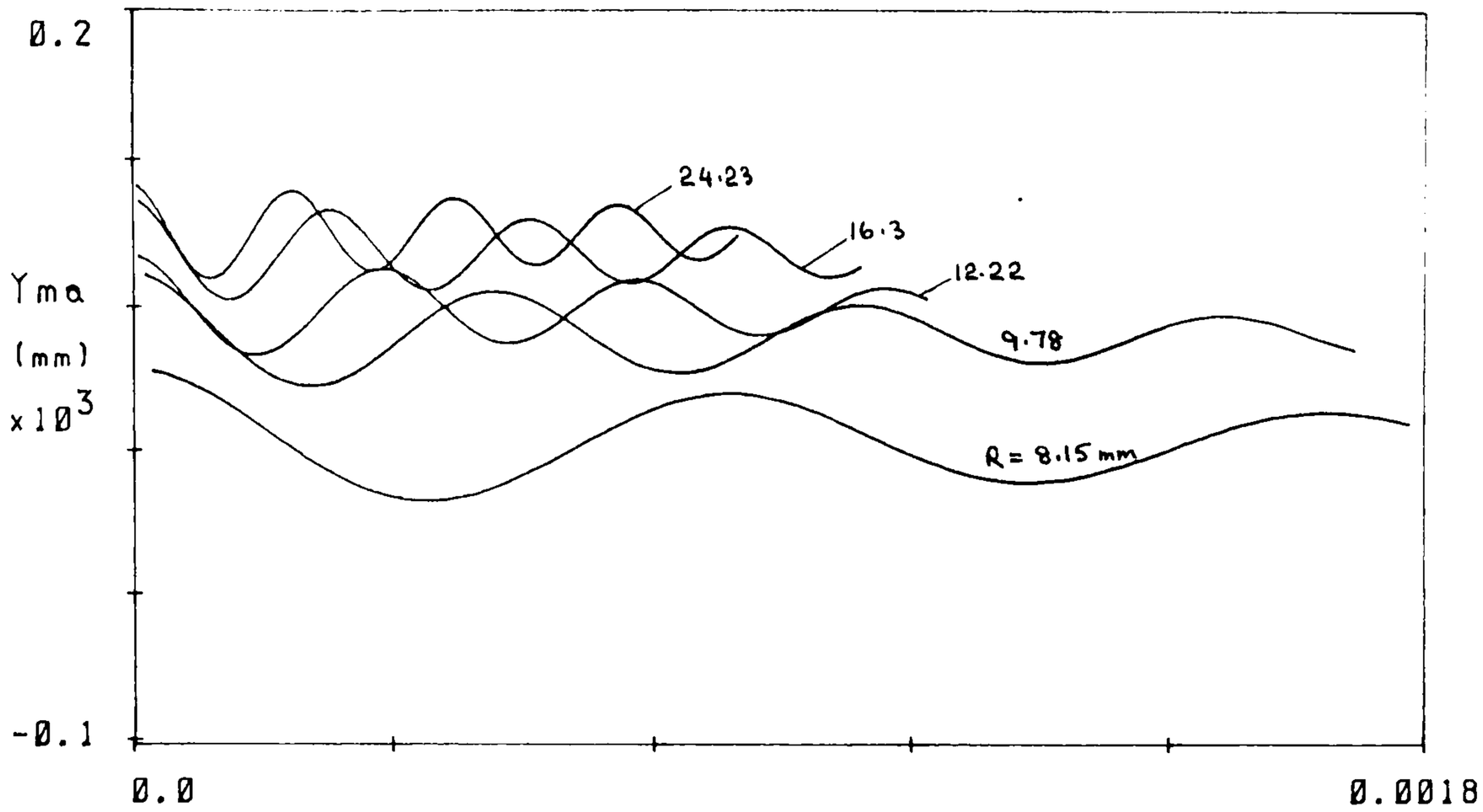

FIGURE 4.9

GEAR <A> DISPLACEMENT (Yma) Vs TIME

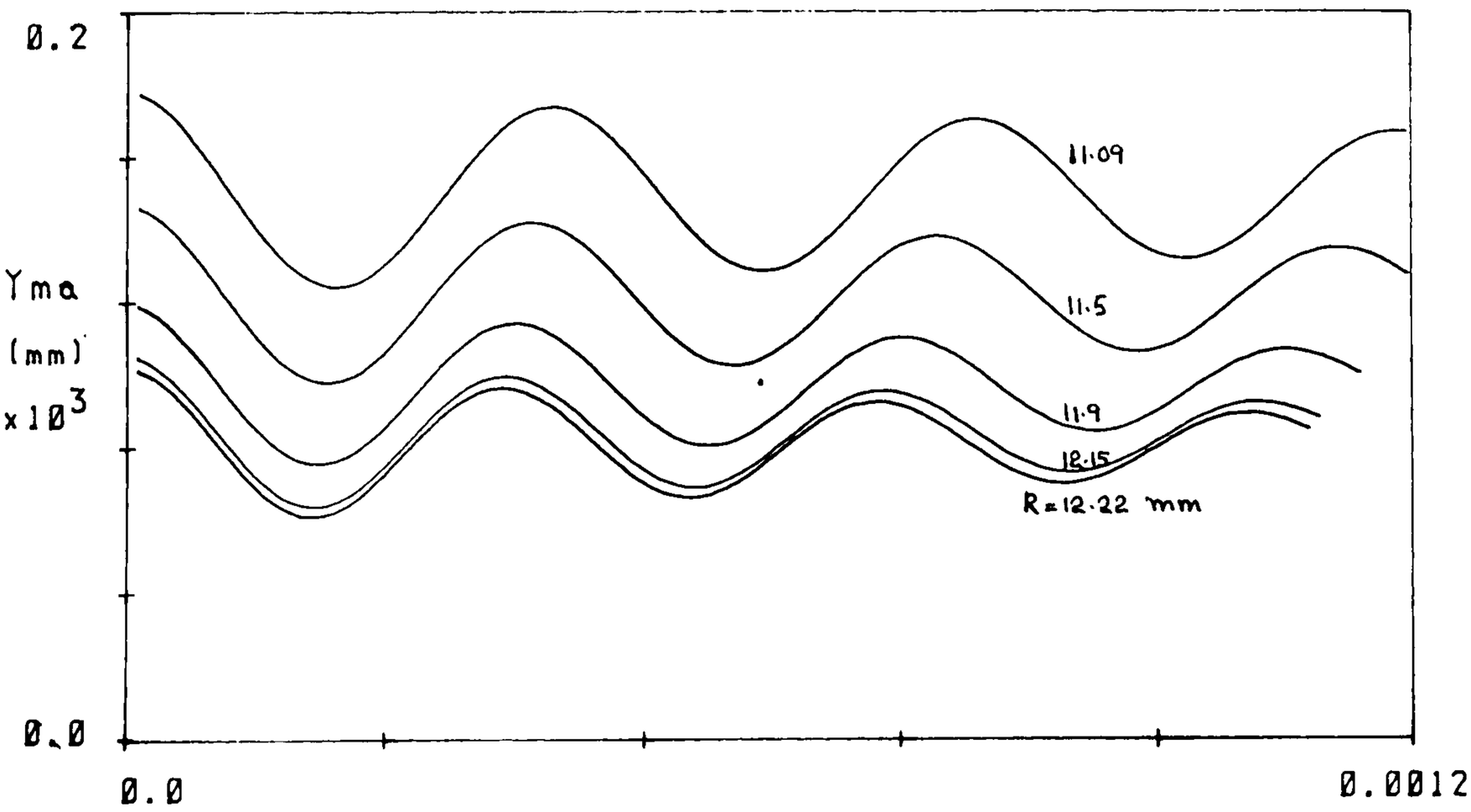

FIGURE 4.10

DAMPING RATIO (ζ) Vs FORCE (FO)

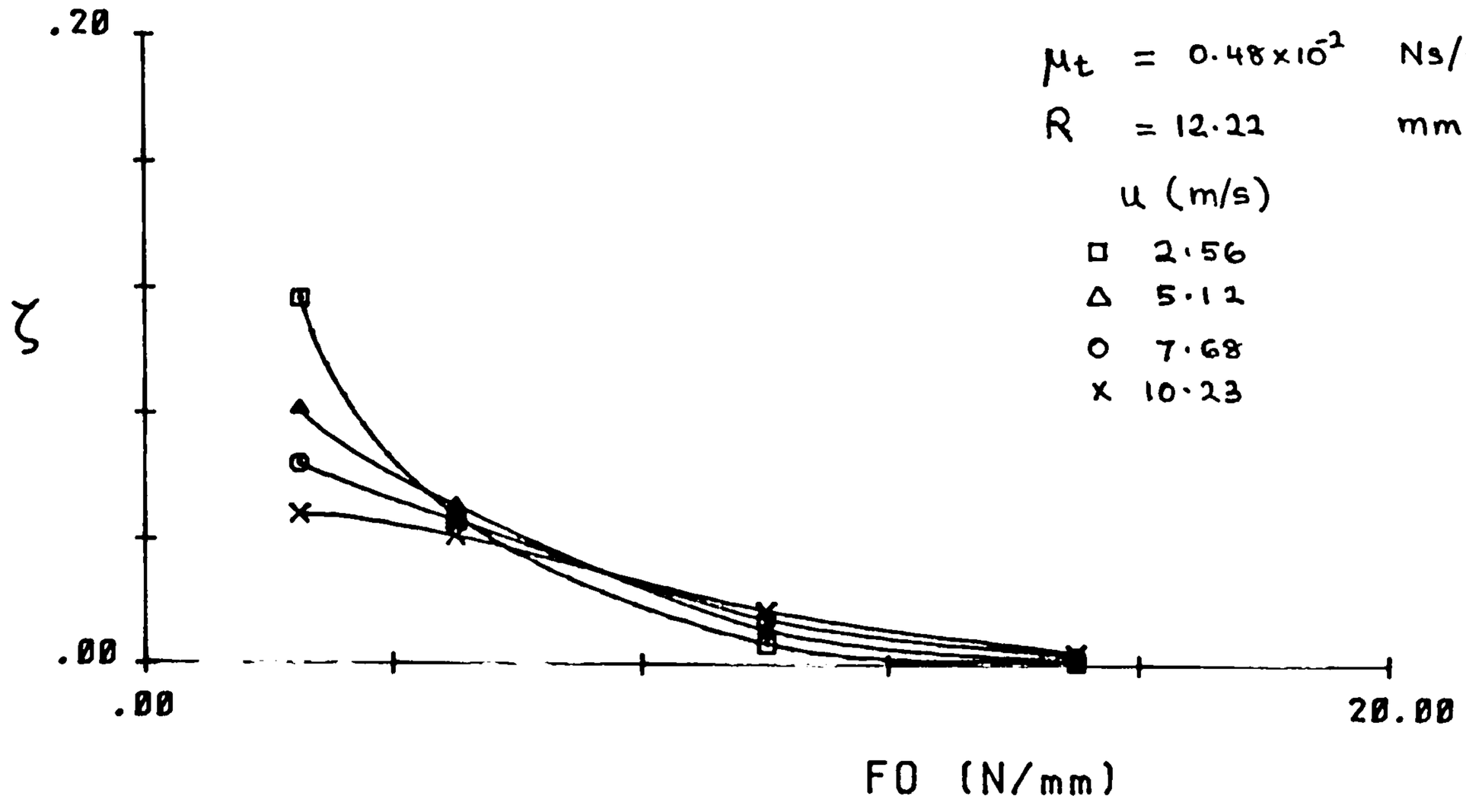

FIGURE 4.11(a)

DAMPING RATIO (ζ) Vs FORCE (FO)

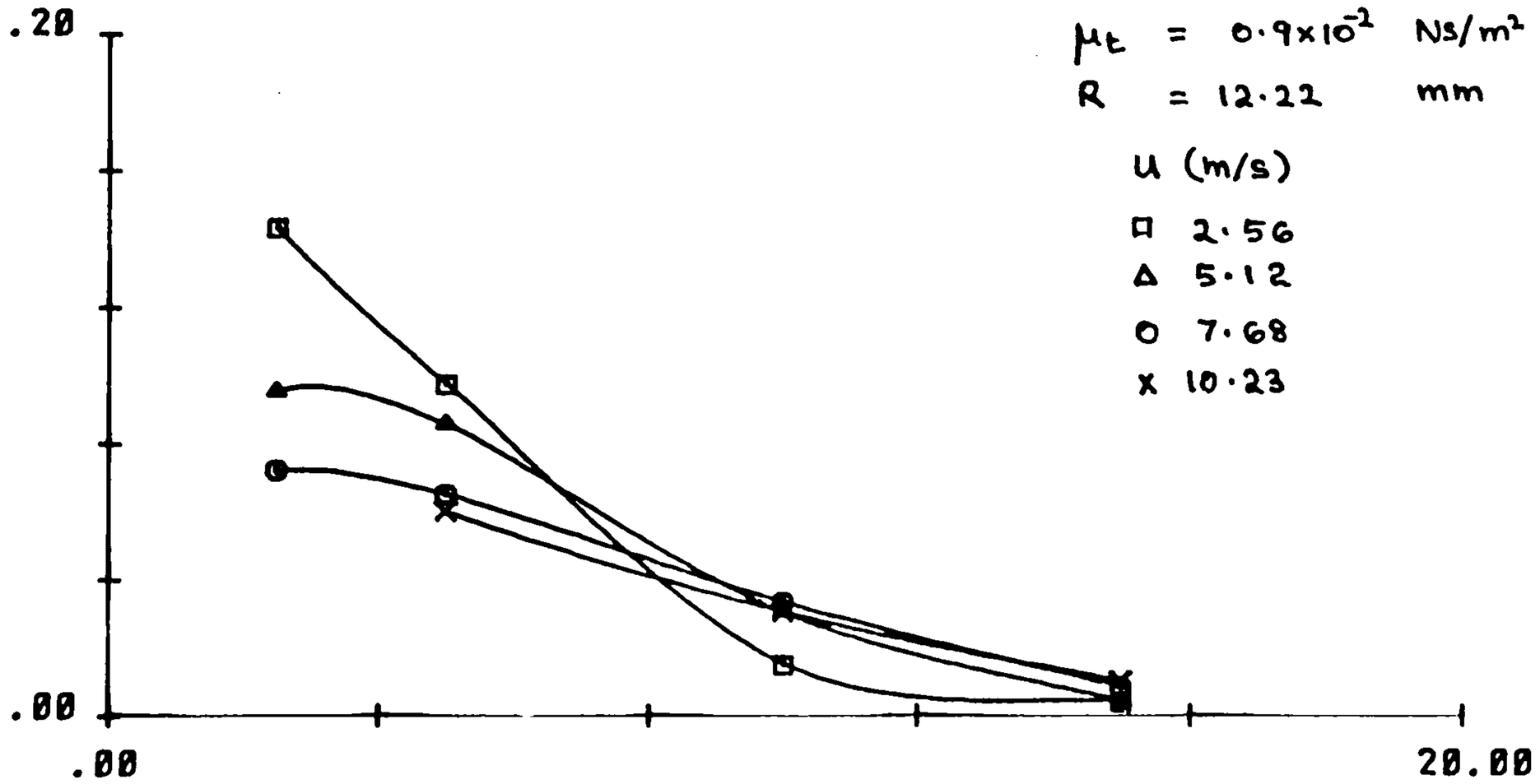

FIGURE 4.11(b)

DAMPING RATIO (ζ) Vs FORCE (FO)

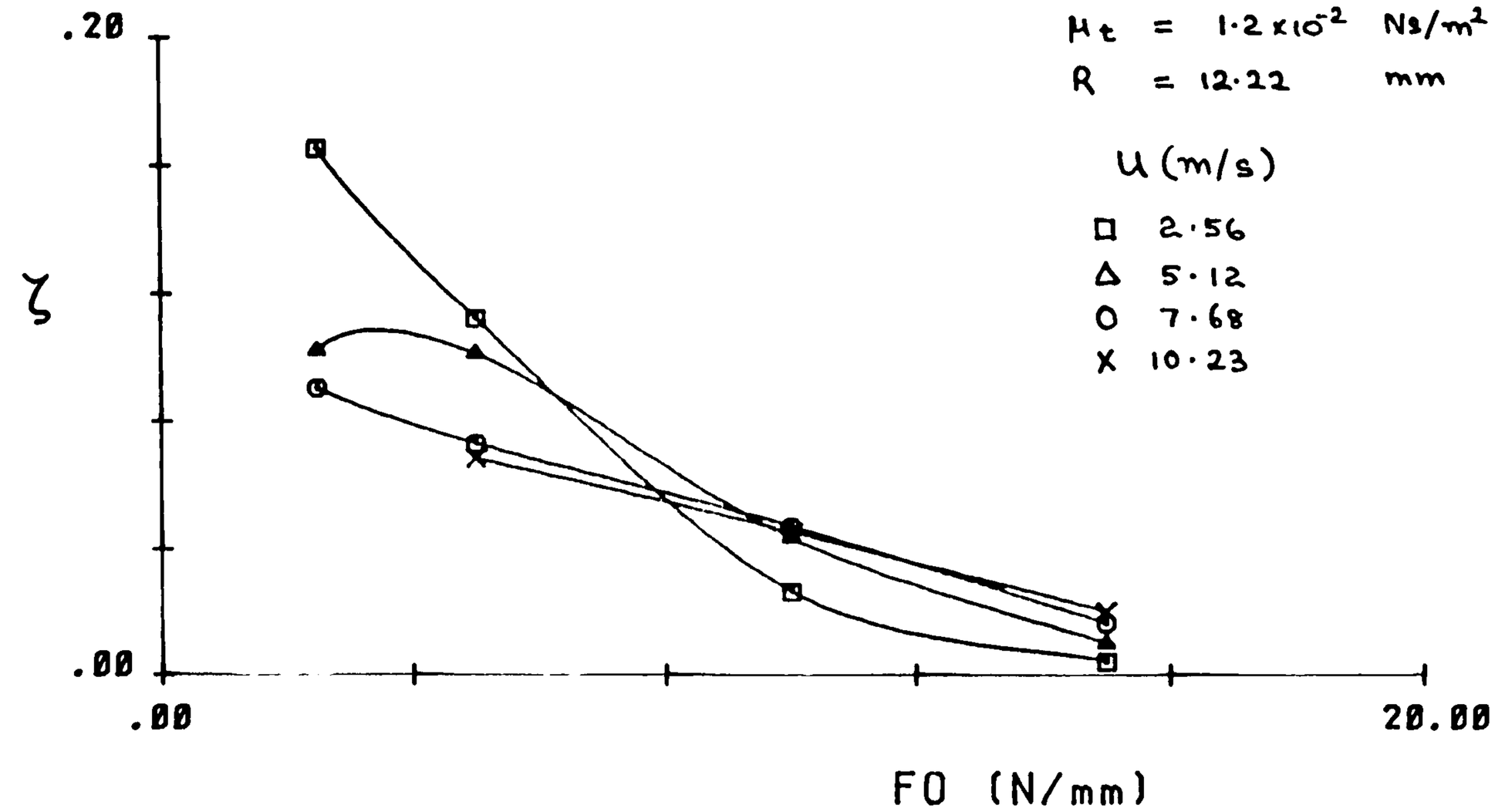

FIGURE 4.11(c)

DAMPING RATIO (ζ) Vs FORCE (FO)

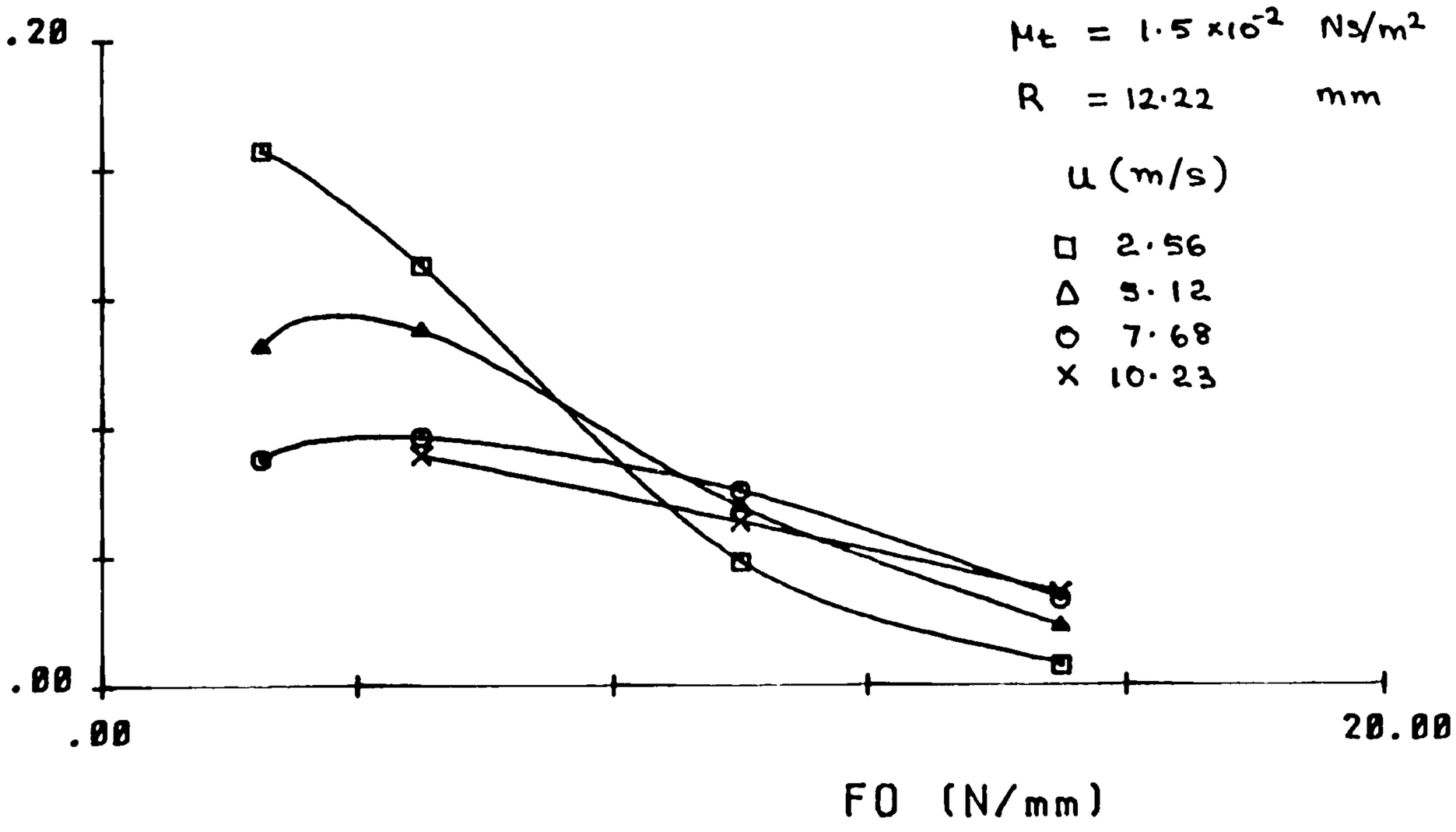

FIGURE 4.11(d)

DAMPING RATIO (ζ) Vs VELOCITY (U)

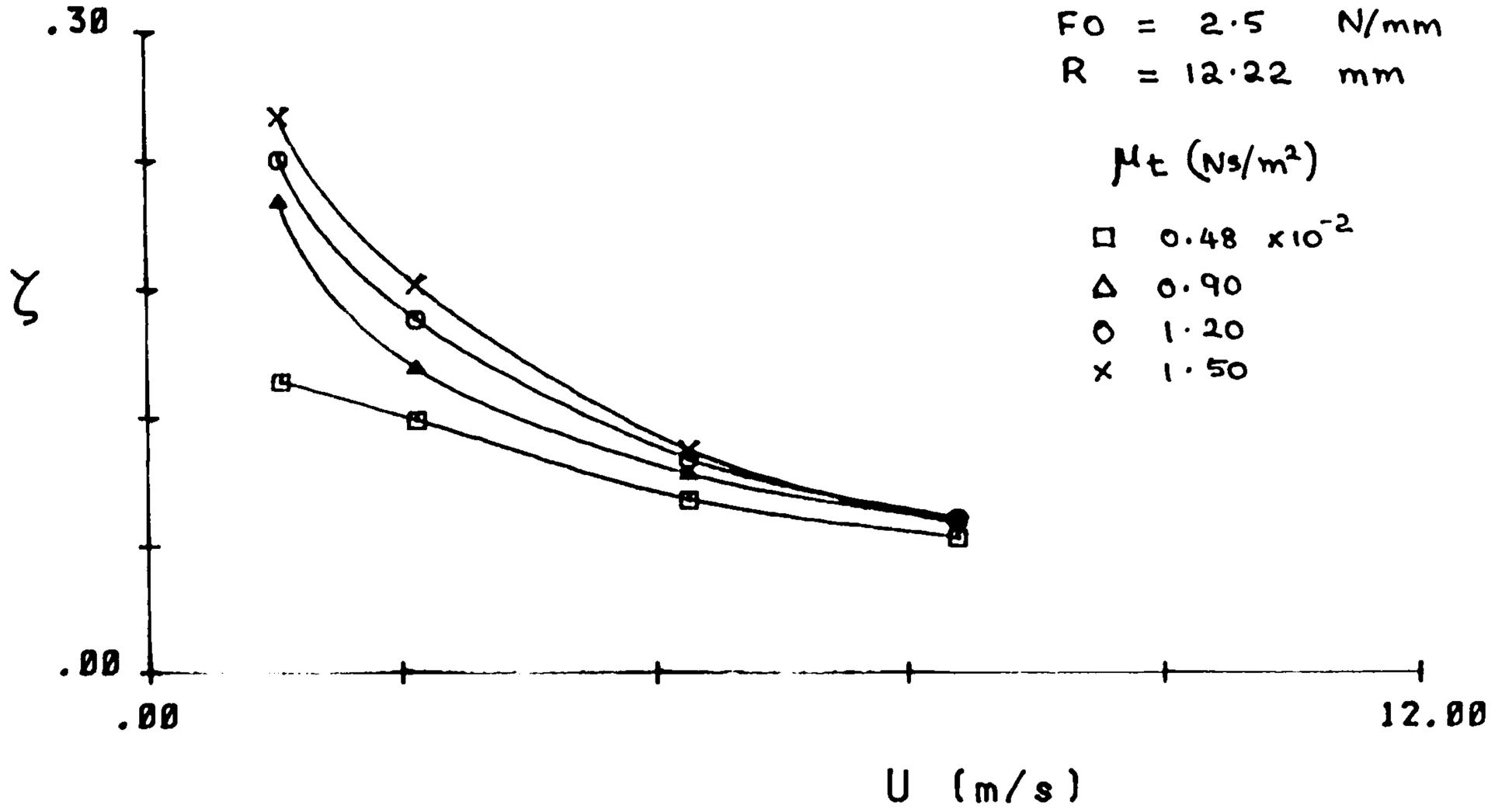

FIGURE 4.12(a)

DAMPING RATIO (ζ) Vs VELOCITY (U)

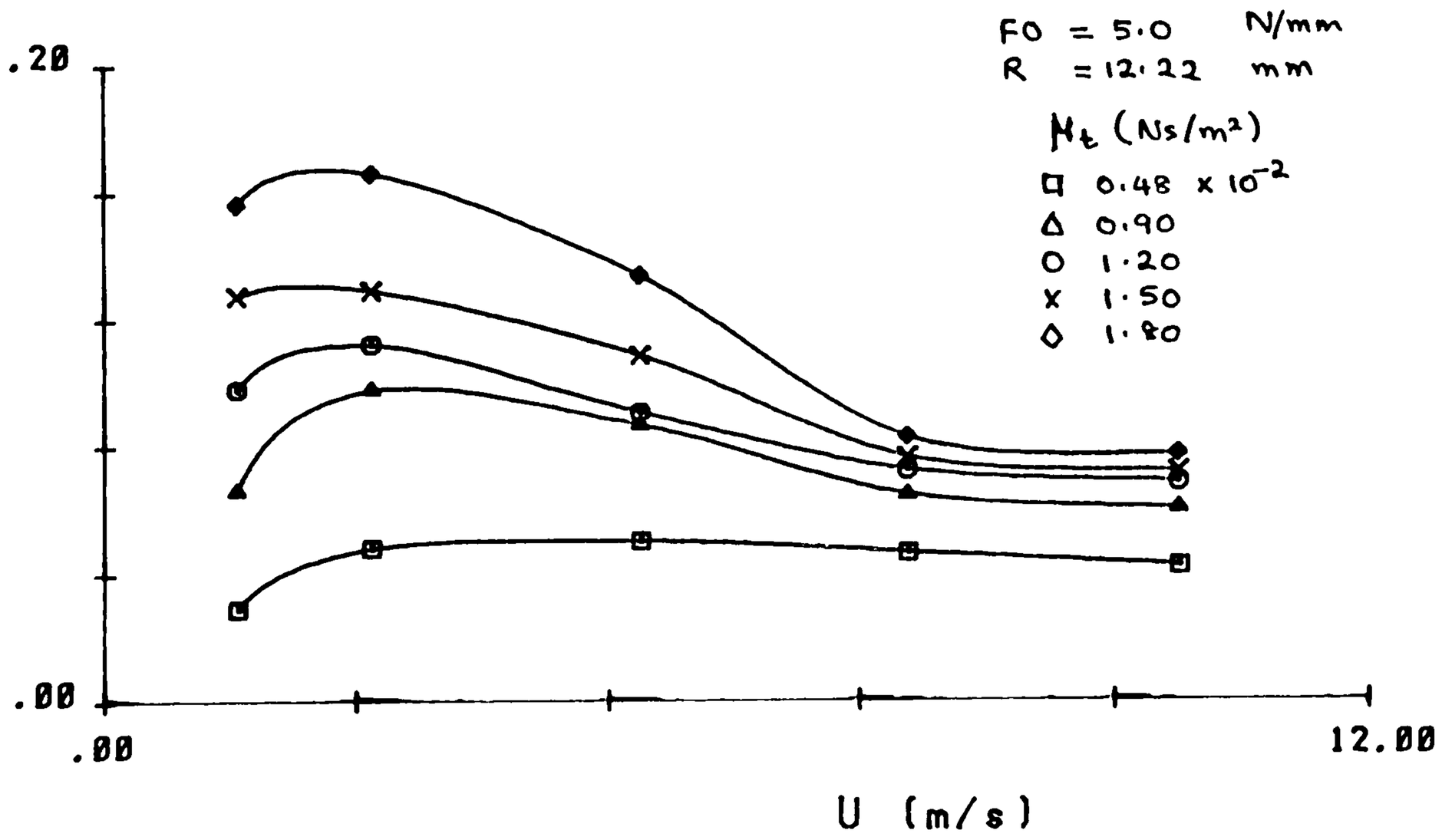

FIGURE 4.12(b)

DAMPING RATIO (ζ) Vs VELOCITY (U)

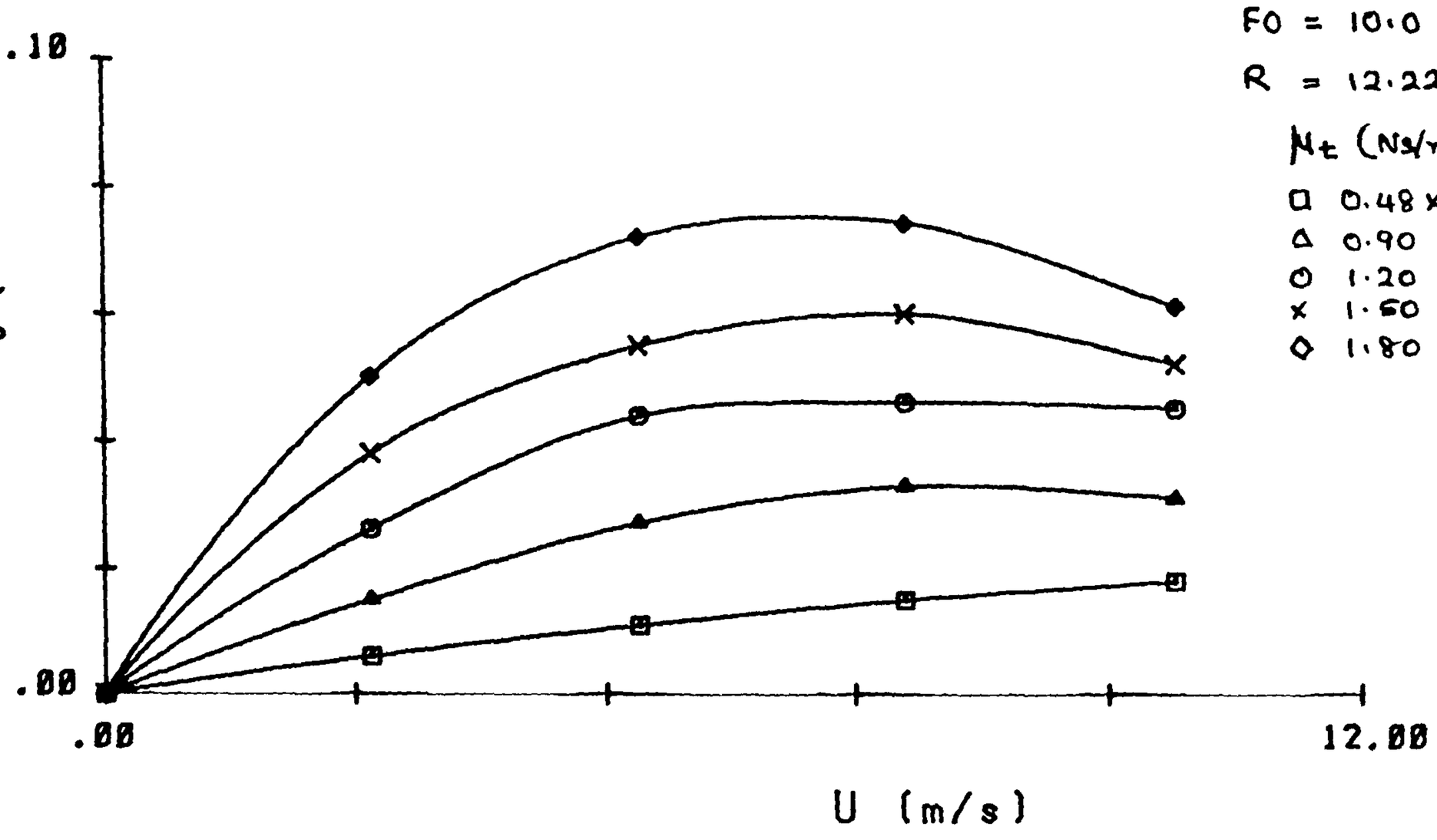

FIGURE 4.12(c)

DAMPING RATIO (ζ) Vs VELOCITY (U)

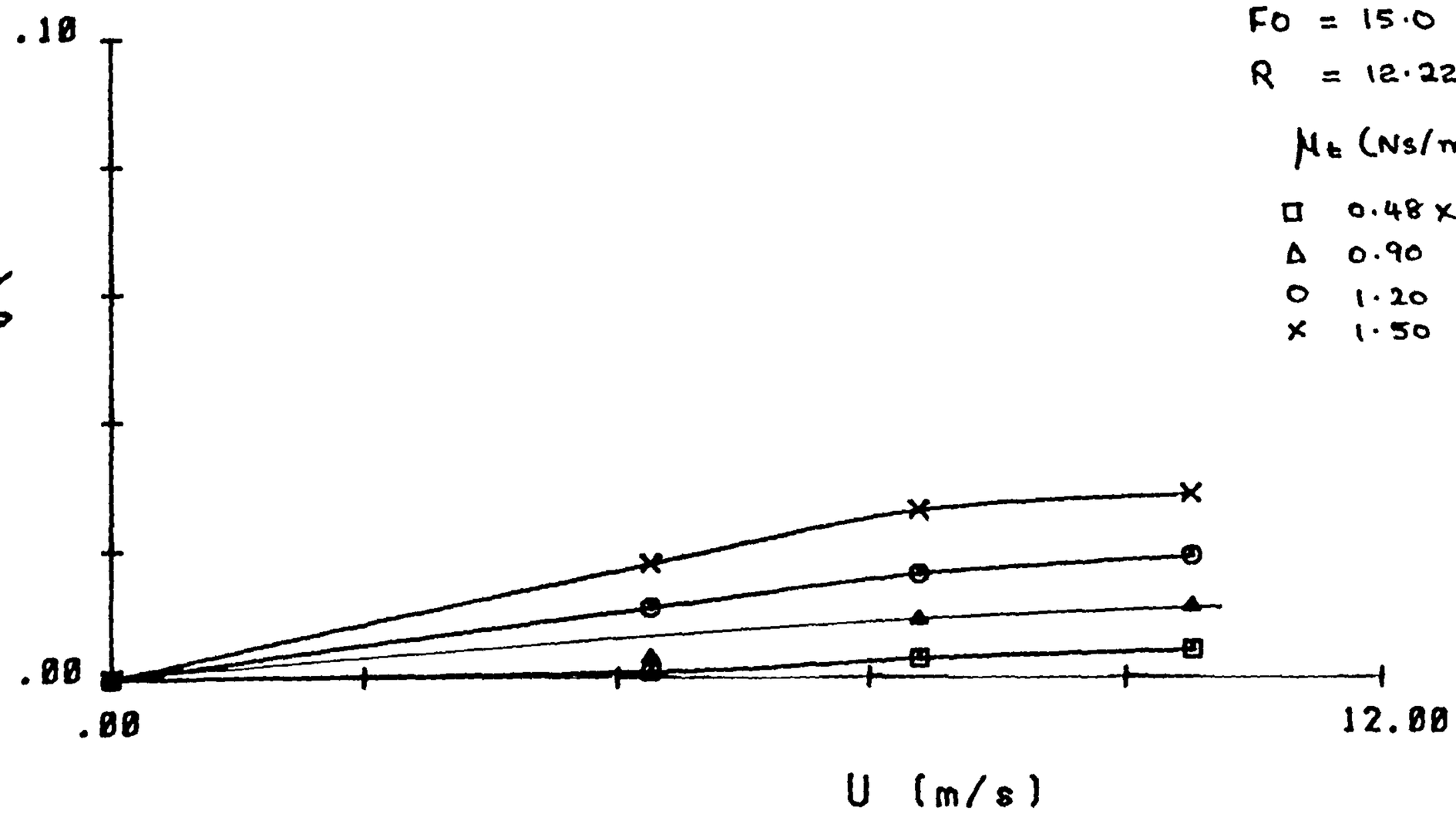

FIGURE 4.12(d)

DAMPING RATIO (ζ) Vs VELOCITY (U)

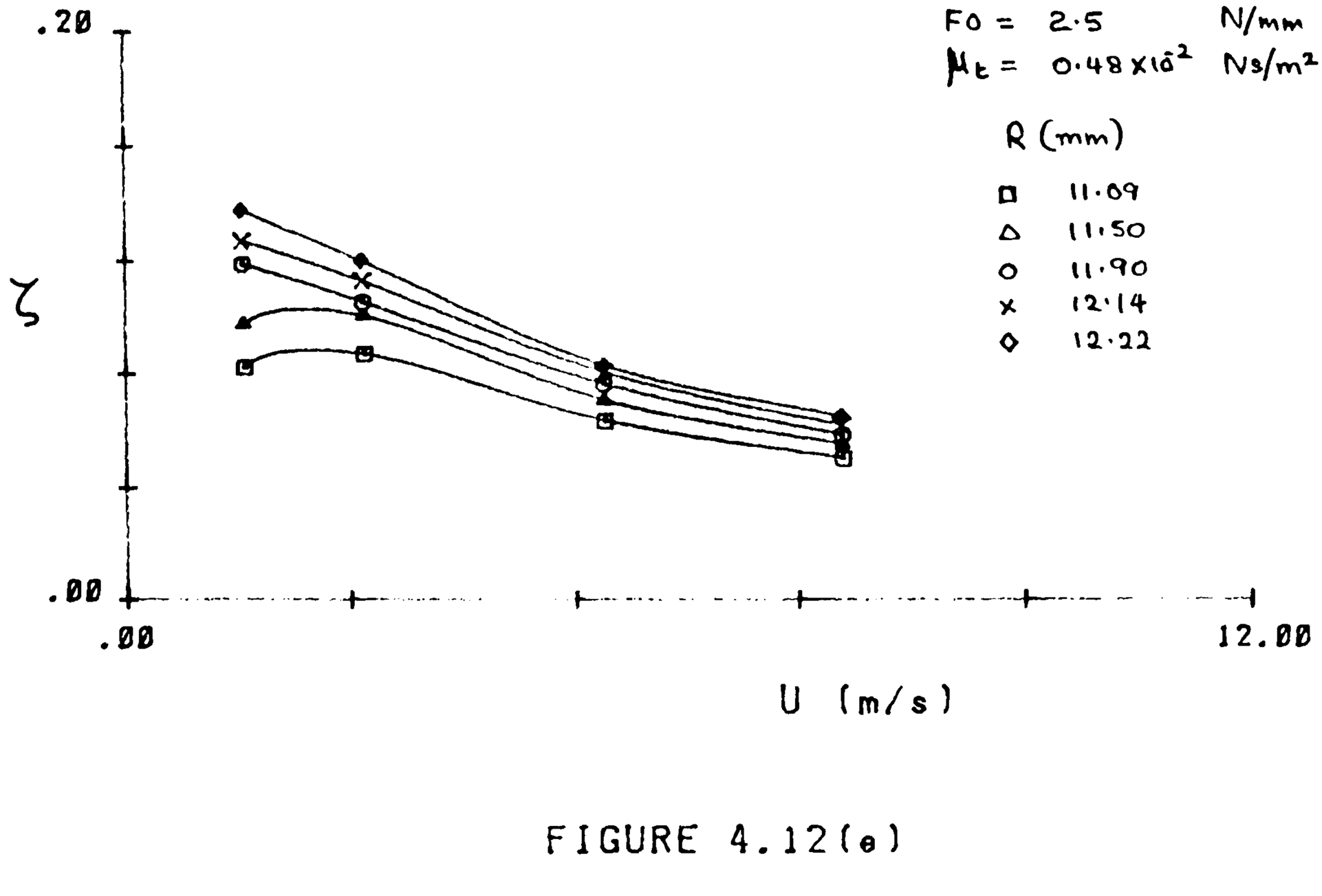

FIGURE 4.12(e)

DAMPING RATIO (ζ) Vs VELOCITY (U)

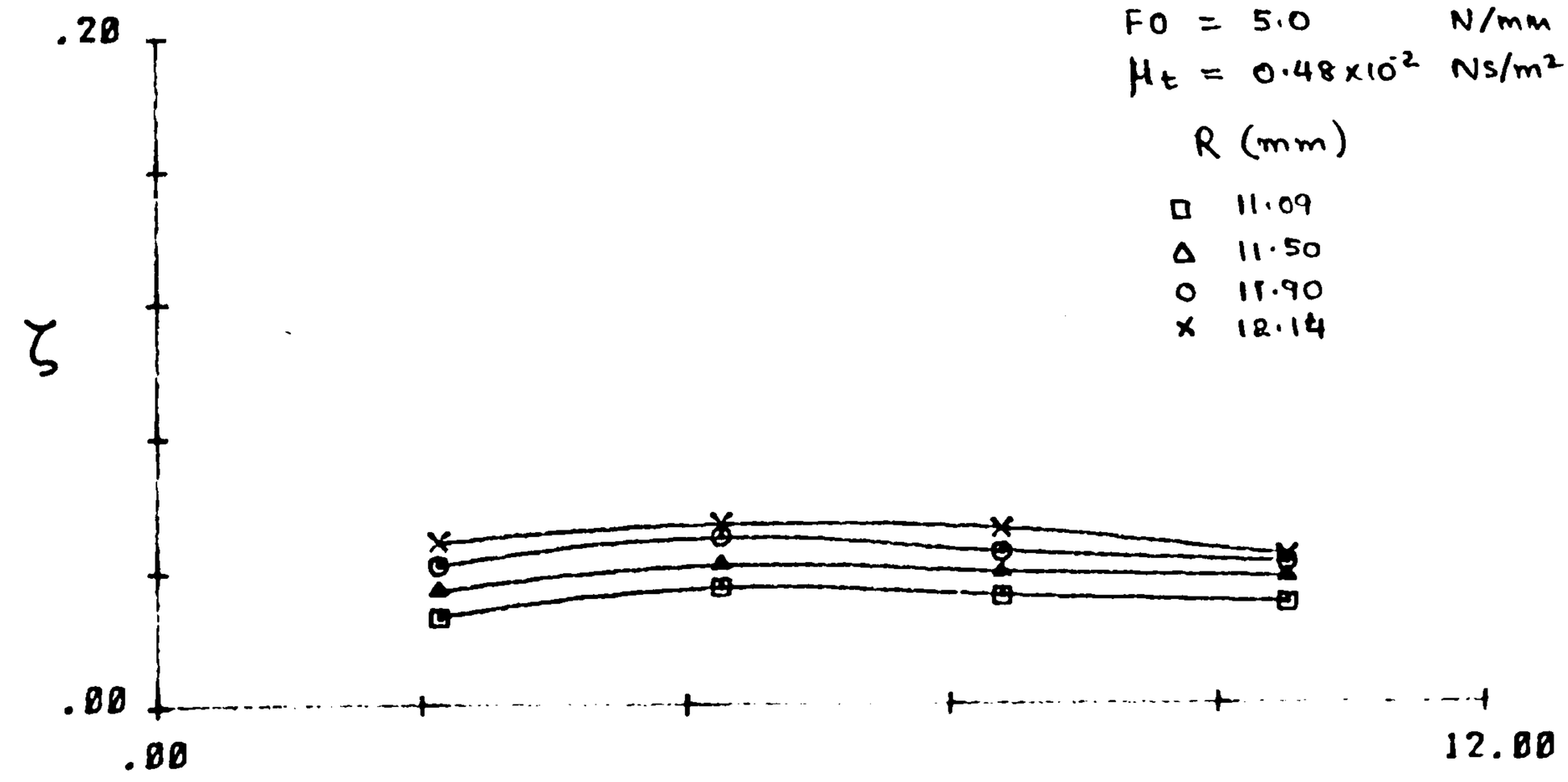

FIGURE 4.12(f)

DAMPING RATIO (ζ) Vs VISCOSITY (μ_t)

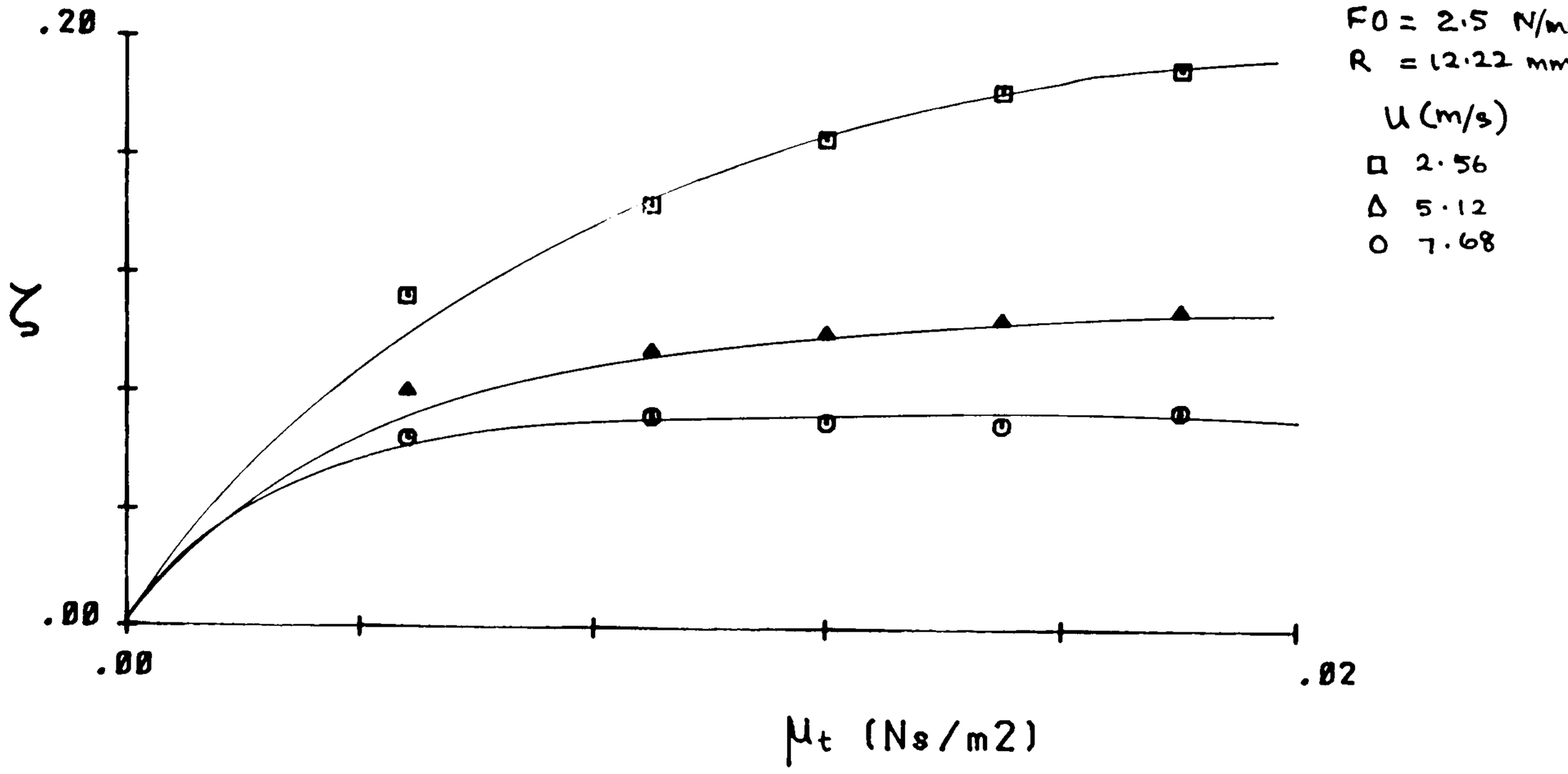

FIGURE 4.13(a)

DAMPING RATIO (ζ) Vs VISCOSITY (μ_t)

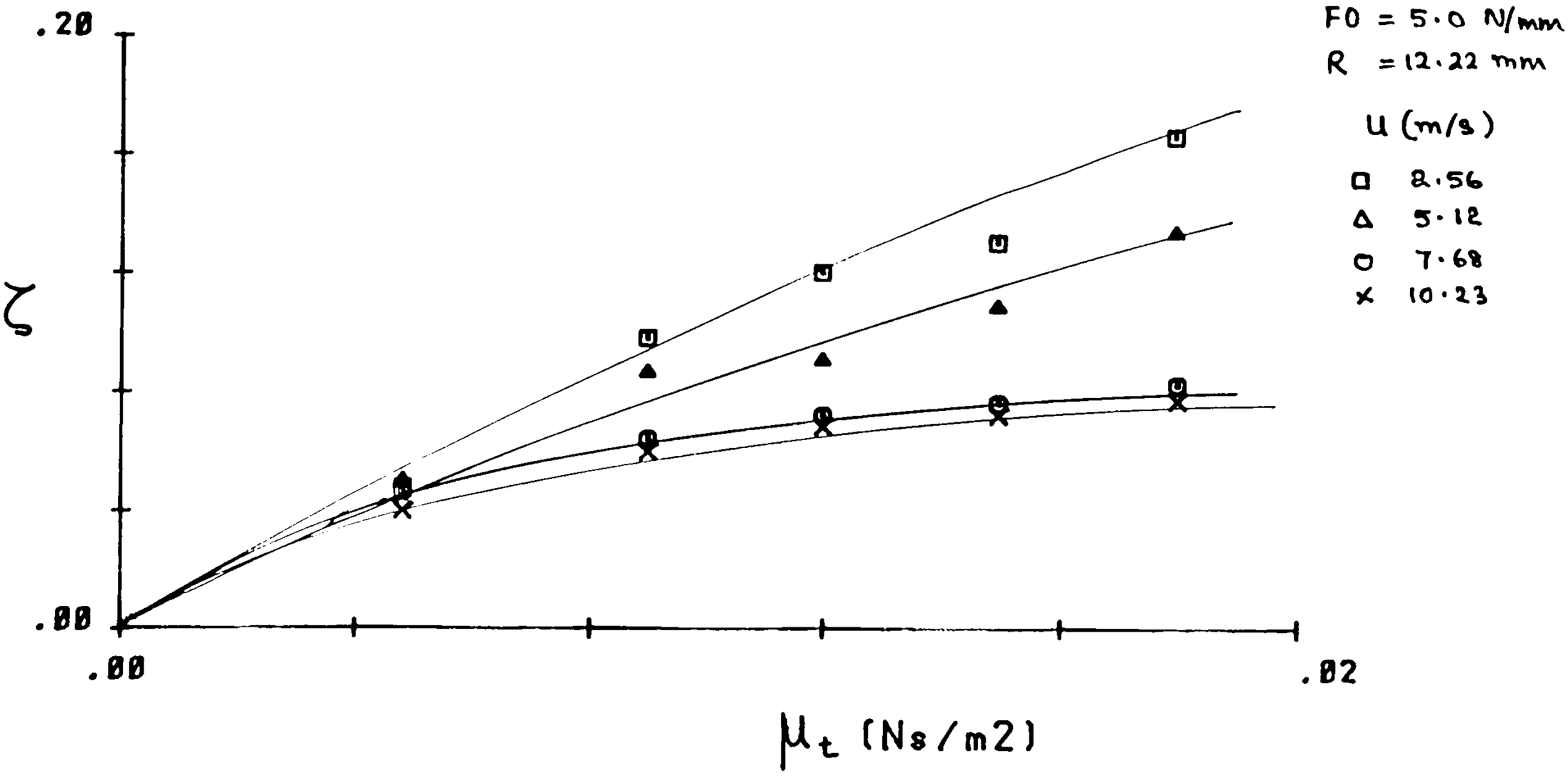

FIGURE 4.13(b)

DAMPING RATIO (ζ) Vs VISCOSITY (μ_t)

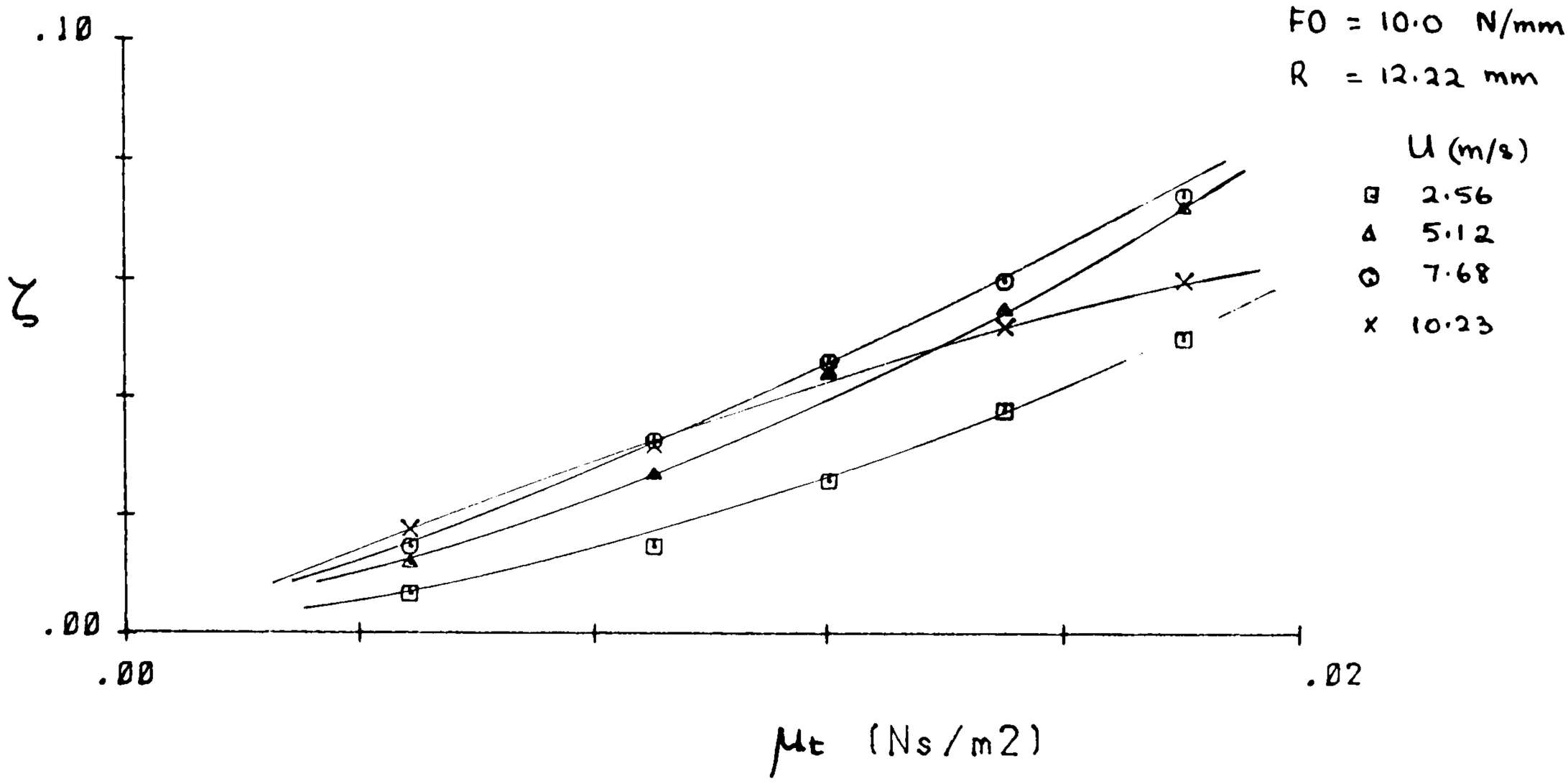

FIGURE 4.13(c)

DAMPING RATIO (ζ) Vs VISCOSITY (μ_t)

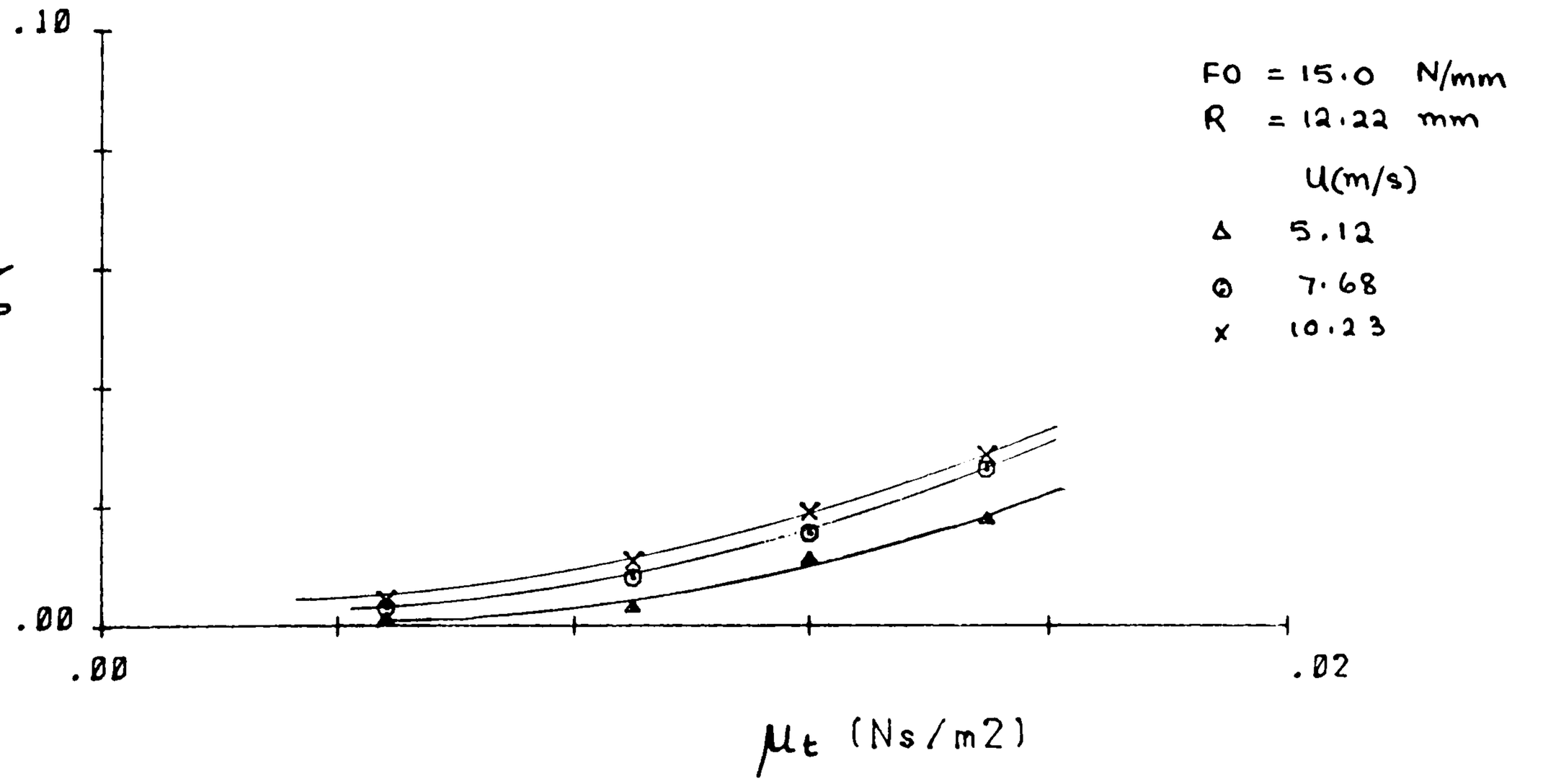

FIGURE 4.13(d)

DAMPING RATIO (ζ) Vs RADIUS (R)

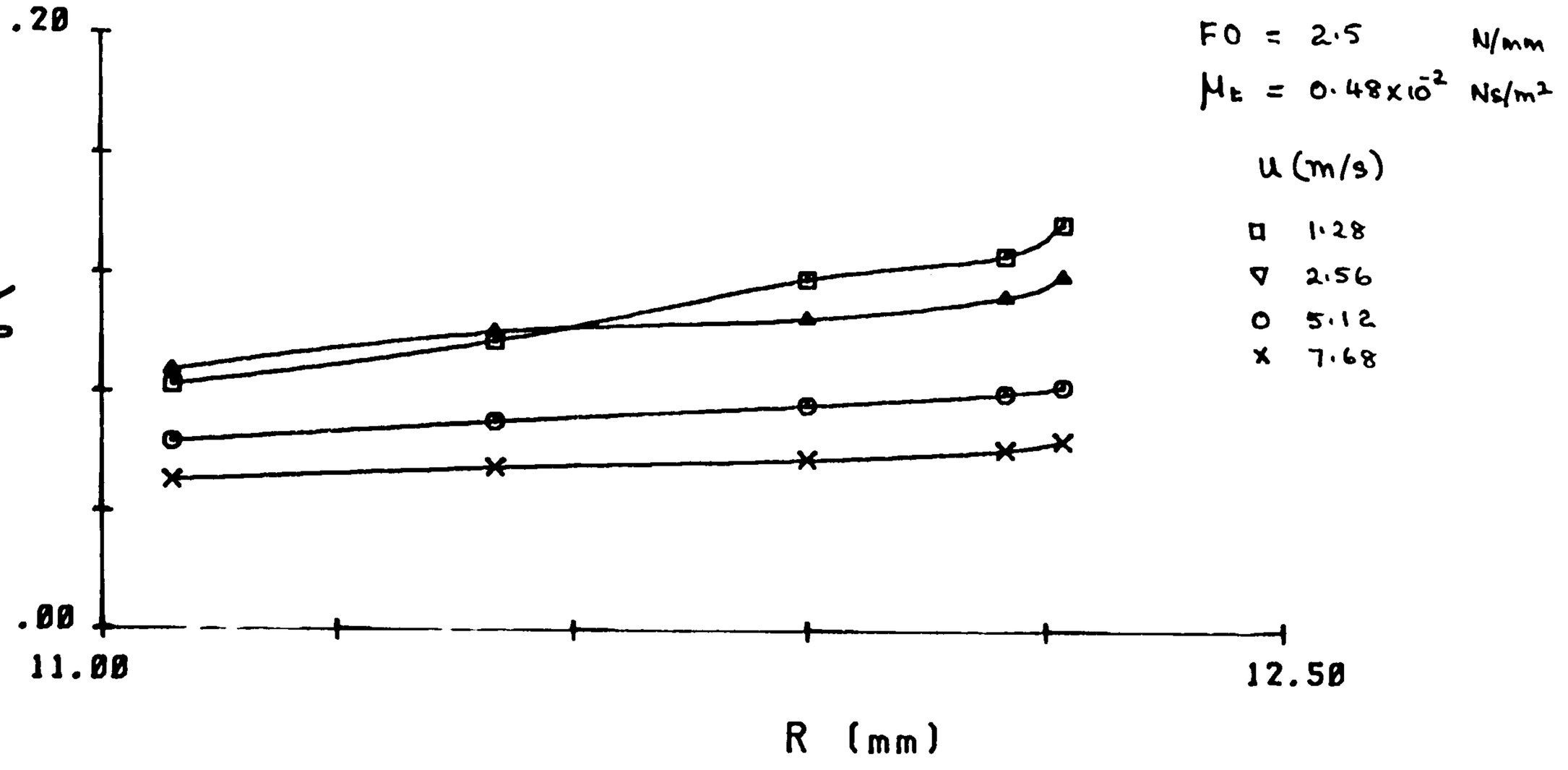

FIGURE 4.14(a)

DAMPING RATIO (ζ) Vs RADIUS (R)

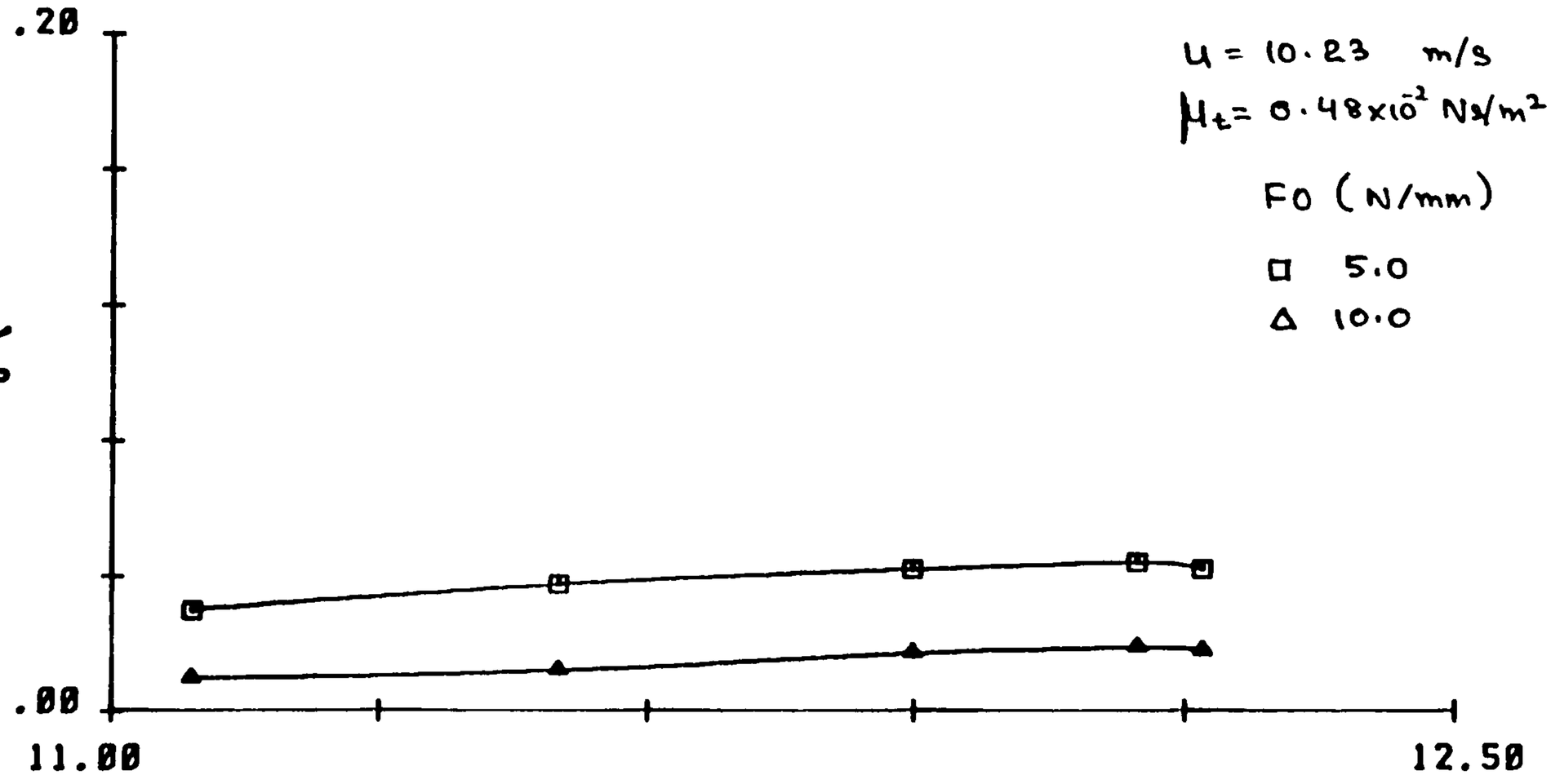

FIGURE 4.14(b)

DAMPING RATIO (ζ) Vs RADIUS (R)

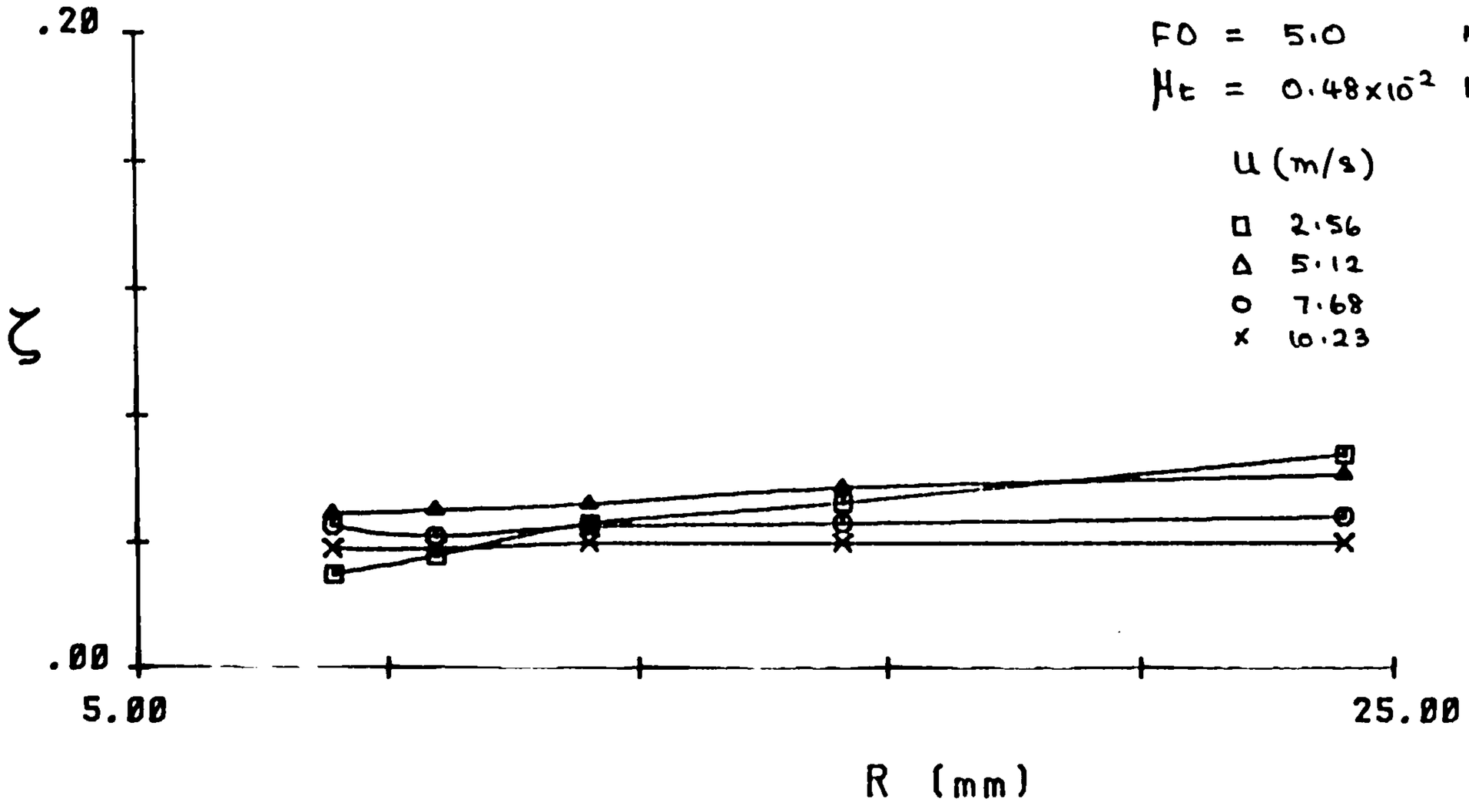

FIGURE 4.14(c)

DAMPING RATIO (ζ) Vs RADIUS (R)

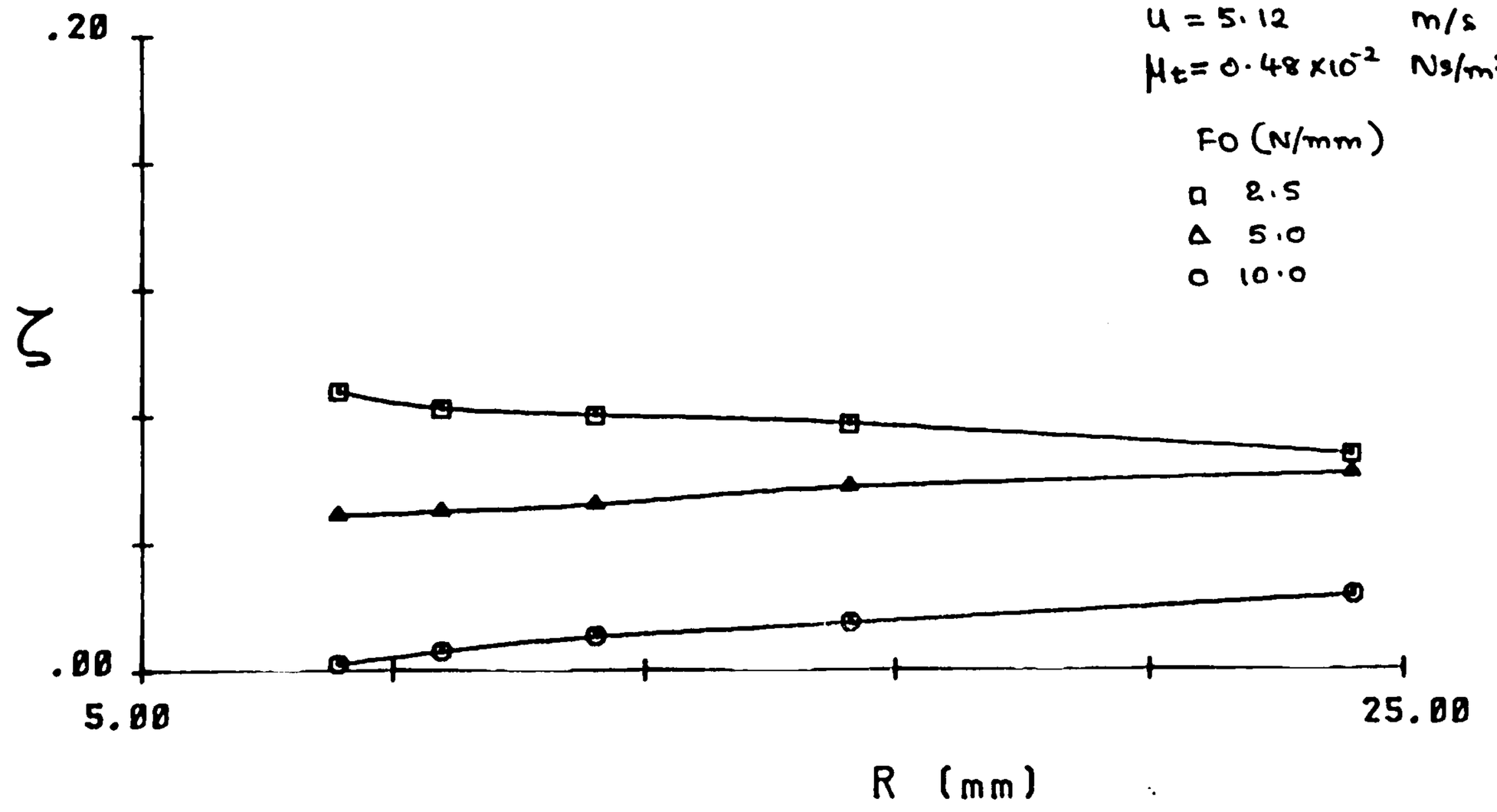

FIGURE 4.14(d)

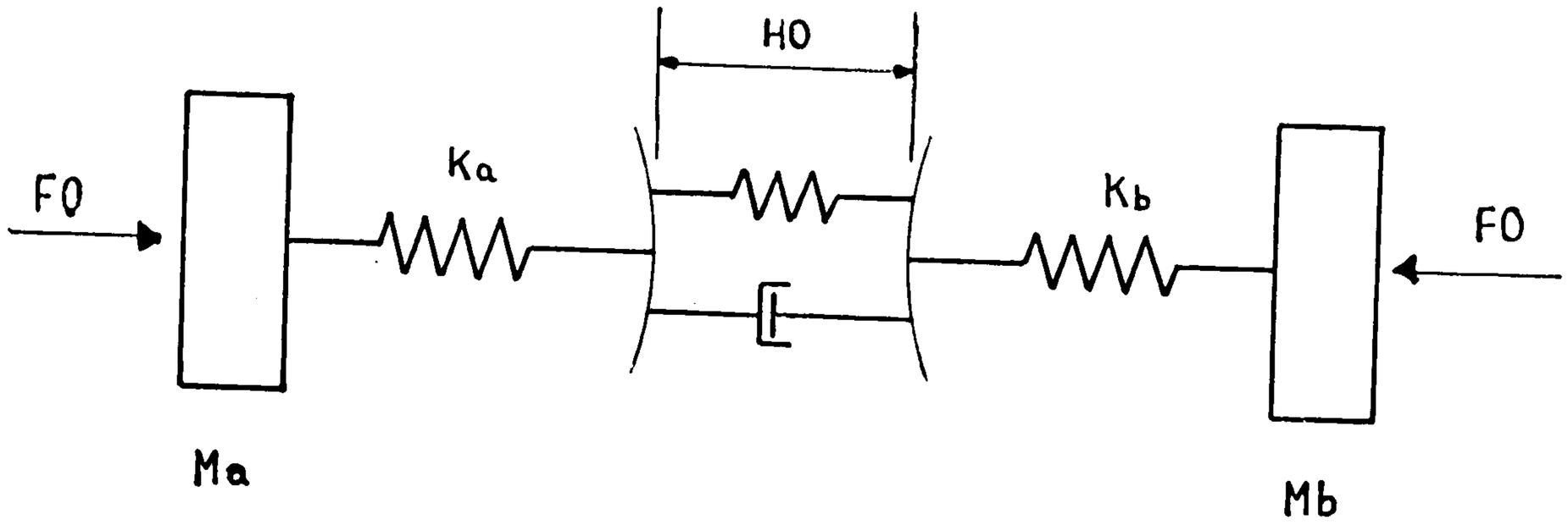

FIGURE 4.15

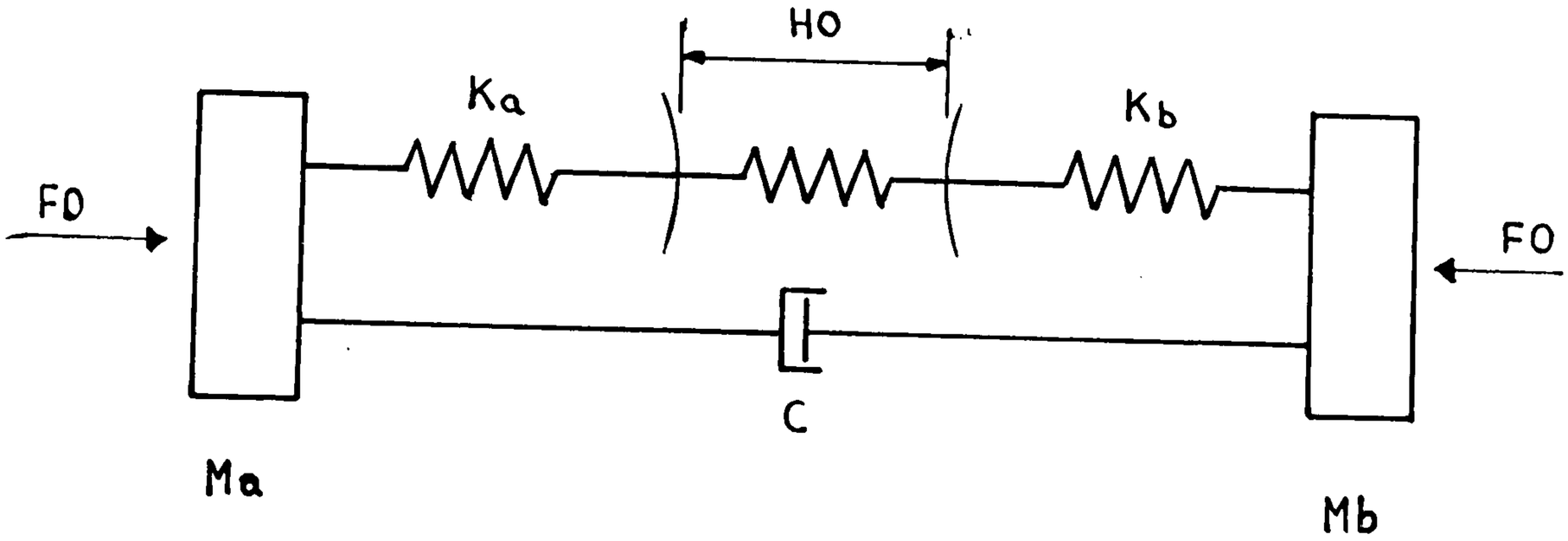

FIGURE 4.16

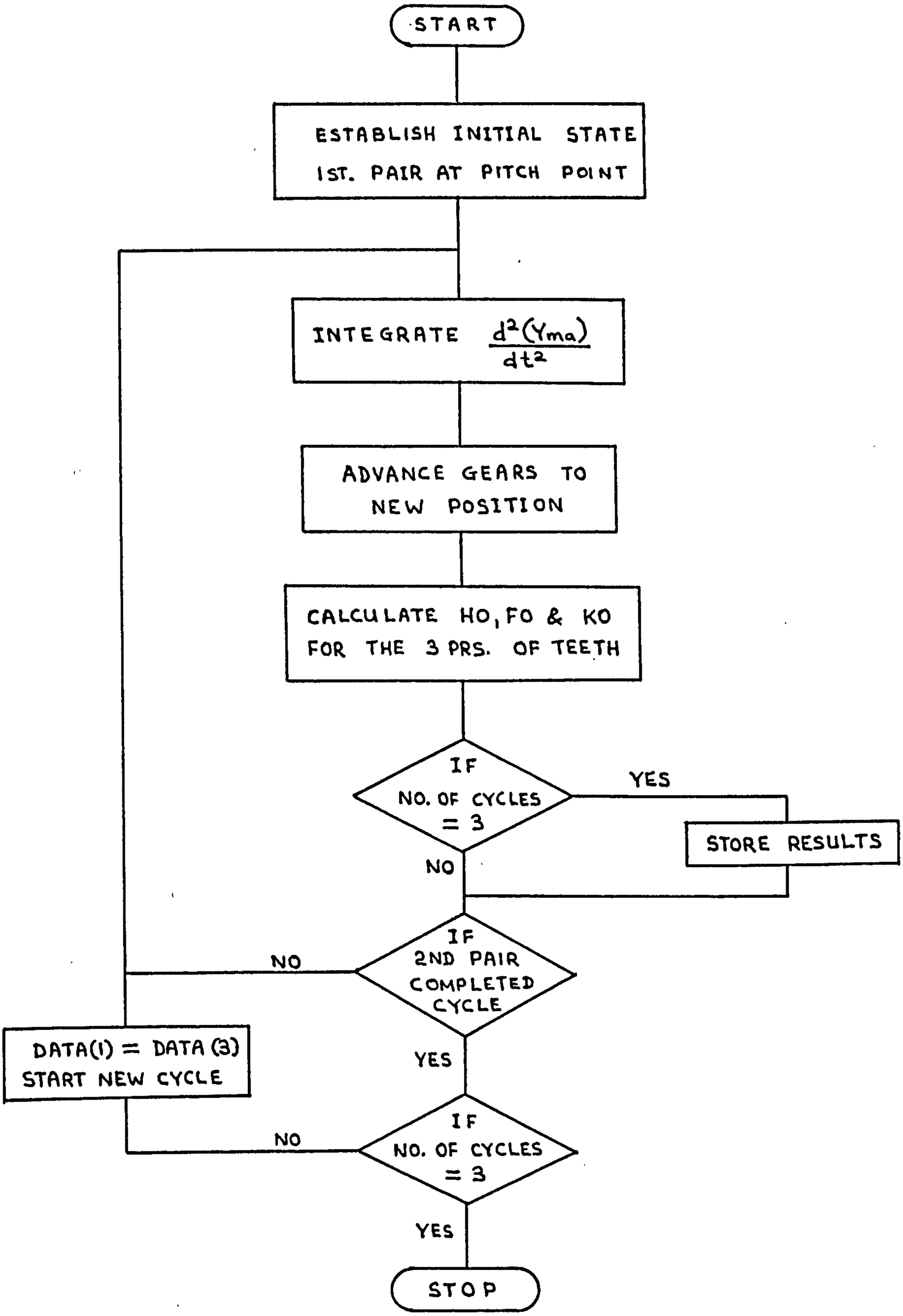

FLOW CHART OF THE DYNAMIC SIMULATION PROGRAMME

FIGURE 4.17

MAXM. DYNAMIC LOAD (DFMX) Vs SPEED (N)

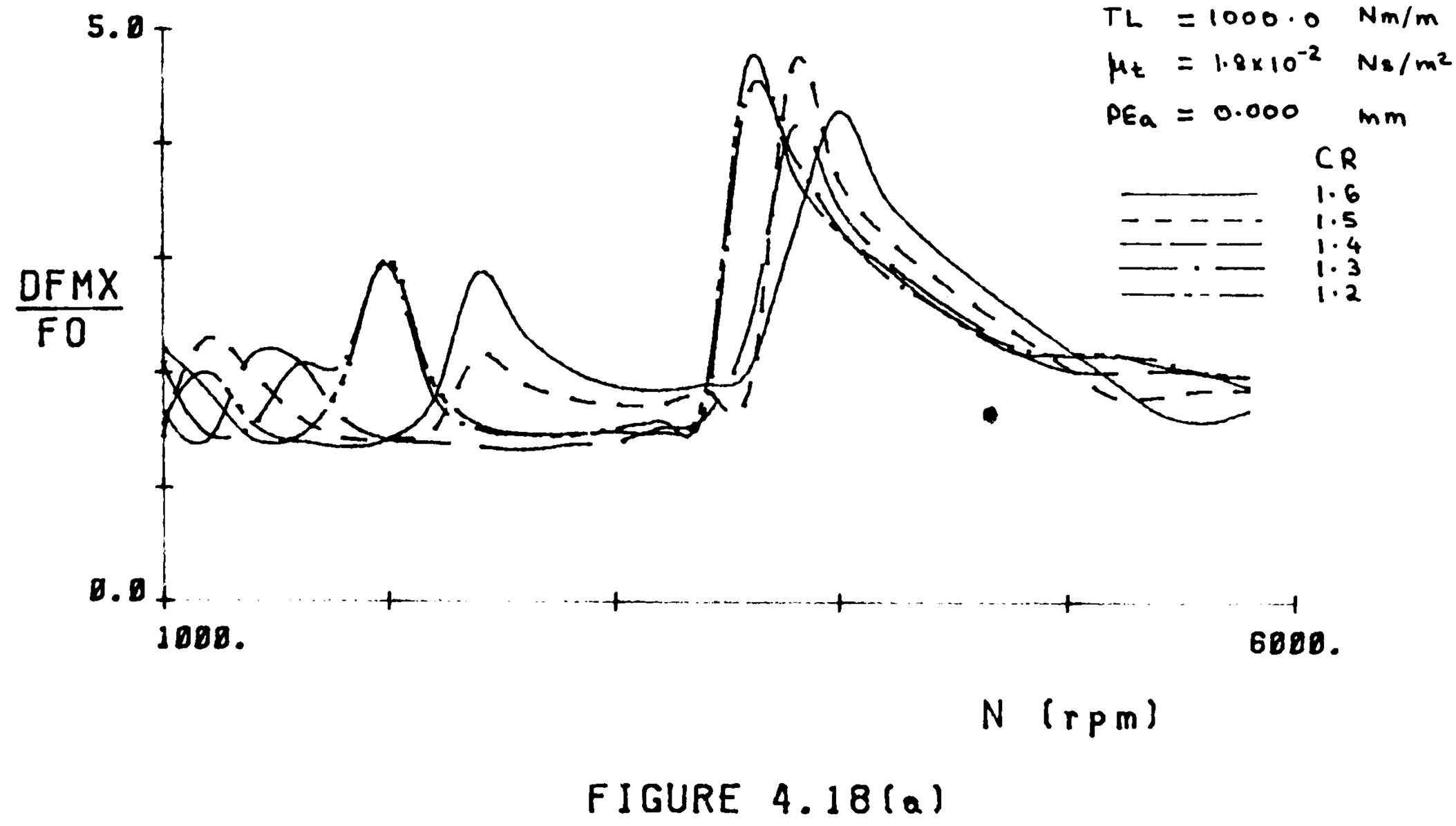

FIGURE 4.18(a)

MAXM. TOOTH FORCE (FMAX) Vs SPEED (N)

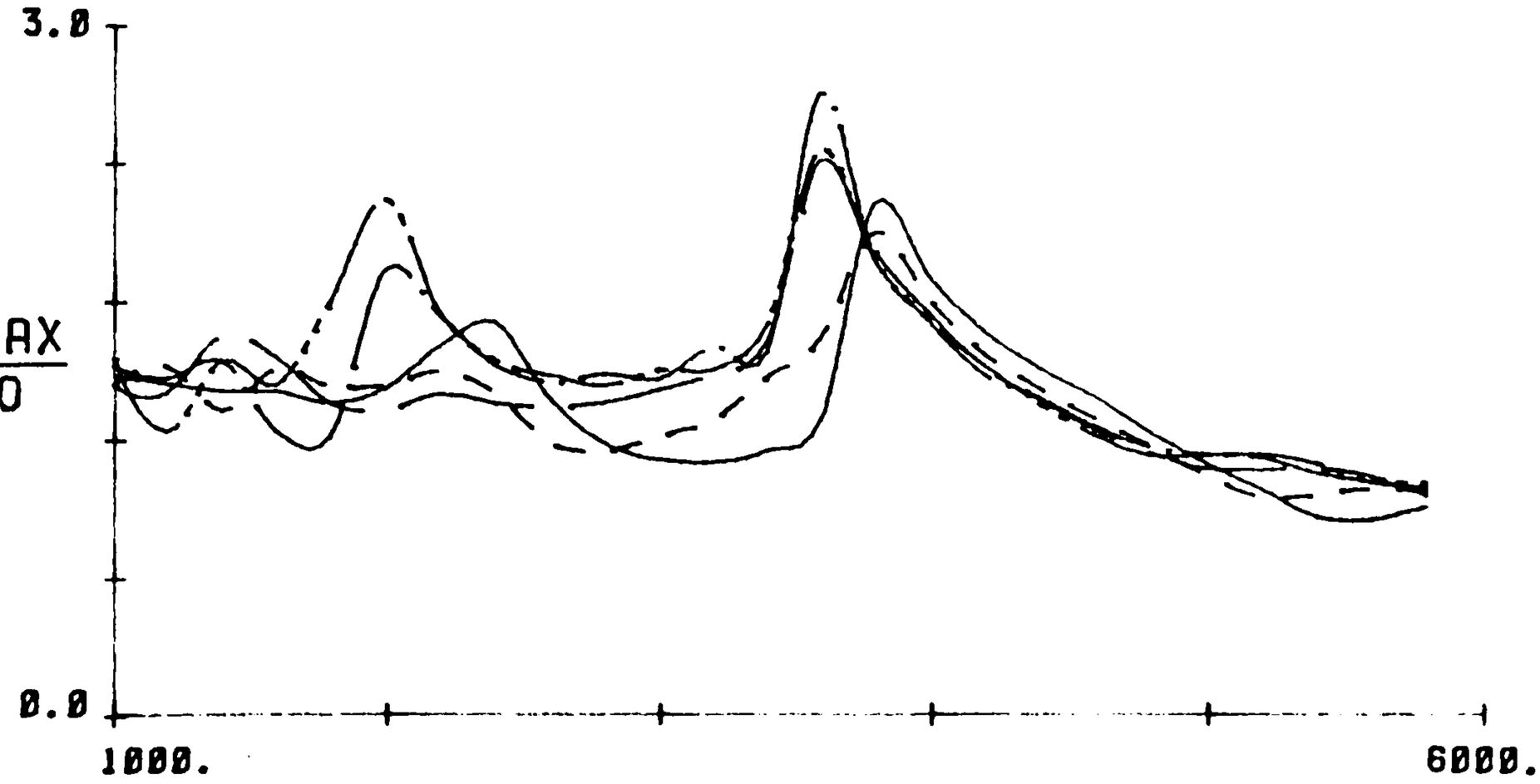

FIGURE 4.18(b)

MAXM. DYNAMIC LOAD (DFMX) Vs SPEED (N)

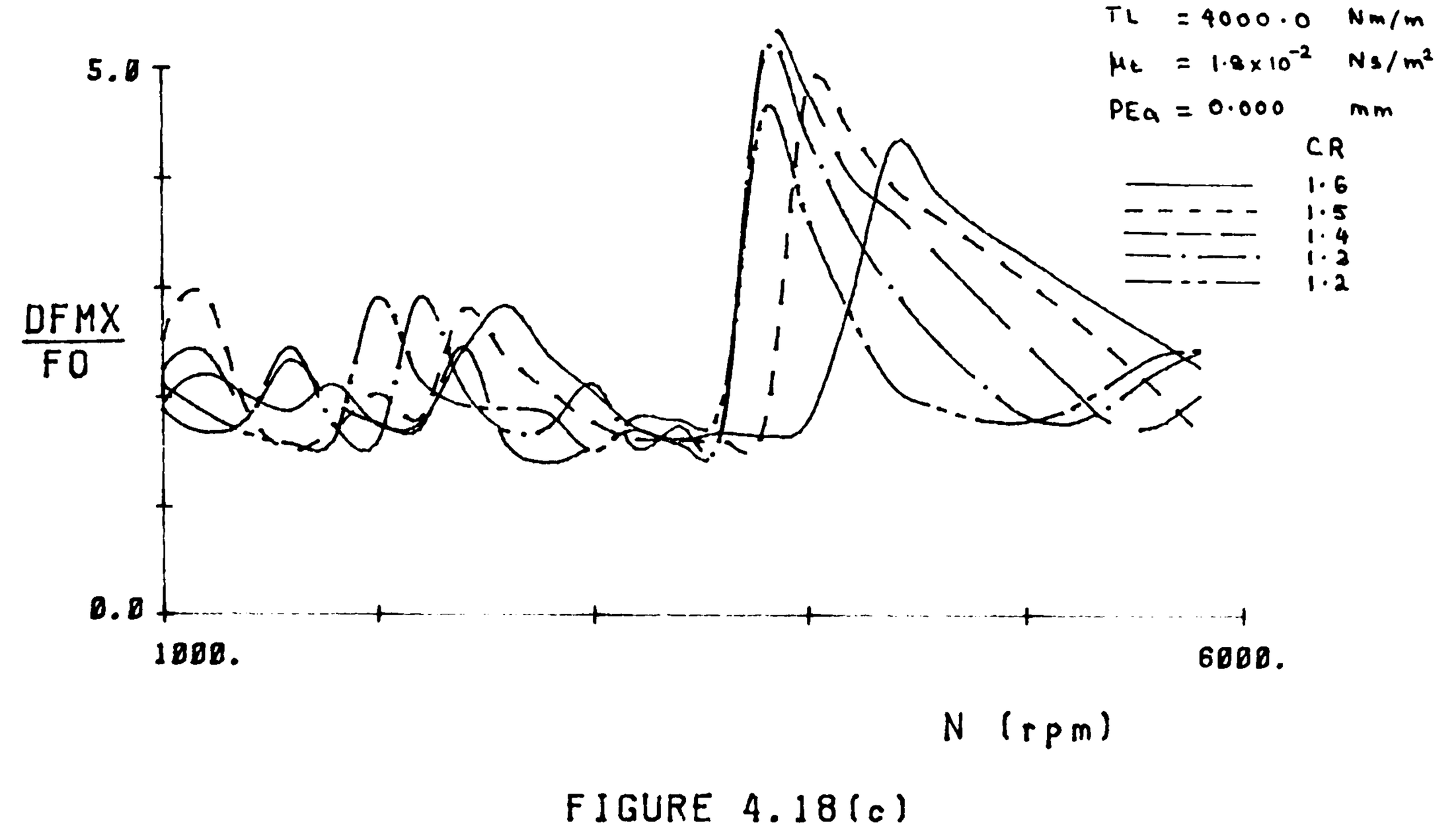

FIGURE 4.18(c)

MAXM. TOOTH FORCE (FMAX) Vs SPEED (N)

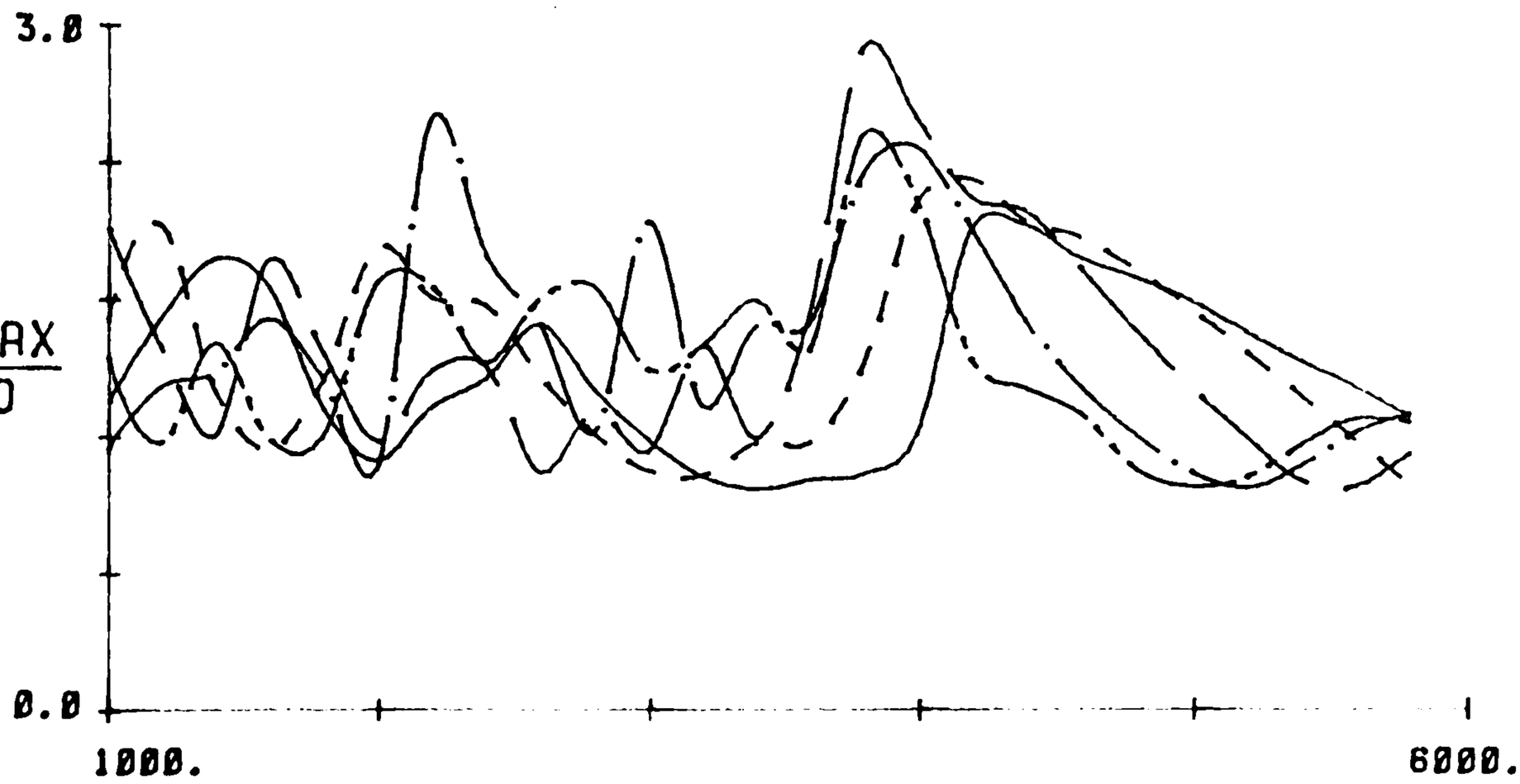

FIGURE 4.18(d)

MAXM. DYNAMIC LOAD (DFMX) Vs SPEED (N)

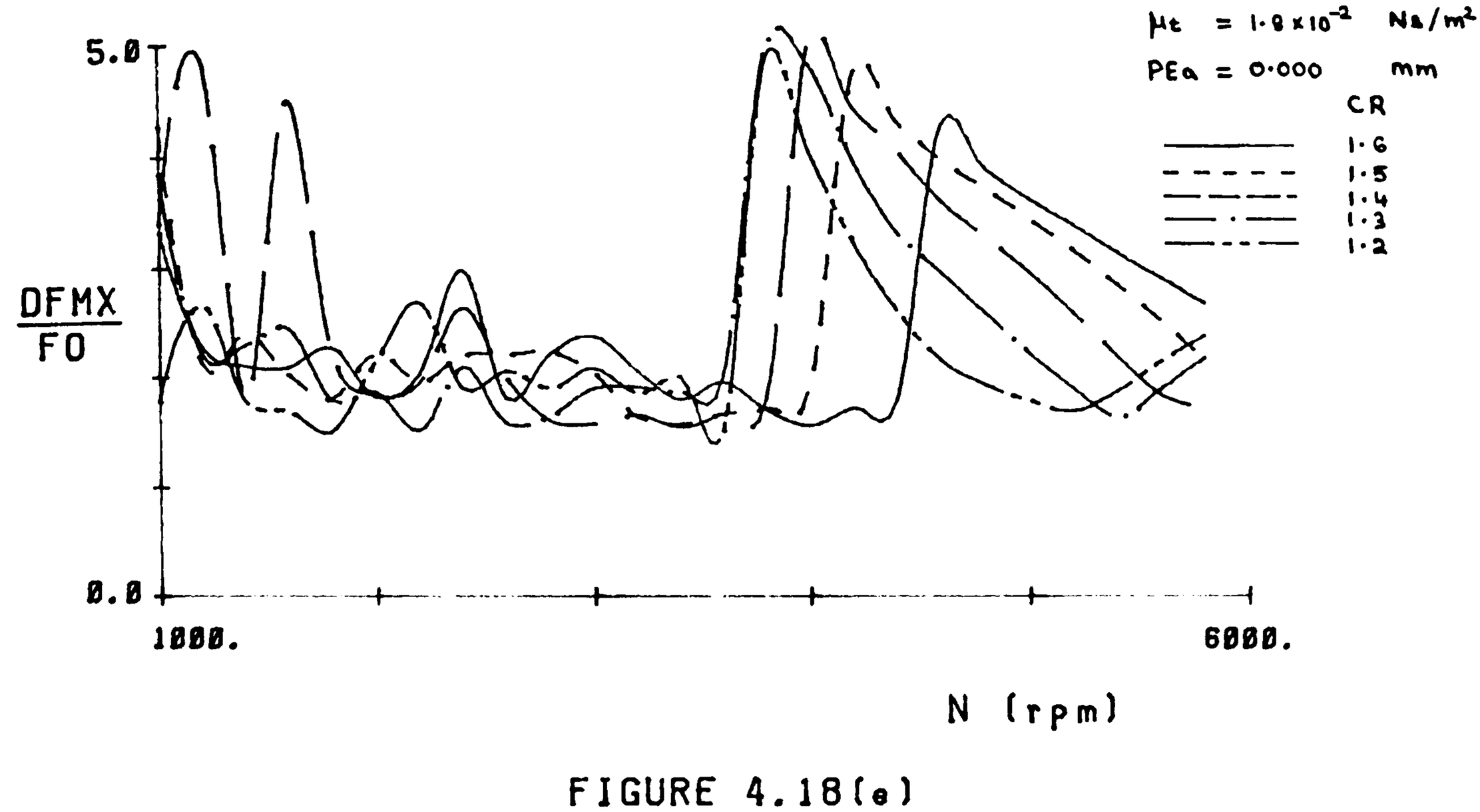

FIGURE 4.18(e)

MAXM. TOOTH FORCE (FMAX) Vs SPEED (N)

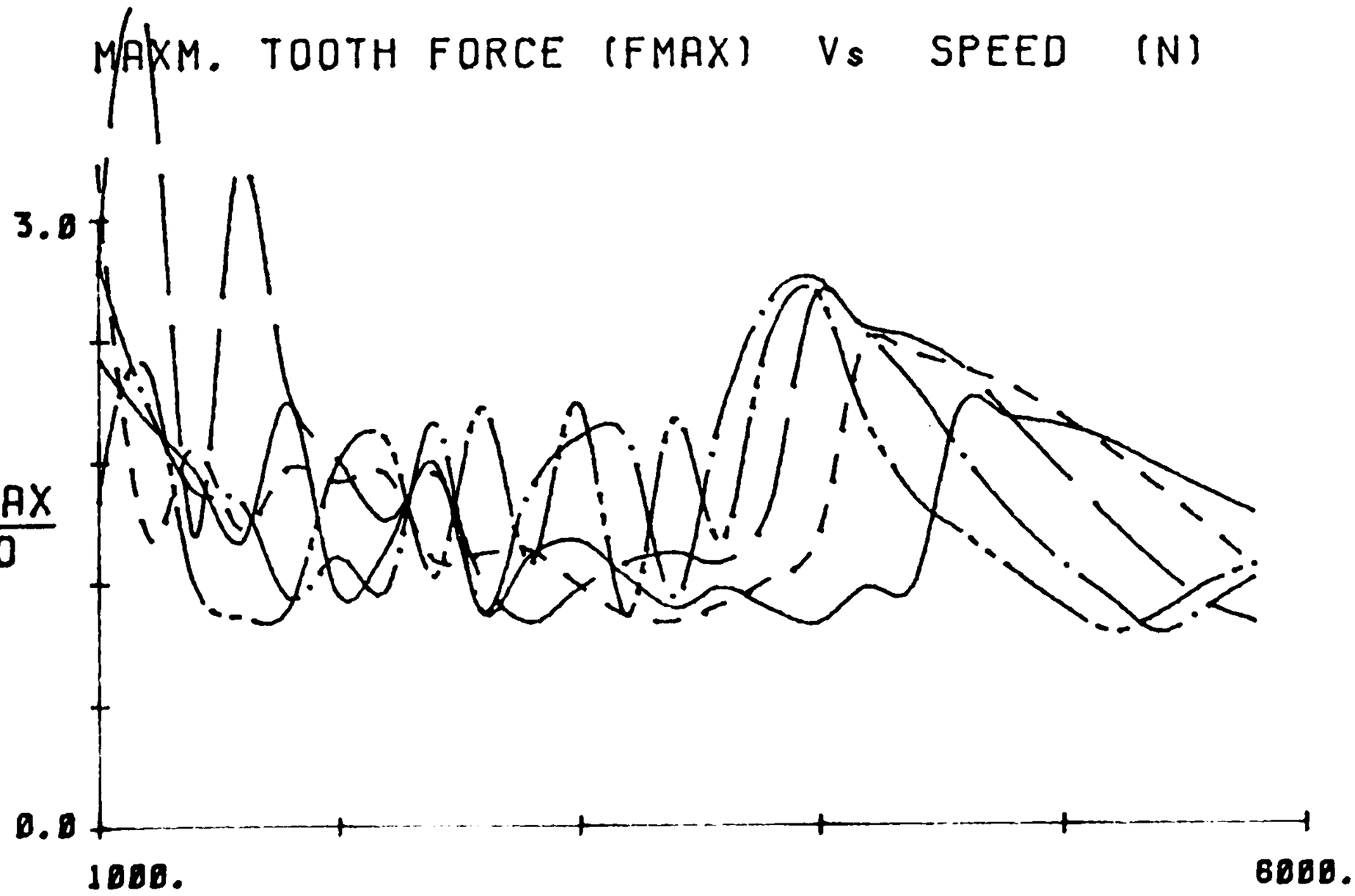

FIGURE 4.18(f)

MAXM. DYNAMIC LOAD (DFMX) Vs SPEED (N)

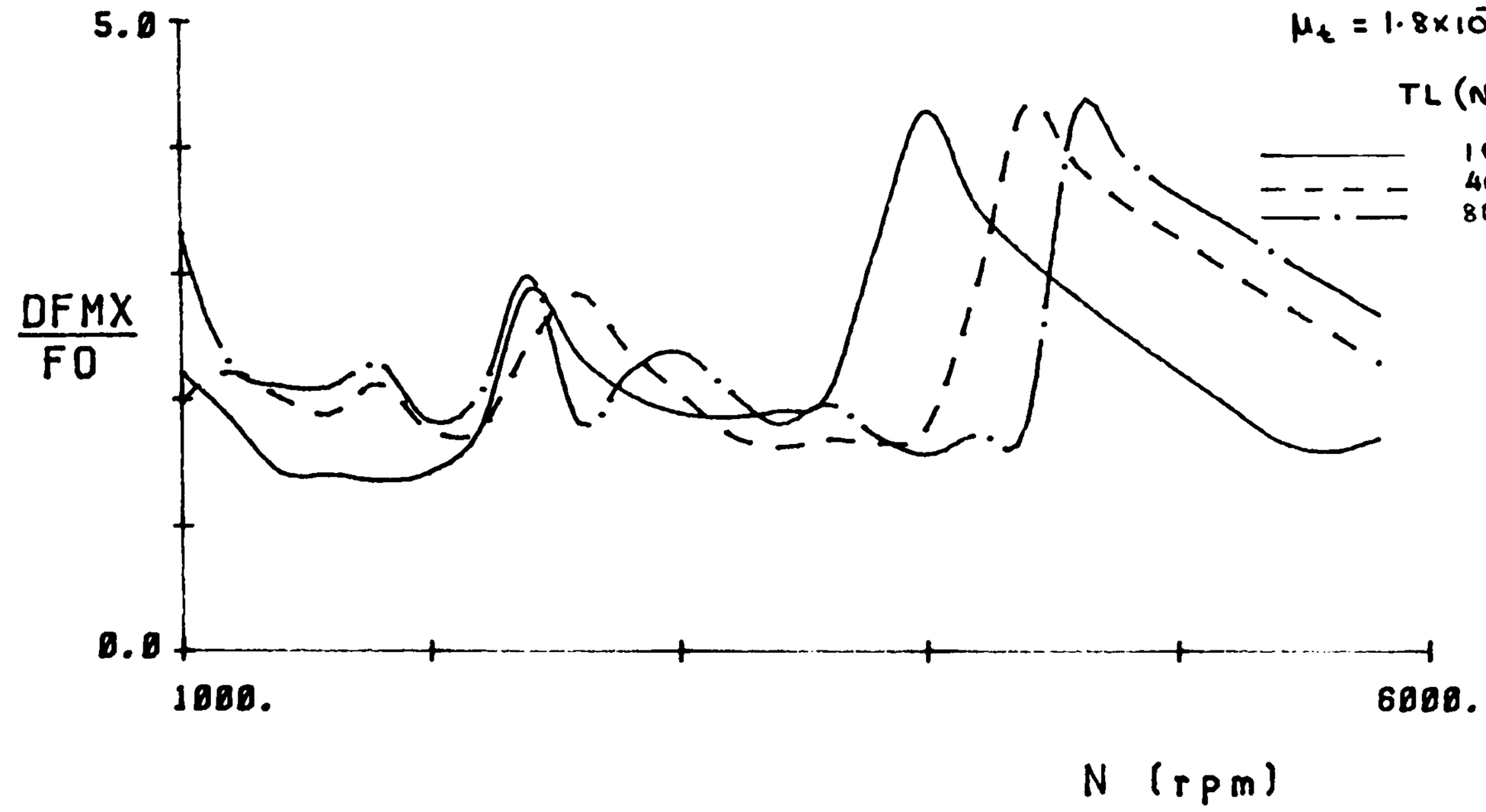

FIGURE 4.19(a)

MAXM. TOOTH FORCE (FMAX) Vs SPEED (N)

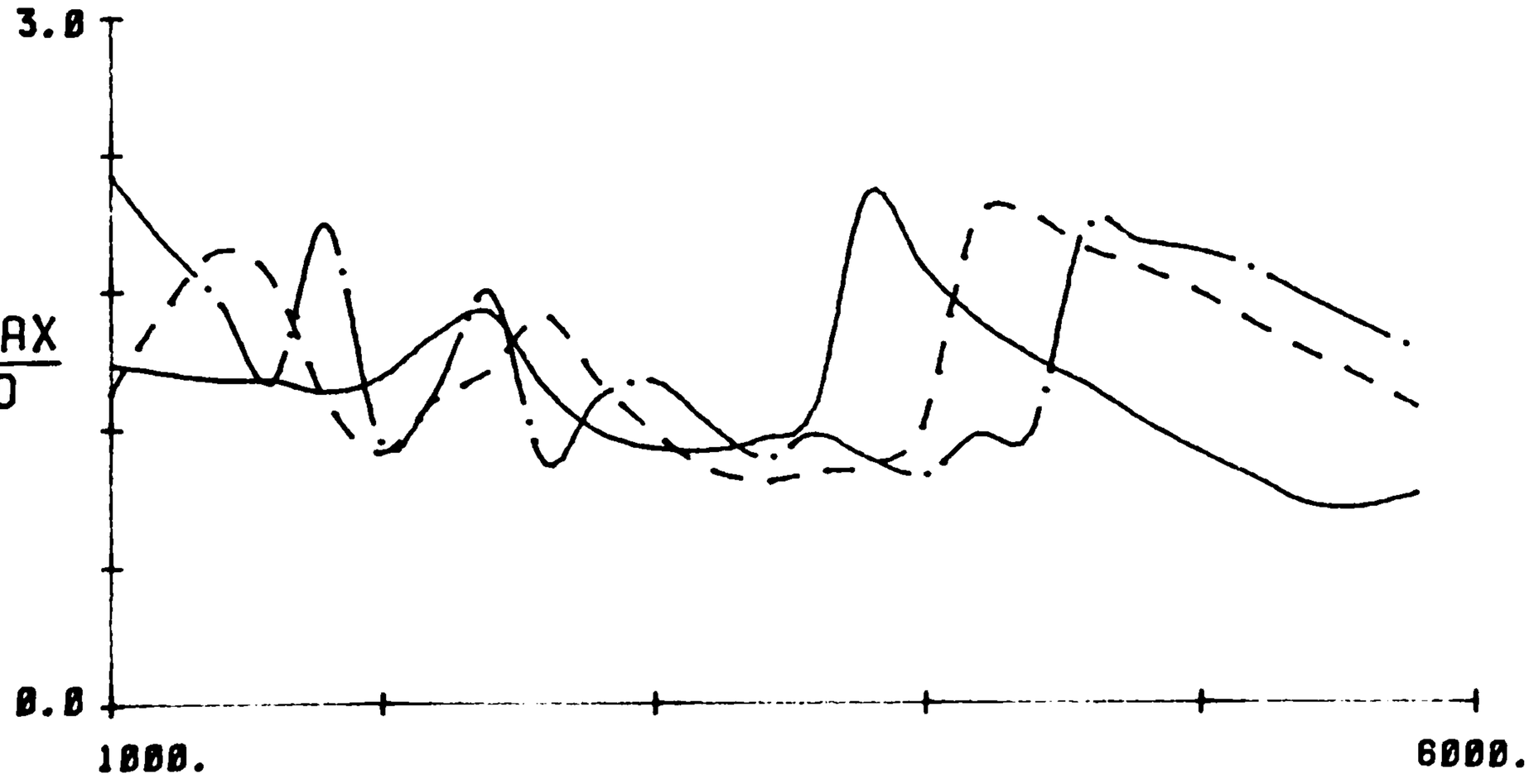

FIGURE 4.19(b)

MAXM. DYNAMIC LOAD (DFMX) Vs SPEED (N)

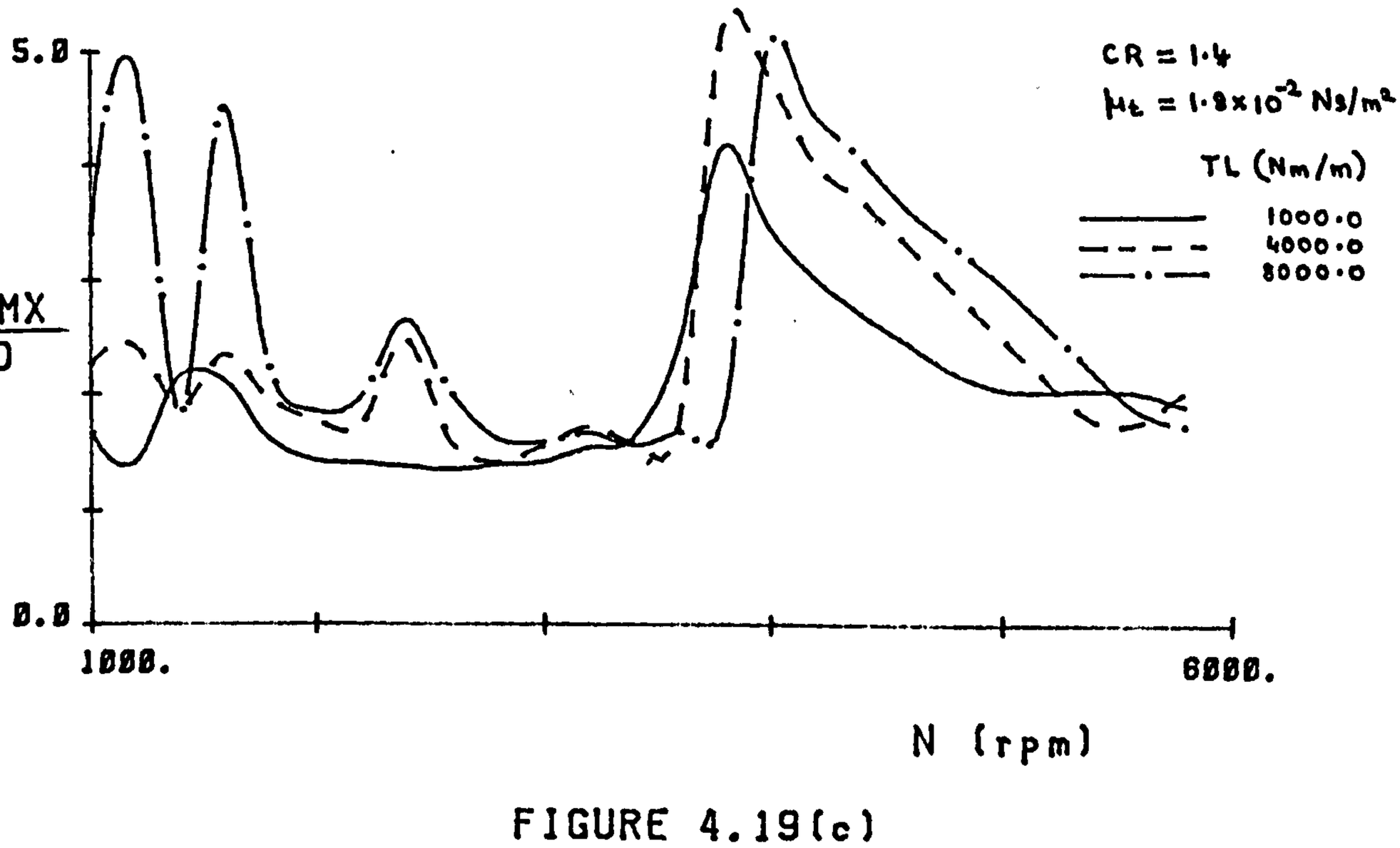

FIGURE 4.19(c)

MAXM. TOOTH FORCE (FMAX) Vs SPEED (N)

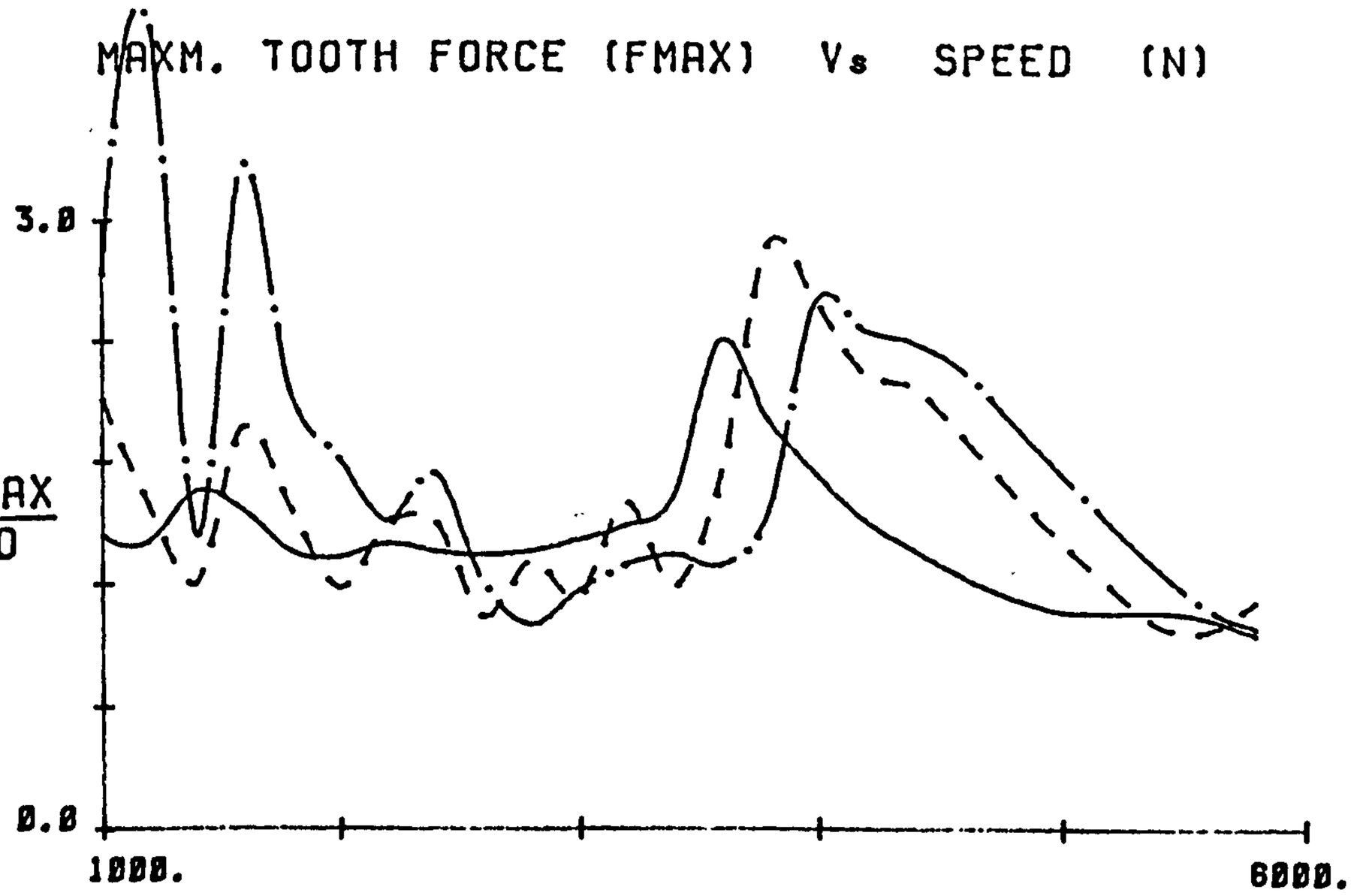

FIGURE 4.19(d)

MAXM. DYNAMIC LOAD (DFMX) Vs SPEED (N)

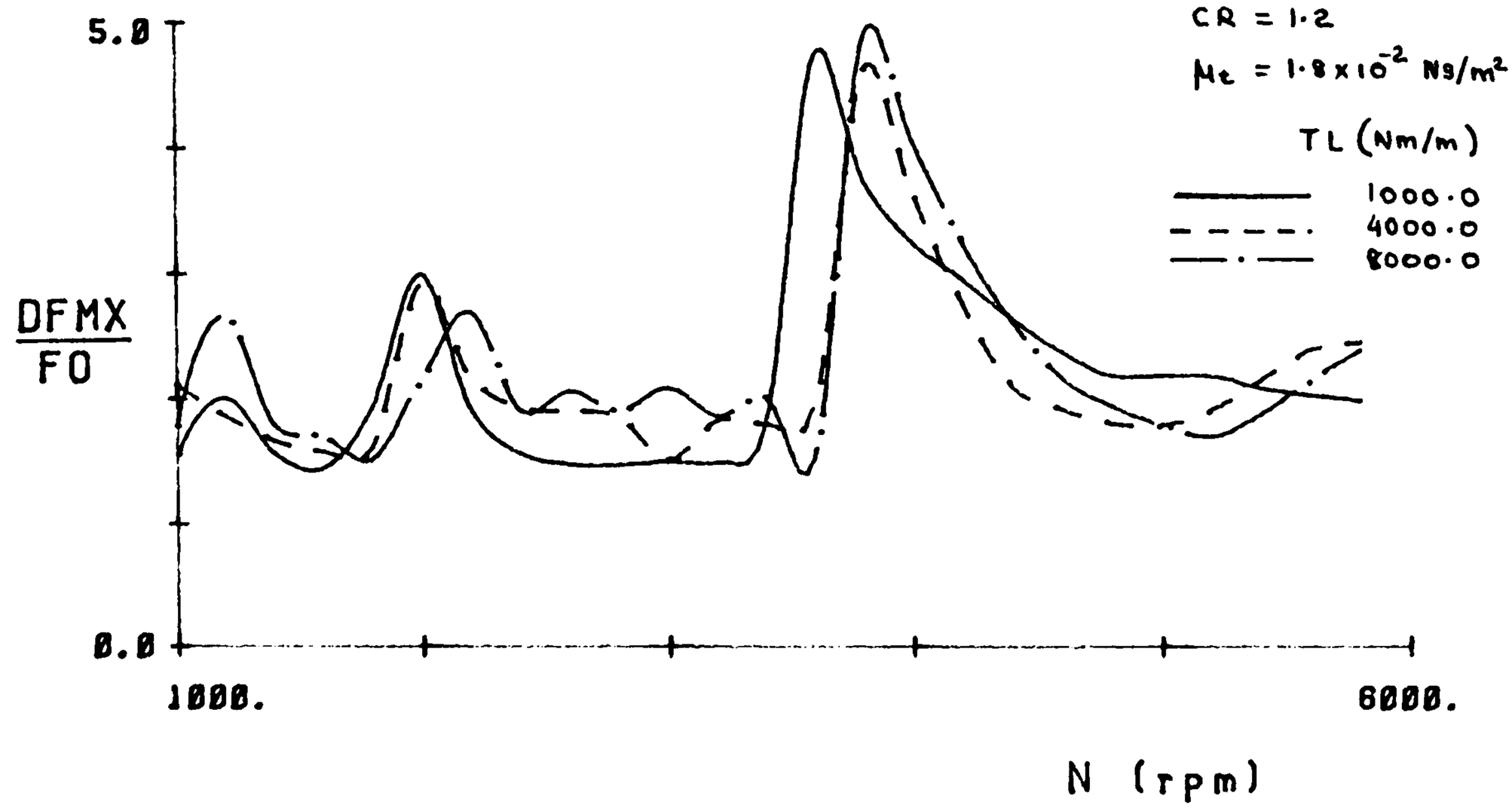

FIGURE 4.19(e)

MAXM. TOOTH FORCE (FMAX) Vs SPEED (N)

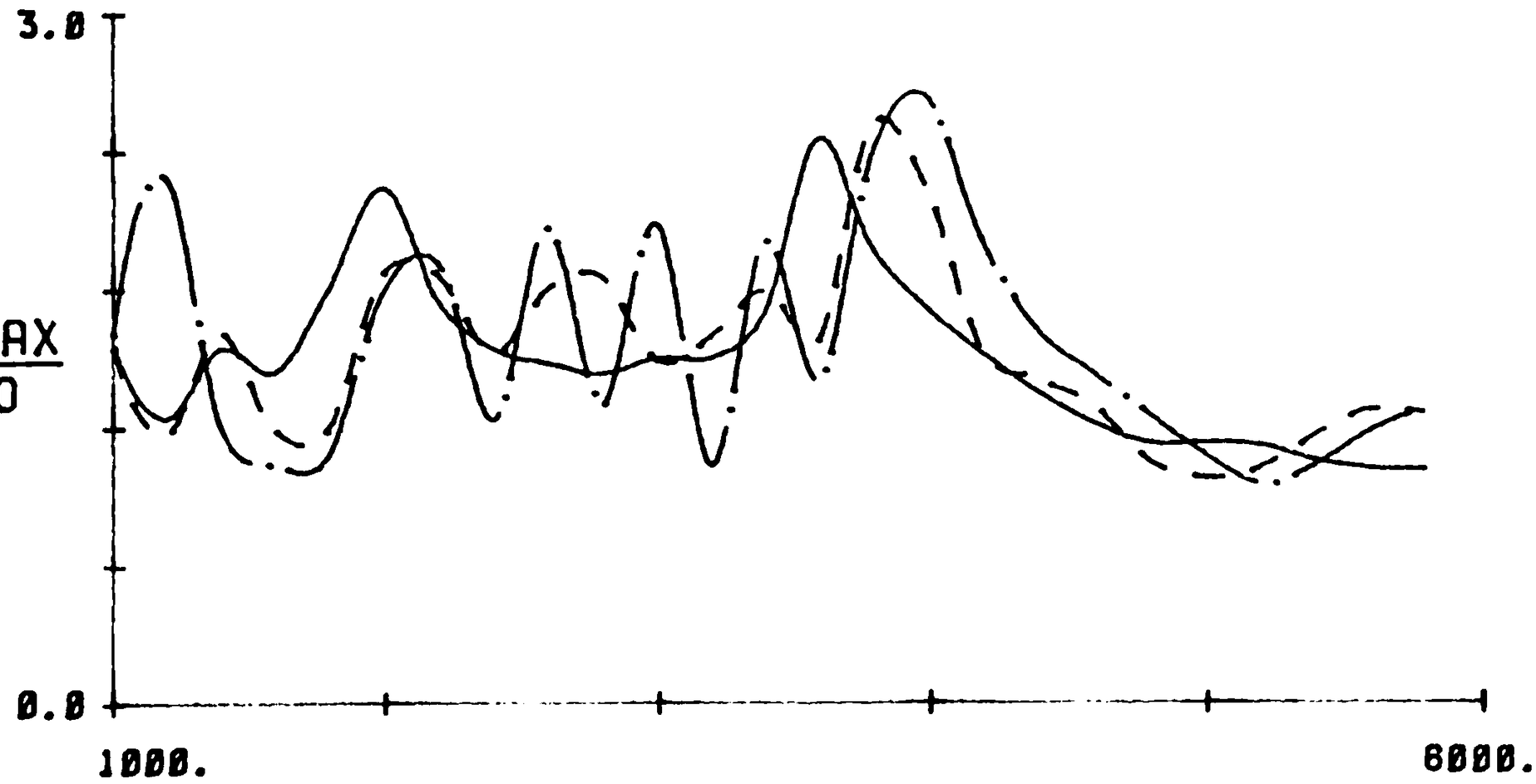

FIGURE 4.19(f)

MAXM. DYNAMIC LOAD (DFMX) Vs SPEED (N)

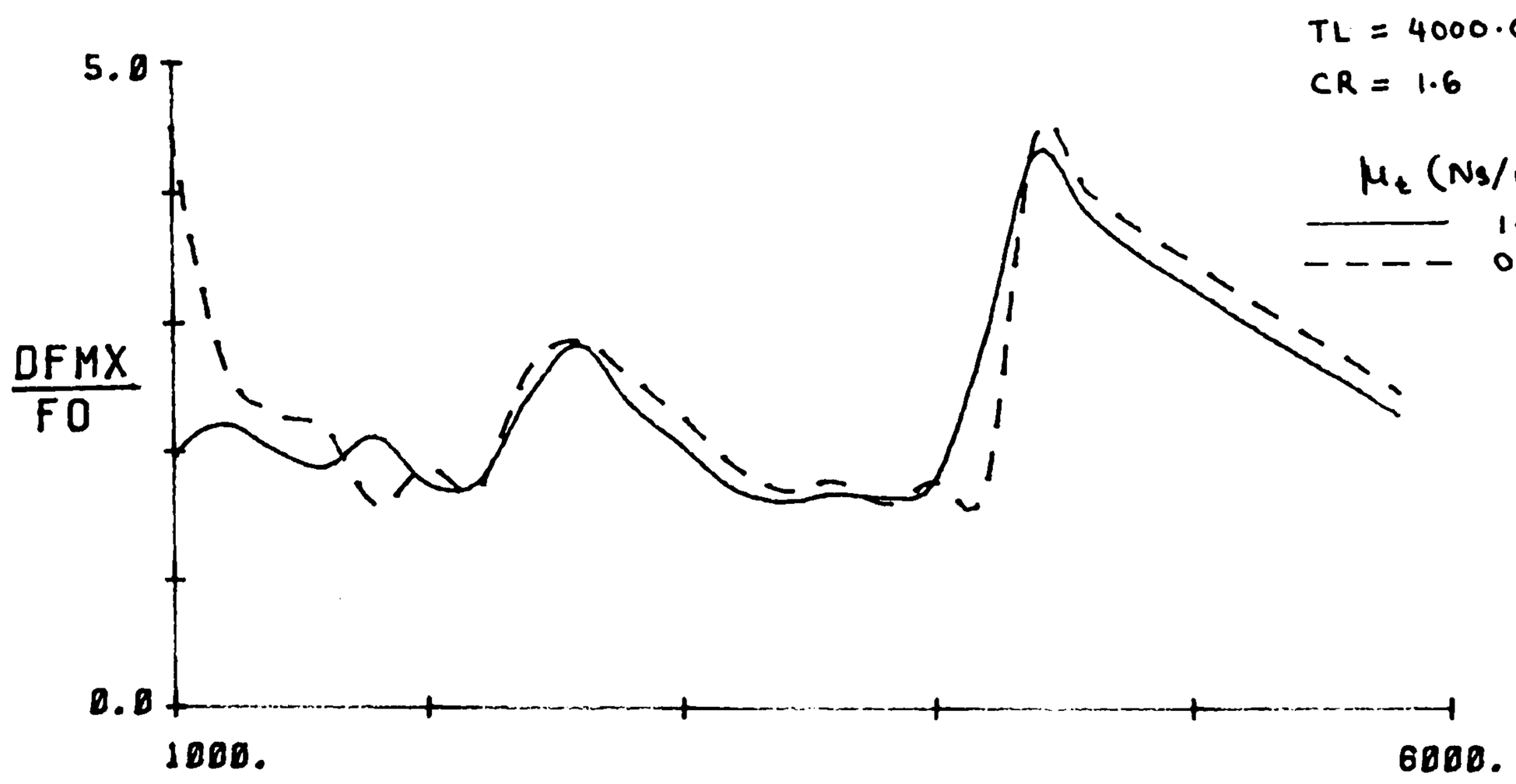

FIGURE 4.20(a)

MAXM. TOOTH FORCE (FMAX) Vs SPEED (N)

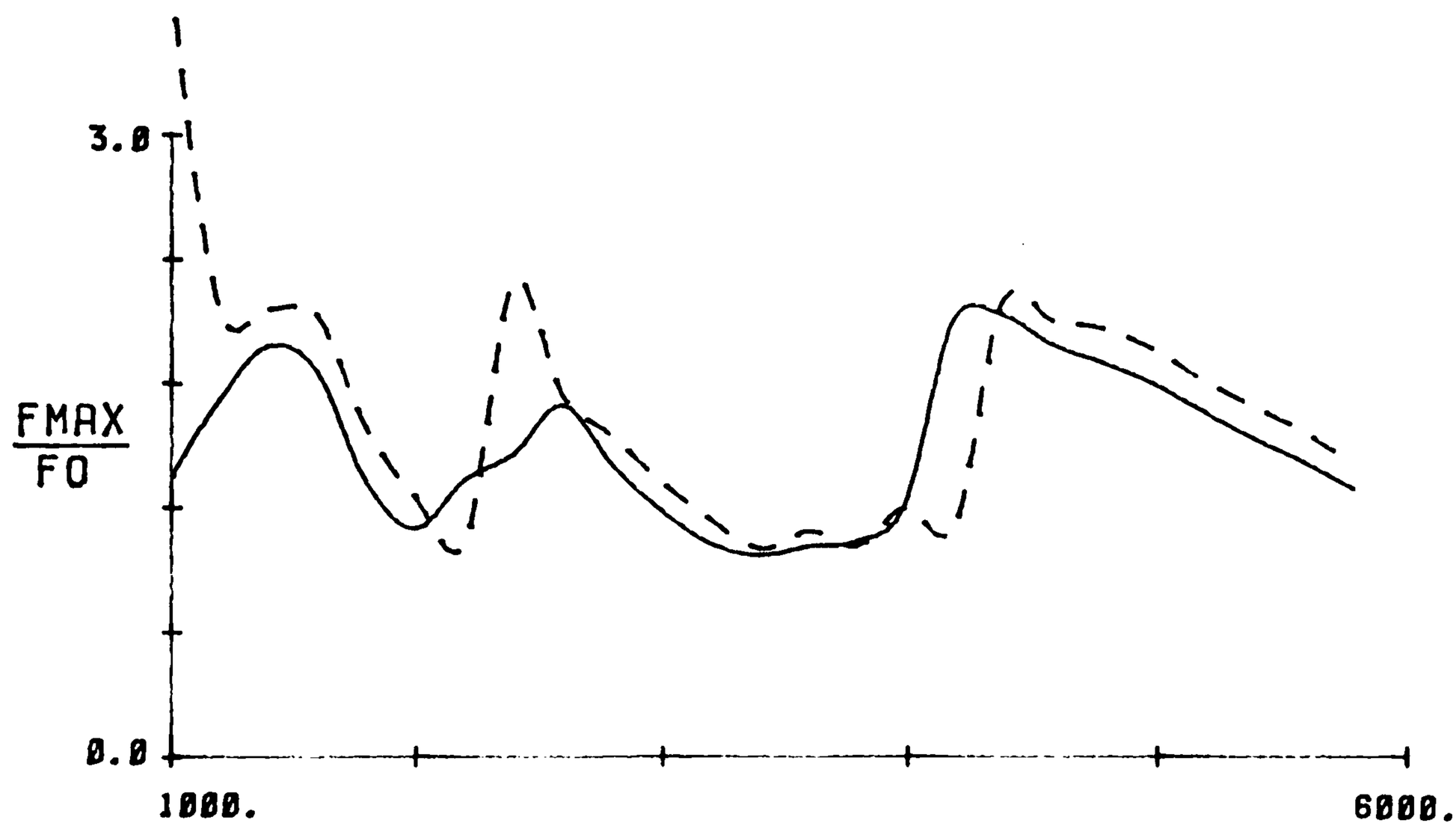

FIGURE 4.20(b)

MAXM. DYNAMIC LOAD (DFMX) Vs SPEED (N)

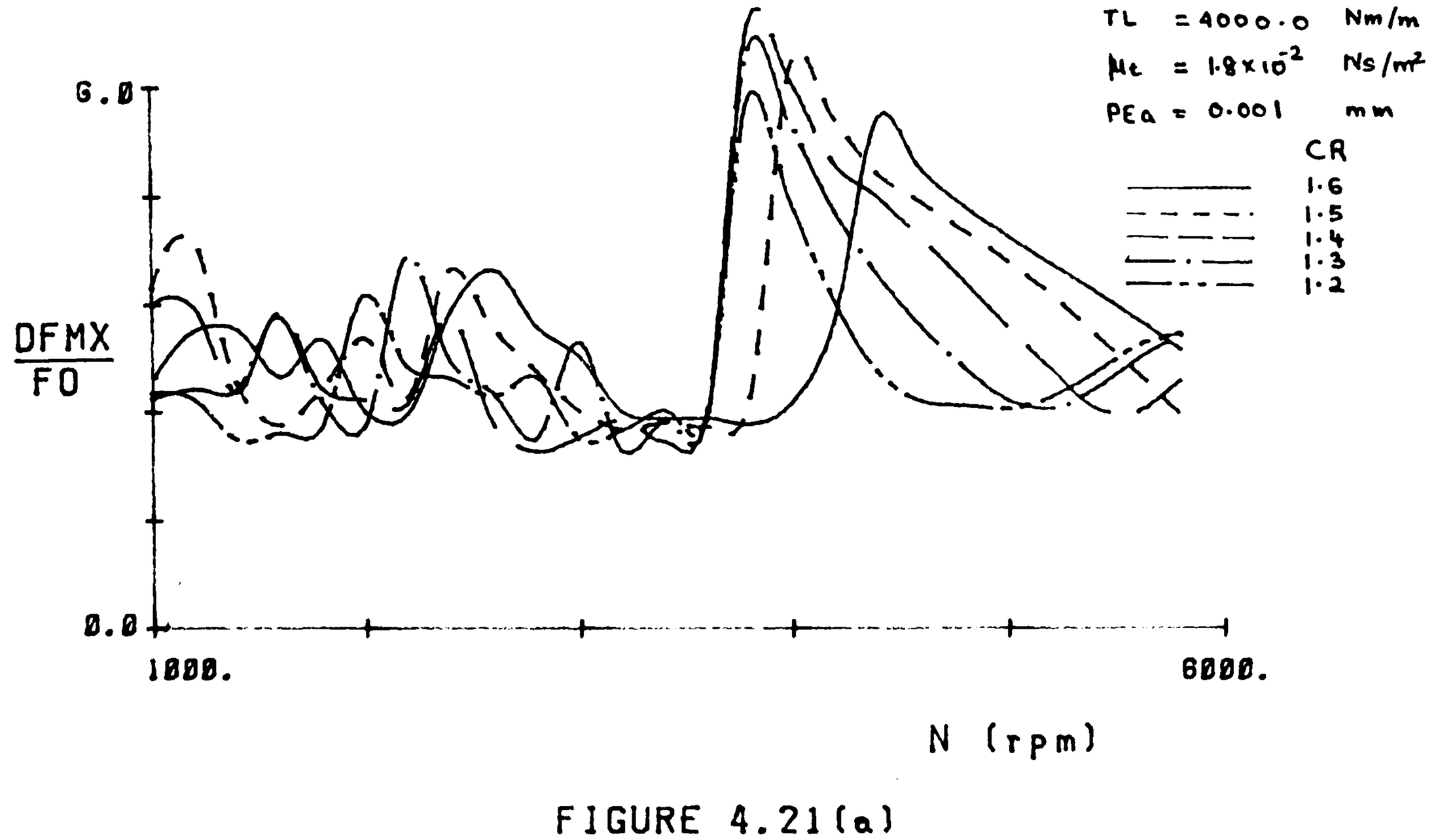

FIGURE 4.21(a)

MAXM. TOOTH FORCE (FMAX) Vs SPEED (N)

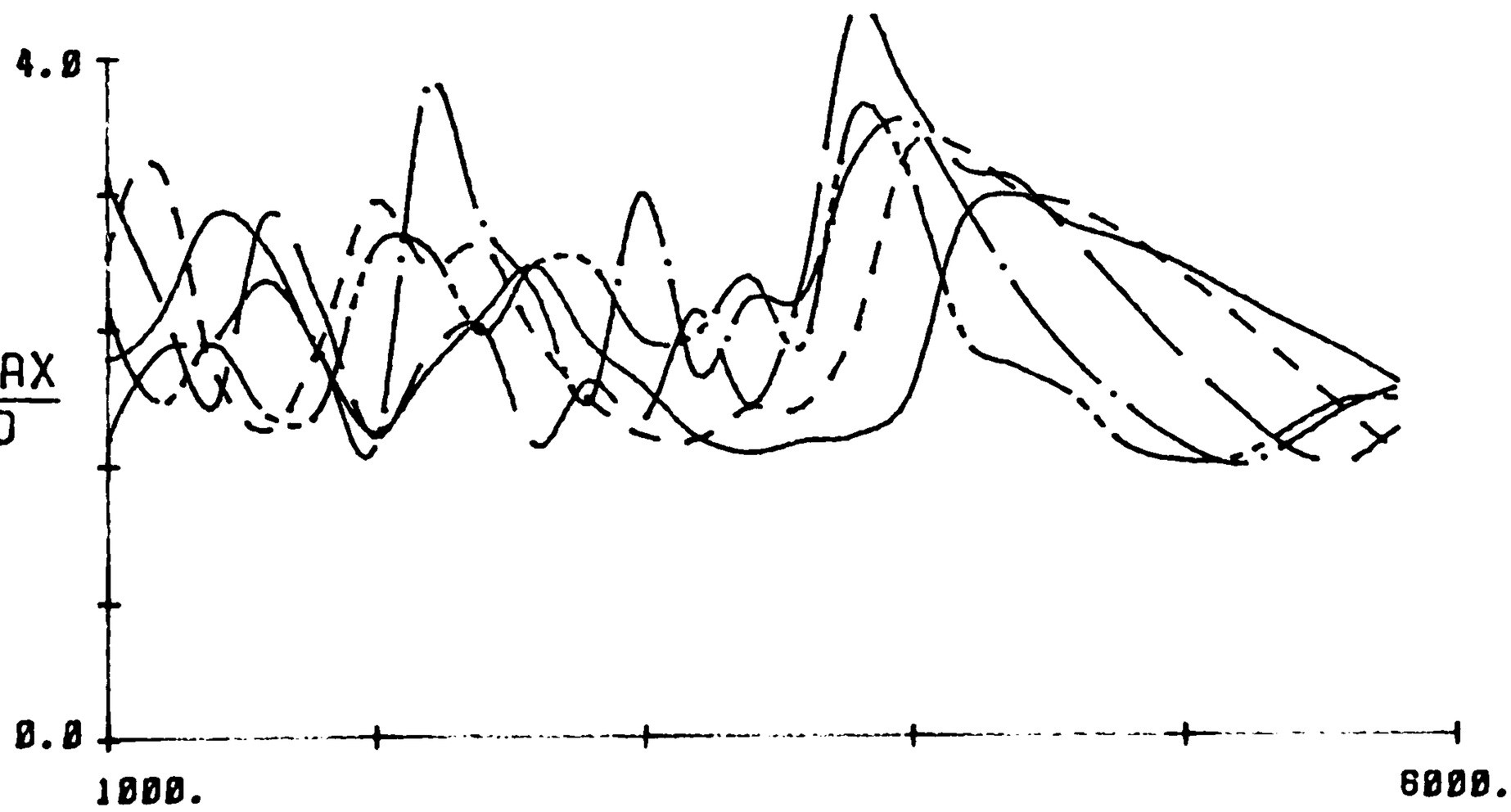

FIGURE 4.21(b)

MAXM. DYNAMIC LOAD (DFMX) Vs SPEED (N)

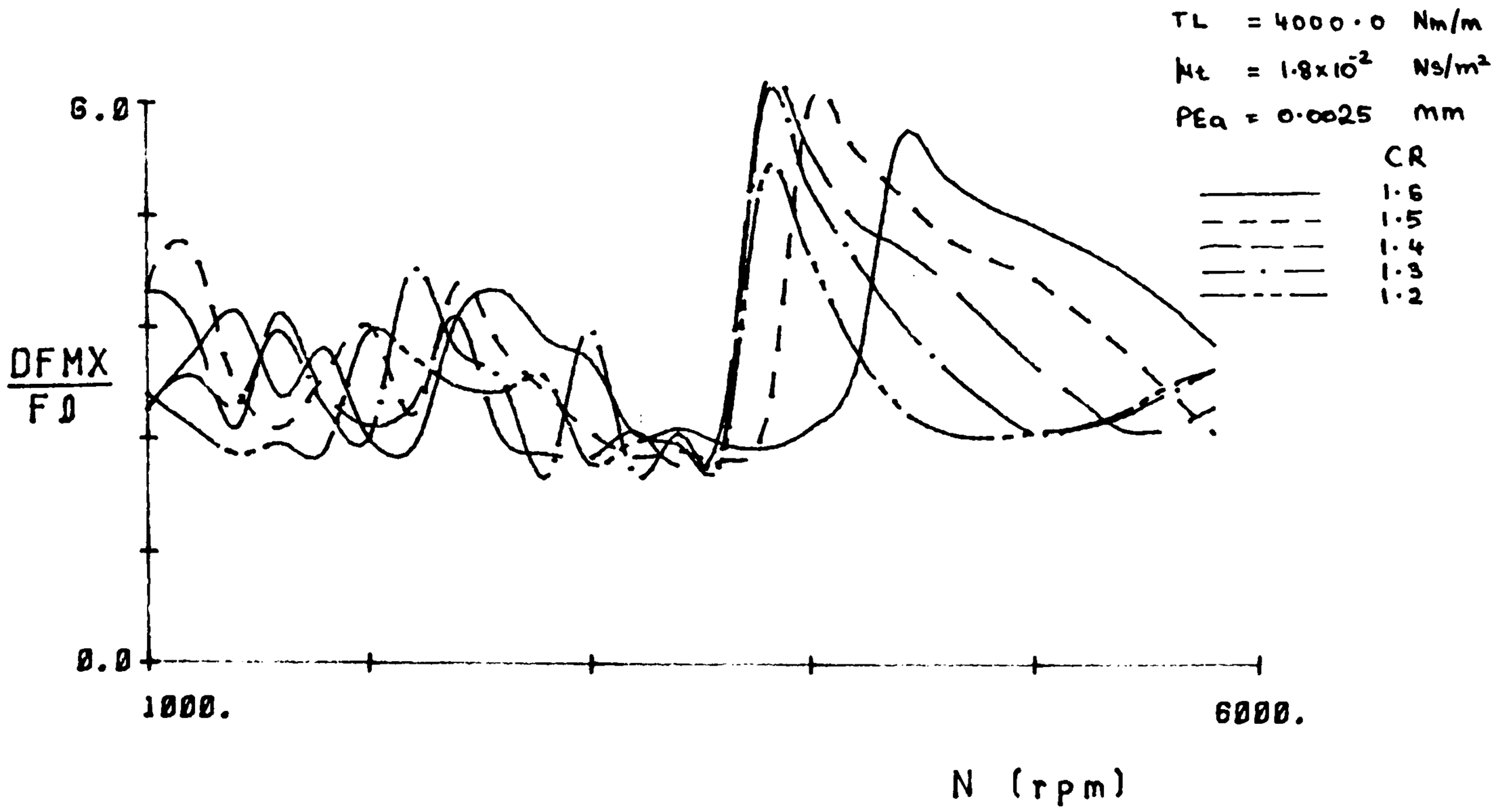

FIGURE 4.21(c)

MAXM. TOOTH FORCE (FMAX) Vs SPEED (N)

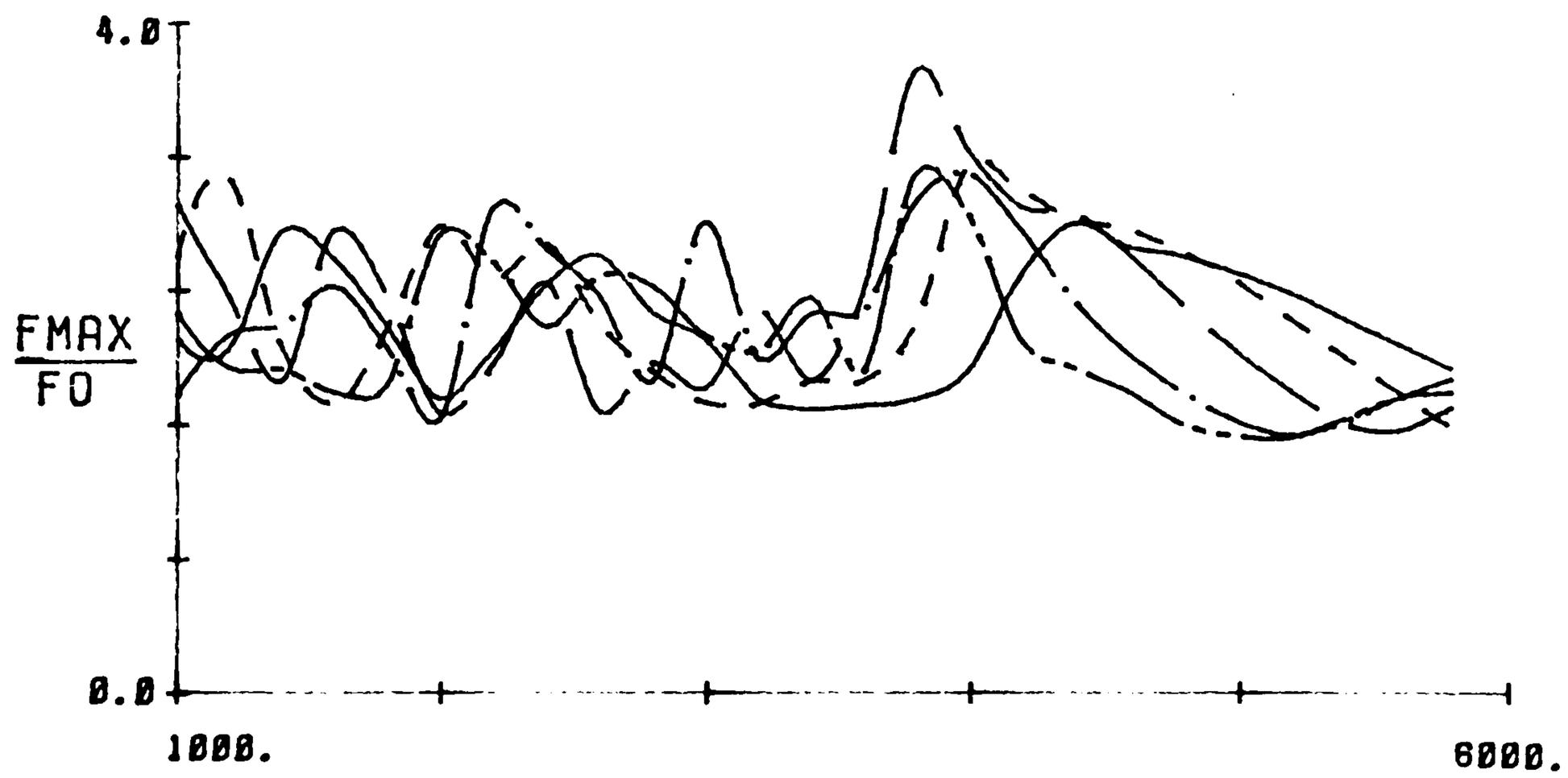

FIGURE 4.21(d)

MAXM. DYNAMIC LOAD (DFMX) Vs SPEED (N)

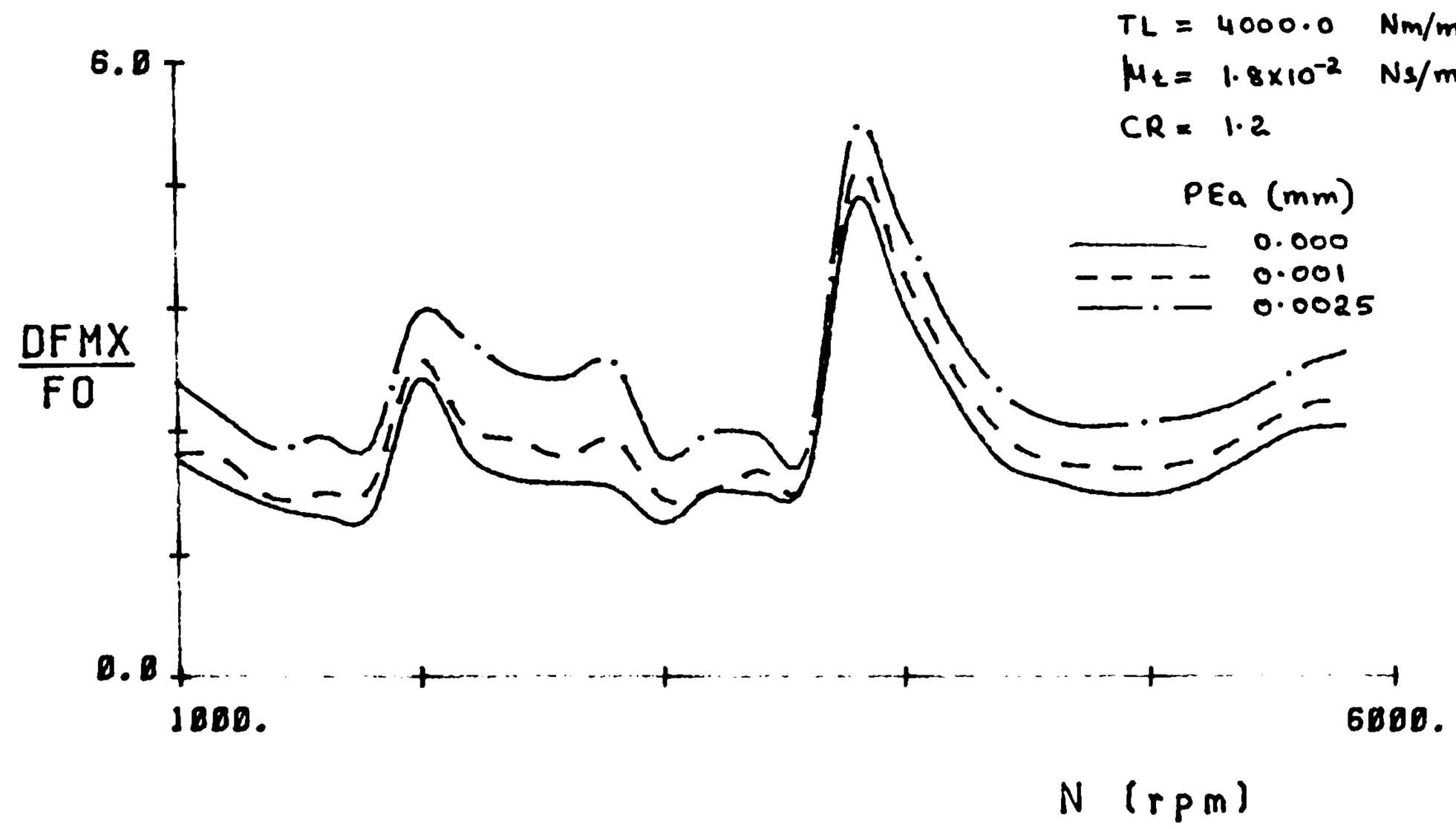

FIGURE 4.21(e)

MAXM. TOOTH FORCE (FMAX) Vs SPEED (N)

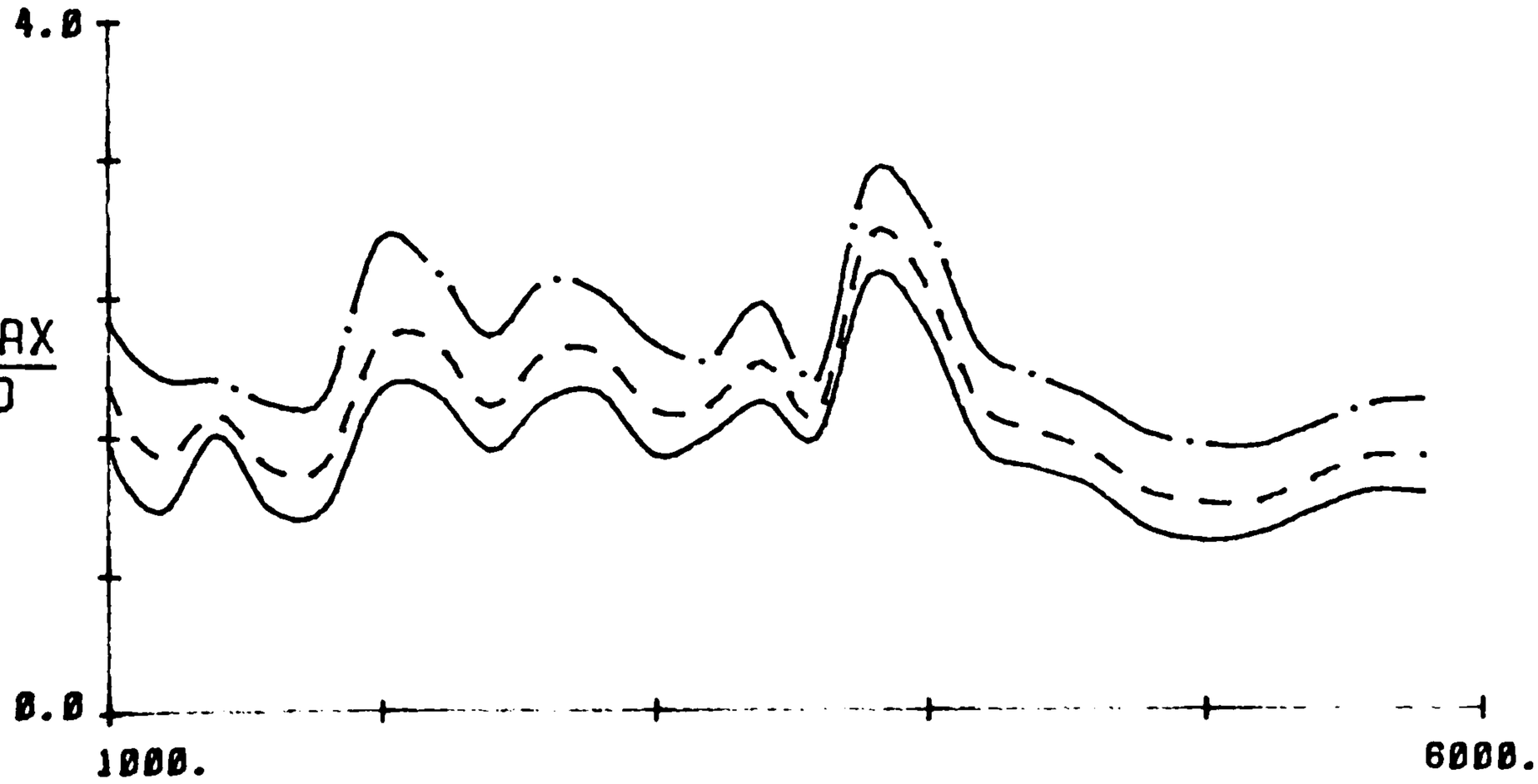

FIGURE 4.21(f)

MAXM. DYNAMIC LOAD (DFMX) Vs SPEED (N)

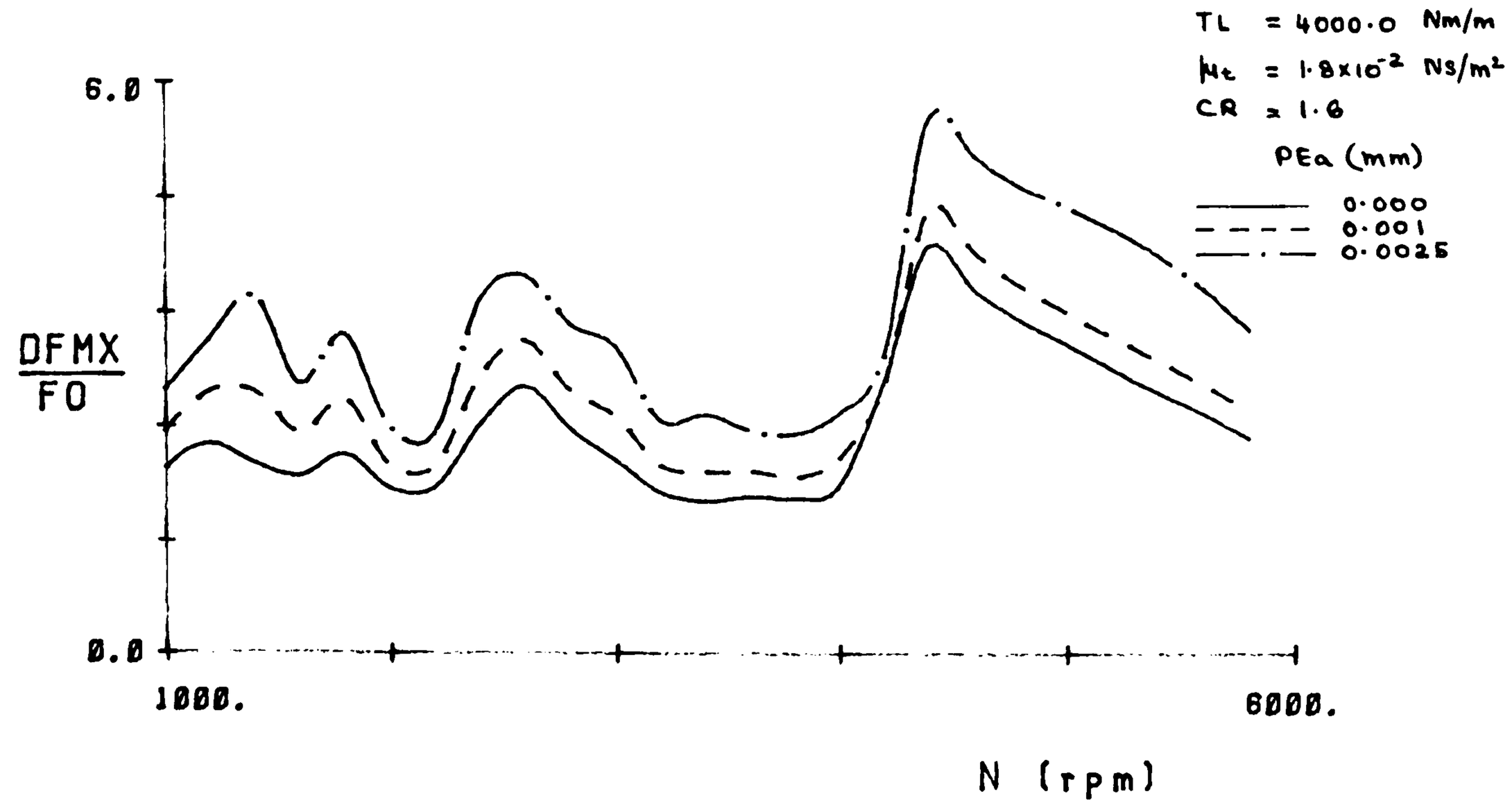

FIGURE 4.21(g)

MAXM. TOOTH FORCE (FMAX) Vs SPEED (N)

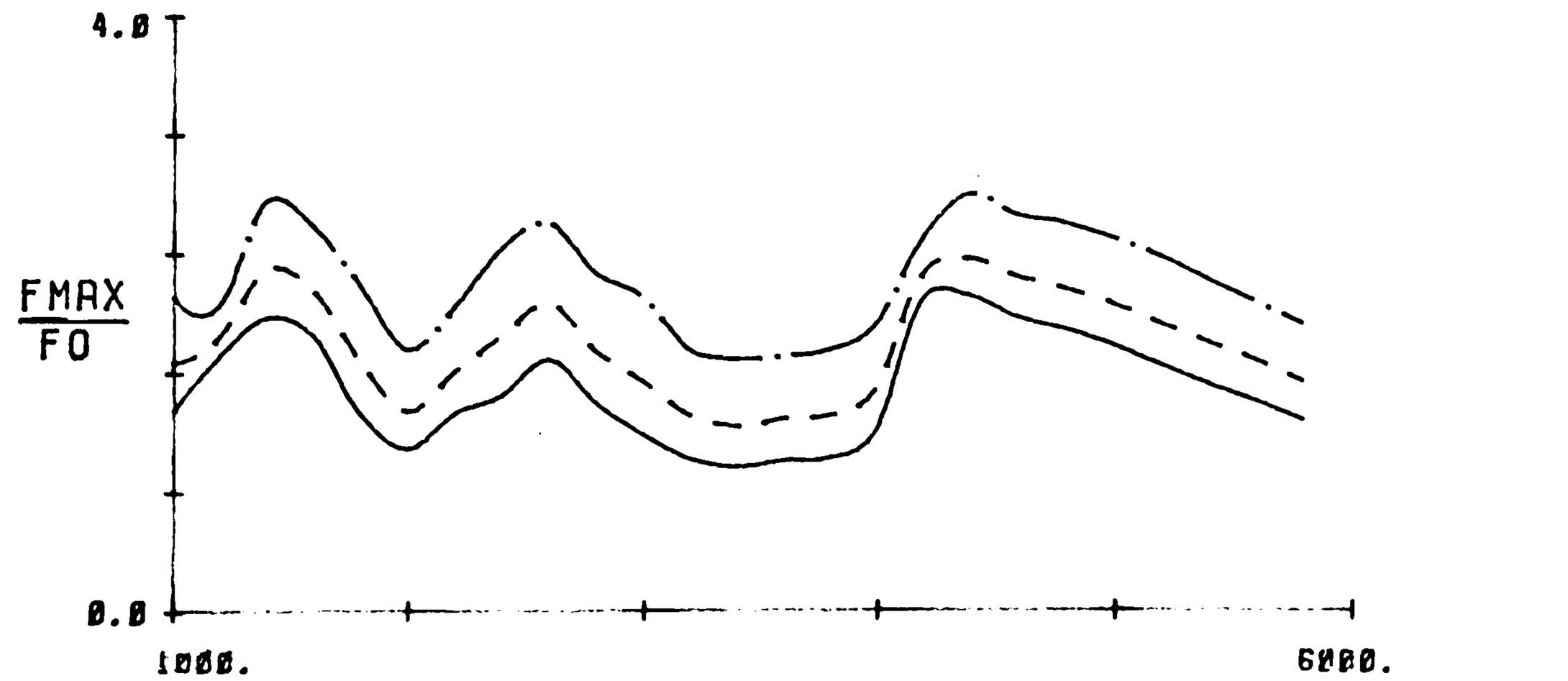

FIGURE 4.21(h)

DYNAMIC LOAD (DF) Vs POSITION OF CONTACT (Yao)

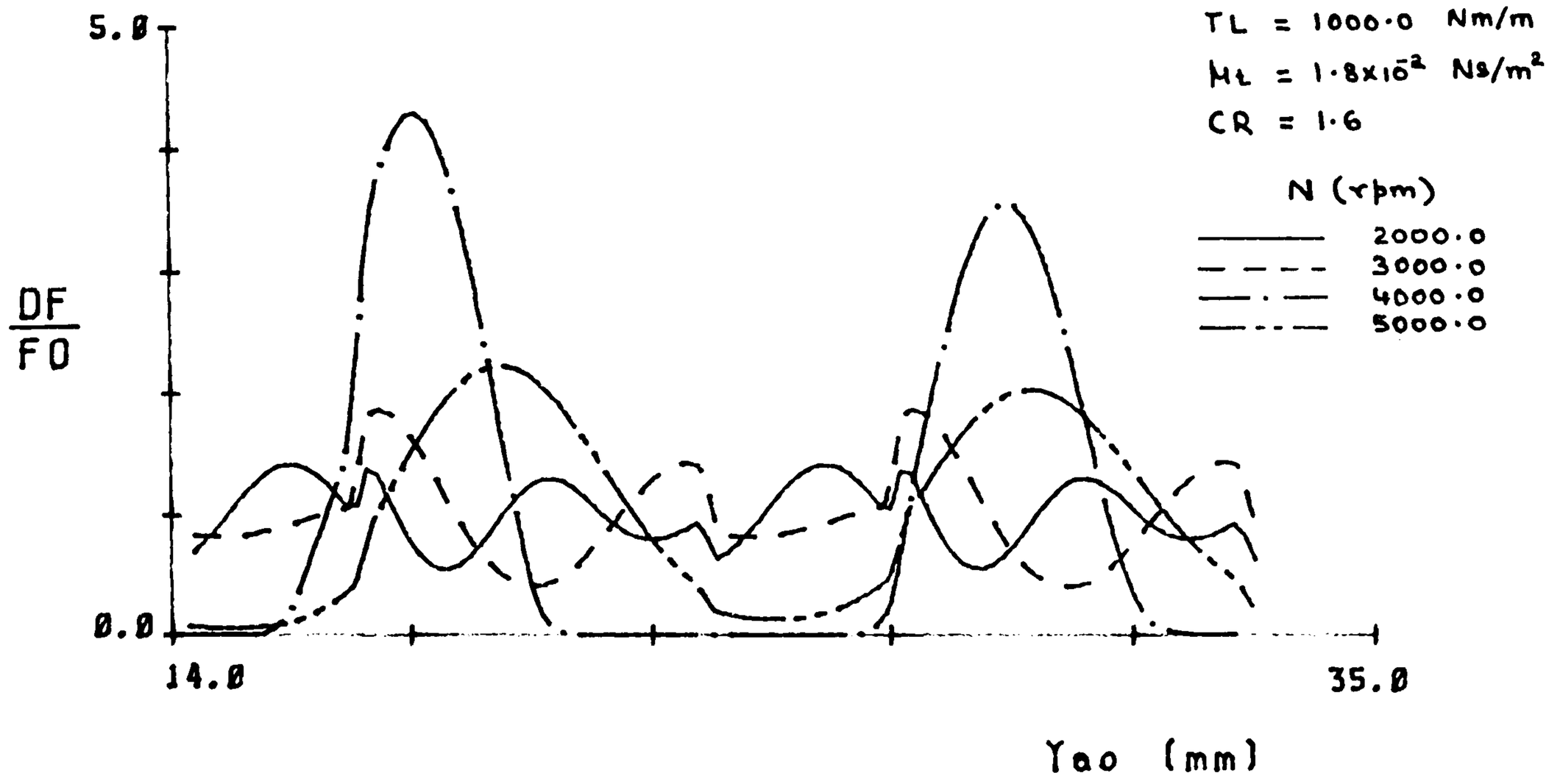

FIGURE 4.22(a)

FORCE (F) Vs POSITION OF CONTACT (Yao)

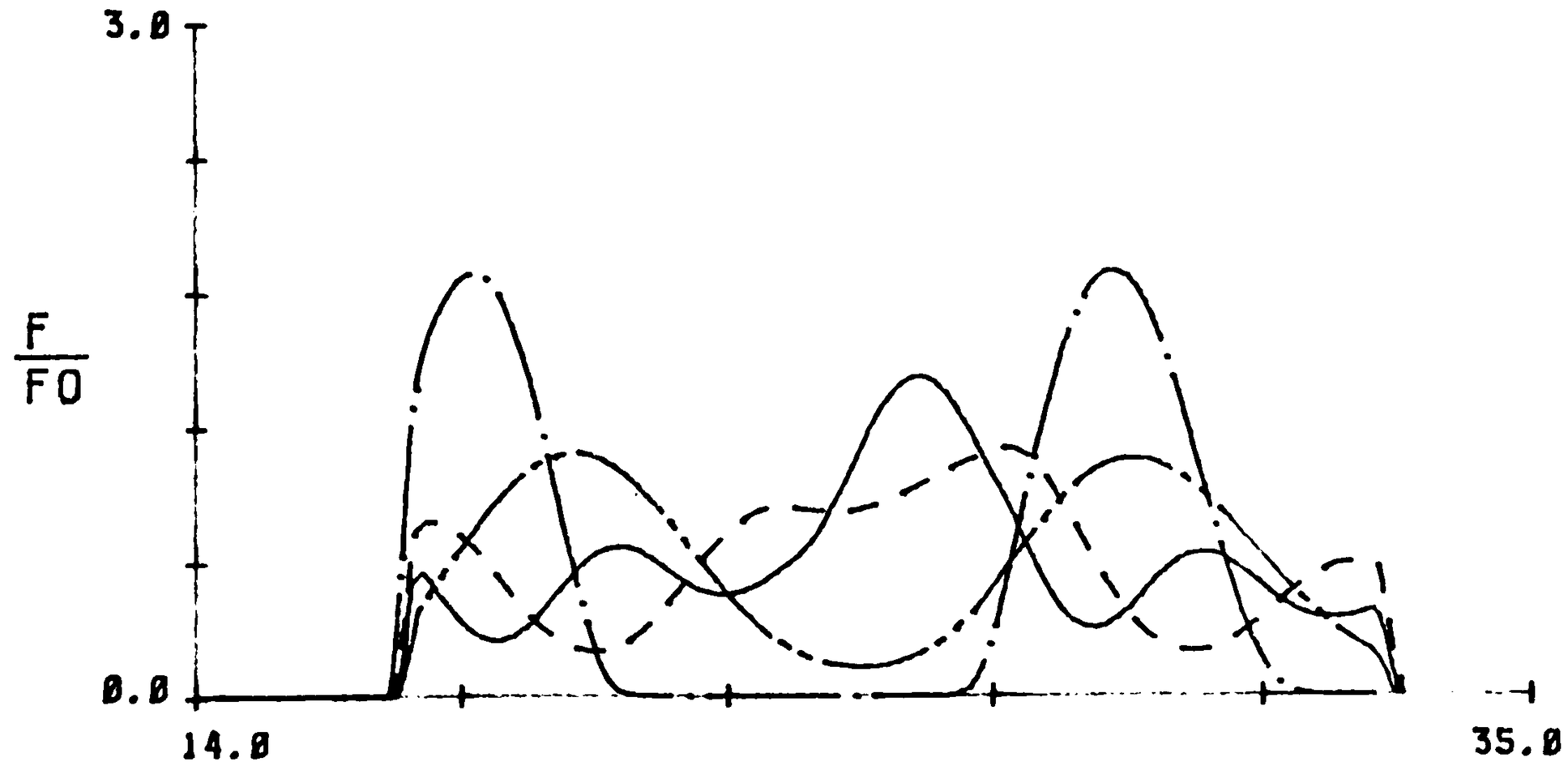

FIGURE 4.22(b)

DYNAMIC LOAD (DF) Vs POSITION OF CONTACT (Yao)

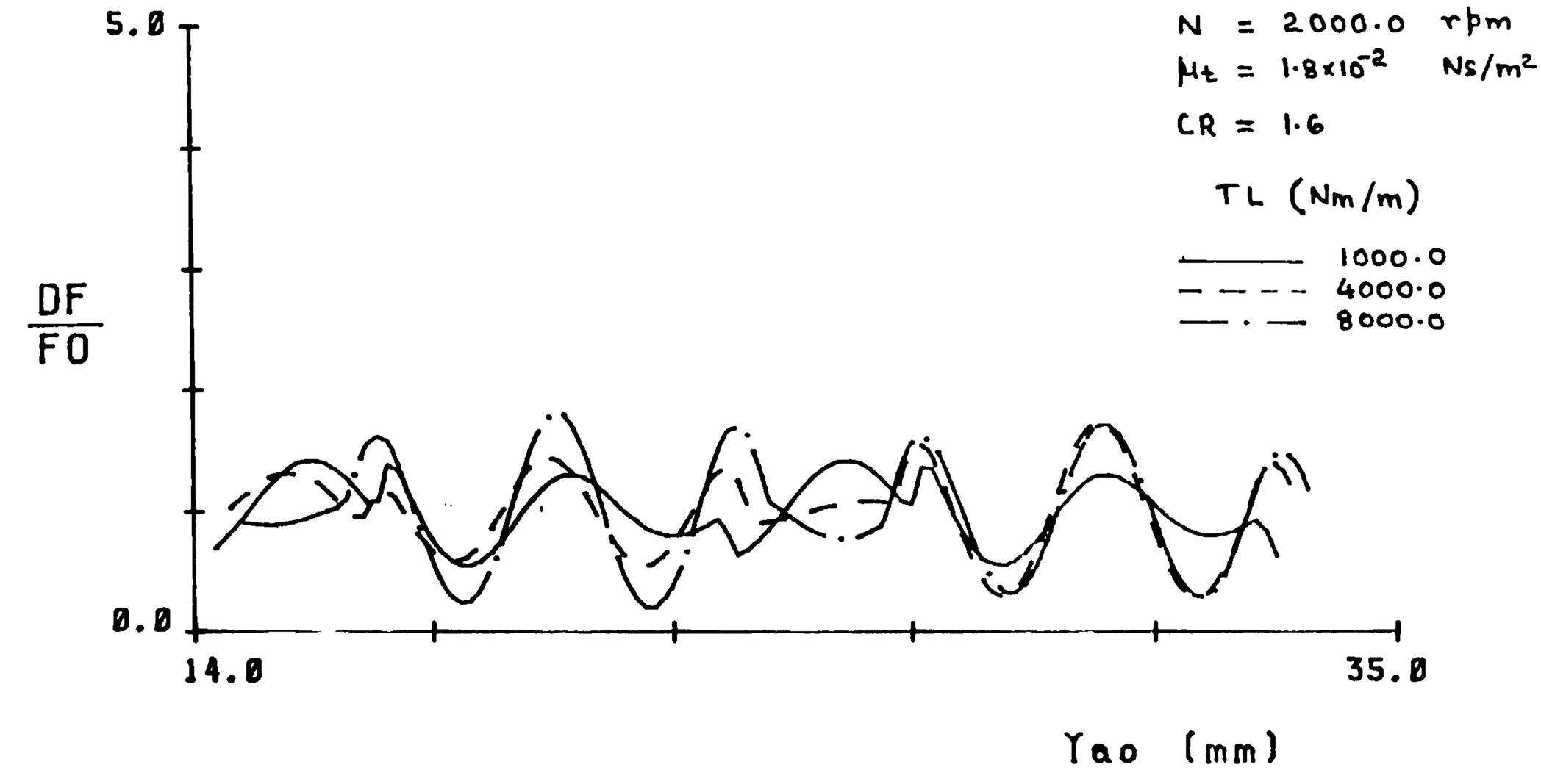

FIGURE 4.22(c)

FORCE (F) Vs POSITION OF CONTACT (Yao)

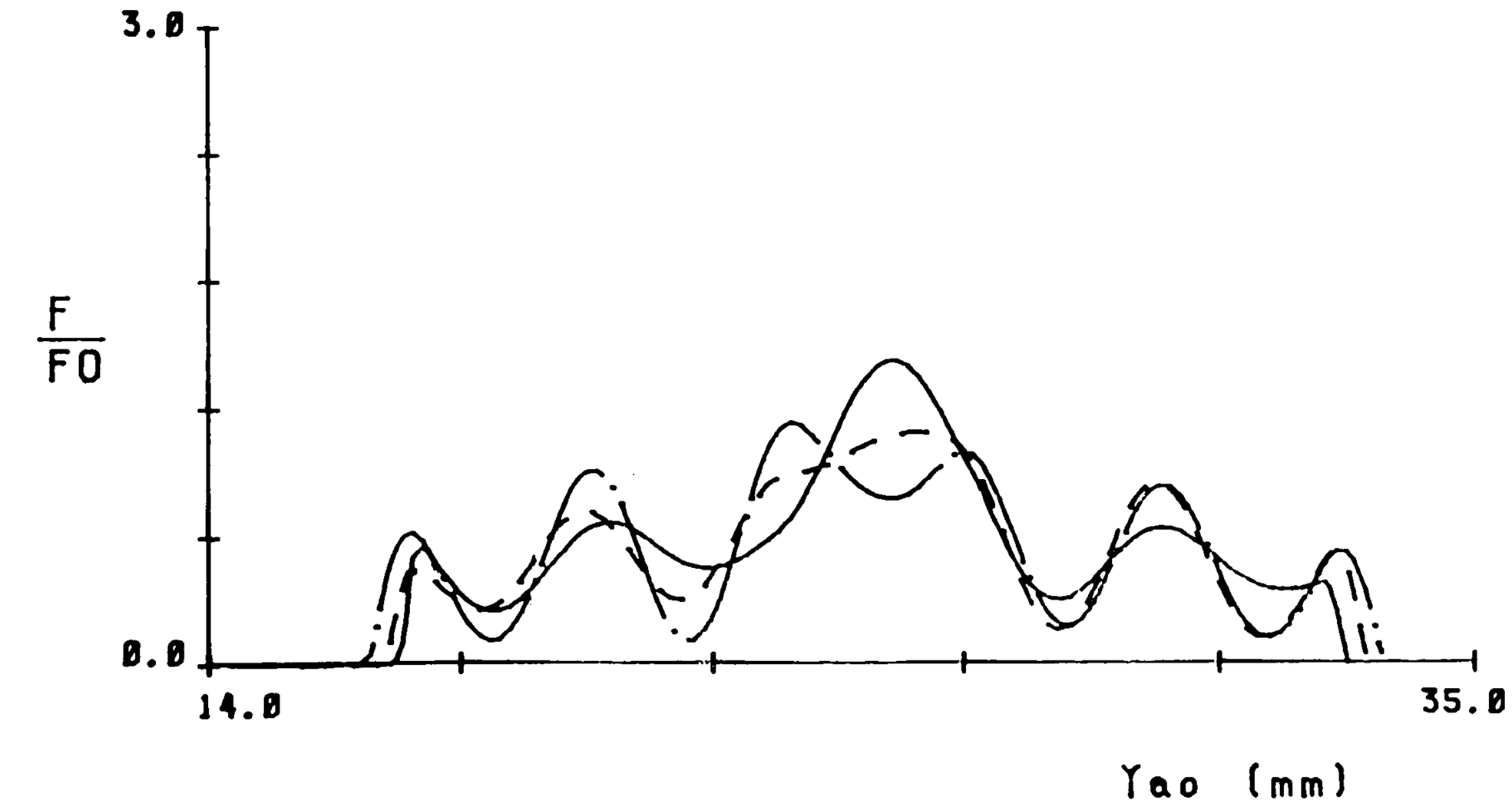

FIGURE 4.22(d)

MESH STIFFNESS (Keq) Vs POSITION OF CONTACT (Yao)

FIGURE 4.23(a)

FILM THICKNESS (HO) Vs POSITION OF CONTACT (Yao)

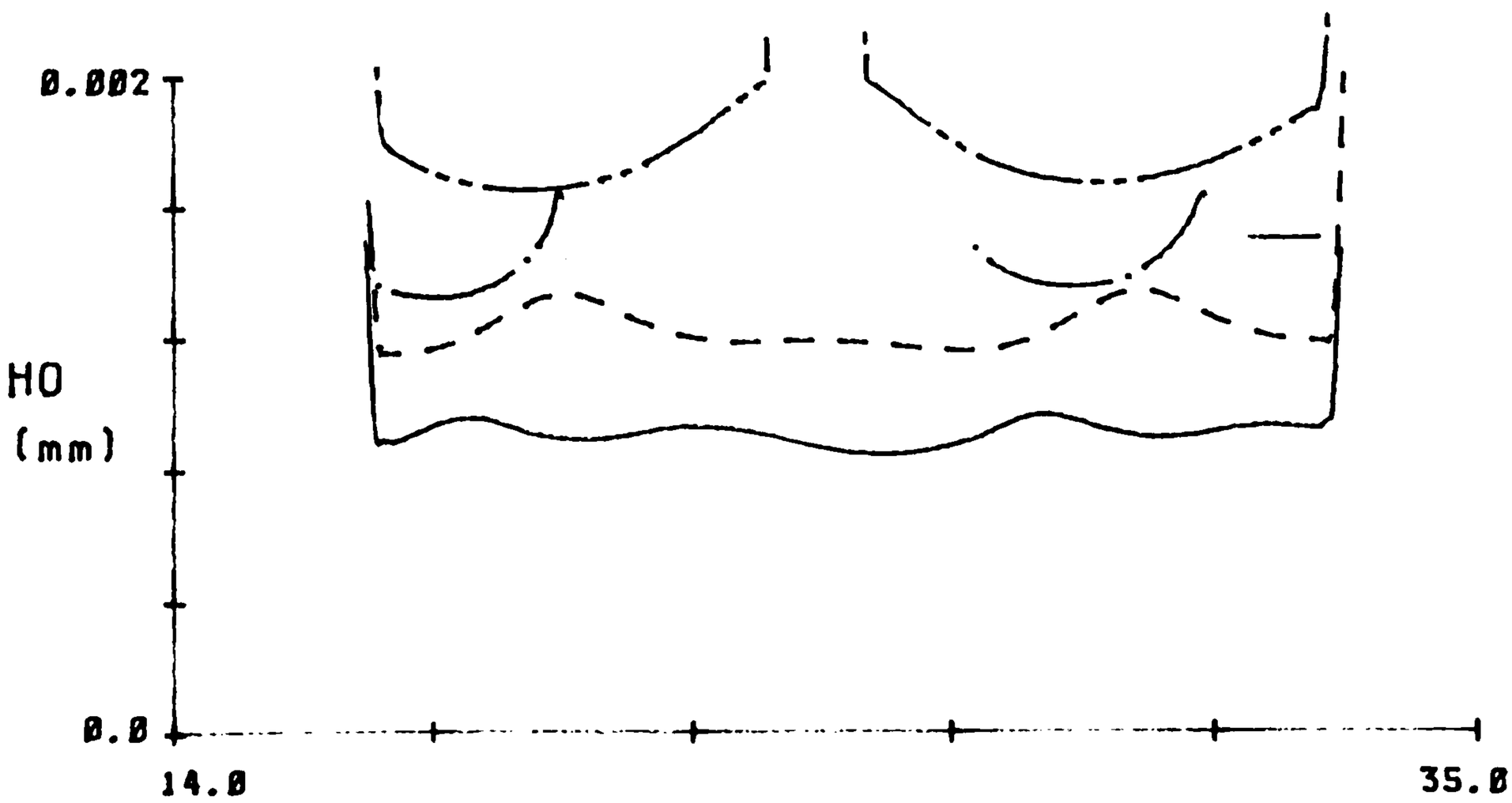

FIGURE 4.23(b)

MESH STIFFNESS (Keq) Vs POSITION OF CONTACT (Yao)

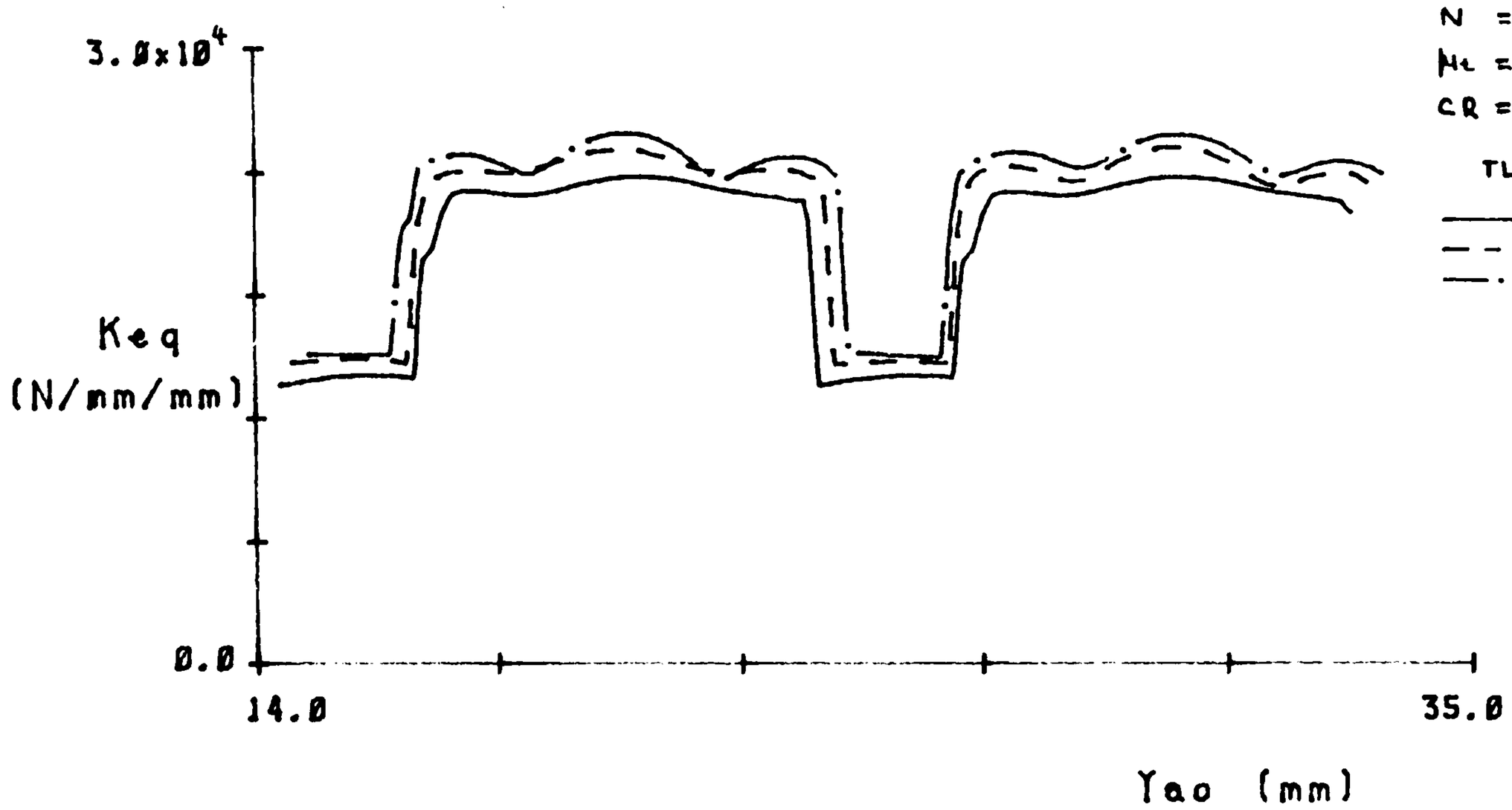

FIGURE 4.23(c)

FILM THICKNESS (HO) Vs POSITION OF CONTACT (Yao)

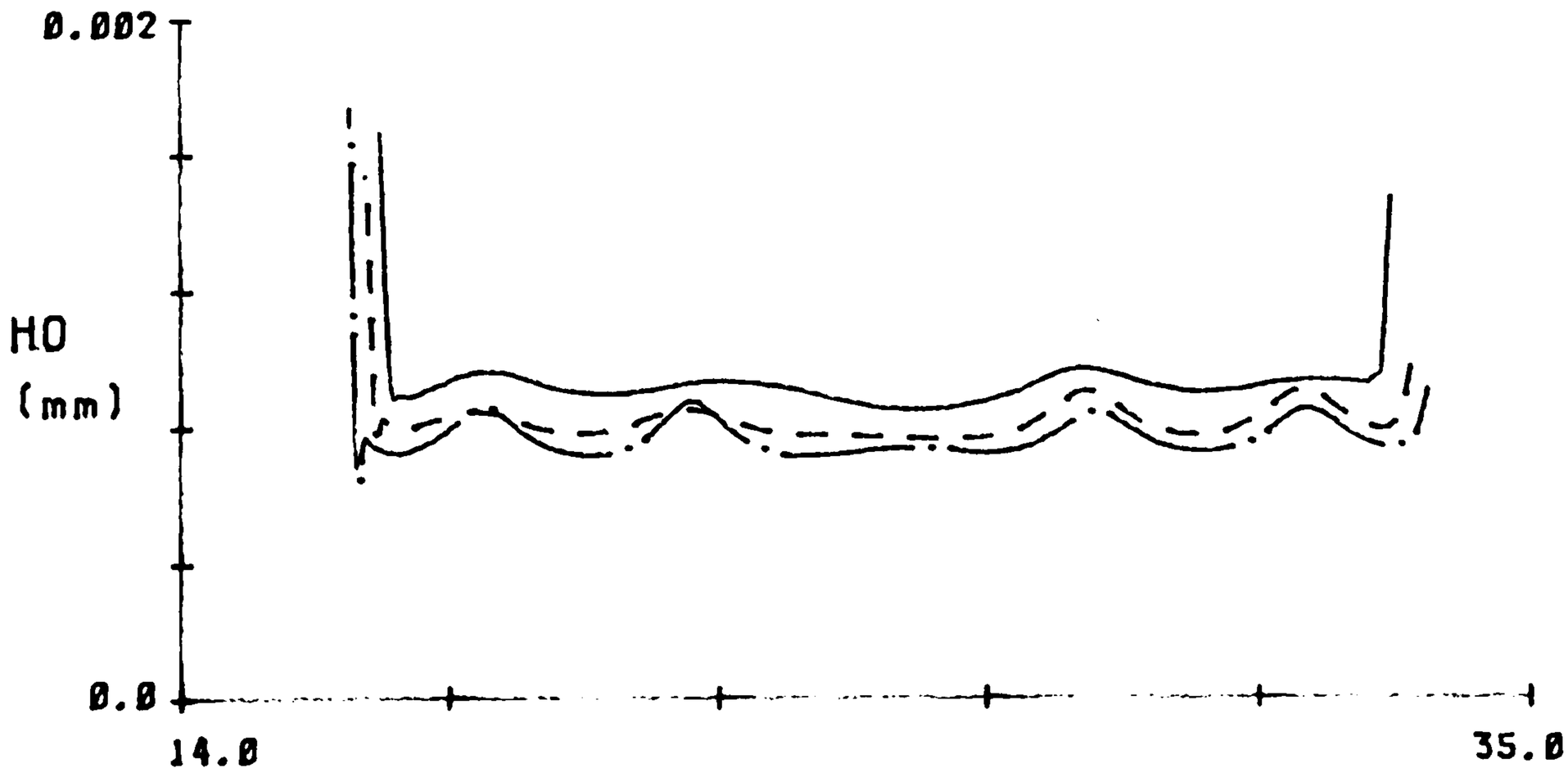

FIGURE 4.23(d)

CHAPTER 5

EXPERIMENTAL OBSERVATIONS

5.1. Introduction

The main difficulty in obtaining accurate analytical solutions for dynamic problems associated with gears is the highly nonlinear nature of the parameters involved. Since they are also inter-dependent it is even more difficult, if not impossible, to analyse them experimentally. As a result many of the investigators turned to disk machines to test the performance of lubricating oil at the tooth mesh. This enabled a steady film to be achieved at the mesh and thus test its performance under steady conditions. These tests have helped to gain invaluable knowledge, especially on matters relating to surface failure. However, disk machines are not capable of simulating the non-steady nature of the parameters at the tooth mesh and the elastic, and hence dynamic characteristics of the gears. A back-to-back gear test rig was, therefore, used in the experiments.

The experiments carried out consisted of two parts: recording of the pattern of the dynamic load, and analysing the characteristics of the mean damping ratio. Both these types of experiments utilised the behaviour of gears at resonance. Thus, a pair of test gears with a natural frequency less than the maximum possible tooth contact frequency was needed and subsequently designed for.

5.2. Test Rig

A back-to-back gear test rig with a fixed centre distance of 91.5 mm was used in the experiments (Figure 5.1). It was driven by a 15 hp variable speed motor with a maximum speed of 2200 rpm. The test gear box was mounted on a cast iron block, while the slave gear box and the motor were mounted on a similar but separate block. The two sections of the rig were connected by two universal couplings, thereby minimising the effect of any misalignments and also isolating the test gears from the rest of the system as far as possible. The power circulating shafts were of 41.0 mm diameter with a distance between the two gear boxes of approximately 1524.0 mm. All the bearings in the system were of the plain journal type. Lubricating oil to these bearings was supplied by an independently driven pump, while a separate pump, but driven by the same motor, supplied lubricating oil to the gears.

5.3. Test Gears

The main requirement in the design of the test gears was that the natural frequency of vibration of them should be as low as possible, and should be below the maximum tooth contact frequency that could be achieved. Hence, in addition to a low natural frequency, this demanded a high tooth contact frequency which meant that the number of teeth of the gear on the driving shaft should be as high as possible.

For a low natural frequency of vibration, the effective inertia of the pair of gears needs to be high, and the tooth mesh stiffness

low. To achieve a high inertia the dimensions of the gears had to be large. Obviously increase in facewidth per unit diameter causes a linear increase in inertia; however, the maximum permissible value was limited to 40.0 mm due to gear box dimensions. The fixed centre distance of the gear box was 91.5 mm and the diameter of the shafts carrying the gears was 44.0 mm. Hence, leaving sufficient material between the root circle and the bore on one gear, the maximum possible pitch circle diameter of the other gear was restricted to about 117.0 mm.

It was thought that if the gears were fitted to the shafts with keys that were tight, both on the shafts and on the gears, the gears would act almost as integral parts of the shafts since the siffnesses of the keys, as far as torsional loads of the system were concerned, were considerably higher than the other flexible elements considered. Under such conditions it was assumed that the effective inertia of the gears would increase as a result of the contribution of the inertia of shafts, especially their free ends which were of a significant length and did not carry any load.

With the stiffness of gear teeth per unit width almost constant, irrespective of their size, the only way of having a low mesh stiffness was by reducing the facewidth of the gear pair. Hence it was decided to use stepped gear blanks to produce them so that the body of the gears had a wider section, while the teeth were cut on the reduced section.

With these assumptions and the restrictions imposed, gears having the following particulars were finally selected (see Figures 5.2 to 5.5 for the rest of the dimensions of the gears).

Gear 'A' (gear on the driving shaft)

Number of teeth	73
Diametral pitch	16
Flank angle at pitch radius	20^{o}
Pitch circle diameter	115.888 mm
Addendum modification	zero
Basic rack BS 436 (1940) Figure 5	
Material	EN 8

Gear 'B' (gear on the driven shaft)

Number of teeth	42
Diametral pitch	16
Flank angle at pitch radius	20^{o}
Pitch circle diameter	66.675 mm
Addendum modification	zero
Basic rack BS 436 (1940) Figure 5	
Material	EN 9

Allowable tooth load calculated according to BS 436 (1940) specification produced a value of 28.3 N/mm for the test gears.

The theoretical contact ratio of the gears was 1.63.

The natural frequency of vibration of the pair of gears was estimated by considering the gears to be separate from the rest of the system. This was thought to be accurate enough, since the shafts connecting the gears were long and had relatively low torsional stiffnesses.

Figure 5.6a shows a sectional view of the test gear box. The slave gear box was identical to this. Figure 5.6b shows the section of the system used in the calculation of the natural frequency of the pair of gears. The inertias of the free ends of the shafts were also added to the respective gears in determining the total effective inertia of this subsystem. The inertias of the elements were as follows:

$$I_a = 5.45 \times 10^{-3} \text{ kg m}^2$$

$$I_{sa} = 0.53 \times 10^{-3} \text{ kg m}^2$$

$$I_b = 0.60 \times 10^{-3} \text{ kg m}^2$$

$$I_{sb} = 0.76 \times 10^{-3} \text{ kg m}^2$$

The rotary system could be represented by an equivalent translatory model for which the effective masses would be:

$$M_a = \frac{(I_a + I_{sa})}{R_{ba}^2} = 2.00 \text{ kg}$$

$$M_b = \frac{(I_b + I_{sb})}{R_{bb}^2} = 1.31 \text{ kg}$$

The equivalent mass $M_{eq} = \frac{M_a M_b}{(M_a + M_b)}$

$$M_{eq} = 0.792 \text{ kg} .$$

Tooth mesh compliance = 8.697×10^{-8} m/N/mm facewidth

$\therefore$ Mesh compliance for a facewidth

of 20.0 mm (H) = 4.35×10^{-9} m/N

Hence the approximate natural frequency of the pair of gears was:

$$\omega_n = \frac{1}{2\pi}\sqrt{\frac{1}{M_{eq}\ H}}$$

$$\omega_n = 2646 \text{ Hz.}$$

The shaft speed corresponding to a tooth contact frequency of this value was 2175 rpm.

5.4. Instrumentation

Detection of resonance:

Subsequent to the preliminary design of the gears, it was decided to utilise the convenience of sound monitoring equipment to pinpoint relevant resonant frequencies. Prominent discrete frequencies were isolated by the analyser. Tooth contact frequency was inevitably one of those, irrespective of speed, and very distinguishable, since it varied linearly with speed. The object was to let the gears

resonate with this tooth contact frequency. To achieve this the speed was increased slowly while watching the peak corresponding to the tooth contact frequency on the analyser display. When resonance occurred the magnitude of this peak reached a very high value. The frequency which gave the highest peak was taken as the natural frequency of vibration of the pair of gears.

The natural frequency of vibration mentioned here is, in fact, one of the many natural frequencies of the gear system. As the speed is increased, the tooth contact frequency will cause resonance to occur at these other frequencies also when they are near enough, resulting in relatively high peaks on the display. To avoid confusing these with the natural frequency corresponding to the pair of test gears, a torsional vibration analysis of the total system was carried out initially (Appendix VI) and approximate values of all the frequencies determined.

Load torque:

The gears were loaded by means of a torque lever and a locking coupling while the machine was stationary. To measure the locked-in torque a torque transducer was constructed using strain gauges mounted on the driving shaft. The output of this was amplified using a strain gauge amplifier before being displayed on a meter. The transducer was initially calibrated by applying known torques using a lever and weights, and this was checked regularly during the course of the experiments.

Frictional torque:

To measure the frictional torque input to the gear system, a torque transducer was installed between this and the driving motor. The output of the transducer was amplified and fed to an analog to digital converter (ADC) fitted in a microcomputer. The outputs of two opto-switches installed near the two test gears were also connected to the ADC. Two reflective markers placed on the shafts prompt the switches to generate pulses as they come in line with their respective switches. Software was developed to ensure that the microcomputer started collecting data (frictional torque transducer output) when the outputs of both opto-switches returned high values. This ensured that data storing always started when a particular pair of teeth was in mesh. This made comparison of different sets of readings easier, since the effects on torque variation due to defects associated with individual teeth were dissimilar.

The computer programme was written in assembly language (Flow chart, Figure 5.7, and listed in Appendix VII) to initiate analog to digital conversion, to read the digital output and to store it. Even though a data collecting rate of around 40 kHz was anticipated, the maximum rate that could be achieved was 23 kHz. This reduced the number of data points that could be collected per cycle to about 10, which was not sufficient to record the true pattern of the torque fluctuation. Details of the torque transducer, the analog to digital converter, and the microcomputer used are given in Appendix VIII.

Speed:

To measure the speed of rotation of the shafts, a toothed wheel and a magnetic pickup was used. The wheel with 54 teeth was fitted to the driven shaft. As each of these teeth passed, the magnetic pickup output generated a pulse and, by counting the number of pulses during a known time, the speed of rotation of the shaft could be found.

5.5. Presentation and Evaluation of Test Results

Frictional torque record:

In a back-to-back gear test rig the power required to drive the gears is only that corresponding to frictional losses in the system. For gears and bearings these losses are functions of the transmitted power. Thus, when the system is subjected to dynamic loads the torque corresponding to frictional losses will also fluctuate according to the same pattern and total losses will synchronize with the dynamic load at resonance. Hence the trace of the frictional torque thus obtained could be assumed to represent the dynamic load pattern of the gears, although the amplitude scale is not identical to the amplitude scale of the true dynamic load.

In addition to the lower rate of data collection attained than expected, a further setback to this test occurred when it was found that the natural frequency of vibration of the pair of test gears was considerably higher than the expected value. Instead of the estimated frequency of around 2650 Hz, resonance occurred at a frequency of about 3400 Hz. This meant that only about seven data

points could be recorded per cycle, which was not at all sufficient to reproduce the true pattern of torque variation. There are two probable causes that could be accounted for the higher natural frequency obtained. They are:

(i) At least one of the gears, especially the pinion, may not have had a tight fit as expected. If this was so, the expected effect of the inertia of the free ends of the shafts would not have been there. This would have reduced the effective inertia of the gears, thereby increasing the natural frequency of vibration.

The natural frequency was then calculated using the inertias of only the gears. This yielded a value of 4065 Hz which left the actual one obtained in between the two extreme values calculated.

(ii) The mesh stiffness was higher than the assumed value.

The mesh stiffness used in the estimation of the natural frequency was an average value. But in practice this varies substantially, especially when contact changes from one pair to two pairs, and vice versa. It is possible that the actual contact ratio of the gears was higher than the design value which was also high. This would have left the gears to operate most of the time with double tooth contact, resulting in a higher average mesh stiffness.

Mesh stiffnesses, calculated using the formulae employed in the analytical section (section 3.4), gave the following values when the total tooth load was 20 N/mm.

(a) For single tooth contact = 0.1565×10^5 N/mm/mm

(b) For double tooth contact (load shared equally between the two pairs) = 0.3028×10^5 N/mm/mm

Whereas the value used in the calculations was only 0.1150×10^5 N/mm/mm, in line with the values used by Tuplin (53) and Gregory, Harris and Munro (18).

The natural frequencies calculated using the above mesh stiffnesses were:

When KO = 0.1565×10^5 N/mm/mm ω_n = 3164 Hz

When KO = 0.3028×10^5 N/mm/mm ω_n = 4400 Hz

Here also this left the natural frequency obtained within the two extreme values calculated.

This high value of natural frequency also meant that the gears had to be run at a much higher speed (at least 3300 rpm) for resonance to occur. But the maximum speed of the driving motor was only 2200 rpm. Thus the readings had to be taken when the exciting frequency was half the natural frequency so that resonance occurred with the first harmonic of the tooth contact frequency. Even though

resonance could be detected at this speed without any difficulty, the response of the system would not have been the same as running at the resonance frequency.

Another aspect that would have influenced the results was the non-uniform load distribution among the bearings. It was found that some of the bearings had reaction forces which decreased with the increase of load (due to tooth load acting opposite to gravitational force). This could have hampered the relationship expected between the load torque and the frictional torque.

In addition to all these, the readings were superimposed on torque fluctuations due to torsional vibrations of the driving section of the test rig. But these could not have affected significantly the torque characteristics during each mesh cycle, since the frequencies of those torsional vibrations were much lower.

Despite the fact that the torsional vibration analysis of the system predicted natural frequencies which were low compared to the natural frequencies of gears, several other resonance frequencies close to the natural frequency of the pair of gears were observed. This could be attributed to the following.

(i) The effect of smaller inertias, such as those of some of the couplings, collars and shafts which were neglected in the analysis.

(ii) Other modes of vibration, especially transverse.

But the noise levels detected for these vibrations were not as great as those due to the vibration of the gears.

Figures 5.8 and 5.9 show spectrum analyser displays when twice the tooth contact frequency was near the natural frequency of vibration of the gears. In addition to the high peak detected on the analyser, resonance was also accompanied by very high overall noise, at least 10-15 dB higher than at other speeds.

Figures 5.10 and 5.11 show the frictional torques recorded experimentally which were assumed to follow the same pattern as that of the dynamic load variation at resonance.

It has to be noted that the torque records shown contain undulations due to noise in the electrical system as well. Figure 5.12 shows a similar torque record taken with the driving shaft running free without the gears on the driven shaft (hence no load). This gives some idea of the level of disturbances in the measuring system.

Figures 5.13 and 5.16 give some enlarged views of the initial few tooth mesh cycles of the torque records at different speeds. Since the gears were driven at slower speeds (twice the tooth contact frequency equal to the natural frequency of the gears at resonance), each cycle corresponding to one base tooth pitch contains about 14 data points at the above speed.

The simulation test predicted cyclic load variations occurring at the natural frequency of gears at low speeds and at the tooth contact frequency at and near resonance. The frictional torque records, too, show a weak similarity to these cyclic variations, but it is difficult to correlate these to the theory for several reasons.

(a) The gears were driven at slow speeds only, at which the dynamic load fluctuations were not very high. According to simulation results, even when the first harmonic of the tooth contact frequency was near the natural frequency of gears, the maximum dynamic load was not very much above the nominal load.

(b) The low stiffnesses of the shafts, those circulating power as well as that of the torque transducer, might have dampened out most of the torque fluctuations which were already weak.

(c) Dynamic simulation results have shown that tooth separation occurs especially at and near resonance. In the practical case this causes reverse contact to take place which again increases frictional losses. Hence a single load torque cycle results in two frictional torque cycles in such situations.

Frequency of Vibration Analysis

The numerical work carried out on computer has given a picture of the nature and extent of dependence of the damping ratio upon various parameters. Using these data, the instantaneous damping

ratio can be calculated for a set of given operating conditions. Most of the data on which damping ratio depend vary during the course of each mesh cycle. Hence, with the available techniques, it is not possible to observe this variation in damping during the mesh cycle. What was attempted in this section of the experiments was to analyse the influence of load and the viscosity of the lubricating oil on the mean damping ratio. Since the damping ratio can not be measured directly, the natural frequency of vibration of the pair of gears which depends on the damping ratio was used instead. The natural frequency of the pair of gears was recorded for various loads and lubricating oil viscosities, and the results were then compared with the computed values.

For this test, the test gears were connected to the rest of the rig through two torsionally flexible couplings. With their comparatively low torsional stiffnesses, these couplings effectively isolate the test gears from the rest of the system from vibrational effects. This was expected to bring the pair of gears closer to the theoretically assumed two inertia, single degree of freedom system.

But the inertias of the couplings were found to be significant in comparison with those of the gears and the short shaft lengths between them and the gears also resulted in high torsional stiffnesses. Therefore, a separate torsional analysis of this half of the system was then considered to be necessary. Figure 5.17 shows the elements the sub-system was comprised of, and Figure 5.18

shows an equivalent rotary system with the tooth mesh also represented by a shaft of equivalent stiffnesses (K2).

The inertias and stiffnesses of the equivalent system were:

$$I_{c1} = 1.20 \times 10^{-3} \text{ kg m}^2$$

$$I_a = 5.45 \times 10^{-3} \text{ kg m}^2$$

$$I_{beq} = 4.00 \times 10^{-3} \text{ kg m}^2$$

$$I_{ceq} = 3.64 \times 10^{-3} \text{ kg m}^2$$

$$K_1 = 142.2 \times 10^3 \text{ Nm/rad}$$

$$K_2 = 882.2 \times 10^3 \text{ Nm/rad}$$

$$K_3 = 429.5 \times 10^3 \text{ Nm/rad}$$

The highest three natural frequencies of vibration of this sub-system were then found to be 3595, 2060 and 1600 Hz. The highest of these was obviously due to the vibration of the pair of gears which was confirmed by the mode shape corresponding to that frequency.

This vibrational analysis was repeated with the gears represented by their inertias only (without adding the inertias of the shaft lengths). This gave a natural frequency of 4836 Hz for the pair of gears.

But these were calculated using a mesh stiffness of 0.115 x 10^5 N/mm/mm, whereas the higher mesh stiffnesses obtained from the analytical results would have resulted in a considerably higher upper limit to the natural frequency.

The viscosity of the oil was changed by varying the temperature at which it was supplied to the gears. The oil temperature was varied between $105^{O}F$ and $150^{O}F$. This resulted in a change in viscosity from about 0.055 Ns/m^2 to about 0.015 Ns/m^2 (Figure 5.19). Figures 5.20a to 5.20d show spectrum analyser display records at resonance for different lubricating oil temperatures. Figures 5.21 to 5.23 show the variation of the magnitude of the peak corresponding to the tooth contact frequency in the vicinity of the resonance frequency. These figures show two aspects that hinder the analysis of the results.

(i) The level of excitation and hence noise level at resonance is very low at low loads when oil damping is expected to be high.

(ii) The magnitude of the spike corresponding to twice the tooth contact frequency, which was used to detect resonance, does not have a sharp maximum value. It shows high values throughout a small frequency band. The magnitude of the spike varies only slightly within this band.

The variation of the tooth stiffness as the mesh point moves along the path of contact can be regarded as the cause mainly responsible

for this second aspect. Also when operating near resonance there is a considerable fluctuation in the tooth load and, since the tooth stiffness depends on the load, this too could be considered as one more reason responsible for the natural frequency to spread over a band of frequencies. But the major change in mesh stiffness occurs when the number of pairs of teeth in contact changes. This change is sudden and the amount is very significant.

Table 5.1 gives a summary of the resonance frequencies obtained at different loads and lubricating oil temperatures. The frequencies listed are those corresponding to the highest magnitude of the noise level within the resonance frequency band. This band itself was about 150 Hz wide. Two prominent resonance frequency areas could be found within the band. One around 5070 Hz and the other around 5120 Hz. As the load was increased the resonance frequency shifted from the 5070 Hz area to the 5120 Hz area. This was in contrast to the expected gradual increase in resonance frequency with load.

At very low loads (no load) maximum noise level was found to be around 5130 Hz; higher than at other loads. Although no definite cause could be found for this tooth separation and reverse, impacts may be regarded as possible causes. Also at these very low loads the excitation level was too low to cause any serious gear vibration and it is possible that the frequency recorded here corresponding to the maximum noise level was not the natural frequency of the pair of gears.

In the analytical model used only one pair of teeth was considered to be in contact, whereas in the practical case the number of pairs of teeth which share the load changes during each mesh cycle. The mesh stiffness is also affected as a result. While in the test gear system there were other elements connected to the gears, in the mathematical model only the two inertias representing the gears were considered. This obviously would have yielded a different natural frequency of vibration than the experimental ones. Thus, in order to compare the experimental results with those predicted by the theory, an equivalent system with an undamped natural frequency equal to that of the test gears was used, together with damping characteristics corresponding to a pair of gears similar to the test gears.

It has been shown that damping gradually diminishes as the load is increased. Hence it can be assumed that at high load there is no damping and the resonance frequency measured is the undamped natural frequency of the system.

The undamped natural frequency of a single degree of freedom system can be written as:

$$\omega_o = Ck\sqrt{Km} \qquad (85)$$

where Ck - constant

Km - mean mesh stiffness.

The natural frequency of vibration of the same system with viscous damping is:

$$\omega = \omega_o\sqrt{1 - \zeta^2} \qquad (86)$$

ζ - damping ratio.

The mean mesh stiffness is a function of the load. Hence mesh stiffnesses were calculated for the test gears (one pair of teeth in mesh) at different loads using the formulae described in Chapter 3. These results are presented in Figure 5.24 and were used subsequently to obtain mesh stiffnesses at various loads.

Figure 5.25 shows the computed results of the variation of damping ratio with load for the test gears used at the speed of rotation at which resonance was observed. According to this it can be seen that for loads above 20.0 N/mm damping ratio becomes negligible irrespective of the viscosity of the oil for the range of viscosities considered. This load corresponds to a shaft torque of about 22.0 Nm. It has to be noted, though, that this figure will be higher (almost double) when two pairs of teeth are in mesh, since the load is shared between them. The experimental results show that the resonance frequency is almost the same, irrespective of the oil viscosity, when the torque is 33.0 Nm. It can thus be assumed with confidence that the resonance frequency at 33.0 Nm (i.e. 5123 Hz) is the undamped natural frequency of the gear system at that load. Thus the mesh stiffness at that load and the frequency 5123 Hz was used to calculate the constant Ck of equation (85).

$$Ck = \frac{\omega}{\sqrt{Km}}$$

$$= \frac{5123.0}{(0.16 \times 10^5)^{\frac{1}{2}}}$$

$$Ck = 40.5.$$

Natural frequencies of vibration of the equivalent gear system at other loads and viscosities were then calculated as follows.

(i) Mesh stiffness at the required load was read from Figure 5.24.

(ii) The damping ratio at that load and at the viscosity of the oil considered were obtained from Figure 5.25.

(iii) The undamped natural frequency was calculated using equation (85).

(iv) Results of (ii) and (iii) were used in equation (86) to calculate the natural frequency.

Figures 5.26a to 5.26d give the variation of the natural frequency thus obtained with load, together with the corresponding natural frequencies obtained experimentally. These graphs show that the increase in the frequency according to experimental results as the

load was increased was even less than half the amount predicted by the theory. This could mean that:

(a) the experimental results are not correct;

(b) theoretical results are wrong; or

(c) the theory did not represent the practical situation correctly.

The problem with the experimental results was that resonance was detected over a considerably wide frequency margin which itself was larger than the total increase in frequency observed for the range of loads tested. In fact, the theoretical results have indicated that the natural frequency is not confined to a narrow frequency band, especially when the contact ratio is high. In this way the experimental results seem to agree with the theoretical ones.

Another aspect that cannot be neglected is the variation of the load on the input side of the gears. This too is a time-dependent variable determined by the torsional characteristics of the system. Simulation results have confirmed that the natural frequency depends on the nominal load and, if this were to vary, then the natural frequency also would vary accordingly. While the theoretical calculations were based on the fixed nominal load, in the experiment it was the average, in this case of the noise, over a certain interval of time that was measured.

The natural frequency/viscosity graphs in Figures 5.27a and 5.27b compare the theoretical and experimental results. At the lower load

(6.4 N/mm) the experimental results give a slower rate of reduction of frequency with viscosity than the theoretical ones, while at the higher load (13.88 N/mm) theoretical results predict a slower rate of decrease of natural frequency with viscosity. At even higher loads, theoretical results predict a constant natural frequency while the experimental results maintain its decreasing trend until the load is about 30.0 N/mm (Figure 5.28).

In the theoretical calculations damping force was calculated assuming only one pair of teeth to be in contact, whereas in the experimental test gear pair the contact ratio was over 1.6, and hence most of the time the load was shared by two pairs of teeth. The load sharing between two pairs of teeth creates a situation which produces two opposite results.

(a) The load on an individual pair of teeth is almost halved, thereby (in most situations according to theory) increasing the damping ratio and hence reducing the natural frequency.

(b) The total mesh stiffness is almost doubled, thereby increasing the natural frequency. The mesh stiffness of the equivalent pair of gears used in the theoretical calculation, and hence its natural frequency at high load, was determined based on the resultant natural frequency of the test gear pair. But the variation of the mesh stiffness with load for a single pair of teeth which was used in the theory is different from the variation of the mesh stiffness of the actual pair of gears with part of the cycle under double tooth contact.

It is the results of the above effects which determine the final natural frequency. Since the experimental results showed a lower increase in natural frequency with load than the amount predicted by the theory, it can be said that the effect of (b) was more than the effect of (a) for the pair of test gears used. Hence it can be concluded that in general this rate of increase of the natural frequency depends, apart from the nominal load and the viscosity of oil, on the contact ratio of the pair of gears.

TABLE 5.1

L.O.T. (^{o}F) / L.T. (Nm)	105	120	130	140	150
1.5		5140	5133	5120	5125
5.0		5063/ 5123	5000/ 5122	5040/ 5126	
7.0	5020 5060	5058 5110	5057 5111	5069 5113	5069 5114
15.0	5030	5080	5077	5049 5081	5075
20.0	5026	5061	5076	5080	5060
26.0	5061	5085	5107	5093	5108
29.0	5110	5090	5120	5119	5120
33.0	5135	5120	5120	5120	5132

FIGURE 5.1

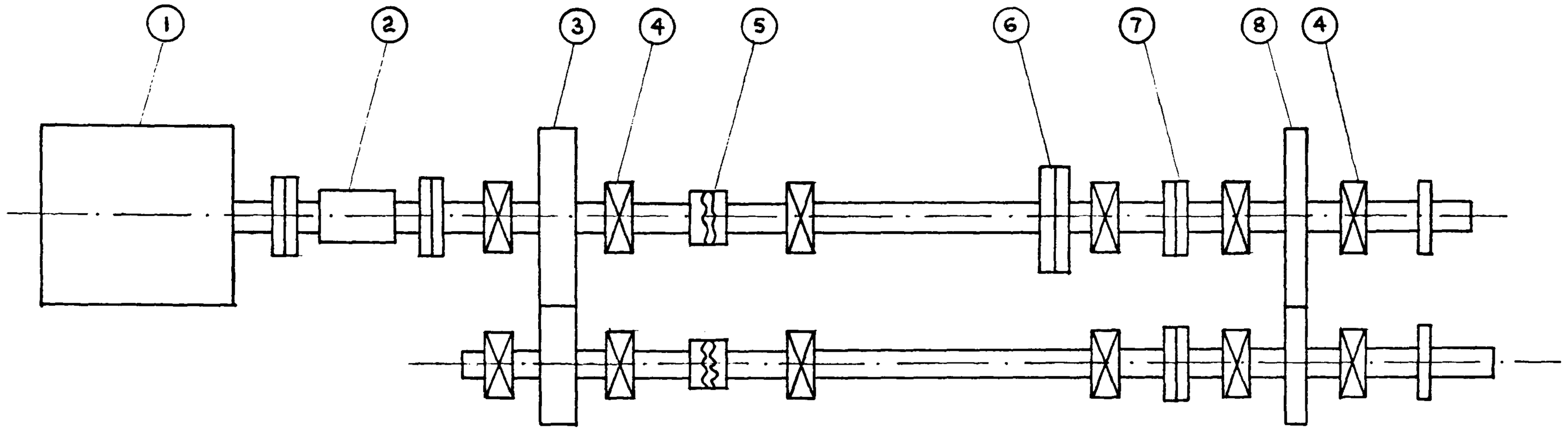

GEAR TEST RIG

1	MOTOR	2	TORQUE TRANSDUCER - FRICTIONAL TORQUE
3	SLAVE GEARS	4	JOURNAL BEARING
5	UNIVERSAL COUPLING	6	LOADING COUPLING
7	COUPLING	8	TEST GEARS

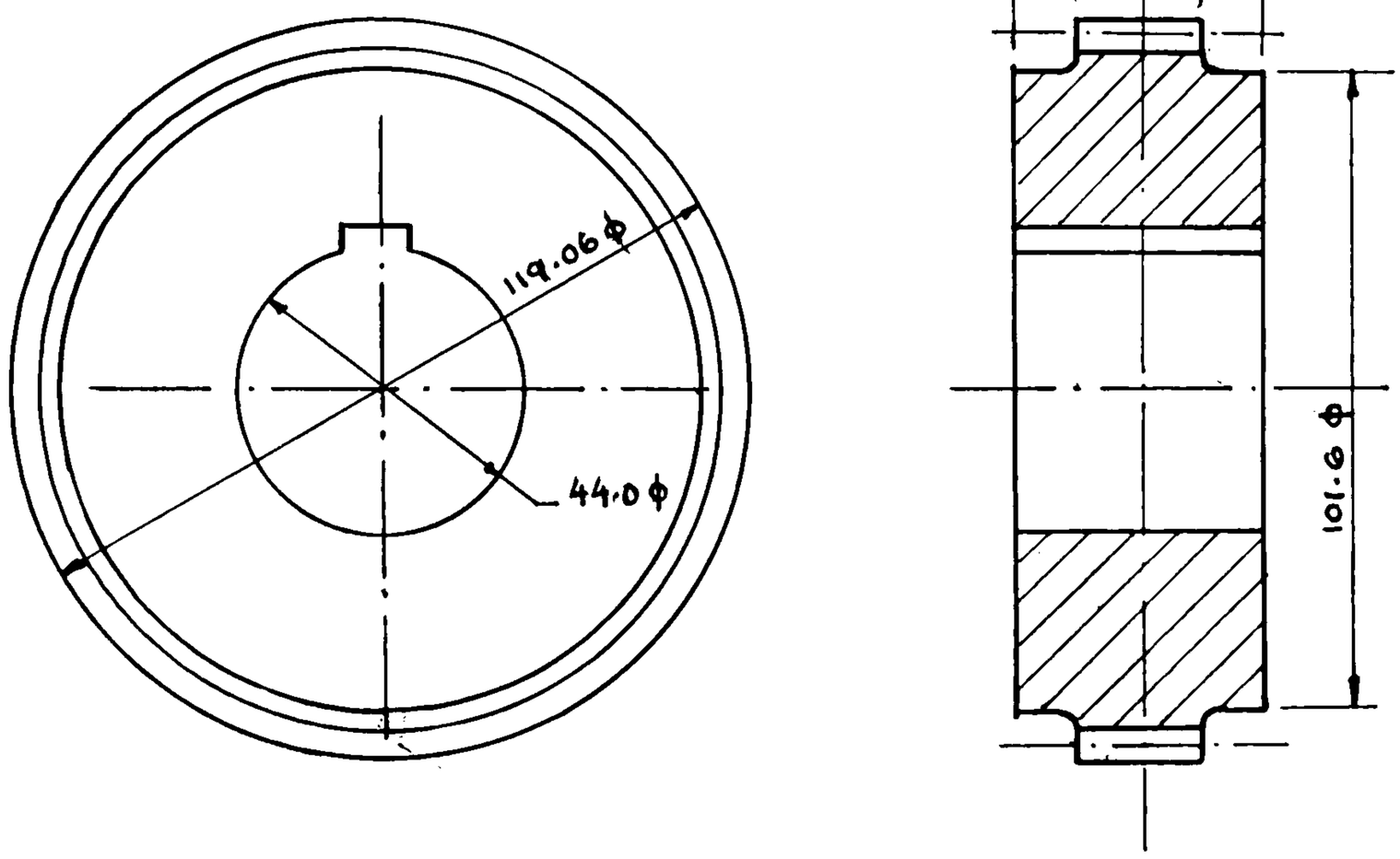

FIGURE 5.2

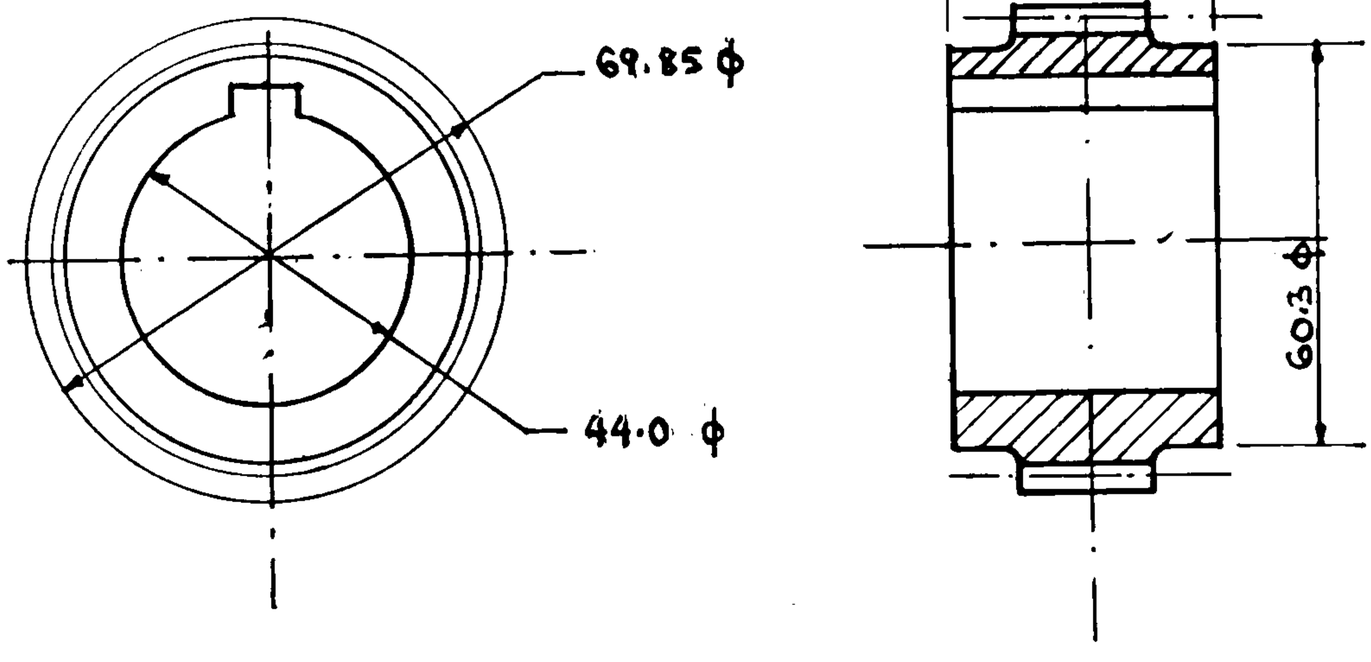

FIGURE 5.3

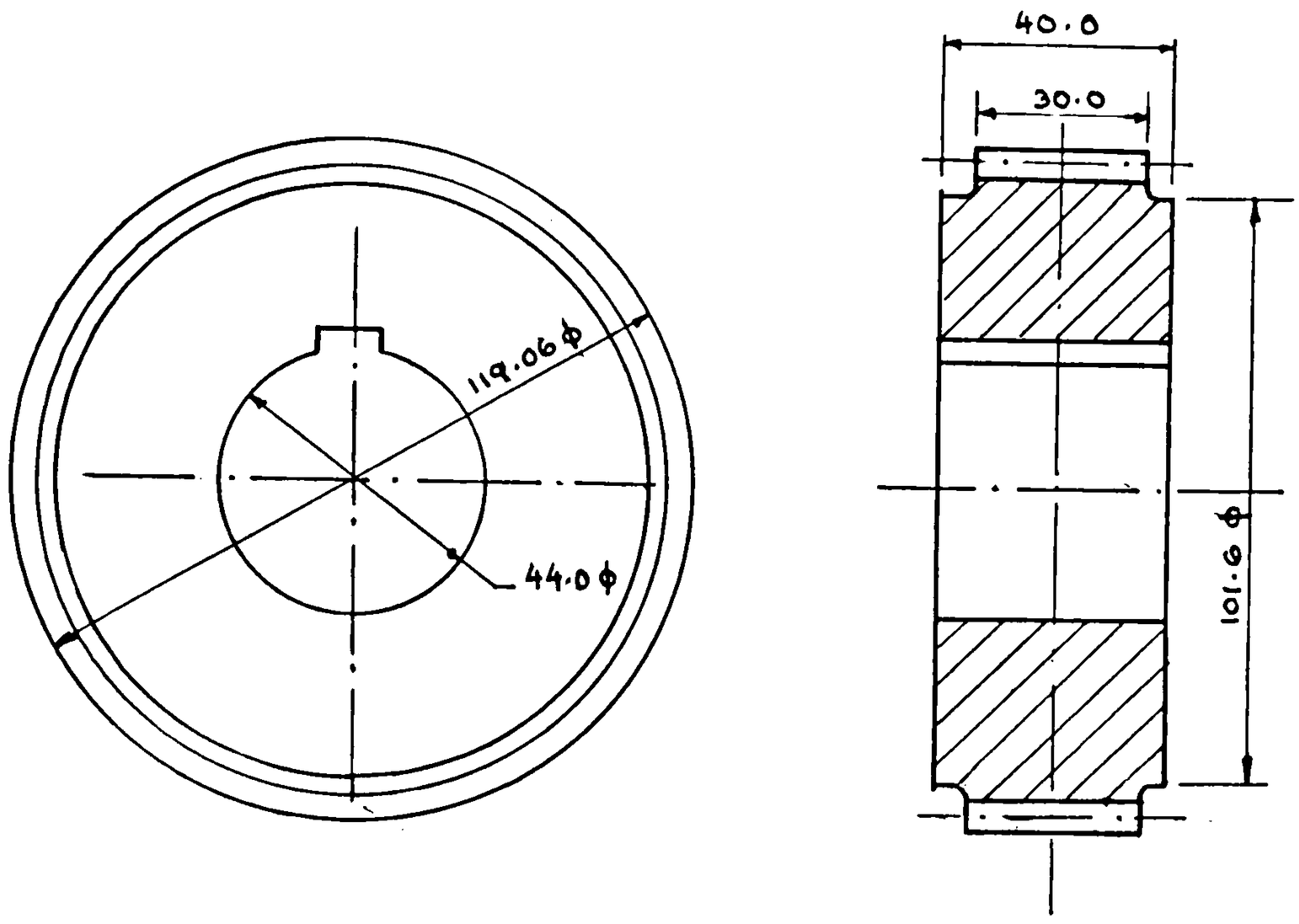

FIGURE 5.4

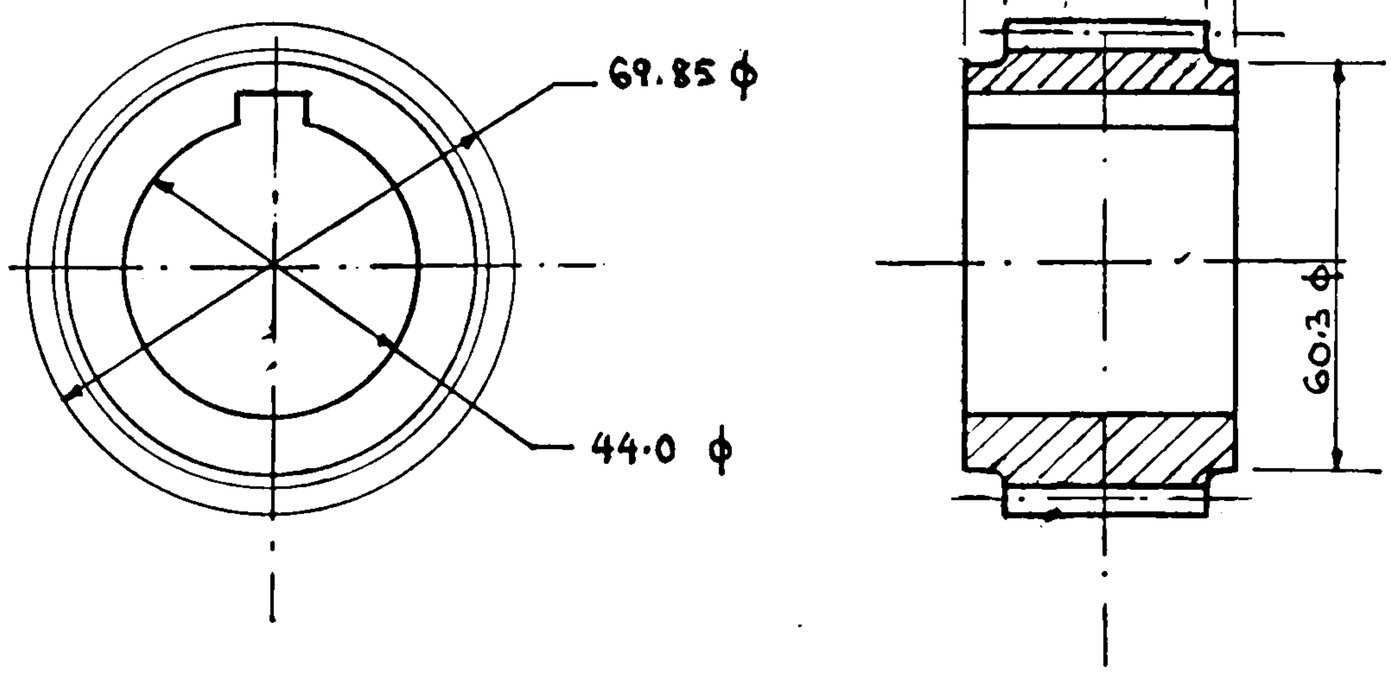

FIGURE 5.5

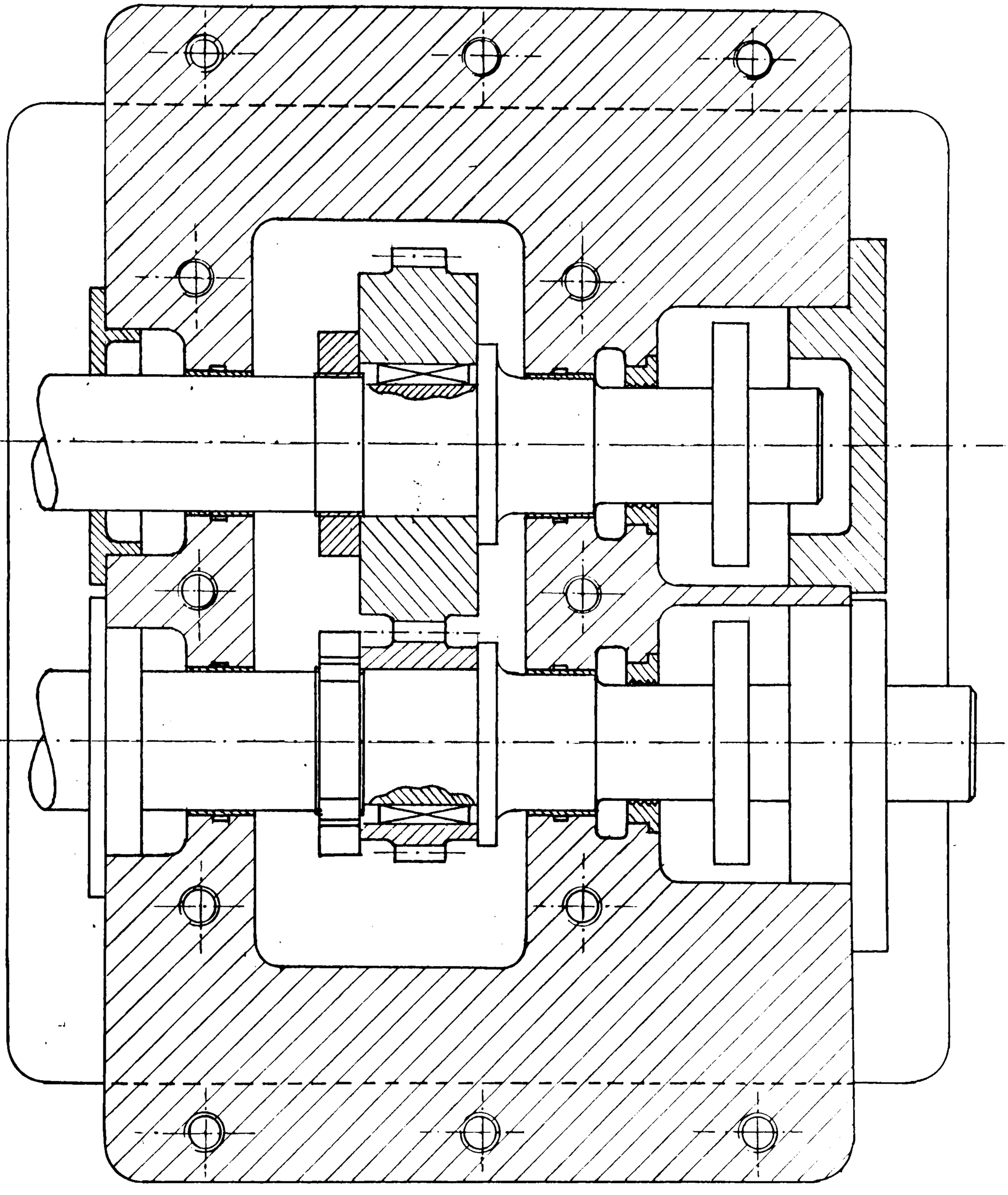

GEARBOX ASSEMBLY

FIGURE 5.6(a)

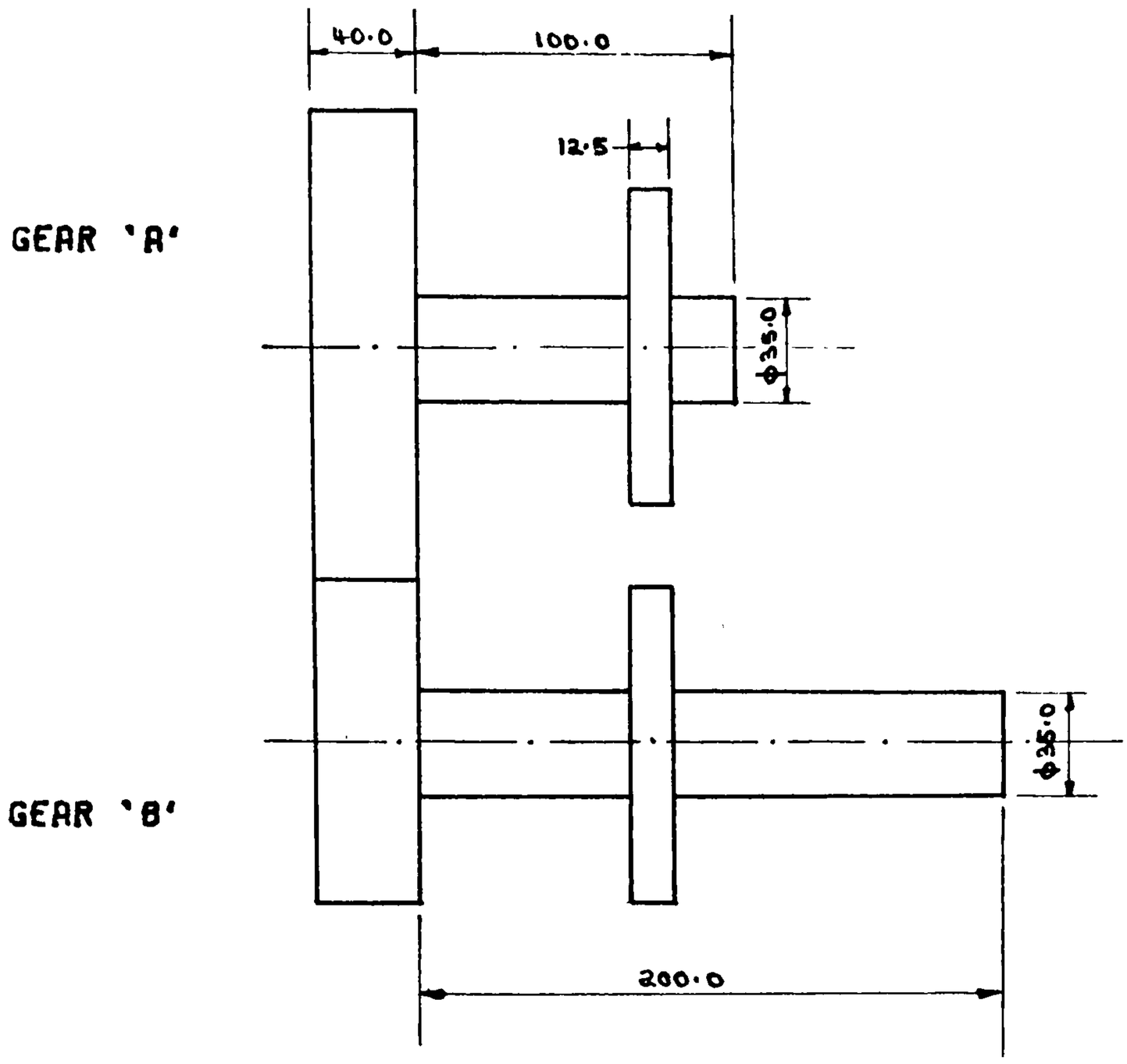

SECTION CONSIDERED FOR CALCULATING THE NAT. FREQ. OF GEARS

FIGURE 5.6(b)

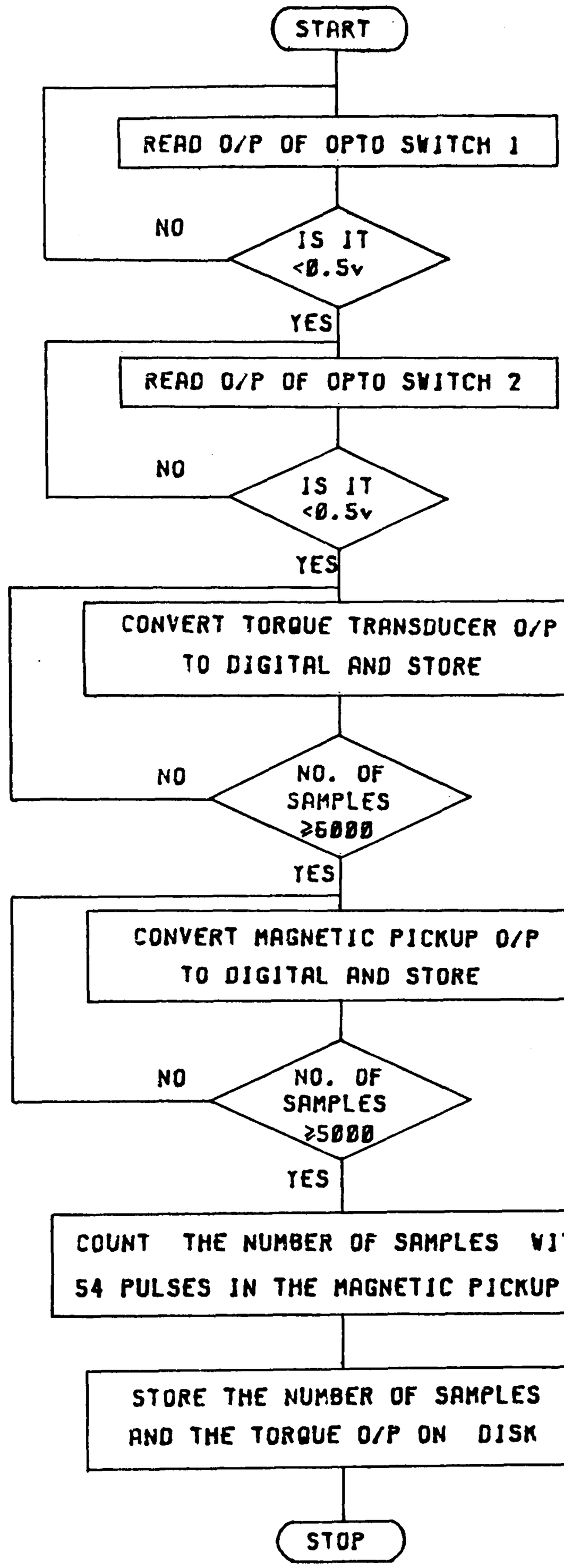

DATA COLLECTING AND STORING SEQUENCE

FIGURE 5.7

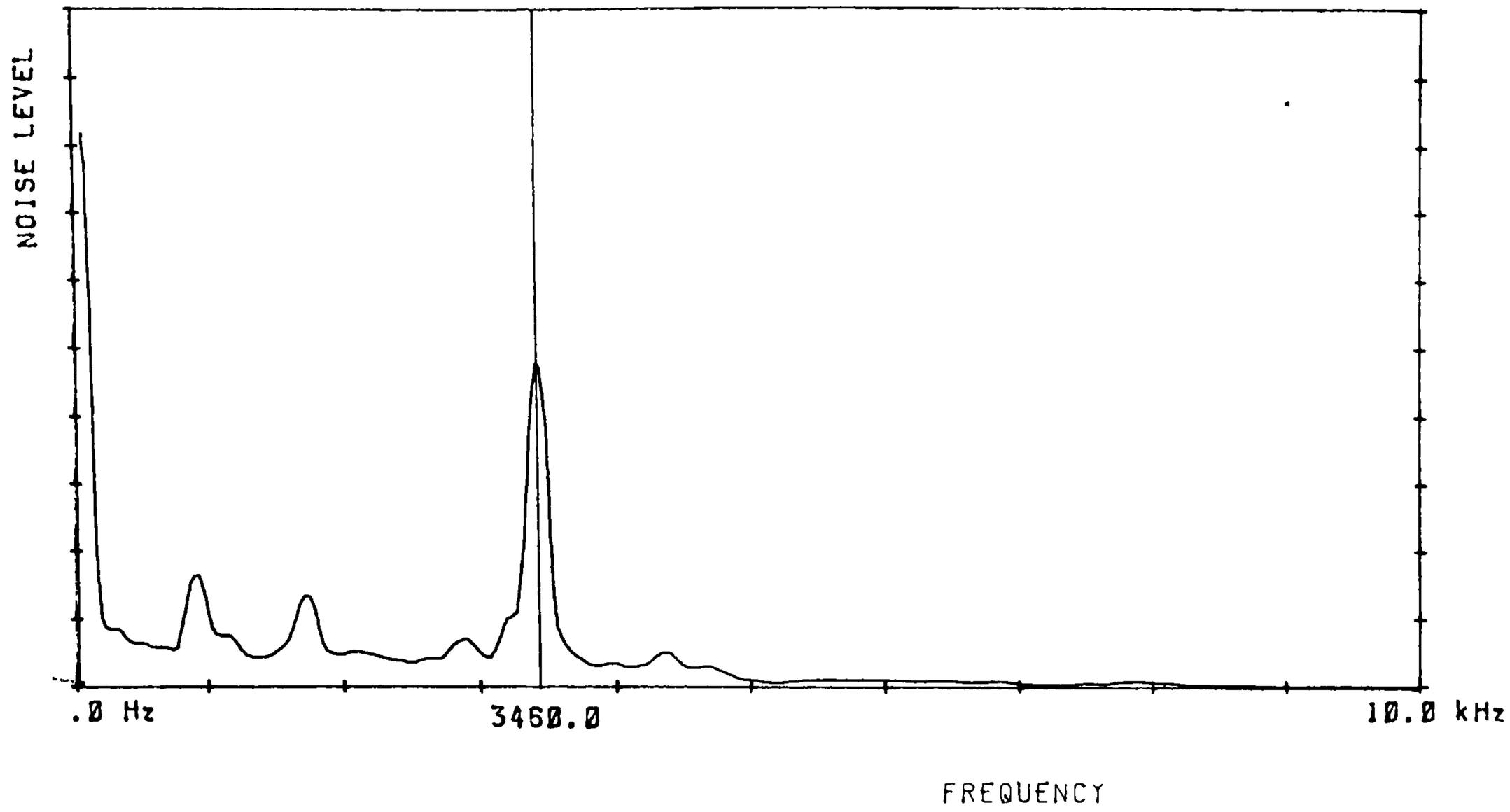

FIGURE 5.8

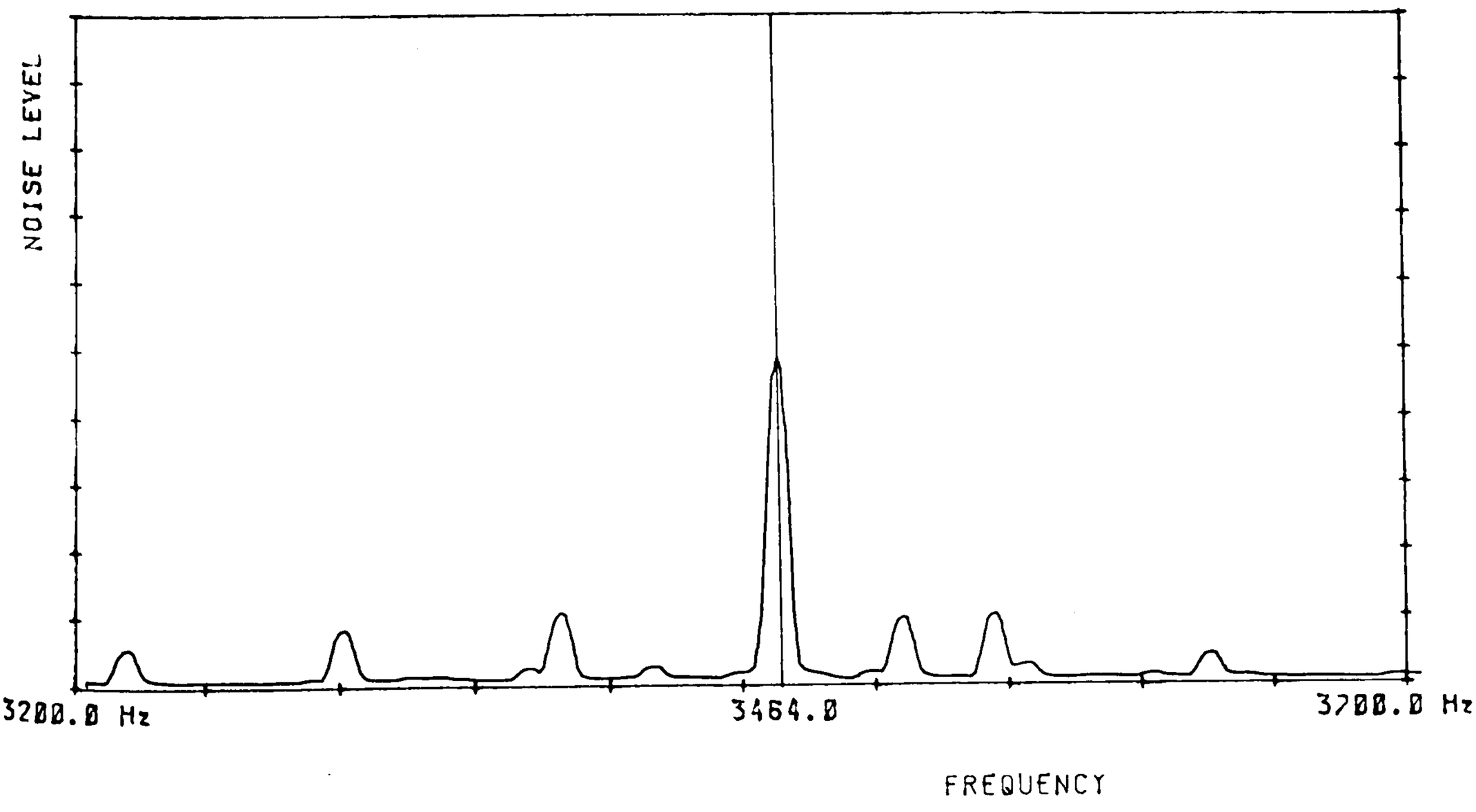

FIGURE 5.9

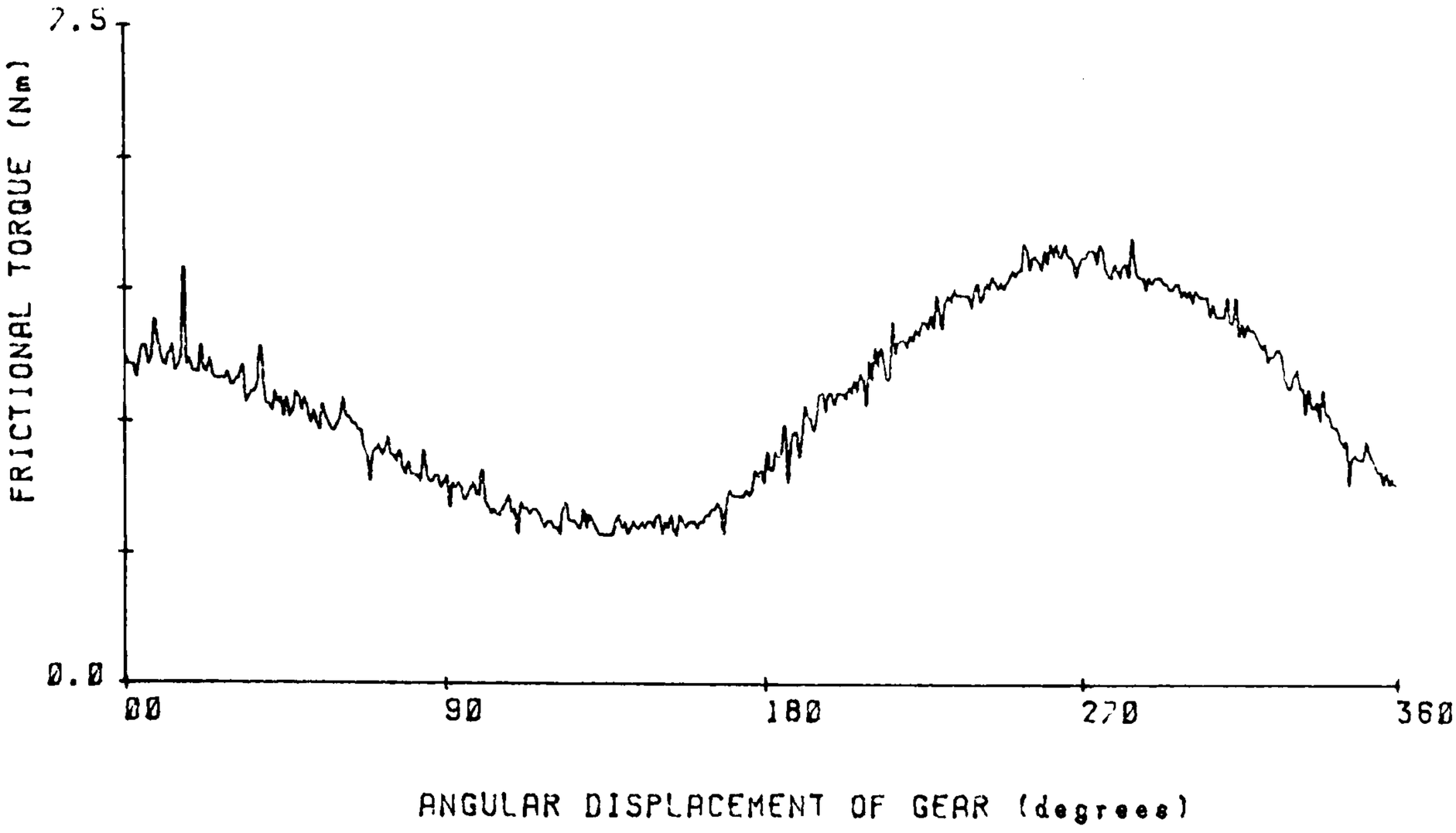

FIGURE 5.10(a)

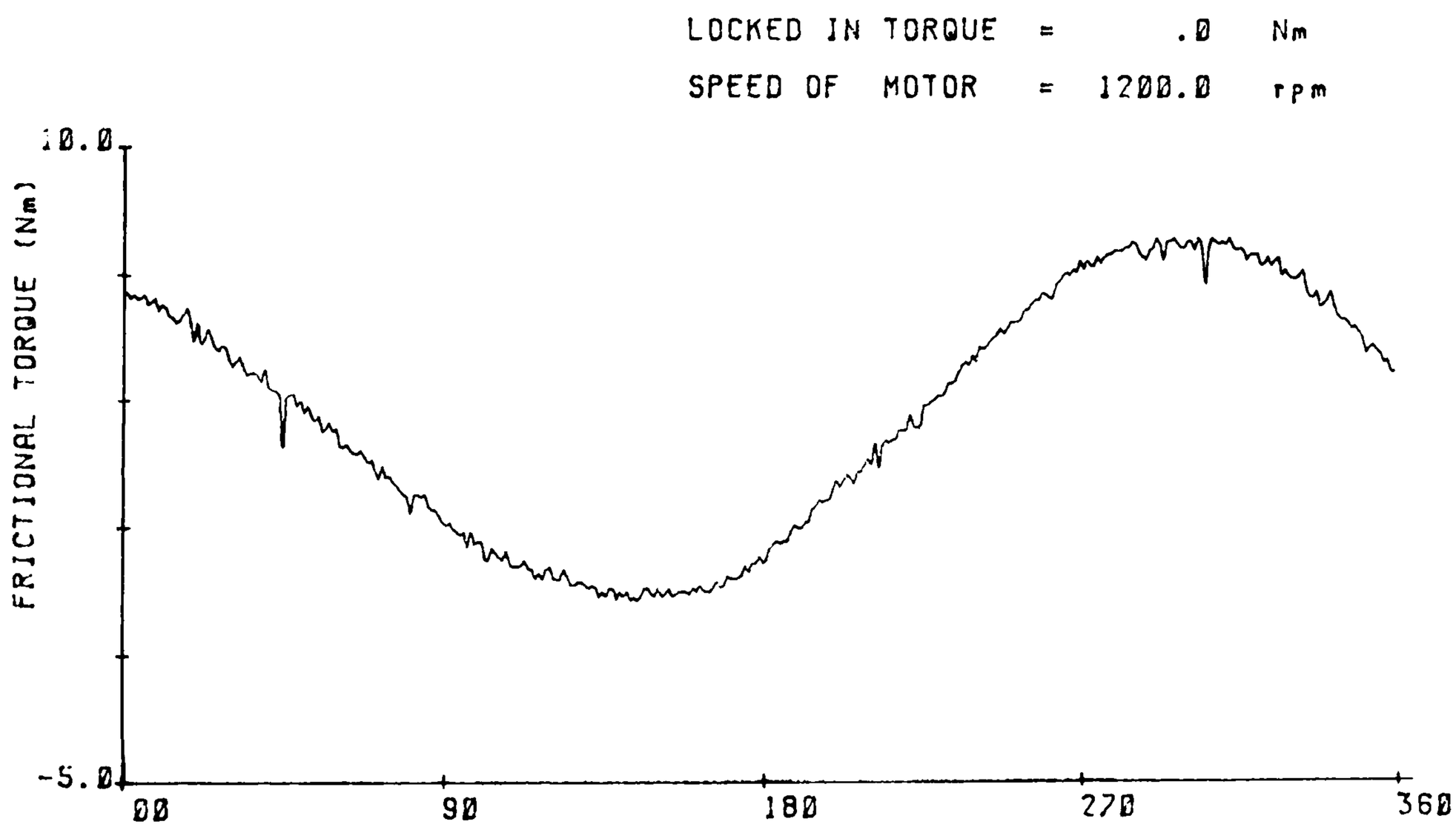

FIGURE 5.10(b)

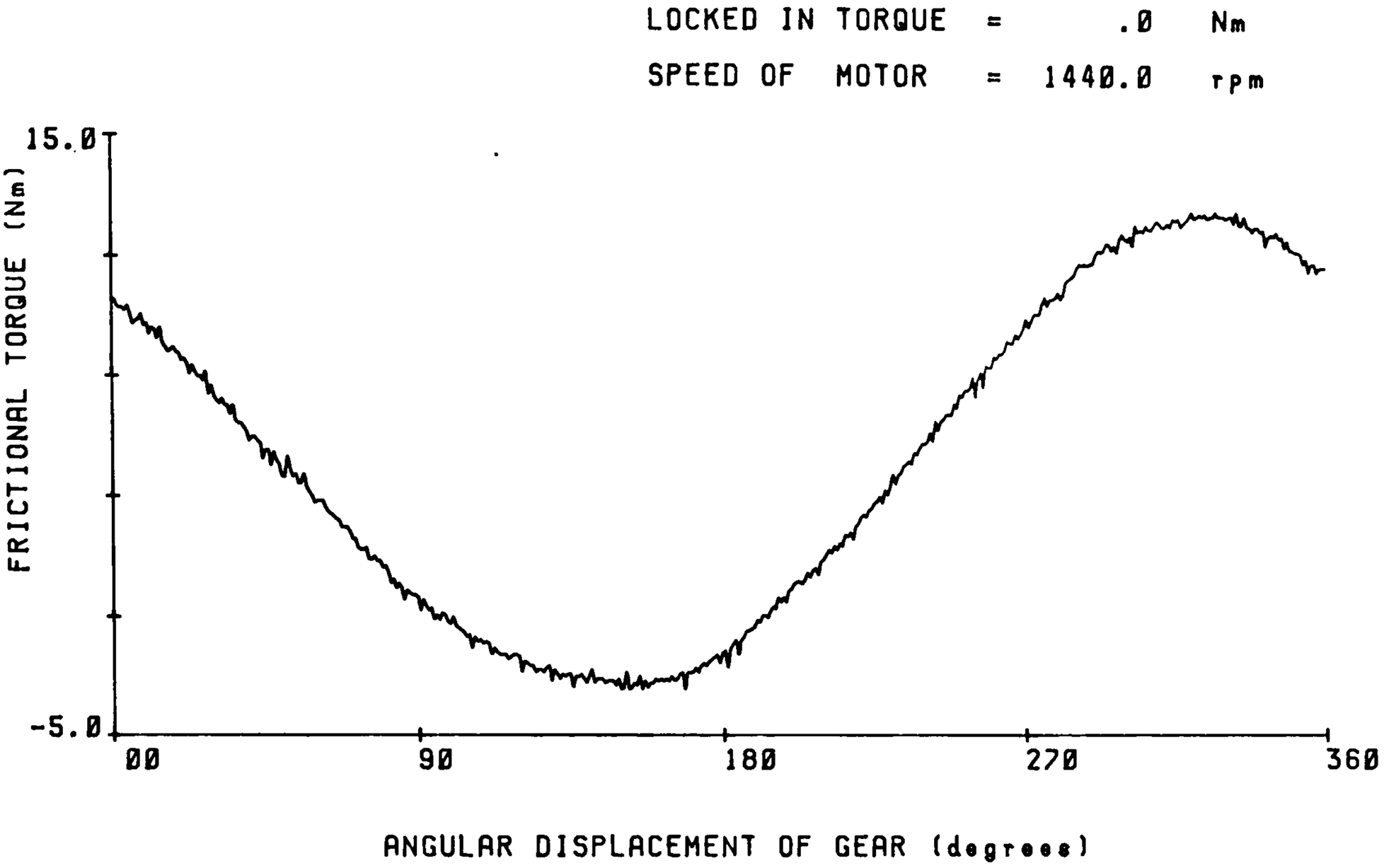

FIGURE 5.10(c)

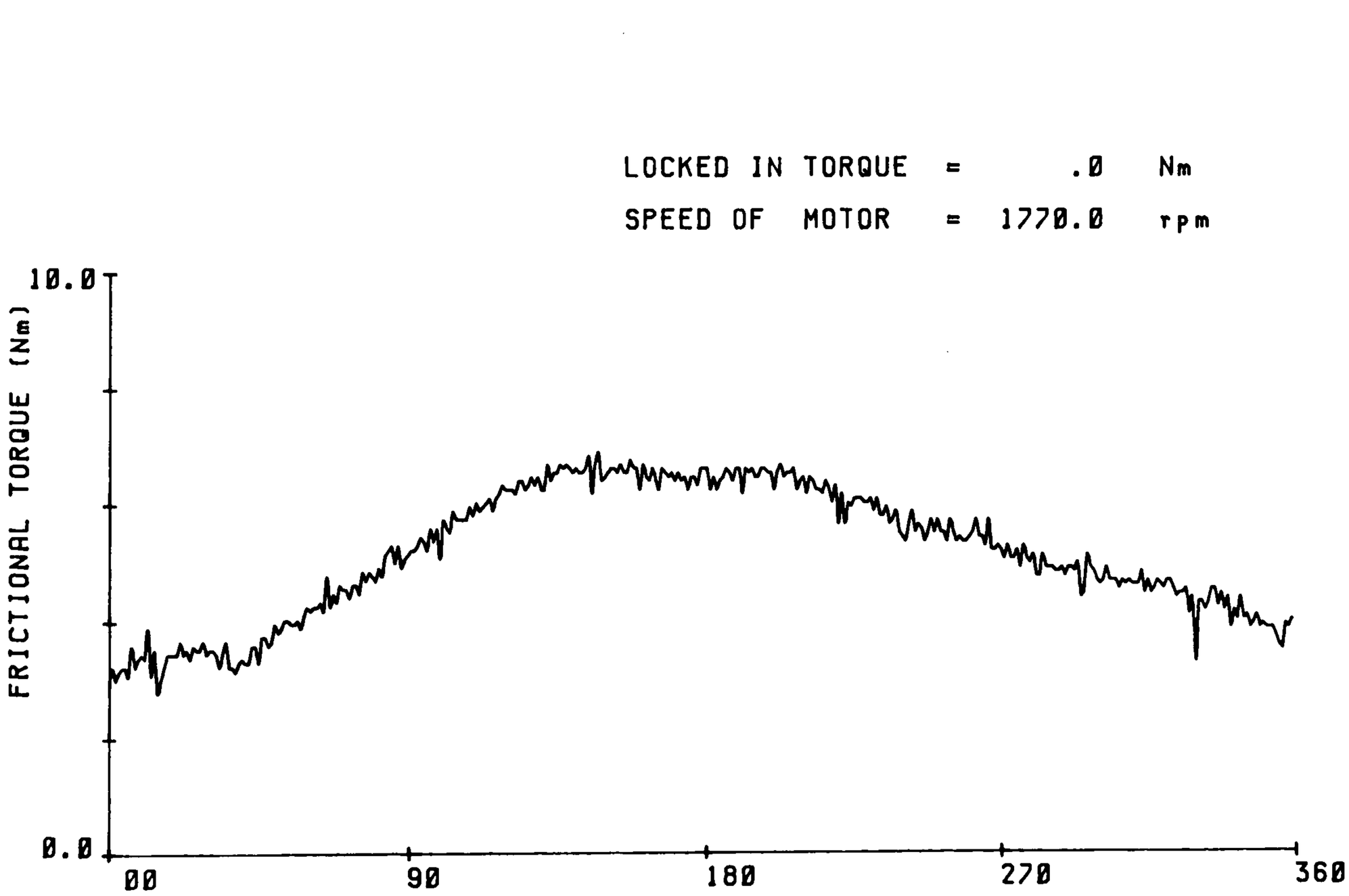

FIGURE 5.10(d)

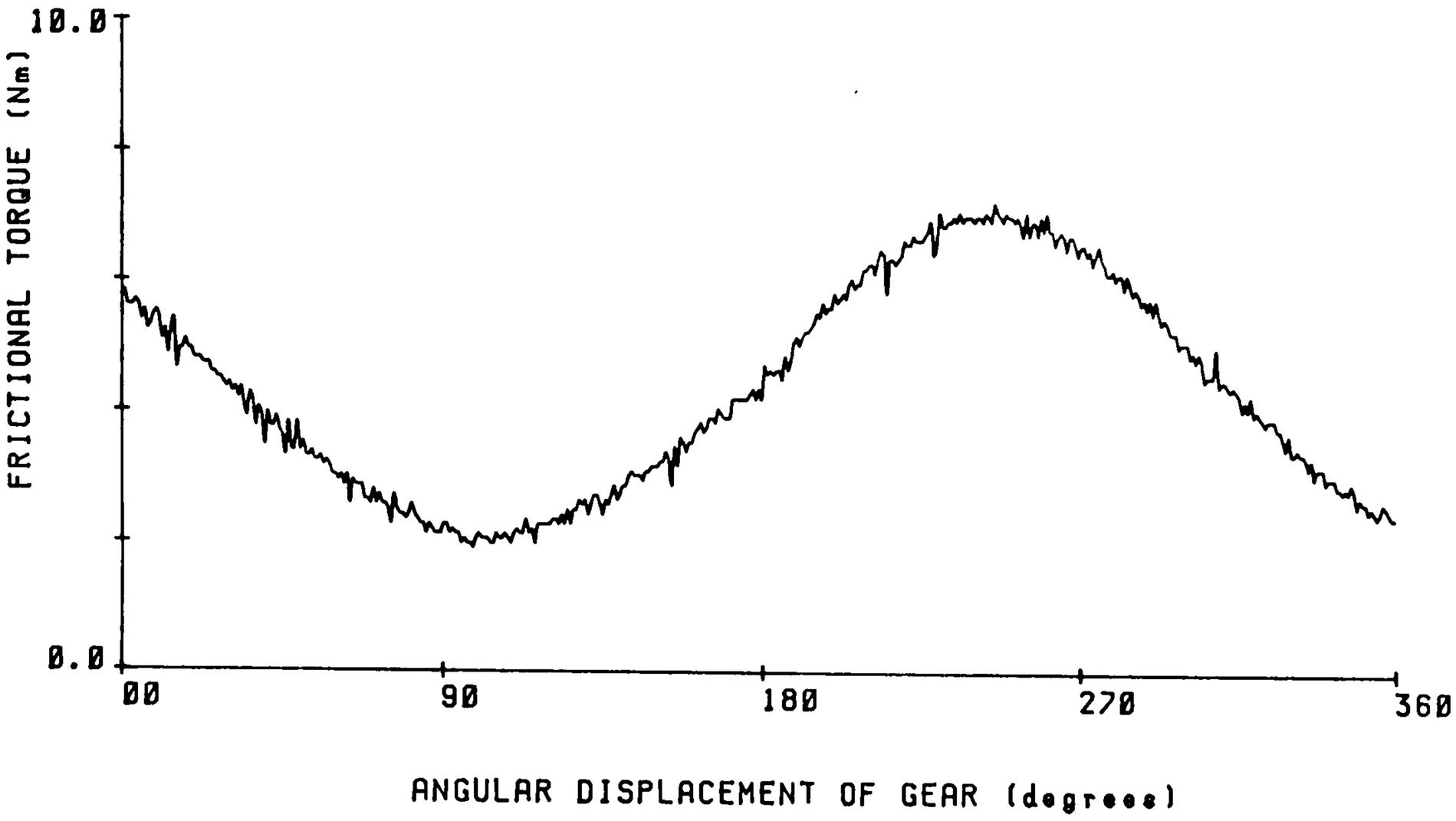

FIGURE 5.11(a)

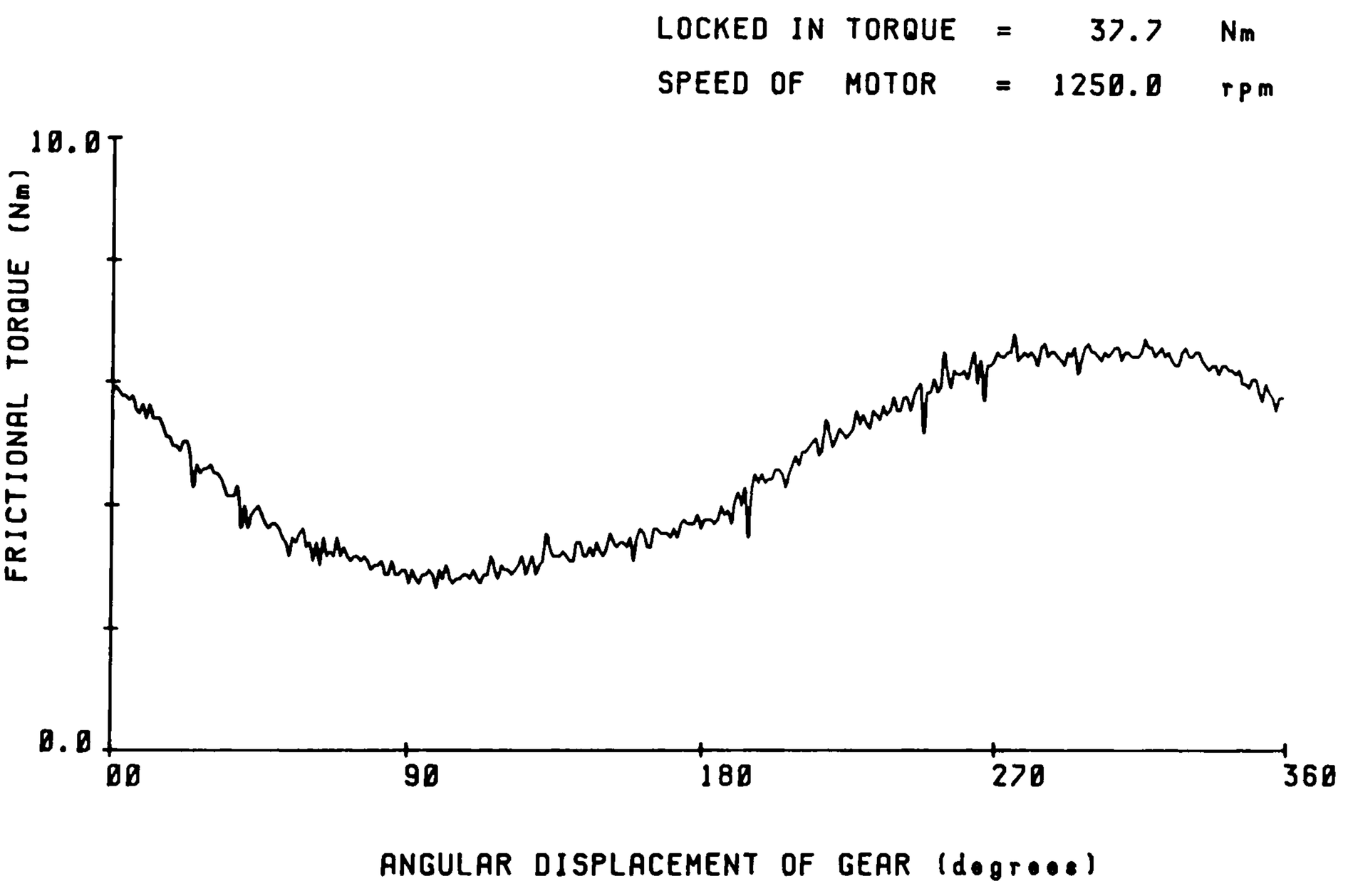

FIGURE 5.11(b)

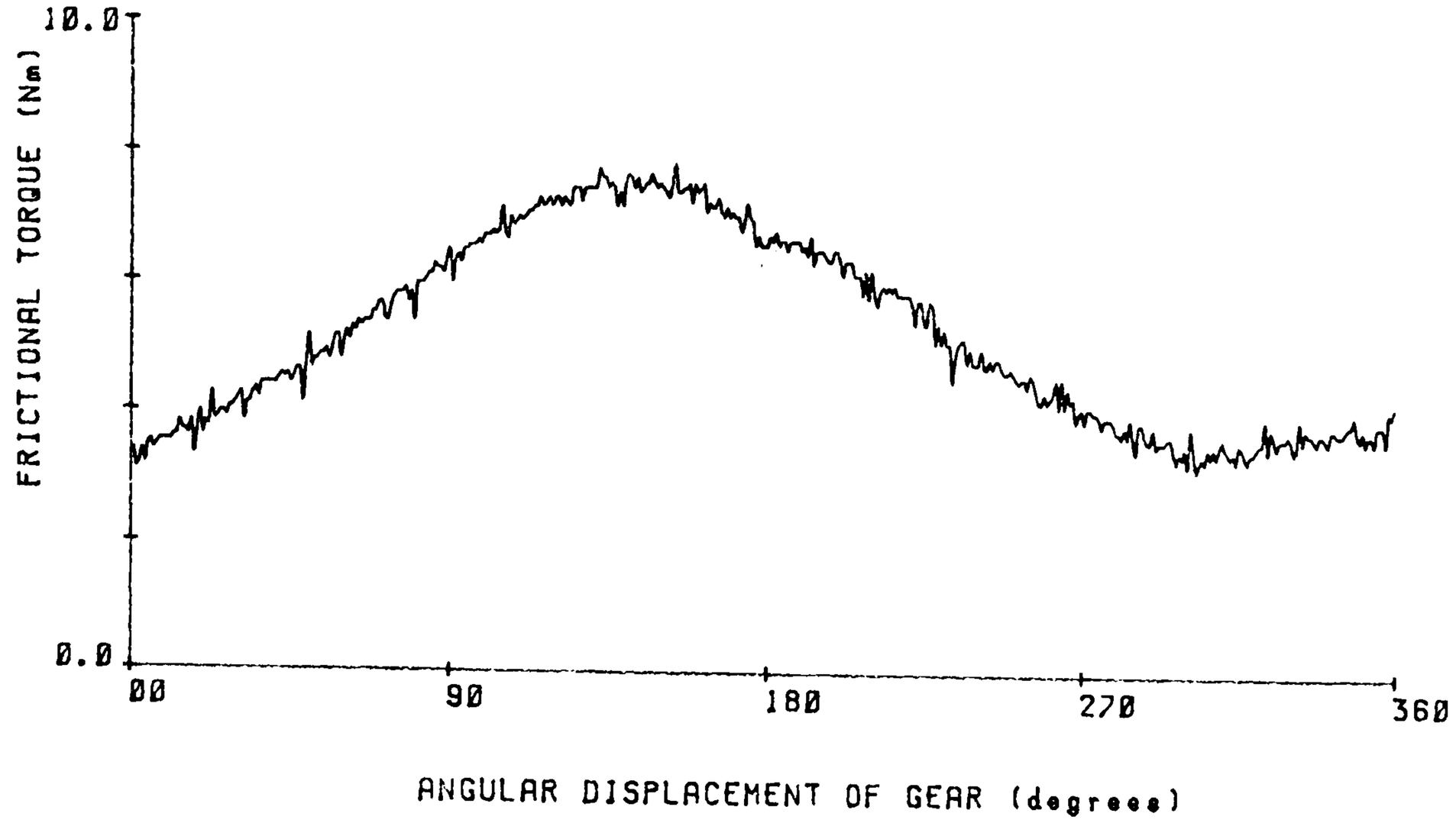

FIGURE 5.11(c)

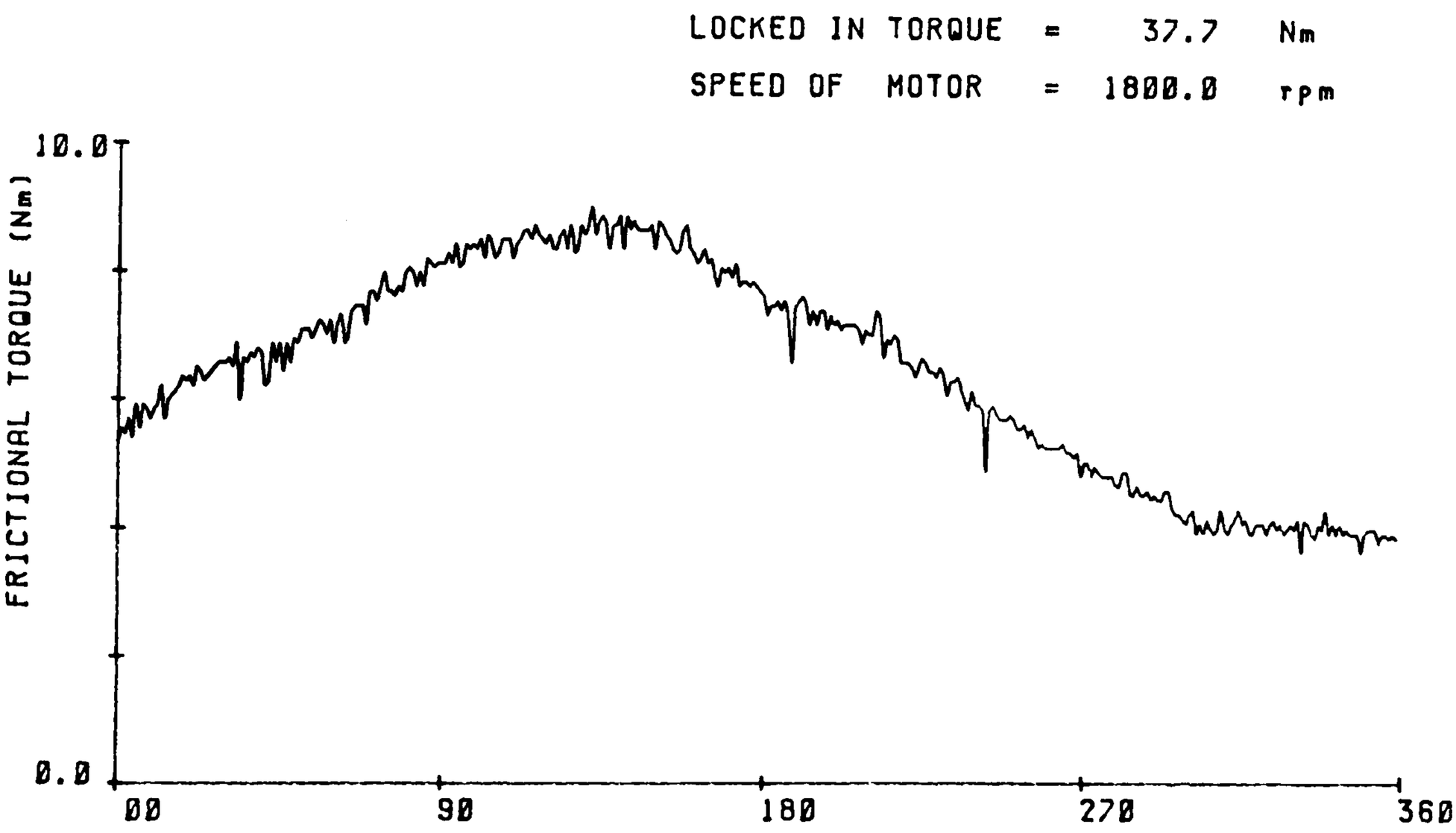

FIGURE 5.11(d)

DRIVING SHAFT ONLY

SPEED OF MOTOR = 1014.0 rpm

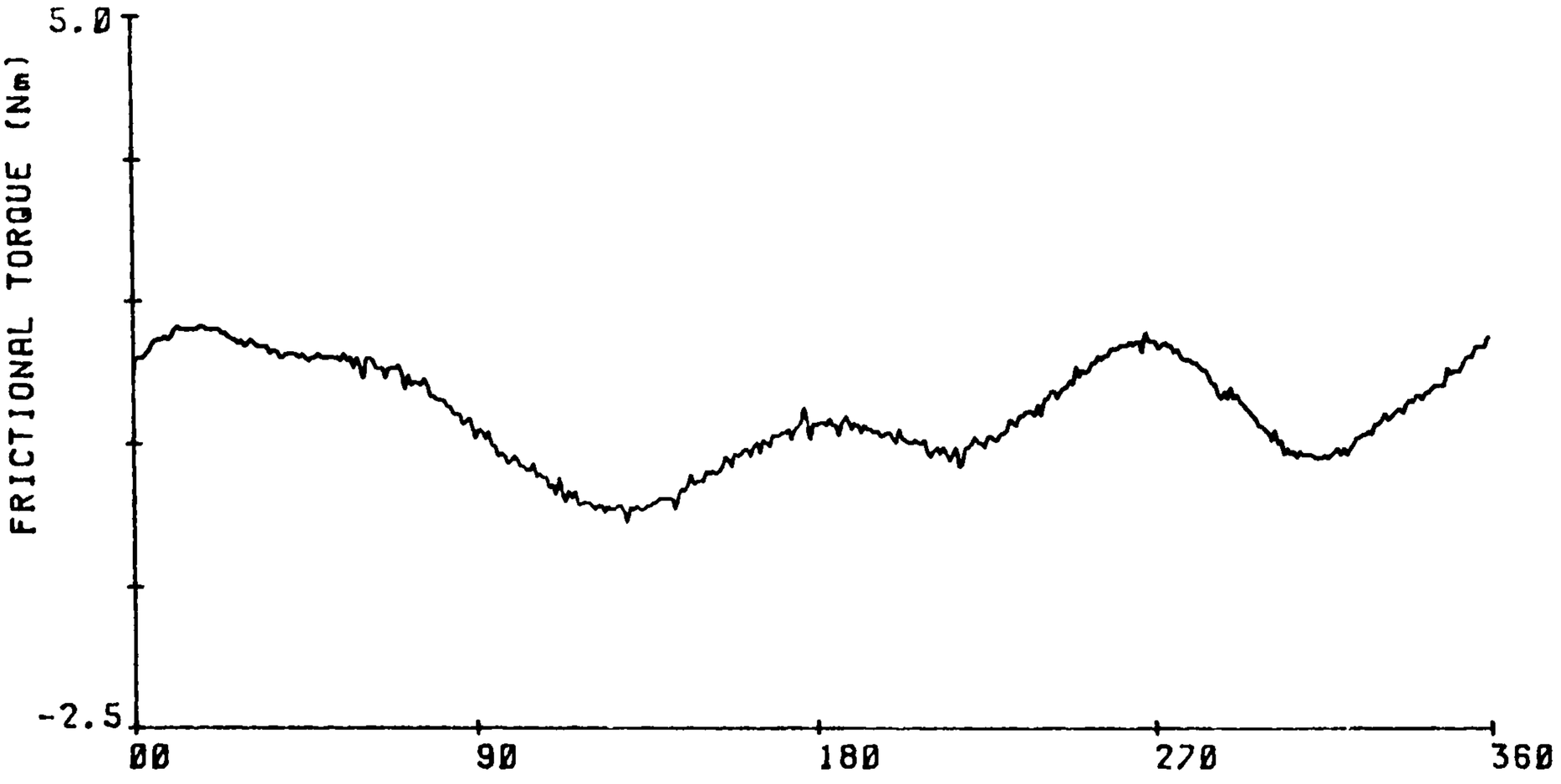

FIGURE 5.12

VARIATION OF FRICTIONAL TORQUE WITH TIME

LOAD TORQUE = 0.0 Nm

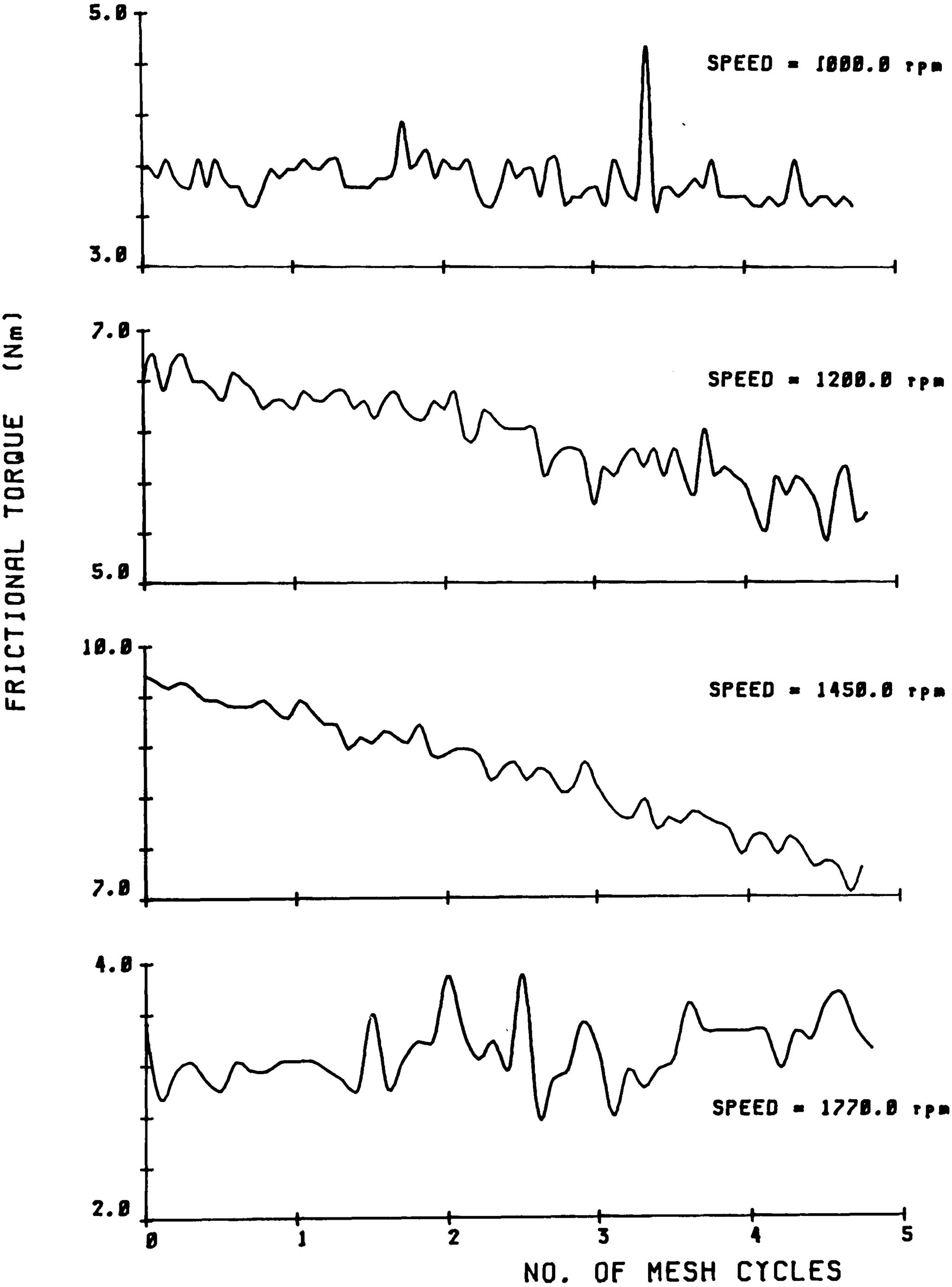

FIGURE 5.13

VARIATION OF FRICTIONAL TORQUE WITH TIME

LOAD TORQUE = 14.5 Nm

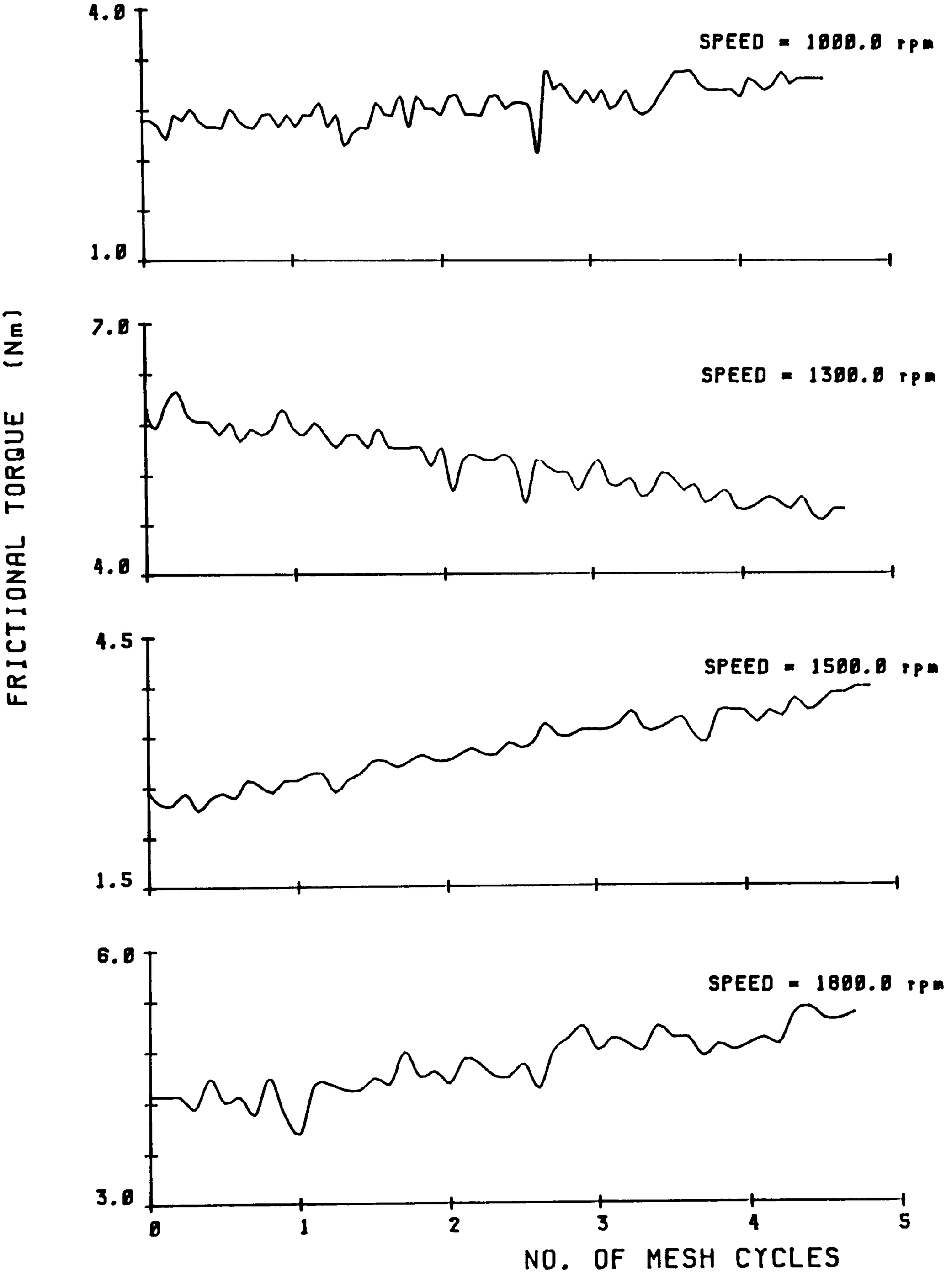

FIGURE 5.14

VARIATION OF FRICTIONAL TORQUE WITH TIME

LOAD TORQUE = 21.0 Nm

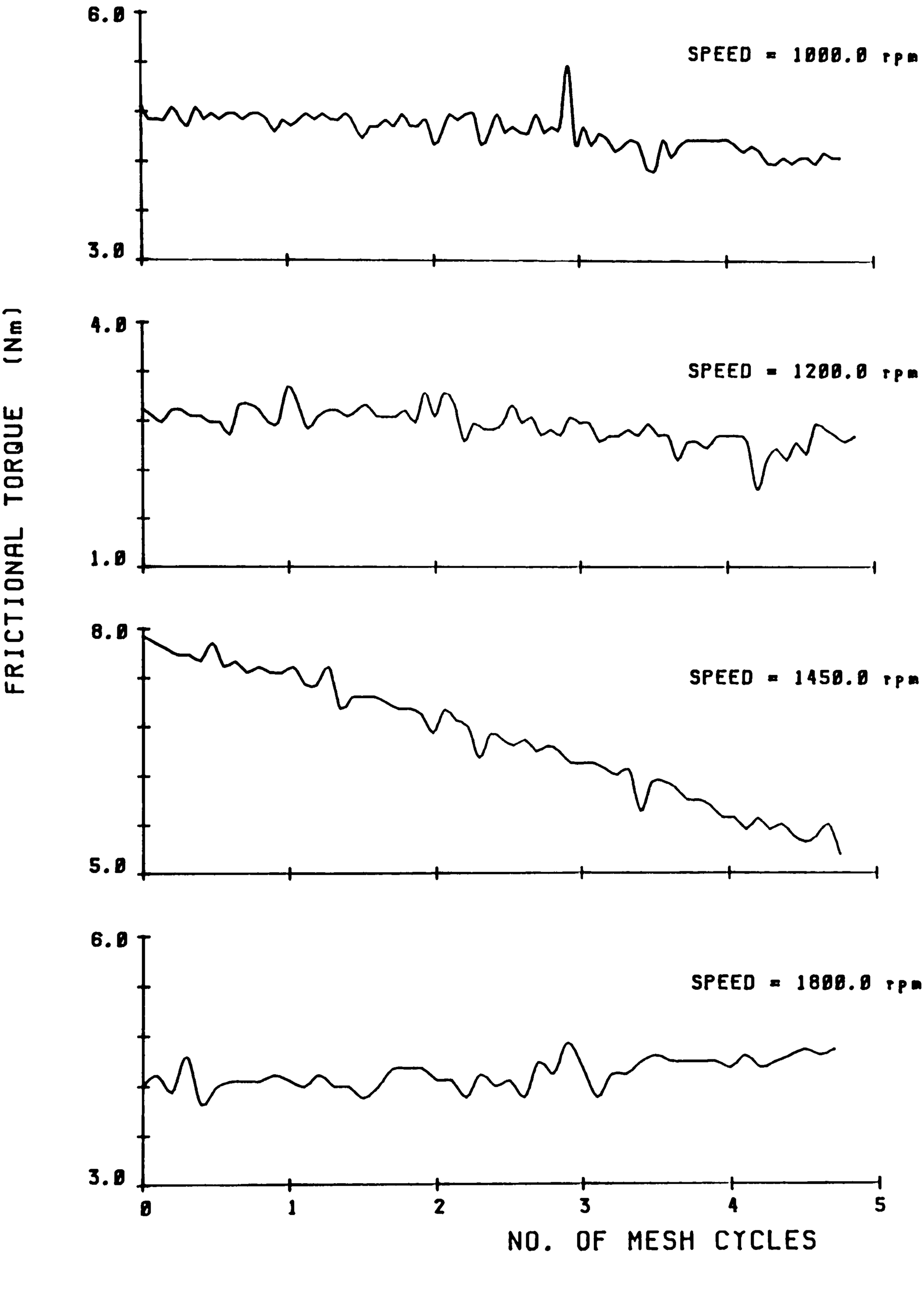

FIGURE 5.15

VARIATION OF FRICTIONAL TORQUE WITH TIME

LOAD TORQUE = 37.7 Nm

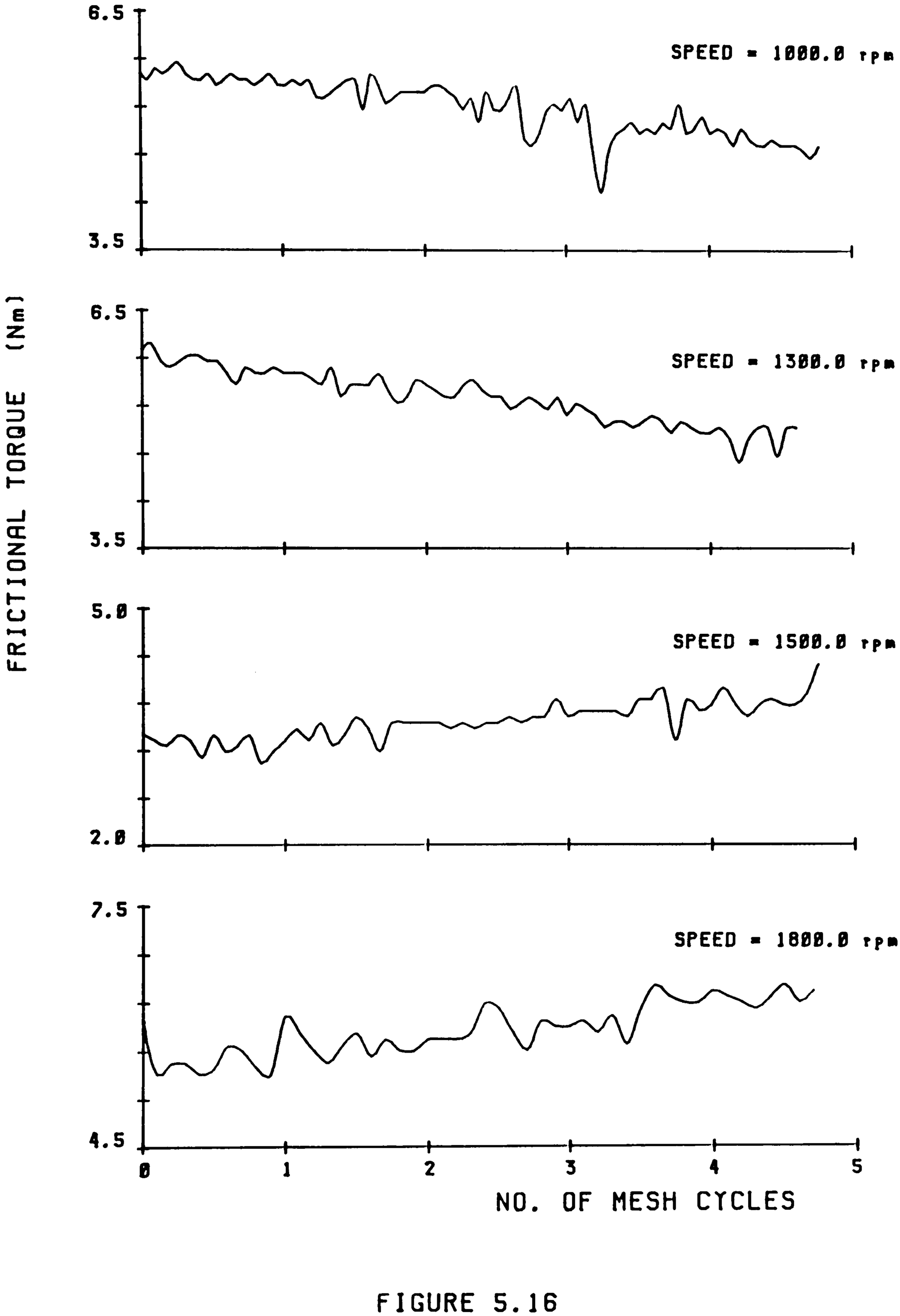

FIGURE 5.16

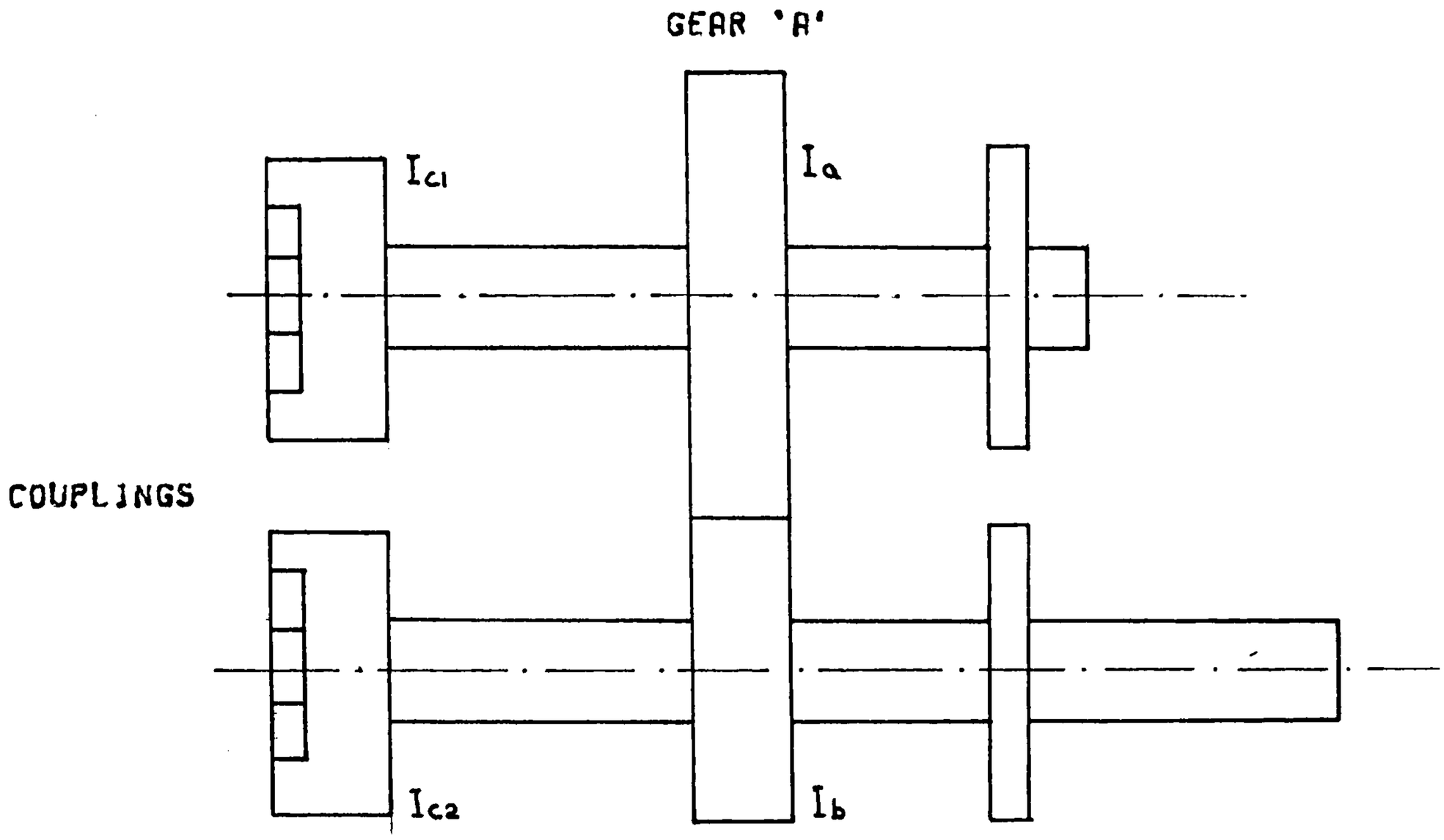

SUB SYSTEM USED FOR THE CALCULATION OF NATURAL FREQUENCIES

FIGURE 5.17

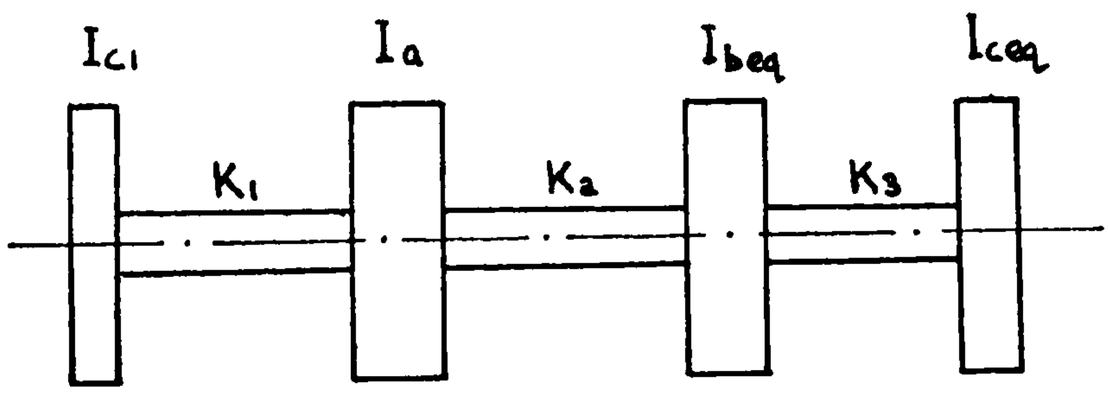

EQUIVALENT FOUR INERTIA MODEL

FIGURE 5.18

LUB. OIL VISCOSITY (μ_t) Vs TEMPERATURE

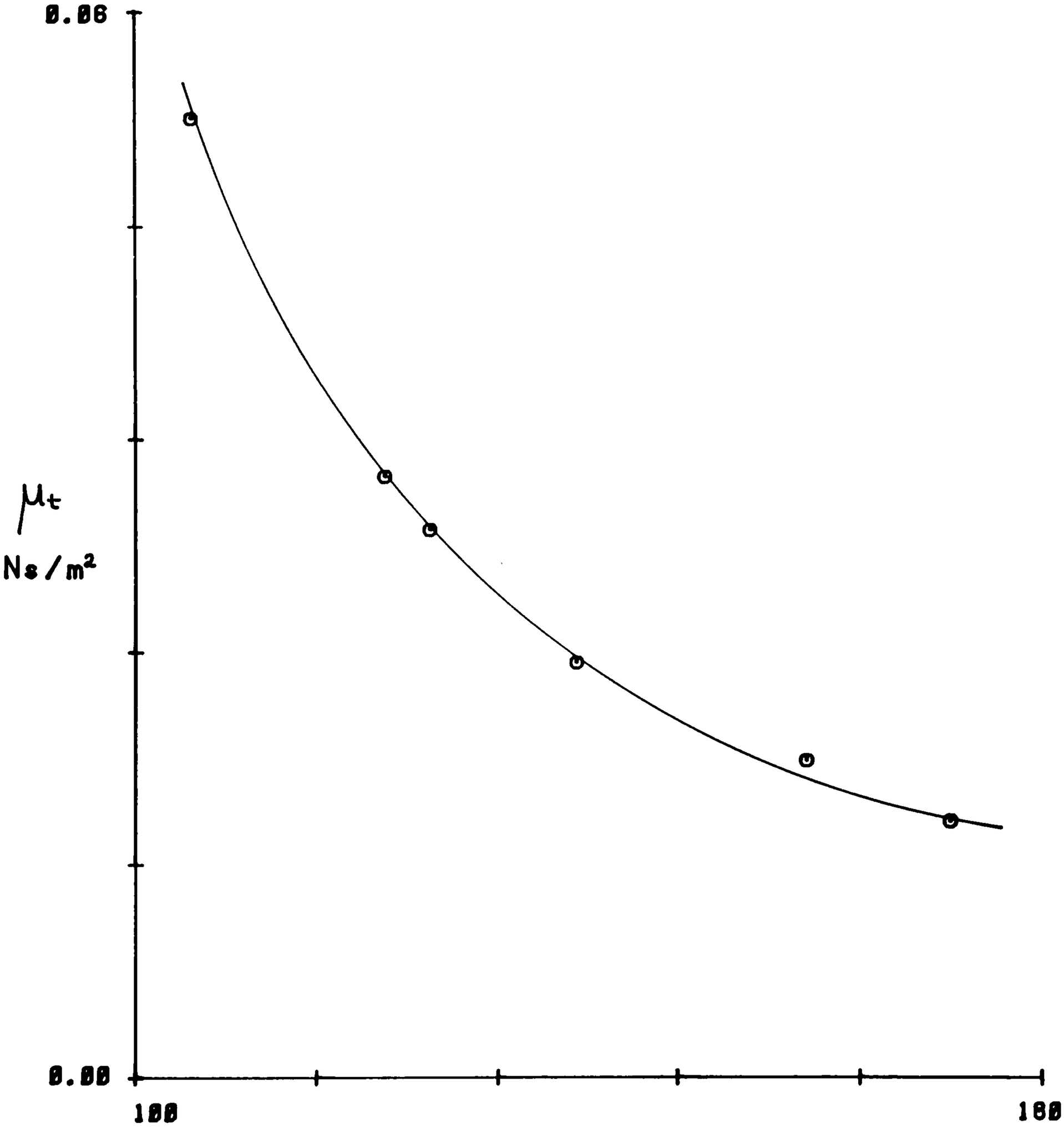

FIGURE 5.19.

SPEED = 2100.0 rpm LOAD TORQUE = 7.0 Nm

T.C.F. = 2555.0 Hz LUB. OIL TEMP. = 120.0 F

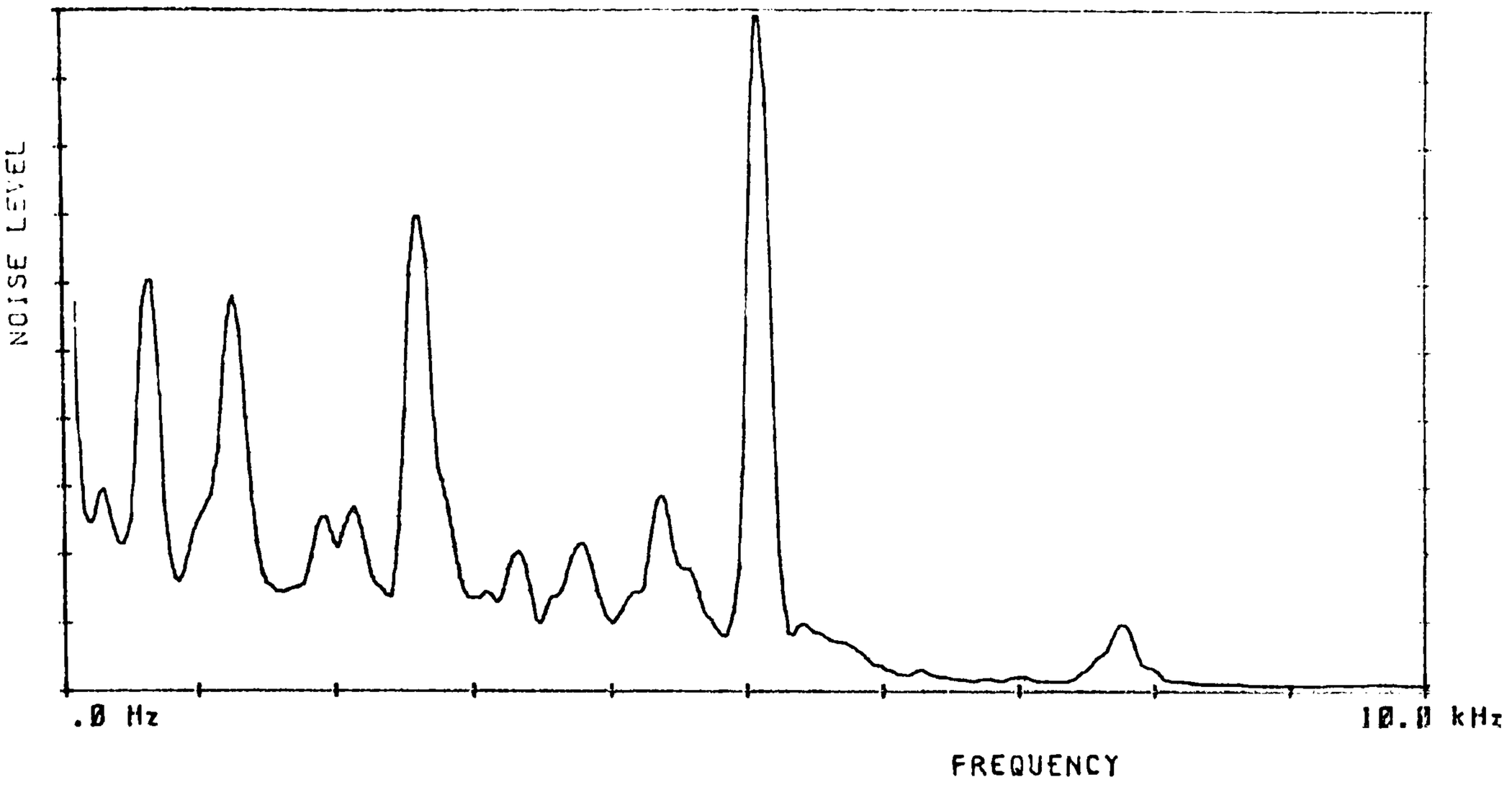

FIGURE 5.20(a)

SPEED = 2103.0 rpm LOAD TORQUE = 7.0 Nm

T.C.F. = 2558.6 Hz LUB. OIL TEMP. = 130.0 F

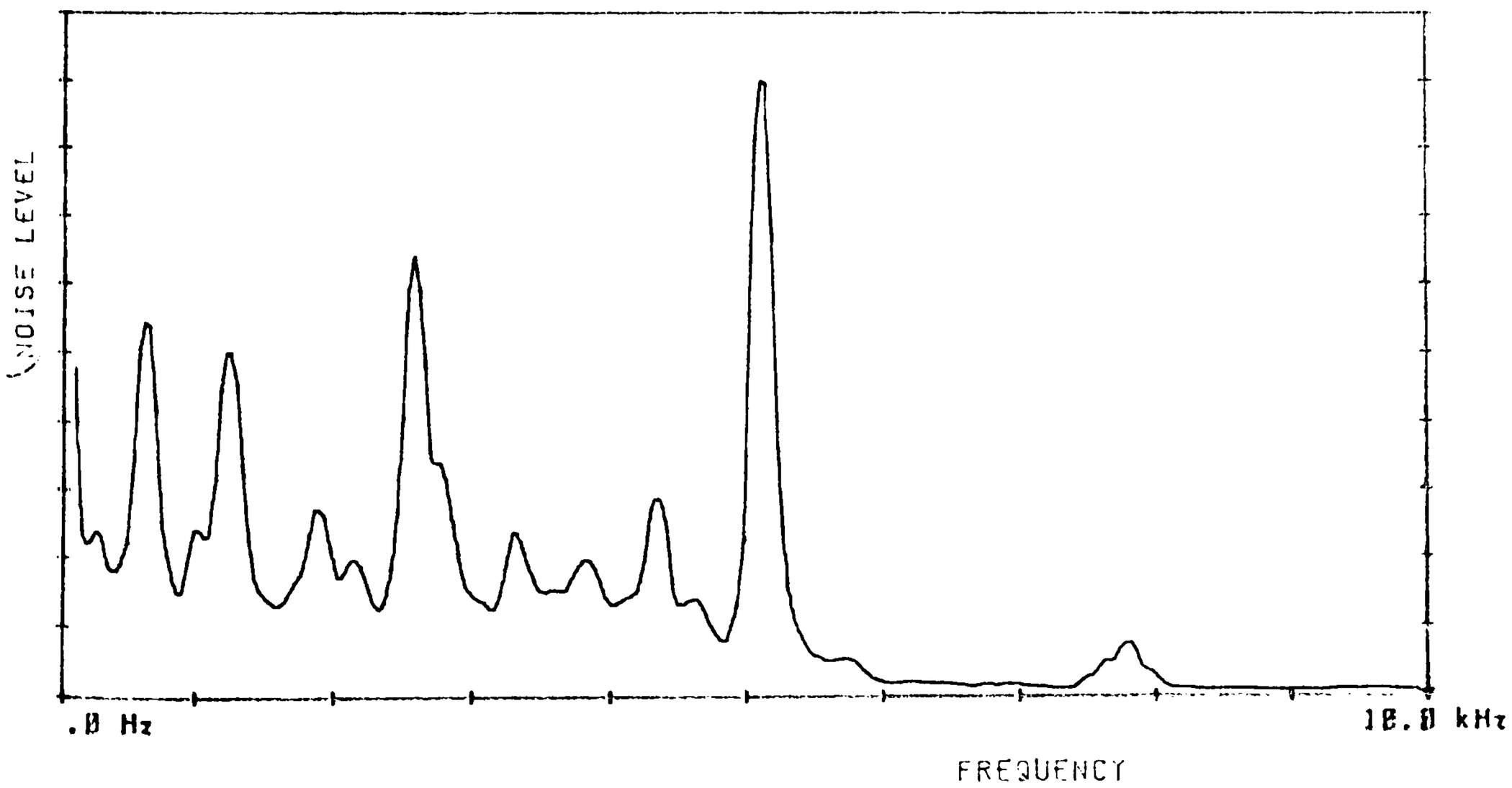

FIGURE 5.20(b)

SPEED	=	2109.0	rpm	LOAD TORQUE	=	7.0	Nm
T.C.F.	=	2565.9	Hz	LUB. OIL TEMP.	=	140.0	F

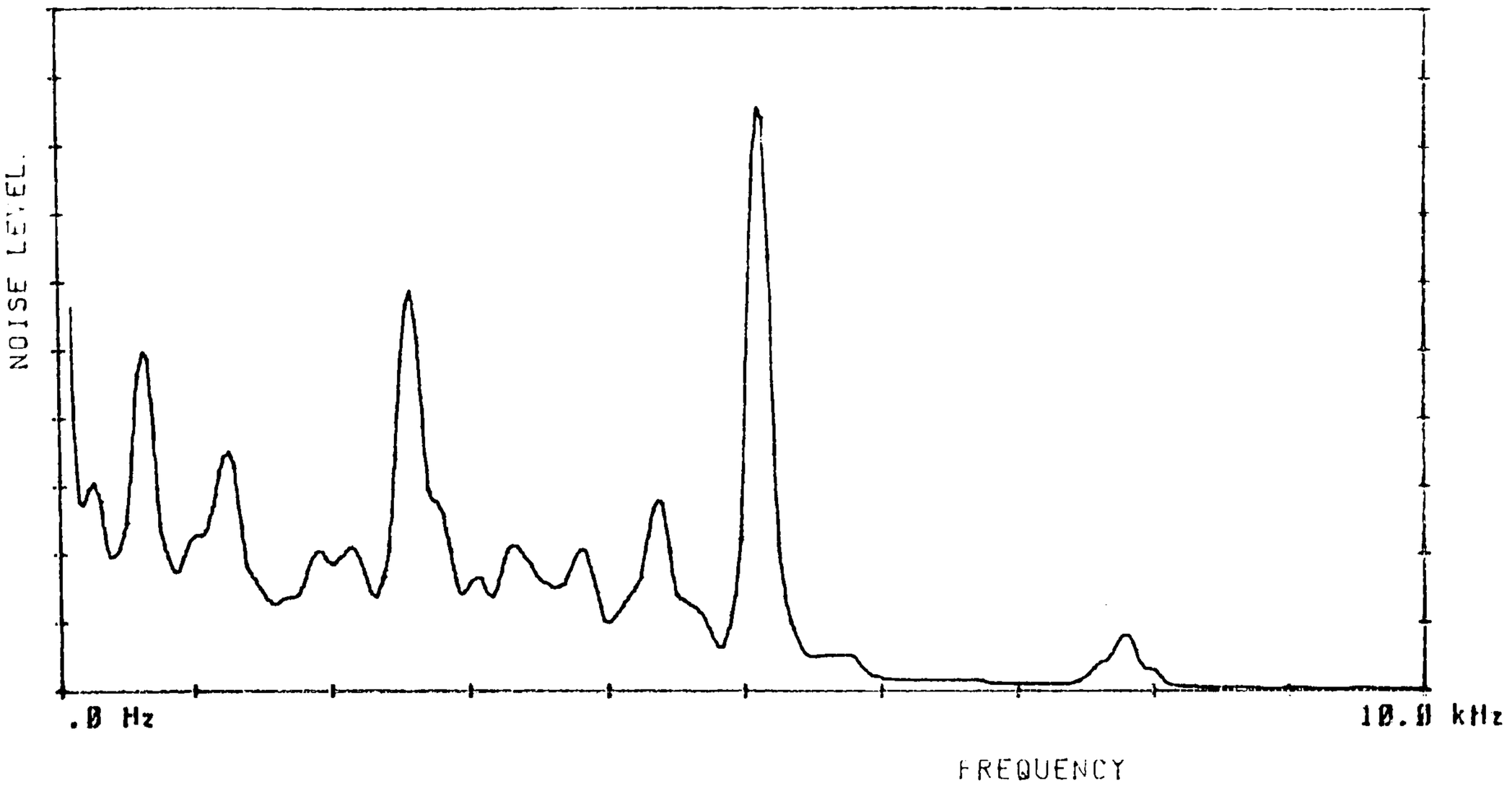

FIGURE 5.20(c)

SPEED	=	2083.0	rpm	LOAD TORQUE	=	7.0	Nm
T.C.F.	=	2534.3	Hz	LUB. OIL TEMP.	=	150.0	F

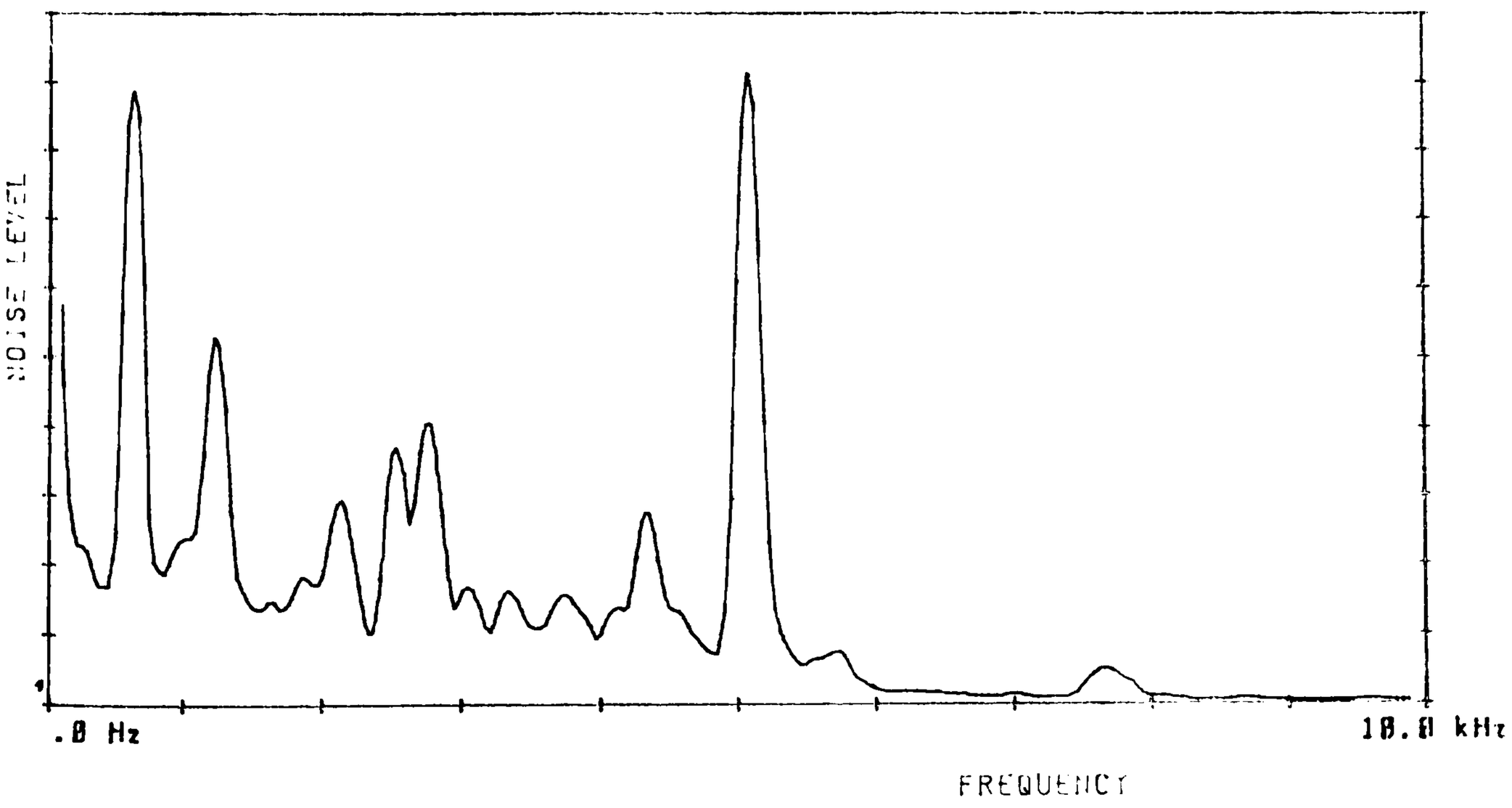

FIGURE 5.20(d)

NOISE LEVEL AT T.C.F. Vs TOOTH CONTACT FREQUENCY

LUB. OIL TEMP. = 120.0 F
LUB. OIL RATE = 1.300 l/min

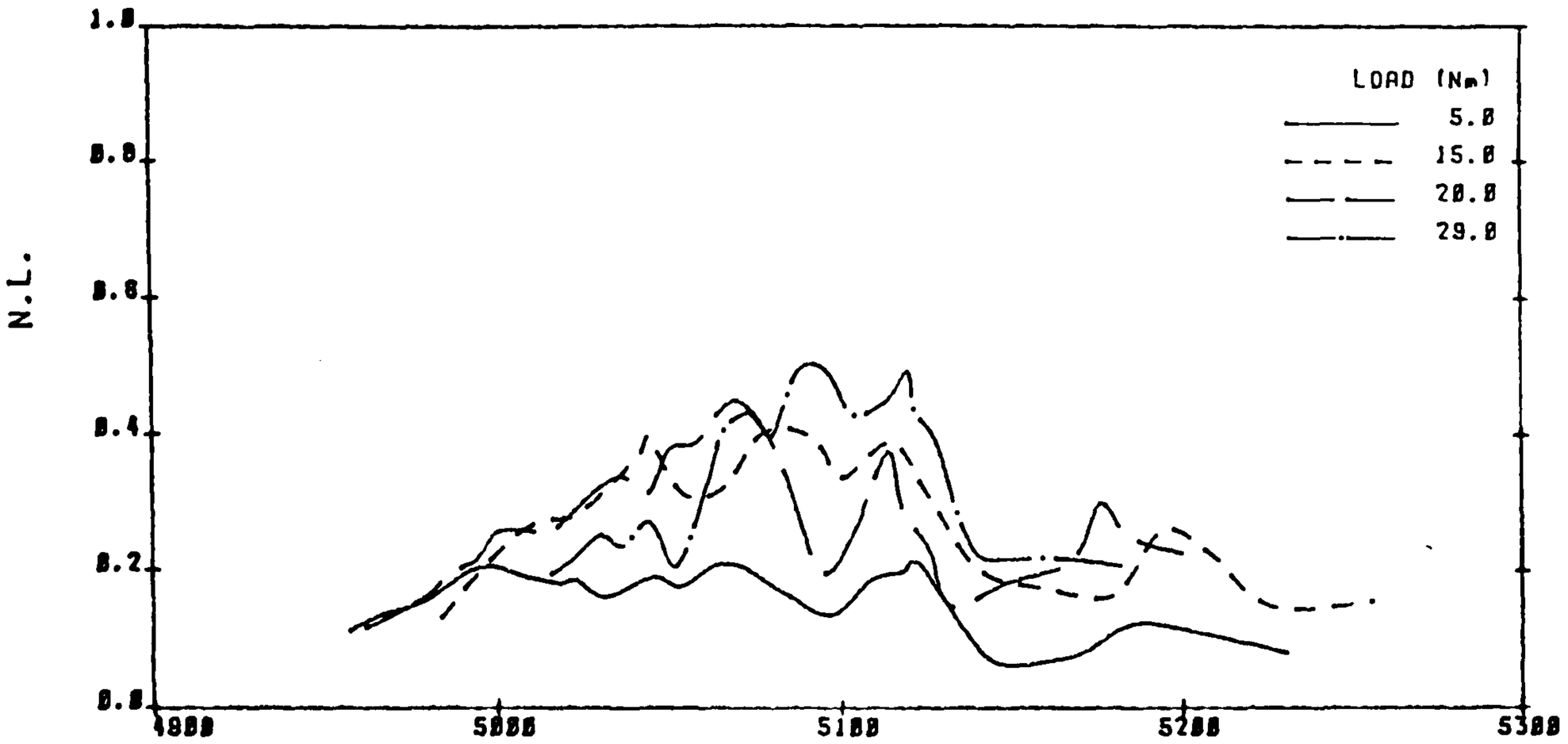

FIGURE 5.21(a)

NOISE LEVEL AT T.C.F. Vs TOOTH CONTACT FREQUENCY

LUB. OIL TEMP. = 130.0 F
LUB. OIL RATE = 1.500 l/min

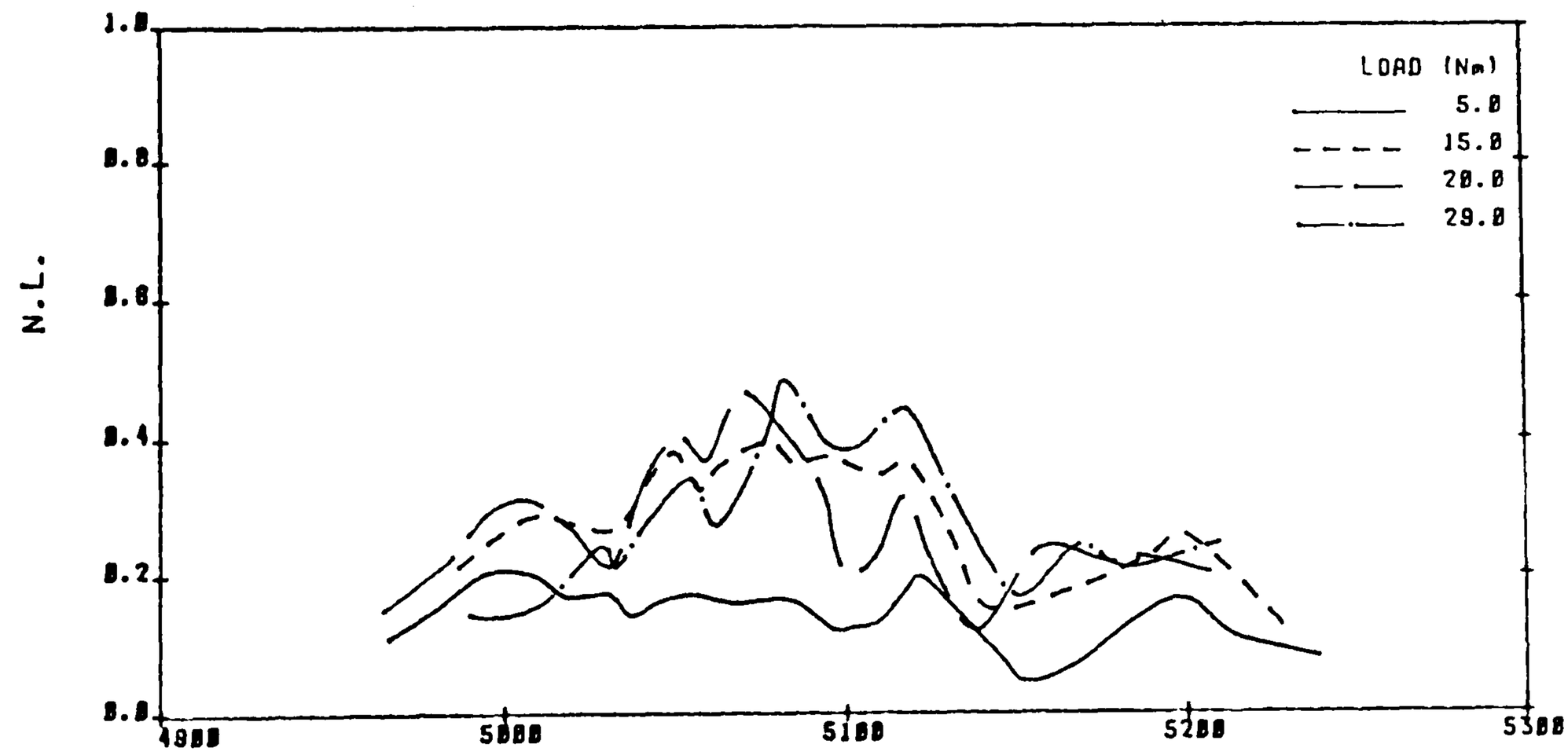

FIGURE 5.21(b)

NOISE LEVEL AT T.C.F. Vs TOOTH CONTACT FREQUENCY

LUB. OIL TEMP. = 140.0 F
LUB. OIL RATE = 1.500 l/min

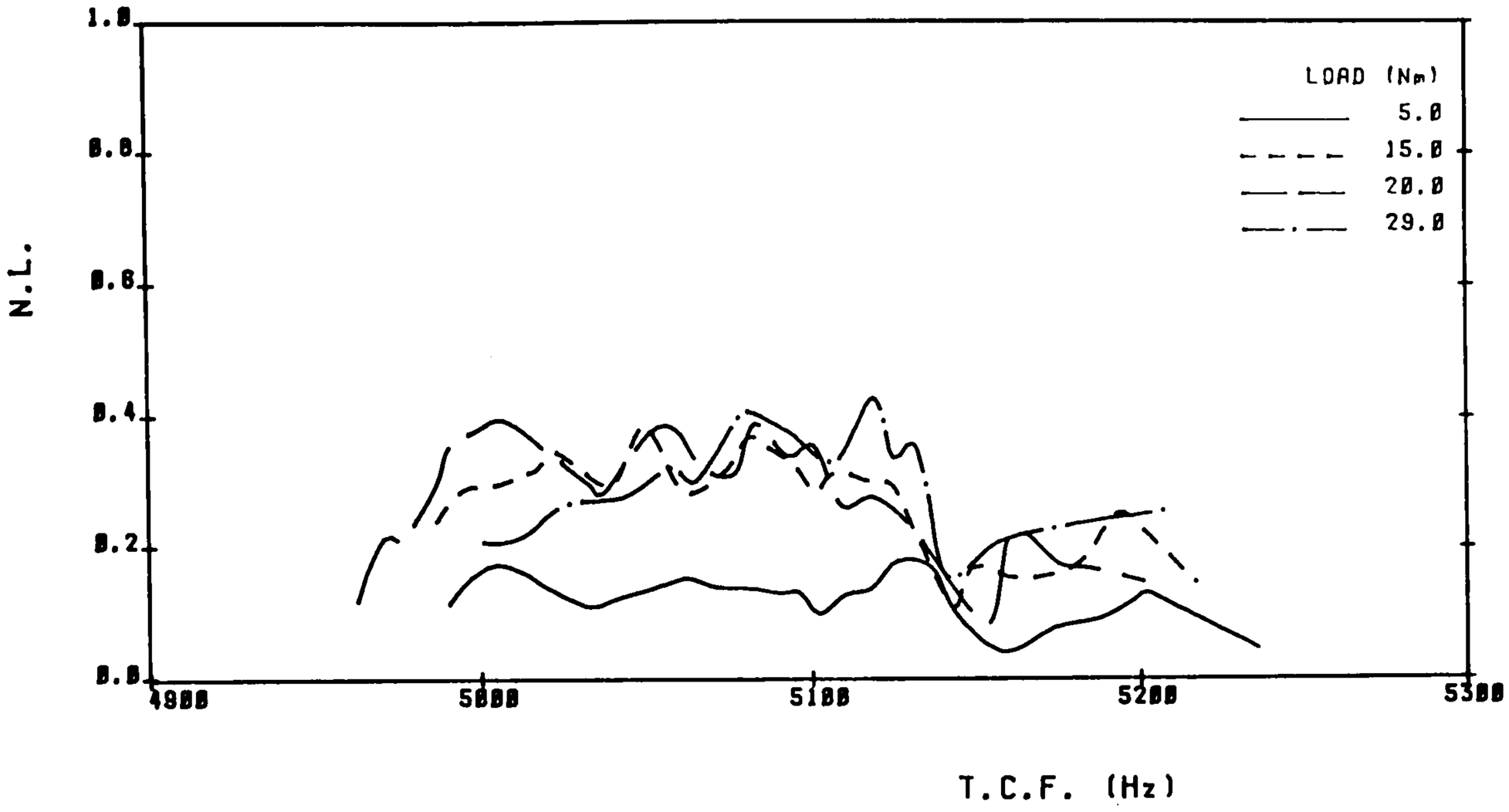

FIGURE 5.21(c)

NOISE LEVEL AT T.C.F. Vs TOOTH CONTACT FREQUENCY

LOAD TORQUE = 5.0 Nm
LUB. OIL RATE = 1.300 l/min

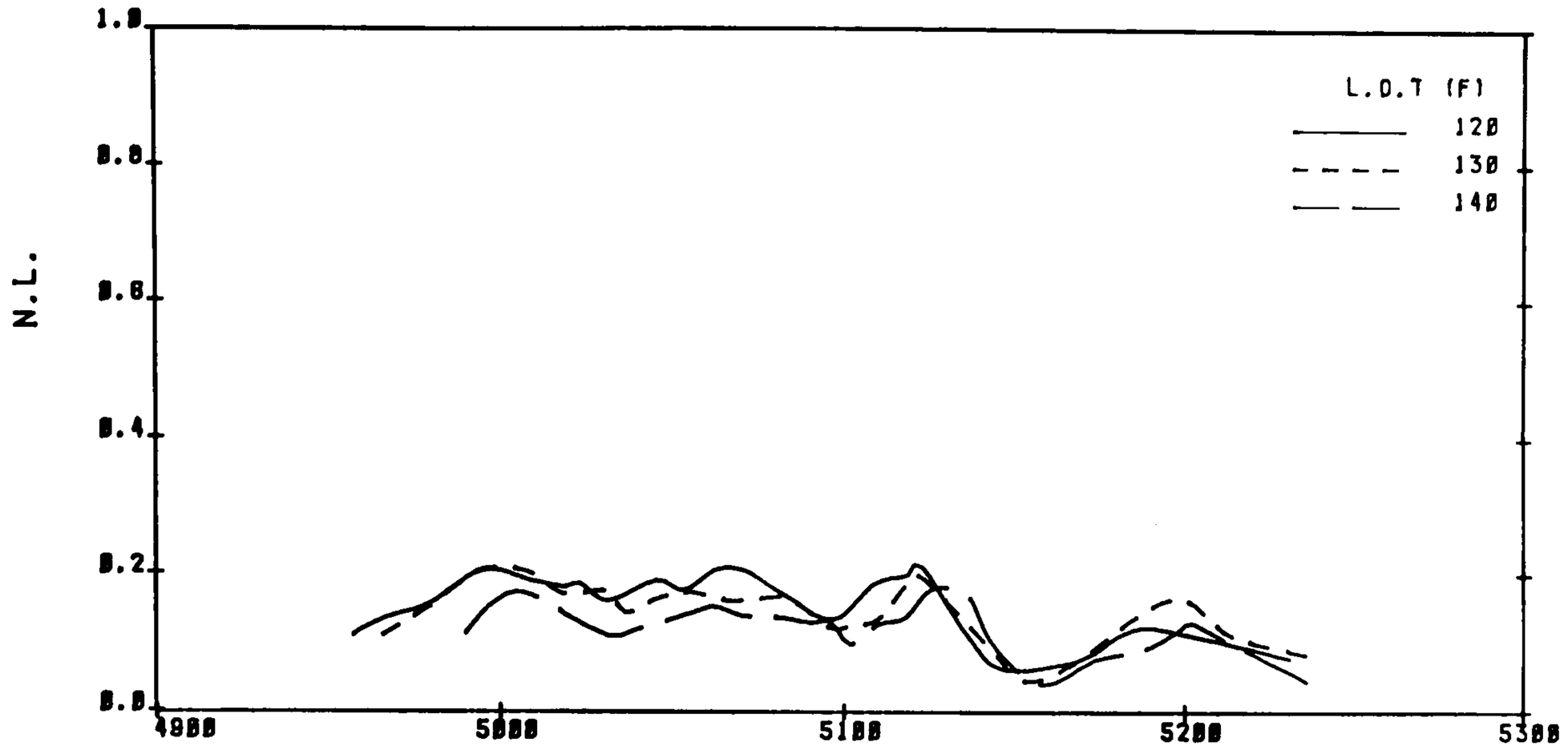

FIGURE 5.22(a)

NOISE LEVEL AT T.C.F. Vs TOOTH CONTACT FREQUENCY

LOAD TORQUE = 15.0 Nm
LUB. OIL RATE = 1.300 l/min

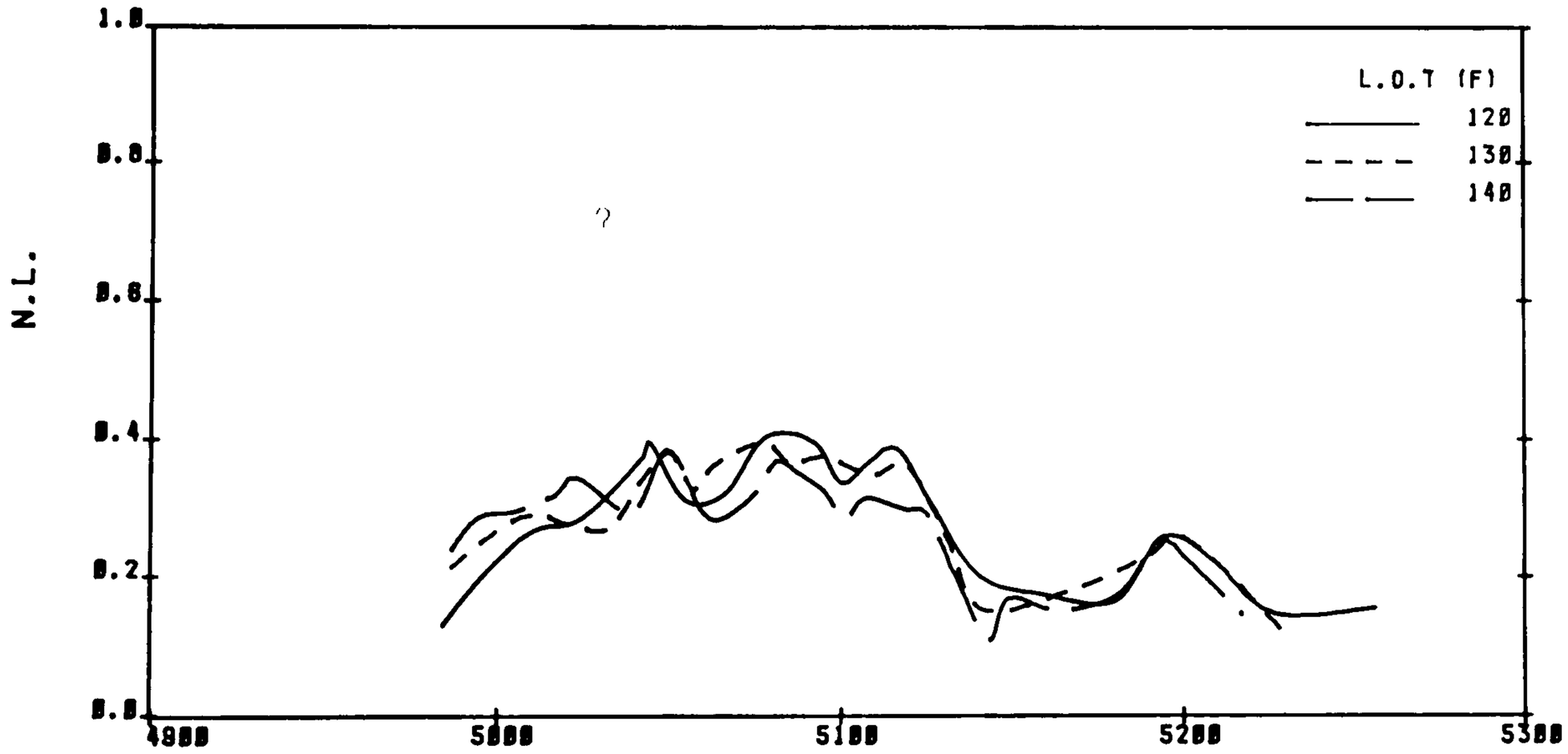

FIGURE 5.22(b)

NOISE LEVEL AT T.C.F. Vs TOOTH CONTACT FREQUENCY

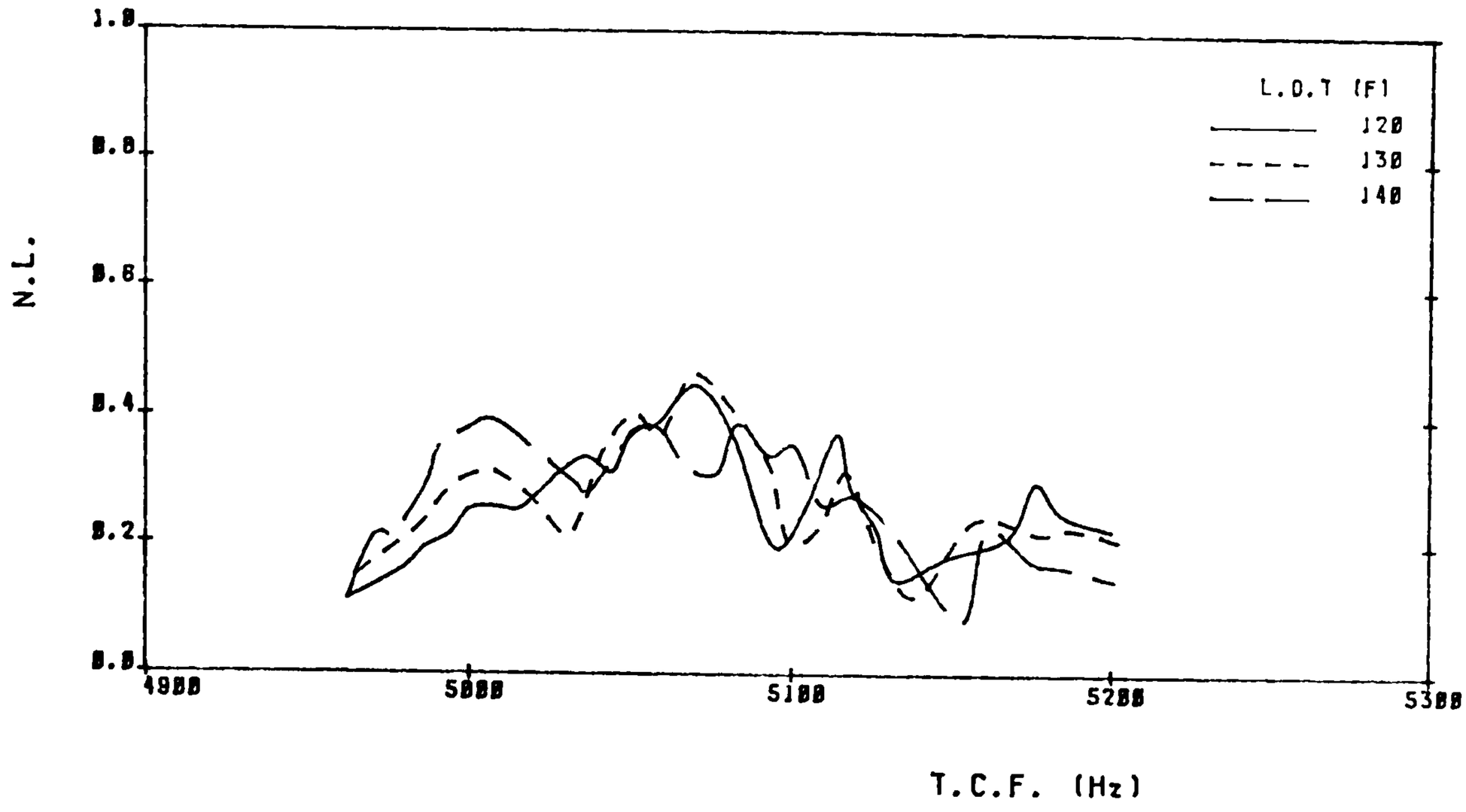

FIGURE 5.22(c)

NOISE LEVEL AT T.C.F. Vs TOOTH CONTACT FREQUENCY

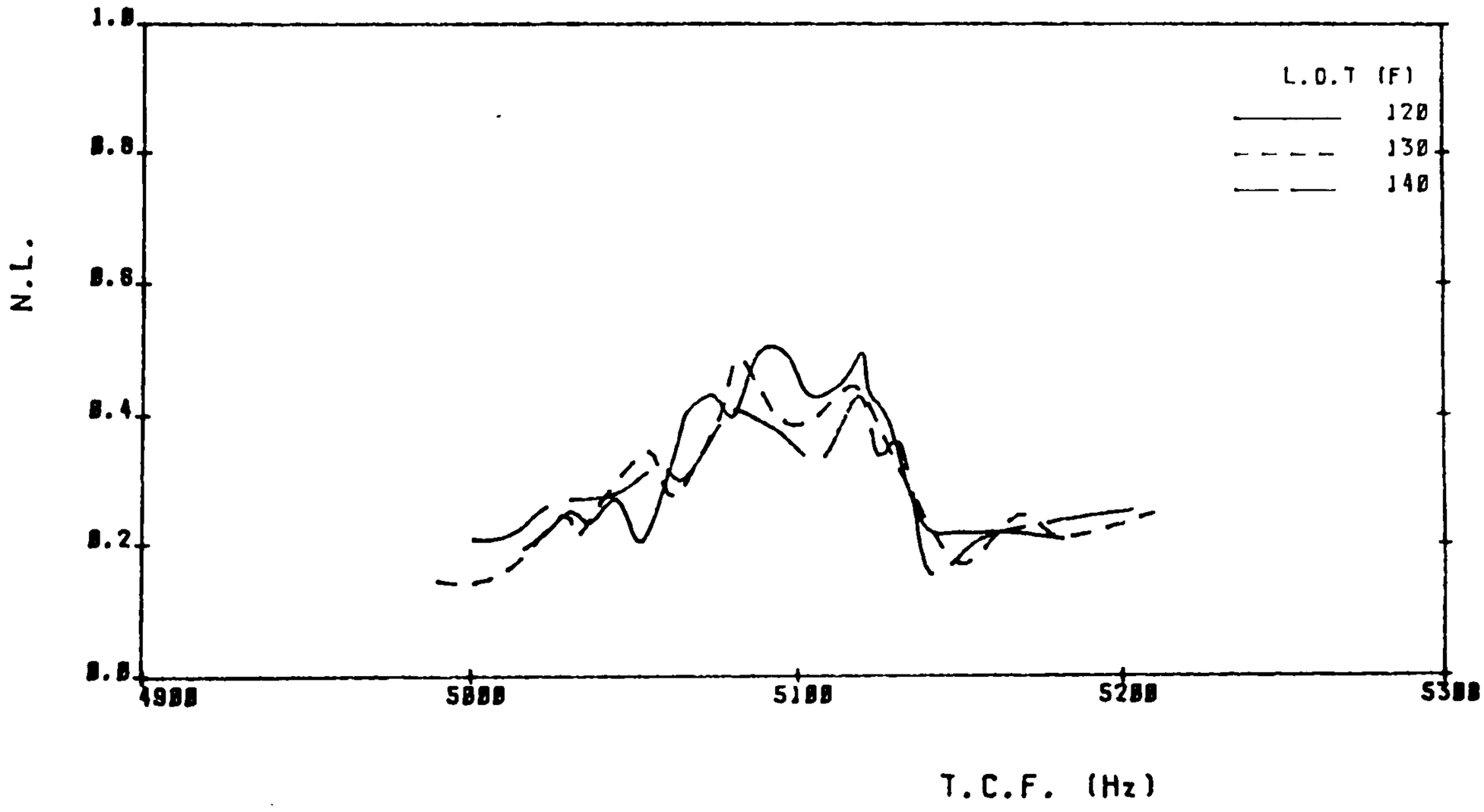

FIGURE 5.22(d)

NOISE LEVEL AT T.C.F. Vs TOOTH CONTACT FREQUENCY

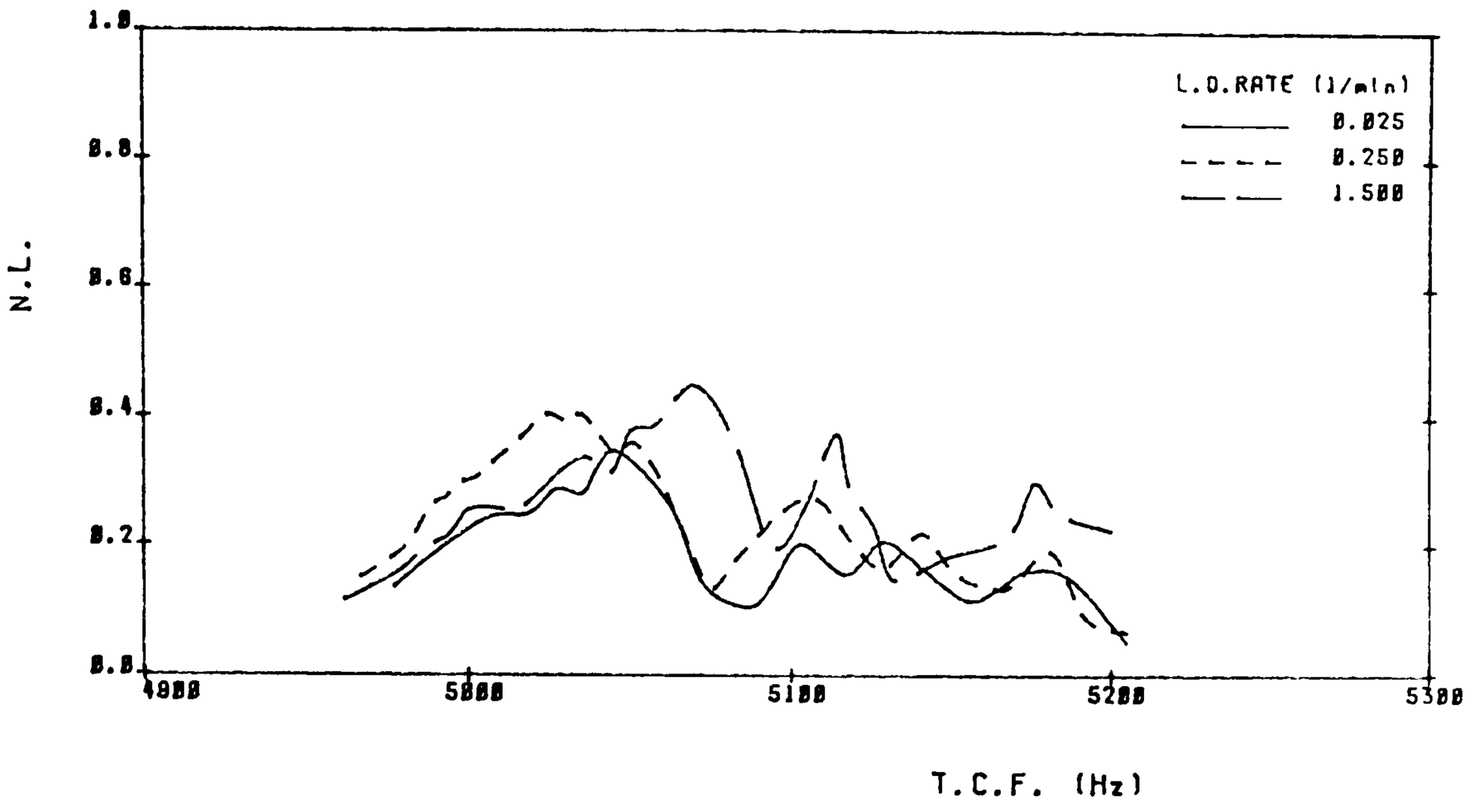

FIGURE 5.23(a)

NOISE LEVEL AT T.C.F. Vs TOOTH CONTACT FREQUENCY

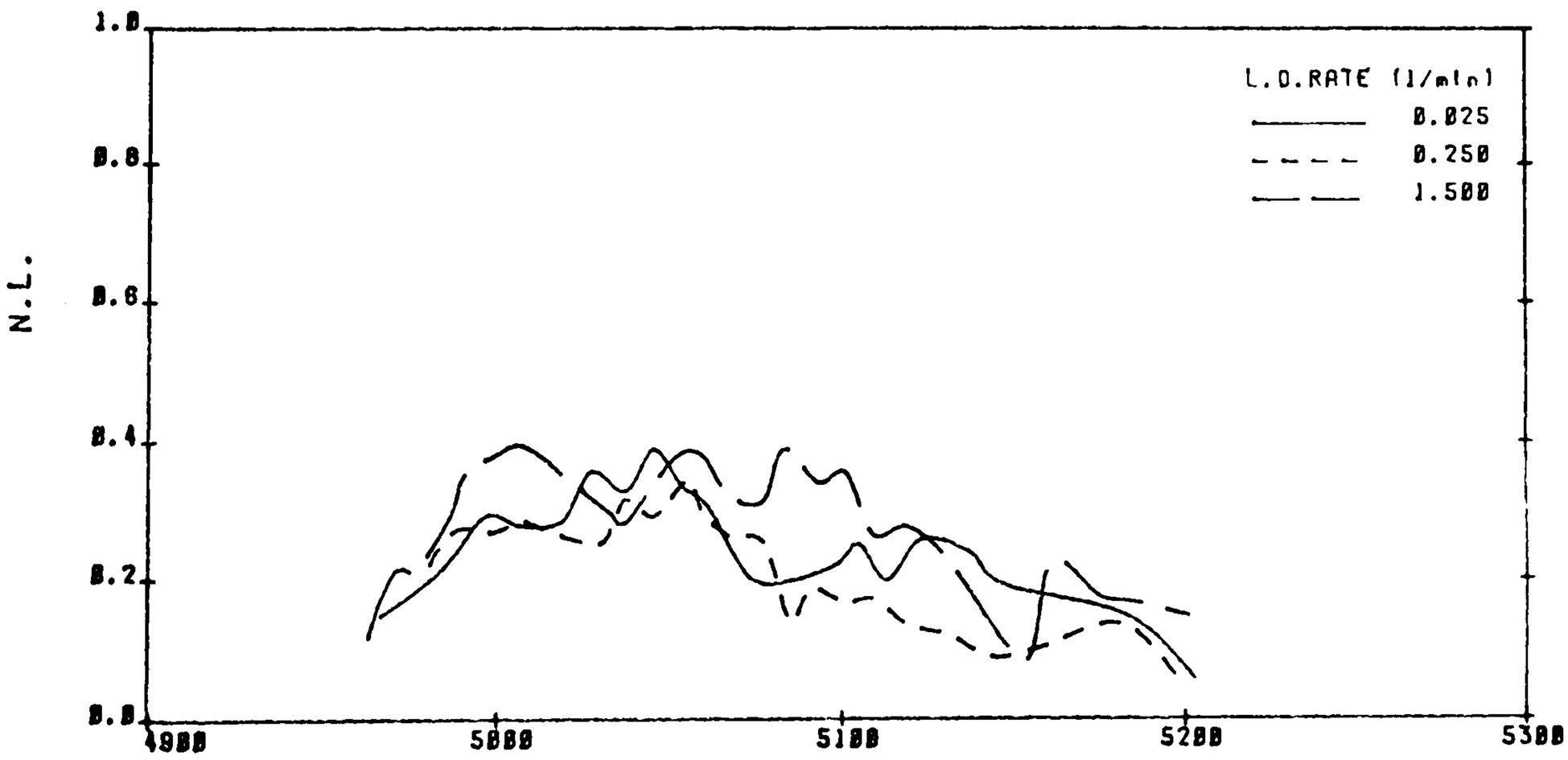

FIGURE 5.23(b)

MESH STIFFNESS (K) Vs FORCE (F)

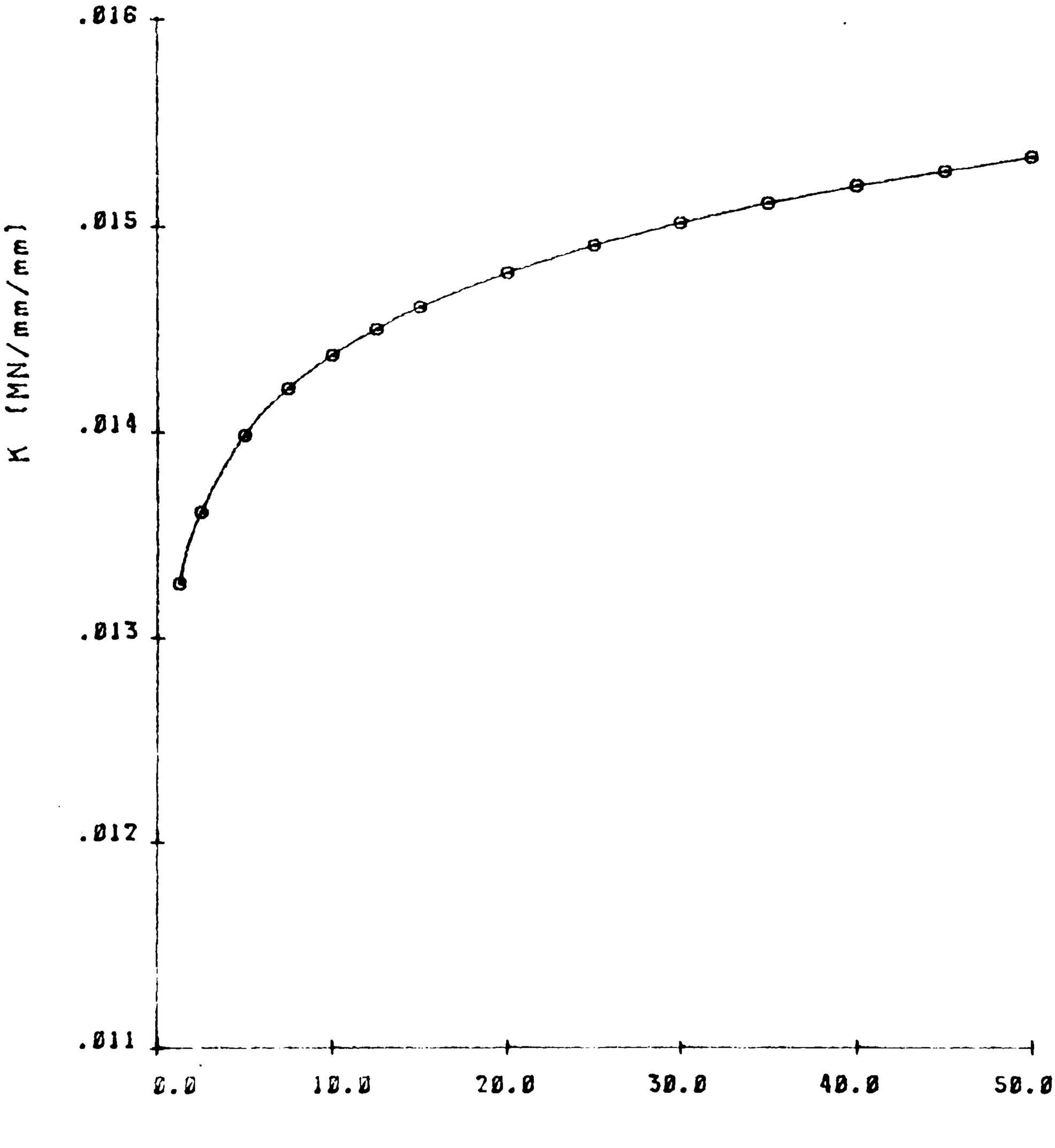

FIGURE 5.24

DAMPING RATIO (ζ) Vs VISCOSITY (μ_t)

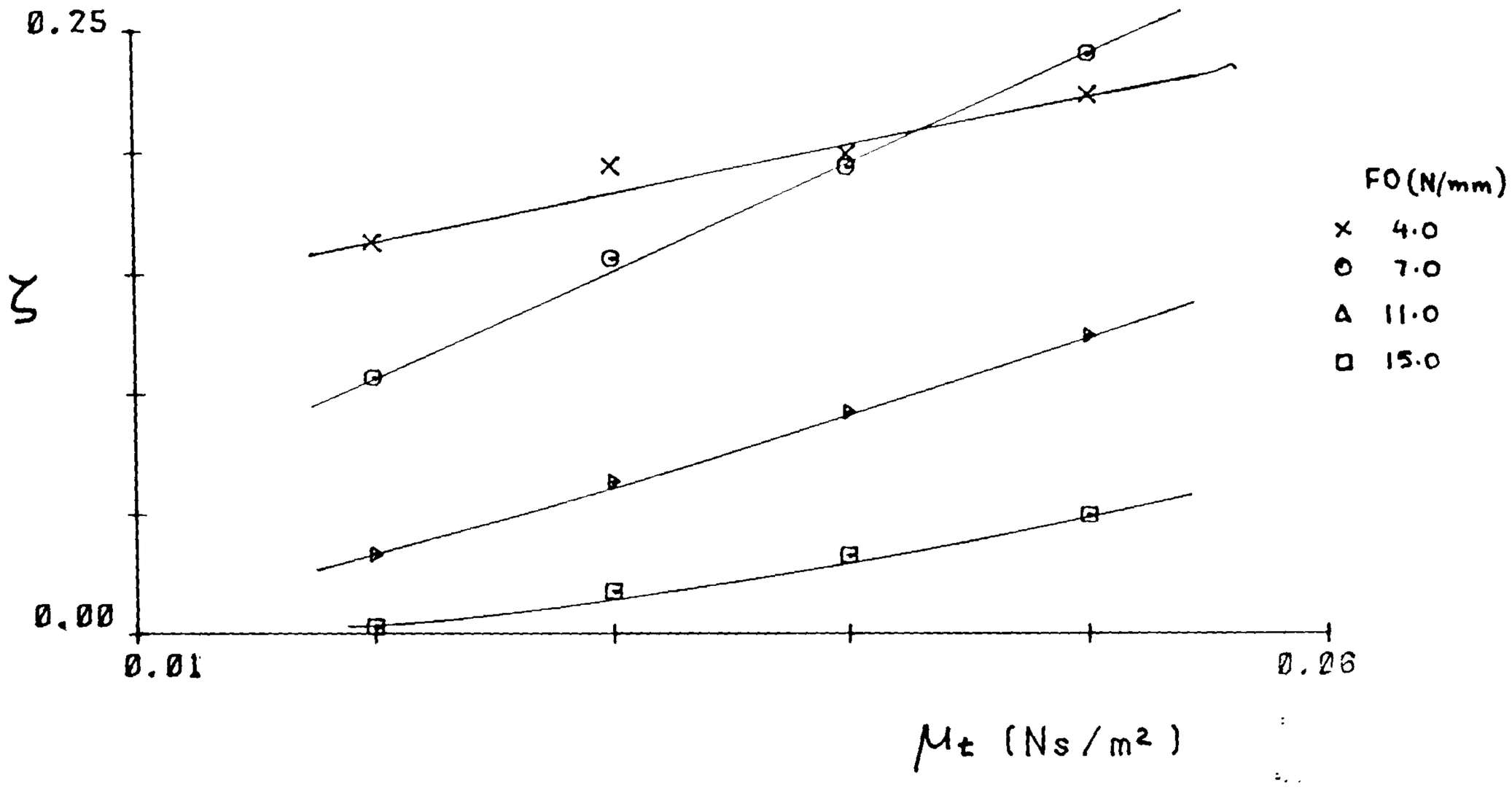

FIGURE 5.25(a)

DAMPING RATIO (ζ) Vs FORCE (FO)

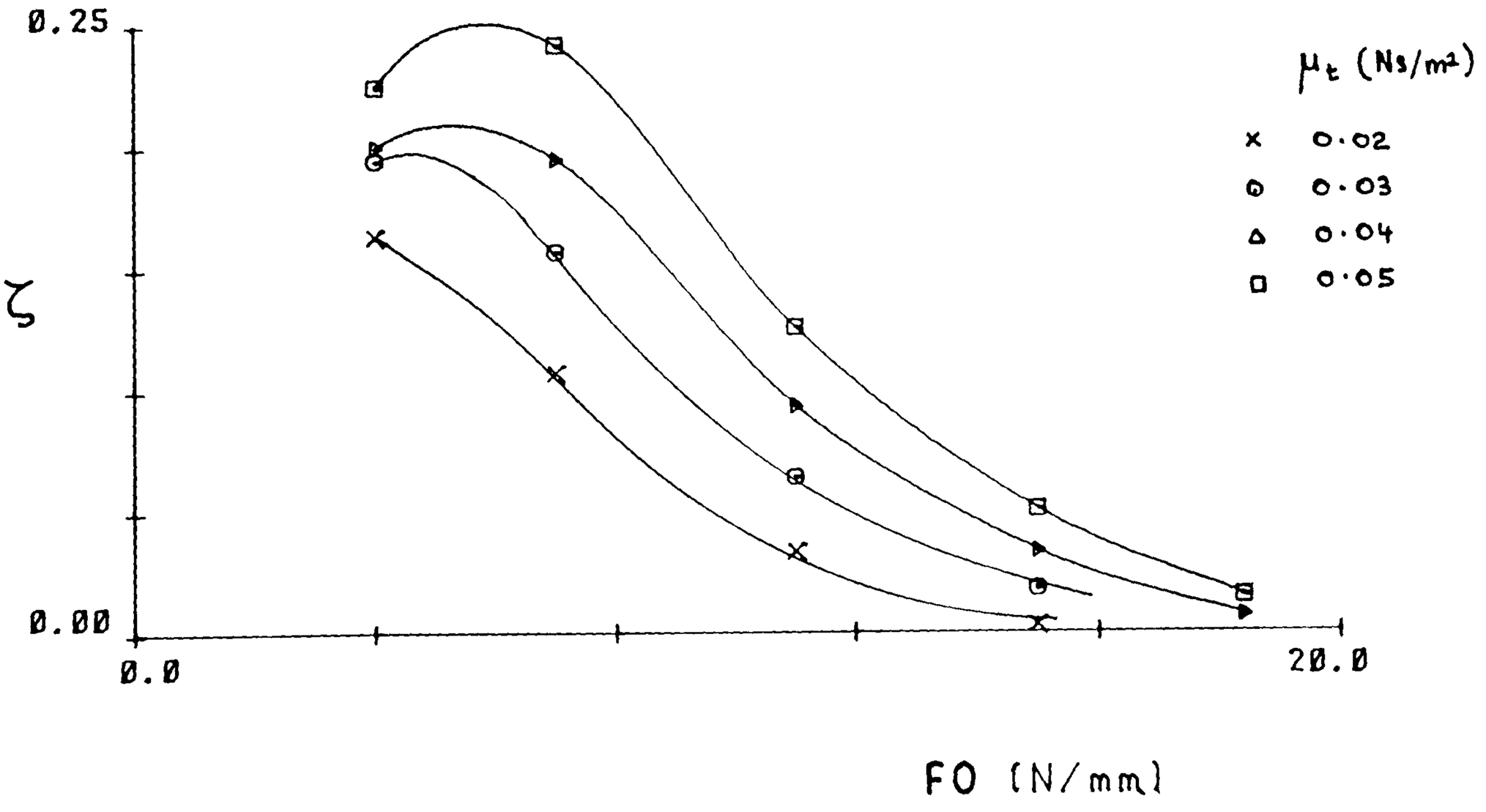

FIGURE 5.25(b)

NATURAL FREQUENCY (ω_n) Vs FORCE (FO)

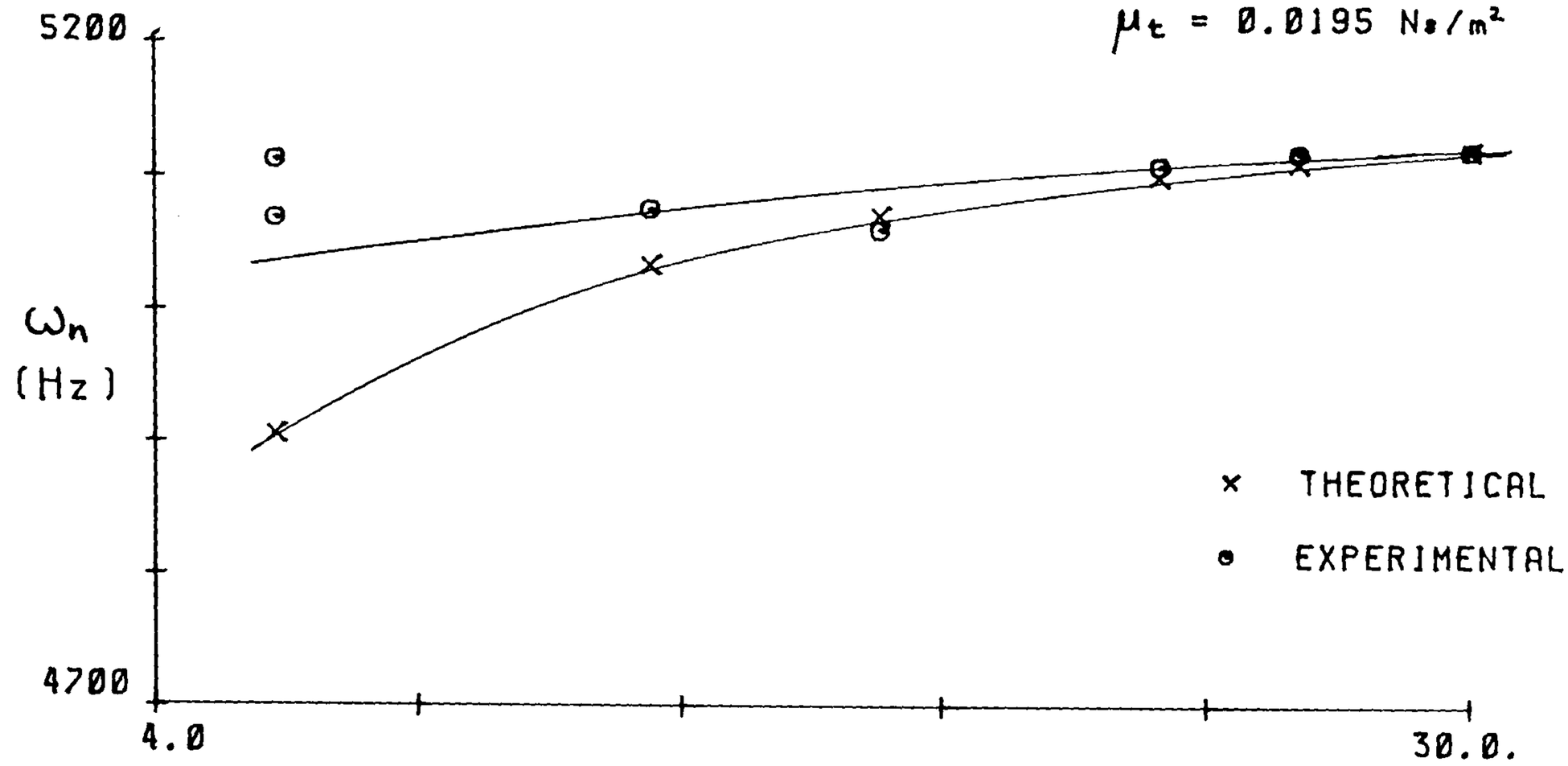

FIGURE 5.26(a)

NATURAL FREQUENCY (ω_n) Vs FORCE (FO)

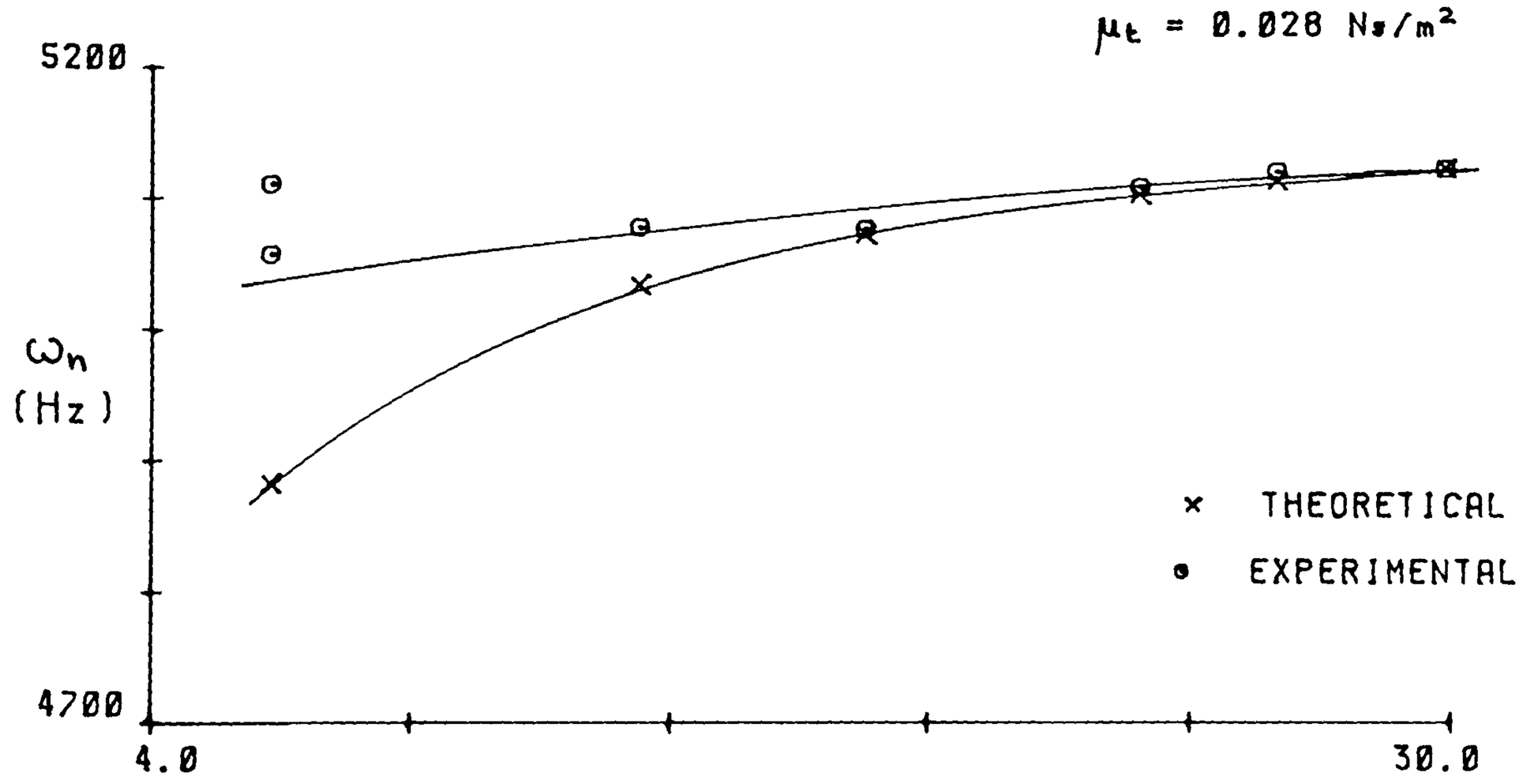

FIGURE 5.26(b)

NATURAL FREQUENCY (ω_n) Vs FORCE (FO)

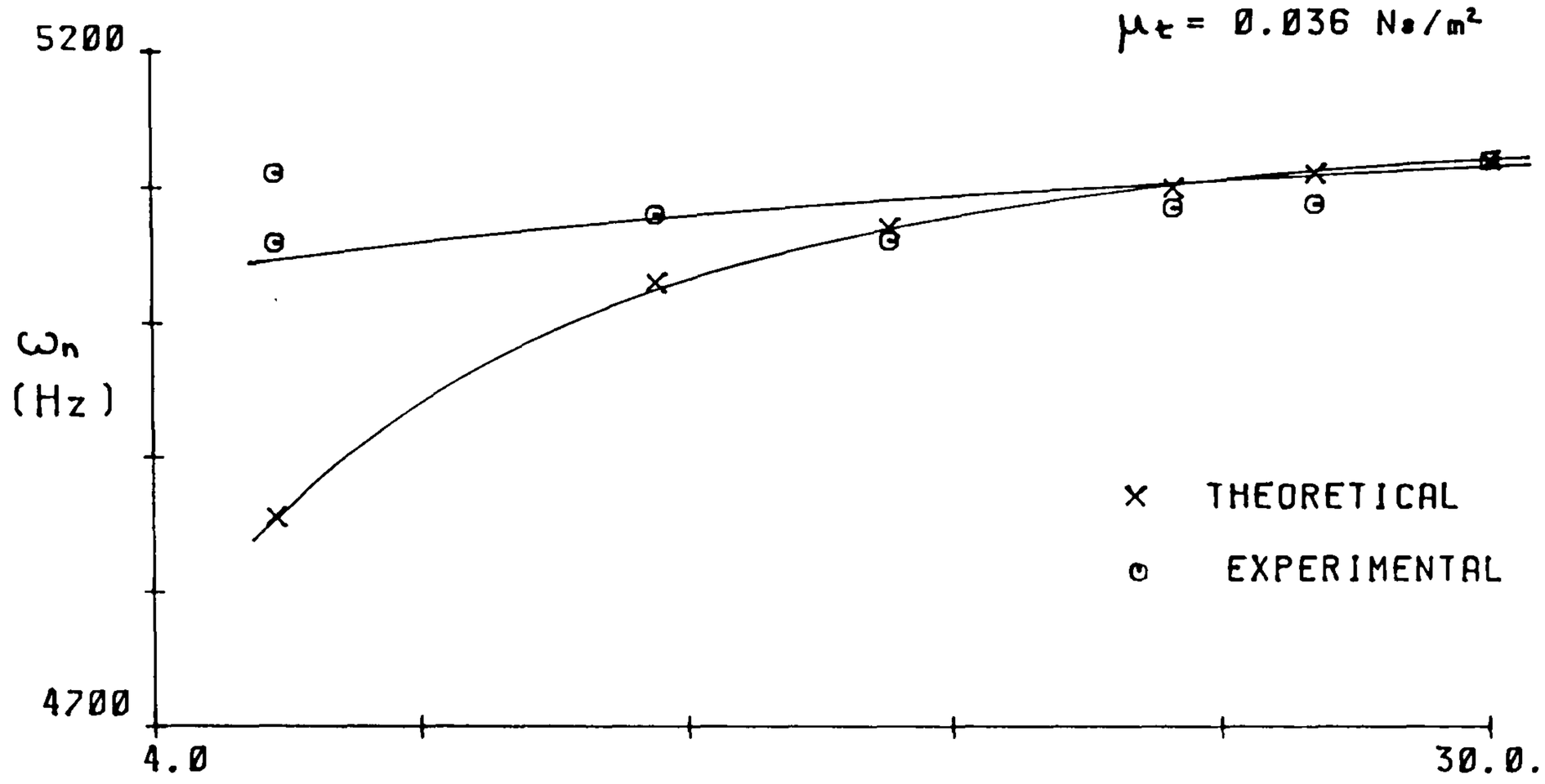

FIGURE 5.26(c)

NATURAL FREQUENCY (ω_n) Vs FORCE (FO)

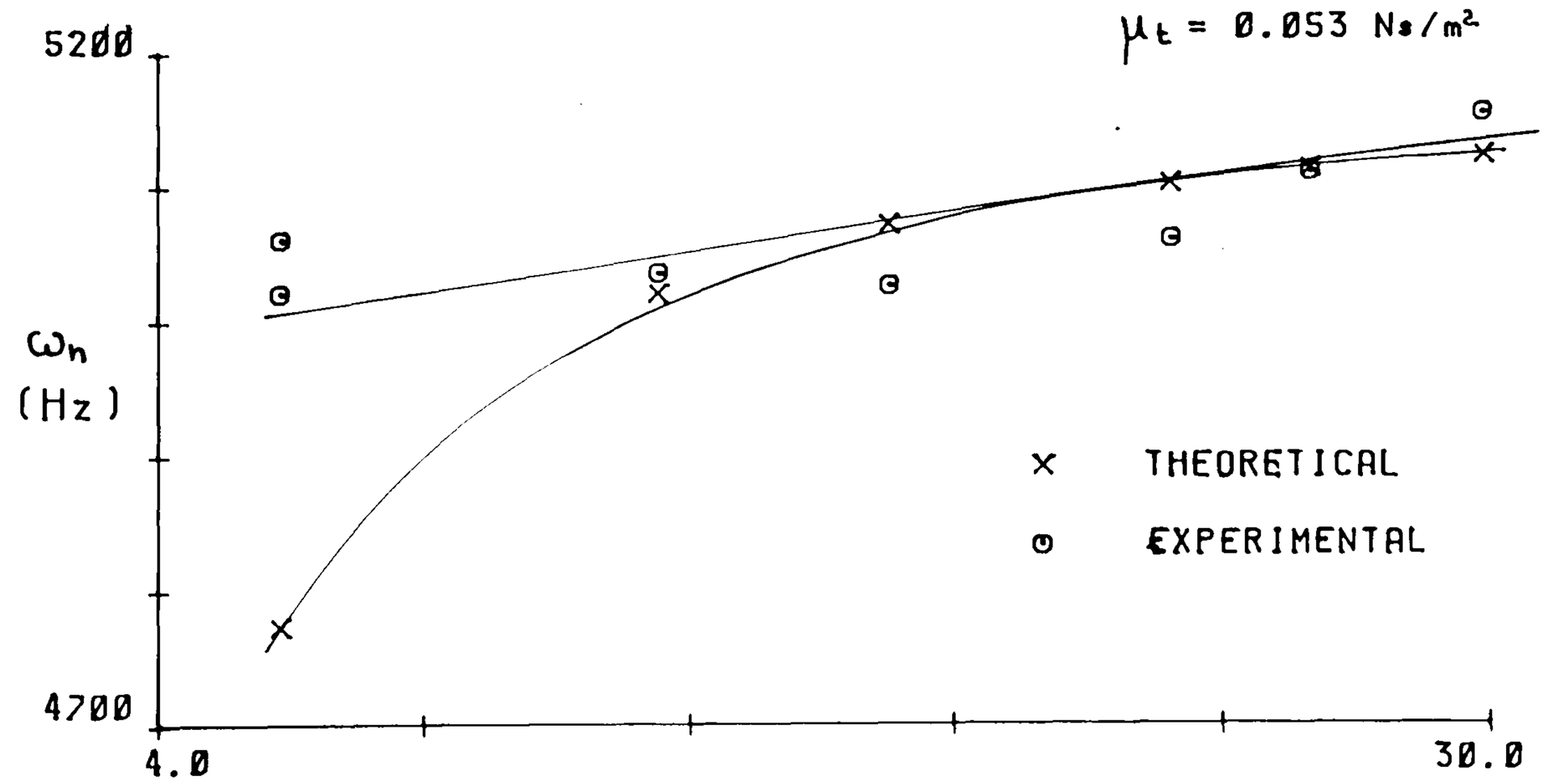

FIGURE 5.26(d)

NATURAL FREQUENCY (ω_n) Vs VISCOSITY (μ_t)

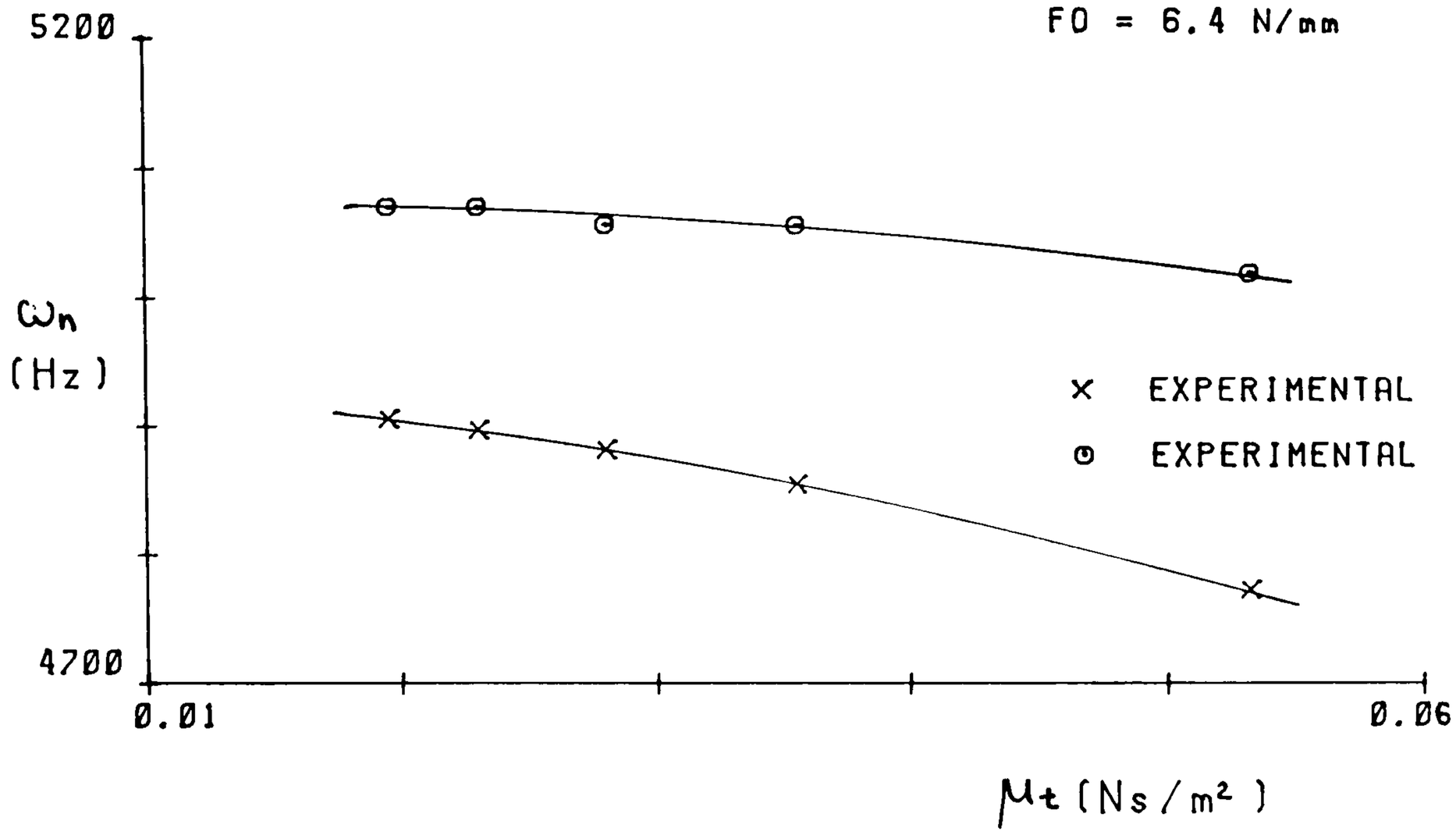

FIGURE 5.27(a)

NATURAL FREQUENCY (ω_n) Vs VISCOSITY (μ_t)

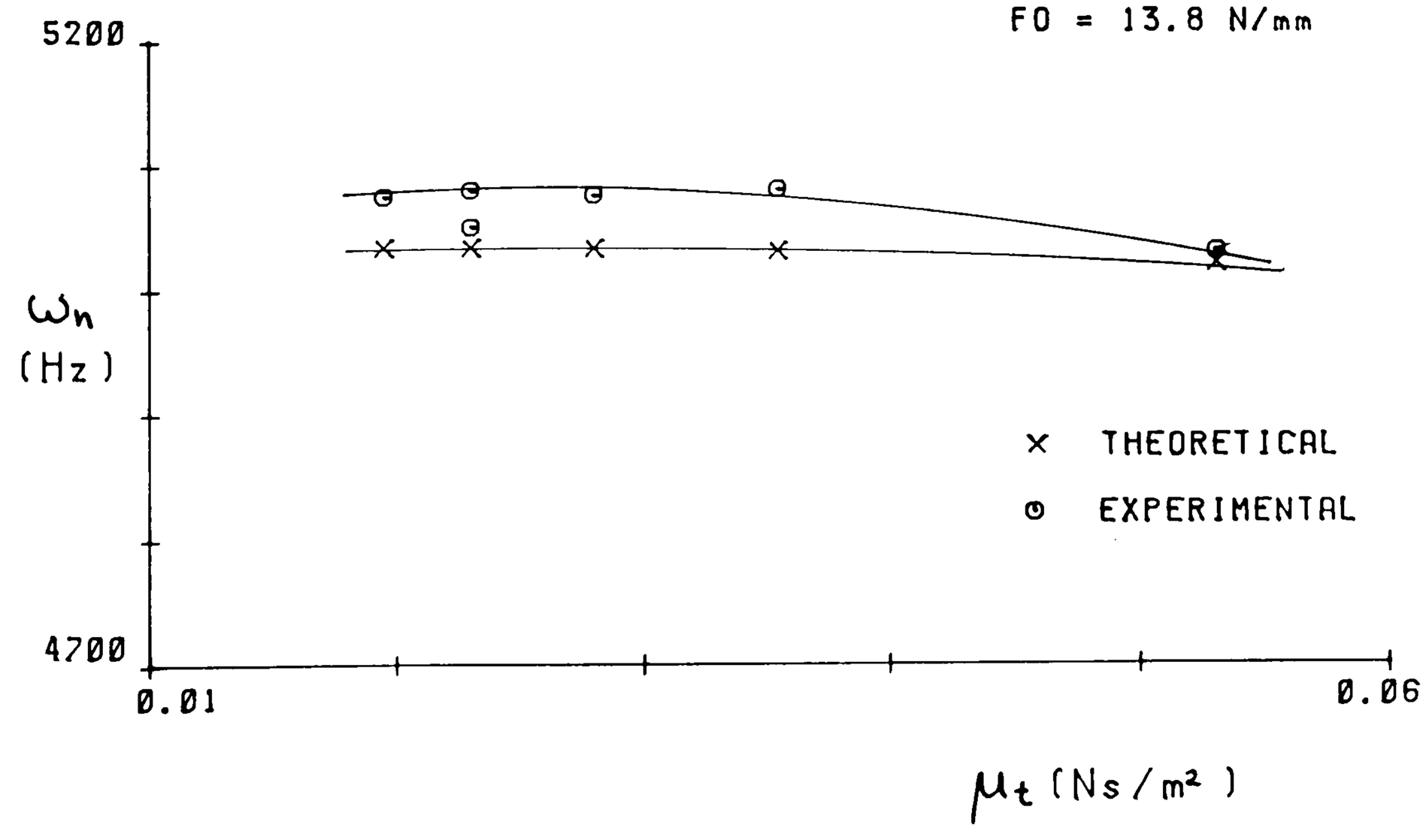

FIGURE 5.27(b)

NATURAL FREQUENCY (ω_n) Vs VISCOSITY (μ_t)

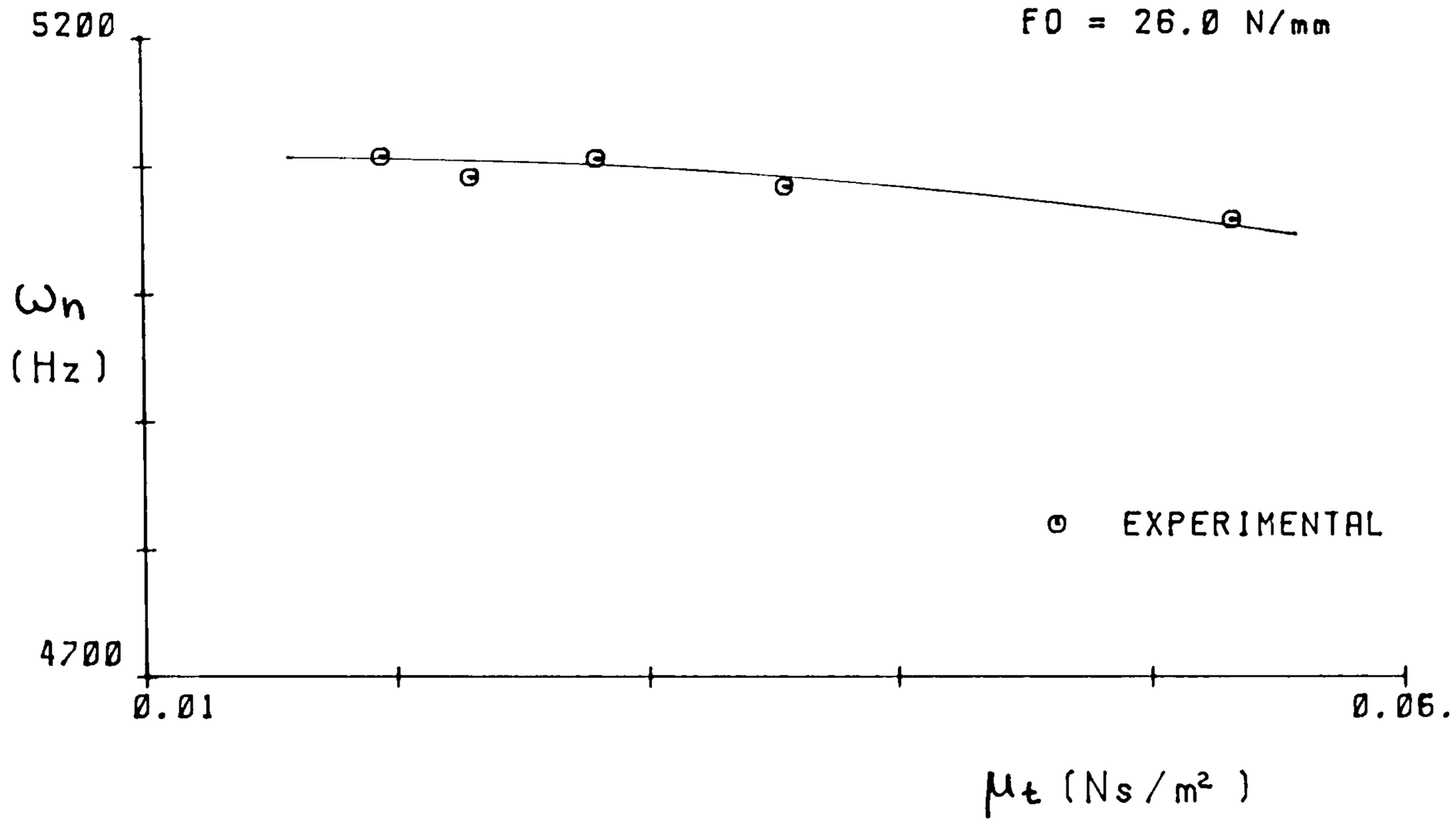

FIGURE 5.28(a)

NATURAL FREQUENCY (ω_n) Vs VISCOSITY (μ_t)

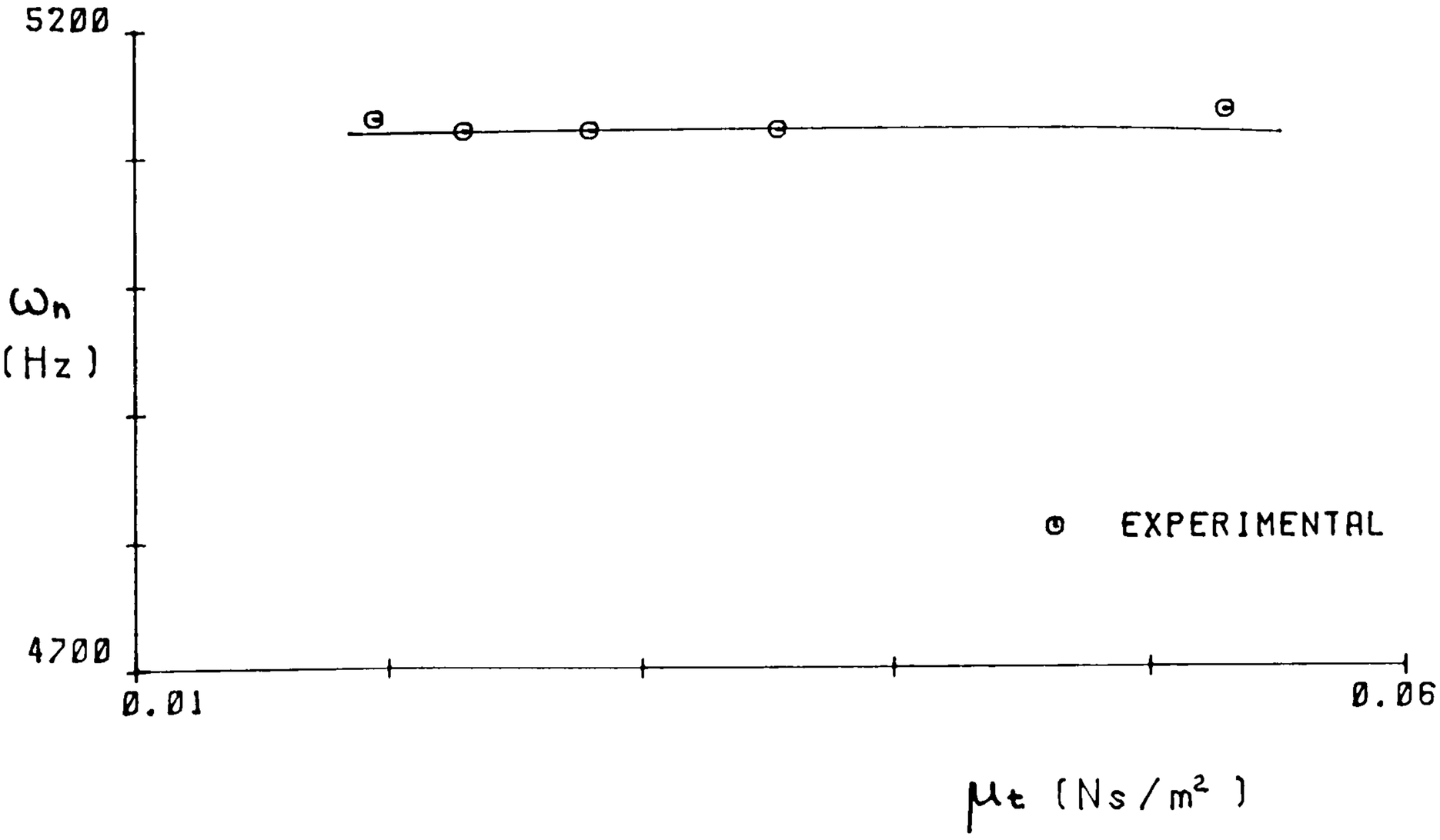

FIGURE 5.28(b)

CHAPTER 6

CONCLUSION

The theoretical and experimental work carried out has confirmed the importance of including the subject of lubrication in the analysis of gear dynamics. This study has merely shown the way for further research and that it is possible to achieve realistic and useful results that could help in the design of gears.

So far no one has tried to express the damping force due to the lubricating oil film as a variable dependent on the instantaneous running conditions at the gear tooth mesh. Investigators on gear dynamics in the past either neglected damping completely or used an arbitrary, constant, viscous damping factor in their analysis. This was not primarily because the role of damping in gear dynamics was not important, but mainly due to insufficient knowledge available on its extent and form. On the other hand, the mesh stiffness, which could be expressed more easily and could be verified easily by experimental means, was used as a variable in dynamic analyses. The theoretical work carried out has shown that the variation in mesh stiffness, apart from that due to the change in the number of pairs of teeth in mesh, is not very significant whereas the damping ratio undergoes more drastic changes during the mesh cycle. Hence, representing the damping ratio as a variable dependent on the operating parameters seems equally, if not more, important than representing the mesh stiffness as a variable.

Oil film thicknesses calculated using basic hydrodynamic theory and assuming rigid teeth resulted in film thicknesses at low loads far in excess of those obtained using Grubin theory which, of course, is intended for situations involving high tooth loads. Hence it can be recommended that in dynamic simulation tests the oil film thickness needs to be represented more flexibly employing a method that gives correct thicknesses for a wide range of loads, since the load on gear teeth undergoes large oscillations. Even though it is the lowest thickness that is of interest from the design point of view, which occurs usually when the load is at a maximum, a true variation of the film thickness over the complete mesh cycle is important since it is actively involved in the dynamic behaviour of the pair of gears that ultimately determines the characteristics of the load cycle.

The film thicknesses calculated assuming a fixed tooth profile yielded film thicknesses that varied sharply with load at low loads, and it also increased almost linearly with the increase of the speed, lubricating oil viscosity and the effective radius at the point of contact. This agrees with the earlier theories based on isoviscous lubricating oil and rigid teeth. But whereas these theories predicted such relationships to continue irrespective of load (which eventually led to the failure of those theories), the film thicknesses calculated based on a pressure-dependent viscosity showed that they became less dependent on load as the nominal load is increased. Presumably due to the assumption of a rigid tooth surface, the film thicknesses predicted nevertheless dropped to

values less than those given by Grubin formula at higher loads, although they tended to reach a constant value much earlier.

This suggests that to calculate the film thickness accurately both the variation of the oil viscosity and the deformation of the contact surfaces need to be taken into account. Any simplified formula thus derived from such theory to predict the film thickness should express the exponent of the load as a variable mainly dependent on the load itself.

Another aspect that needs attention is the thickness of the oil film generated when a new pair of teeth come into mesh. Especially since they mesh early when the operating load is high the full tooth face of the driven gear is not available to create the hydrodynamic film and to take up the load. This also means that the effect of rolling and sliding motions of the two faces will be at a minimum and the oil film is created mainly by the relative movement of the pair of teeth along the line of action. This could result in two things:

(a) Relatively high damping due to the squeeze film effect.

(b) Very low film thicknesses since the squeeze force is the only significant force available to resist the tooth load.

Despite the higher damping, low film thicknesses at the start of the mesh cycle could cause scuffing to take place, especially if it is accompanied by high impact loads such as those predicted by the dynamic simulation test to occur near the resonance speed.

Oil film damping was found to be present only at very low loads, but it had the effect of stabilising the system. Whatever the nominal load is, the dynamic load can be expected to oscillate almost sinusoidally and if it does not reach low loads for damping to come into effect, then there will not be anything to worry about since during the other half of the load cycle it can safely be assumed that the dynamic load will not exceed twice the nominal load.

It has to be noted that there are other sources of damping as well, especially the damping in the material which could increase with load and perhaps reach a significant level. This means that there could be some form of damping at the two extremes of the cycle which act as effective limiters to the amplitudes of vibration and hence to the maximum dynamic load.

Damping due to the oil film alone, calculated for a pair of gears with a speed ratio of unity, showed that it behaved in a considerably complicated manner. It increased rapidly with load initially and then gradually decreased with further increase of load. This was the general pattern, and the maximum value reached by the damping ratio and the load at which it occurred was determined by the other parameters, speed being the most influential of them, i.e. at very low loads low speeds produced higher damping, while at higher loads speed had the reverse effect.

Increasing the viscosity generally raised the value of damping ratio at all loads and speeds, though when the loads were low and the

speeds high, it did not seem to have much effect.

The relationship between damping ratio and speed was slightly similar to that between the damping ratio and load. Here, too, it increased initially with speed and then decreased gradually. But the initial rate of increase was largely governed by the load with low loads producing a steeper increase. Unlike in the case with load damping ratio tended to reach a constant value at very high speeds.

The damping ratio did not seem to depend on the effective radius of curvature to any significant extent. It showed a near-linear relationship with the radius, with lower speeds producing higher rates of change. When the radius was changed by changing the size of the gears (i.e. by varying the diametral pitch) damping ratio decreased at low loads, while at high loads it increased. When the radius was changed by varying the position of contact, the change in damping ratio obtained seemed to be more than in the previous case, considering the relatively small change in the radius achieved. Since the only significant difference between the two methods was the presence of sliding velocity in the second case (apart form the slight variation in the mesh stiffness), this higher variation of the damping ratio could be attributed to that, and thus further research into the effect of sliding speed seems appropriate.

Neglecting the effect of the radius of curvature the above relationships of the three parameters (load, speed and viscosity),

were combined so that the damping ratio for the pair of gears tested could be expressed by an approximate formula. This resulted in the following:

$$\zeta = Ae^{-B(C-F)^2}$$

where $A = 18.24 \frac{\mu_t}{u^{1.09}} + \ln\left[\frac{1.1193}{u^{0.027}}\right]$

$$B = \frac{0.1535}{u}$$

$$C = 39.08\, u\mu_t + 57.0\, \mu_t + 1.15 \ .$$

Although this is intended for the particular pair of gears only, the analysis shows that it is possible to develop a general formula to evaluate the damping ratio at any given operating condition for any pair of gears.

Dynamic simulation tests of the pair of gears carried out have revealed that dynamic factors of the order of 3-5 could occur at the resonance speed depending on the pitch error, contact ratio and the viscosity of the lubricating oil. But those results were obtained assuming unlimited backlash and hence, in practice, the maximum dynamic factor could be less.

Several minor resonances were also detected at speeds corresponding to tooth contact frequencies of n/2, n/3 and n/4. Of these the

speed at n/4 seemed to cause instabilities in the system at high nominal loads. Under stable conditions the dynamic factors at all the above speeds remained below 3.0 and at speeds away from resonances the maximum dynamic factor was around 1.8.

The load on individual pairs of teeth which could be considered to be more important than the total load, from the gear designer's point of view, recorded maximum values of around 2.5 to 3.0 times the nominal load at the resonance speed.

It was also found that:

There was a particular contact ratio that generated the maximum dynamic load at resonance. This was about 1.4 for the pair of gears tested.

Lower contact ratios had a sharper peak at resonance and hence a narrower high-load speed range than higher contact ratios.

There was no particular difference in the performance of the system at speeds away from resonance for different contact ratios.

Pitch errors caused a general increase in the dynamic factor and the maximum individual tooth load at all speeds and loads tested.

The natural frequency of vibration of the pair of gears increased slightly with the increase of the contact ratio and the nominal load.

The effective contact ratio increased significantly with the load due to the deflection of gear teeth which caused the incoming pair to come into mesh earlier.

The pair of gears vibrated at their natural frequency at speeds below resonance, and at speeds above resonance it vibrated at the tooth contact frequency.

The maximum tooth load occurred near the pitch point at low speeds (below resonance) while at and above the resonance speed they occurred at the beginning of contact.

Experimental results showed a general qualitative agreement with the theoretical predictions.

APPENDIX I

Tooth deflections calculated using the assumed tooth shapes and true involute profiles :

RF = Radius at which the force is acting (mm)
Z1 = Deflection of the assumed tooth (mm)
Z2 = Deflection of the involute tooth (mm)
ER = Error (mm)
ER% = Percentage error
O'LL% = Error as a percentage of the total tooth deflection

Number of teeth = 45
Diametral Pitch = 8

RF	Z1	Z2	ER	ER%	O'LL%
67.468750	.000005	.000000	-.000005	.000000	.000000
68.405030	.434695	.427734	-.006961	-1.627361	-.046427
69.341310	.950949	.924508	-.026441	-2.860017	-.176356
70.277590	1.630094	1.568647	-.061447	-3.917168	-.409835
71.213870	2.567705	2.449398	-.118306	-4.830019	-.789078
72.150150	3.883568	3.677733	-.205835	-5.596794	-1.372875
73.086430	5.741602	5.414309	-.327293	-6.044971	-2.182975
74.022710	8.397996	7.917135	-.480861	-6.073670	-3.207235

Number of teeth = 73
Diametral Pitch = 16

RF	Z1	Z2	ER	ER%	O'LL%
55.959370	.000000	.000000	.000000	.000000	.000000
56.429880	.396238	.395908	-.000330	-.083398	-.002202
56.900390	.865367	.865520	.000153	.017692	.001021
57.370900	1.475941	1.480328	.004387	.296330	.029258
57.841410	2.311604	2.329203	.017599	.755595	.117384
58.311920	3.480658	3.530960	.050302	1.424592	.335502
58.782420	5.135698	5.258667	.122969	2.338409	.820177
59.252930	7.522932	7.792321	.269389	3.457105	1.796763

Number of teeth = 42
Diametral Pitch = 16

RF	Z1	Z2	ER	ER%	O'LL%
31.353120	-.000009	.000000	.000009	.000000	.000000
31.820870	.443824	.434738	-.009086	-2.090024	-.060602
32.288610	.971732	.937365	-.034367	-3.666338	-.229220
32.756360	1.668489	1.588095	-.080394	-5.062284	-.536210
33.224100	2.632907	2.476171	-.156736	-6.329789	-1.045397
33.691840	3.987987	3.712461	-.275527	-7.421675	-1.837703
34.159580	5.900996	5.452079	-.448917	-8.233875	-2.994180
34.627330	8.631389	7.952111	-.679277	-8.542102	-4.530631

APPENDIX II

Integration of the tooth deflection formulae

The total height LO of the assumed tooth shape was chosen in such a way that its thickness at the base (H_r) was equal to the tooth thickness at the root radius (R_r) and its thickness at a height ($R_o - R_r$) from the base was equal to the tooth tip thickness.

The thickness of the assumed shape at a distance x from its tip is given by the equation:

$$H = H_r \left(\frac{x}{LO}\right)^{1/2}$$

If L is the height of the gear tooth, then its tip thickness is:

$$H_o = H_r \left(\frac{LO - L}{LO}\right)^{1/2}$$

$$\therefore \quad LO = \frac{L}{1 - \left(\frac{H_o}{H_r}\right)^2}$$

and the thickness of the assumed shape at any radius R is:

$$H = H_r \left(\frac{R_r + LO - R}{LO}\right)^{1/2}$$

Equating the work done by the force to the stress energy (per mm facewidth of the gear) -

(i) Due to bending:

$$\frac{1}{2} F \, ZB = \frac{1}{2} \int_{R_r}^{R_y} \frac{M^2}{EI} \, dR$$

$$M = F \cos\theta \, (R_y - R)$$

$$I = \frac{1}{12} H^3$$

$$I = \frac{1}{12} H_r^3 \left(\frac{R_r + LO - R}{LO}\right)^{3/2}$$

where

M - Bending moment of the force F about an axis parallel to that of the gears at a radius R on the centre-line of the gear tooth

I - Second moment of area of the tooth's cross-section about the same axis.

Substituting for M and I

$$\frac{1}{2} F\, ZB = \frac{1}{2} \int_{R_r}^{R_y} \frac{F^2 \cos^2\theta (R_y - R)^2}{\frac{1}{12} E H_r^2 \left(\frac{R_r + LO - R}{LO}\right)^{3/2}} dR$$

$$ZB = \frac{12F \cos^2\theta}{E} \frac{LO^{3/2}}{H_r^3} \int_{R_r}^{R_y} \frac{(R_y - R)^2}{(R_r + LO - R)} dR$$

Let $R_r + LO - R = Y$

and $R_r + LO - R_y = LC$

then $R = R_r + LO - Y$

and $dR = - dY$

$$\therefore \int_{R_r}^{R_y} \frac{(R_y - R)^2}{(R_r + LO - R)} dR = - \int_{LO}^{LC} \frac{(Y - LC)^2}{Y^{3/2}} dY$$

$$= - 2 \left[- \frac{8}{3} LC^{3/2} + \frac{LC^2}{LO^{1/2}} + 2LC\, LO^{1/2} - \frac{LO^{3/2}}{3} \right]$$

$$\therefore ZB = \frac{8F}{E} \cos^2\theta \frac{LO}{H_r^3} [8LC^{3/2}\, LO^{1/2} - 3LC^2 - 6LC\, LO + LO^2]$$

(ii) Due to shear:

$$\frac{1}{2} F\, ZS = \frac{1}{2} \int_{R_r}^{R_y} \frac{1.2\, Q^2}{G\, H} dR$$

$$Q = F \cos\theta$$

Q - Shear component of the force F

$$\therefore \quad \frac{1}{2} F\, ZS = \frac{1}{2} 1.2 \frac{F^2 \cos^2\theta}{G} \int_{R_r}^{R_y} \frac{1}{H_r \left(\frac{R_r + LO - R}{LO}\right)^{1/2}} dR$$

$$ZS = 1.2 \frac{F \cos^2\theta}{G} \frac{LO^{1/2}}{H_r} \int_{LO}^{LC} -\frac{1}{Y^{1/2}} dY$$

$$ZS = 2.4 \frac{F \cos^2\theta}{G} \frac{LO^{1/2}}{H_r} (LO^{1/2} - LC^{1/2})$$

(iii) Due to the normal component of the force:

$$\frac{1}{2} F\, ZN = \frac{1}{2} \int_{R_r}^{R_y} \frac{N^2}{EH} dR$$

$$N = F \sin\theta$$

N = Normal component of the force F

$$\frac{1}{2} F\, ZN = \frac{1}{2} \frac{F^2 \sin^2\theta}{E} \int_{R_r}^{R_y} \frac{1}{H_r \left(\frac{R_r + LO - R}{LO}\right)} dR$$

$$ZN = 2.0 \frac{F}{E} \sin^2\theta \frac{LO^{1/2}}{H_r} (LO^{1/2} - LC^{1/2})$$

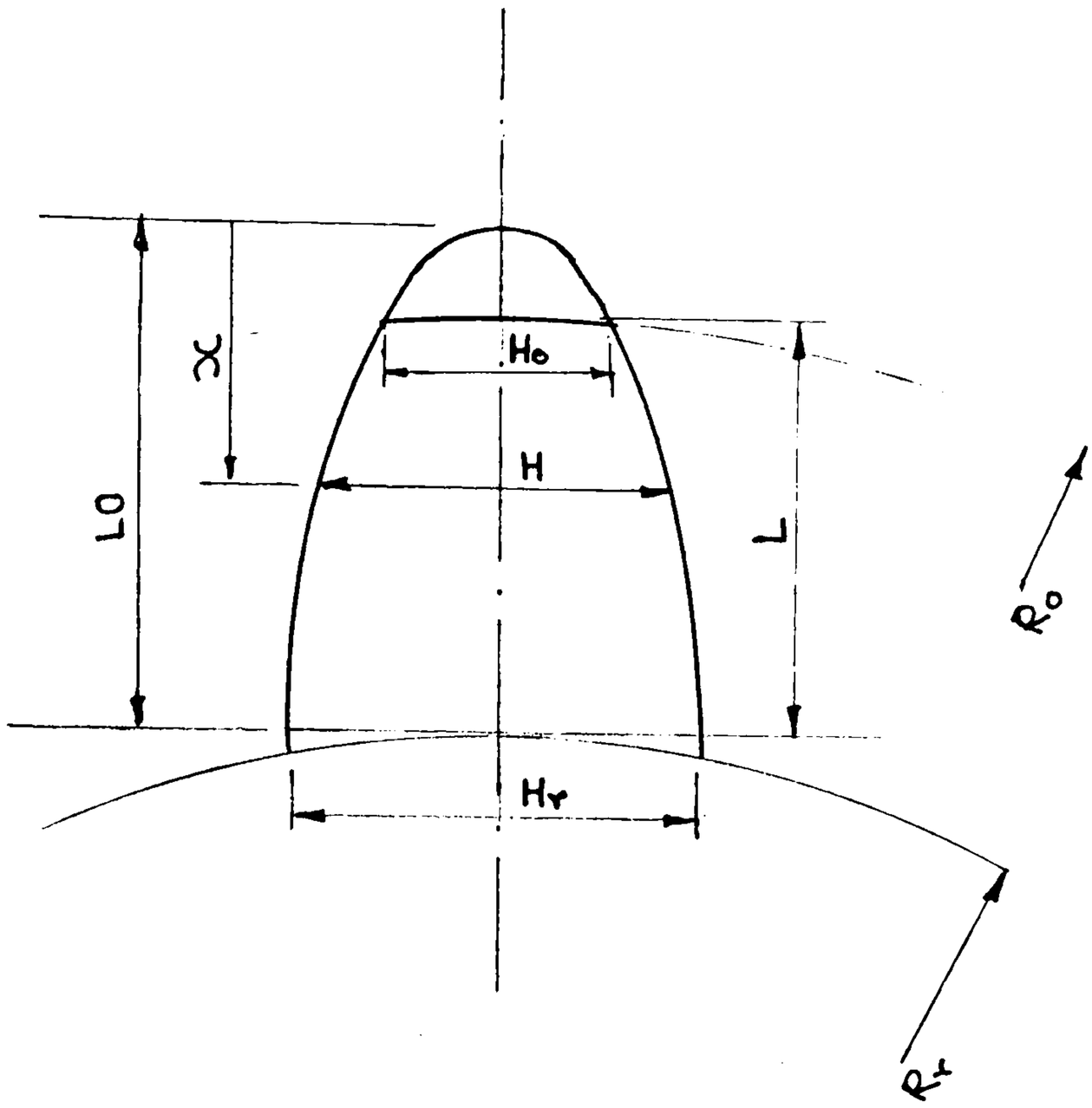

FIGURE II(a)

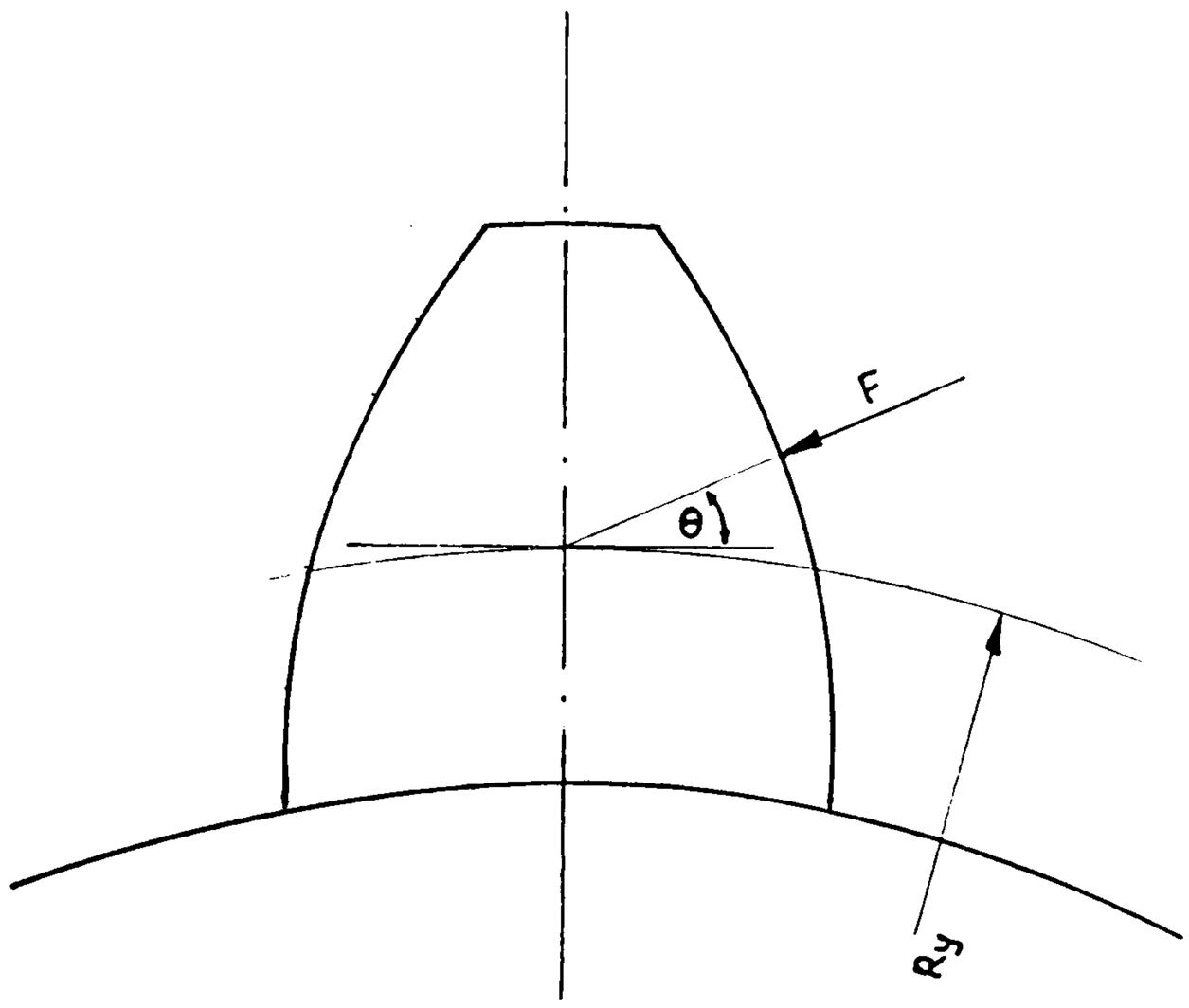

FIGURE II(b)

APPENDIX III

Details of the Fortran computer programme used to calculate the minimum oil film thickness:

The pressure/viscosity coefficient 'α' was calculated according to the following formula suggested by Davenport (13).

$$\alpha = 10^{-6} Y[\ln(\mu_T + 0.5) + D]/p_o$$

where μ_T = viscosity of oil at inlet in cP

Y, D and p_o are constants

$Y = 80.0$

$D = 2.15$

and $p_o = 200.0$

for the lubricating oil considered.

In calculating the shear stress a limiting shear stress as used by Wang and Cheng (56) was employed,

i.e. at high pressure $\tau_{max} = \dfrac{\bar{G}_\infty}{4.0}$

where $\bar{G}_\infty$ is the limit shear modulus for continuous shear, given by the formula:

$$\bar{G}_{\infty} = \frac{1.2p \times 10^{-8}}{2.52 + 0.024\ T}$$

p = pressure (N/m^2)

and T = temperature (^{o}C)

At low pressure

$$\tau_{max} = \frac{1}{4\ K_s}\left(\frac{1}{2.52 + 0.25\ T}\right)$$

For mineral oil $K_s \approx 7.5$

τ_{max} is in GN/m^2

τ is also calculated using the formula derived in Chapter 3. The smallest of the three values is taken as the shear stress at the point considered.

```
C       PROGRAM TO CALCULATE THE OIL FILM THICKNESS, AT STEADY STATE,
C       BETWEEN A PAIR OF SPUR GEAR TEETH IN MESH
        COMMON  /DCNS/RRA,RCA,LA,GNA,CBA,CSA,CNA,C11A,C12A,C22A,CH,V
       1,RRB,RCB,LB,GNB,CBB,CSB,CNB,C11B,C12B,C22B,INVPSY,CBT
        COMMON /ALL/RBA,ROA,RBB,ROB,YY,WA,M,PANG,DT,PI
        COMMON /OIL/DYAO,VISCT,RBTA,MRBTA,TO,ALP,TM,BET
        COMMON /VCNS/ERFX
        COMMON /VCNS2/DELHO
        REAL IA,IB,INVPSY,L,LA,LB,LT,KA1,KB1,KO1,M,MA,MB,MAB,MRBTA,NA
        REAL*8 COMP1,DHO1,HO,HO1,YA,YB,YAO,YBO,YAO1,YBO1,YMA
        INTEGER TA,TB,DP
        DATA SY/20./,FWG/1.0/,FWT/1.0/,E/2.068E5/,GOIL/5000./,G/8.273E4/
        WRITE(*,10) '    NO. OF TEETH - GEAR - A        : '
        READ(*,90) TA
        WRITE(*,10) '    NO. OF TEETH - GEAR - B        : '
        READ(*,90) TB
        WRITE(*,10) '    DIAMETRAL PITCH                : '
        READ(*,90) DP
        WRITE(*,10) '    SPEED OF GEAR  A  (rpm)        : '
        READ(*,30) NA
        WRITE(*,10) '    FO  (N/mm)                     : '
        READ(*,40) FO
        WRITE(*,10) '    VISCOSITY (Ns/m2)              : '
        READ(*,40) VISC
C  SYSTEM PARAMETERS
        GOTO 295
200     ALP=2.32E-8
        DYAO=DYAR
        YAR=YOPH
        RBTA=RBA*TAN(PANG)
        MRBTA=(M+1)*RBTA
        MAB=(MA+MB)/MB
        RAD=YOMX*(YY-YOMX)/YY
        CERFX=E/(2*PI*RAD*(1-V**2))
        ERFX=10.0*SQRT(FO*CERFX)
        ERAL=FO*1.0E-3
C  VISCOSITY IN Ns/m2
        BET=3890.0
        TM=90.0+273
        TO=30.0+273
        VISCT=VISC*EXP(BET*(1.0/TM - 1.0/TO))
C  VISCOSITY/PRESSURE COEFFICIENT
        Y=0.8
        PP=200.0
        D=2.15
        ALCON=1.0E-6*Y/PP
        ALP=ALCON*(ALOG(VISCT*1.0E3+0.5)+D)
        DHO1=0.0
        F1=FO
        YAO1=YAR
C    OIL FILM THICKNESS `GRUBIN' FORMULA
210     RA=YAO1
        RB=YY-YAO1
        R=RA*RB/(RA+RB)
        UA=RA*WA
        UB=RB*WA*M
```

```
U1=(UA+UB)/2
U=VISCT*U1/(EV*R*1E6)
W=FO/(EV*R)
H=1.95*(GOIL*U)**0.727/(W**0.091)
HO=H*R
HO1=HO
DELHO=HO/5.0
CALL OFTH(YAO1,HO1,F1,DHO1,ERAL)
CALL STIF1(YAO1,HO1,F1,COMP1,KO1,KA1,KB1)
YMA=(COMP1-HO1)/MAB
WRITE(*,75)HO1,YMA
GOTO 300
10     FORMAT(A\)
20     FORMAT(A)
30     FORMAT(F9.3)
40     FORMAT(F10.7)
75     FORMAT(7H HO =    E15.7,12H      Yma =    E15.7)
90     FORMAT(I4)
C  SYSTEM PARAMETERS
295    PI=3.14159
       V=0.3
       WA=2*PI*NA/60
       PSY=SY*PI/180
       INVPSY=TAN(PSY) - PSY
       RCA=TA*25.4/(2*DP)
       RCB=TB*25.4/(2*DP)
       CD=RCA+RCB
       RBA=RCA*COS(PSY)
       RBB=RCB*COS(PSY)
       ROA=((TA+2)*25.4+ACA*TAN(PSY))/(2*DP)
       ROB=((TB+2)*25.4+ACB*TAN(PSY))/(2*DP)
       RRA=(TA-2.5)*25.4/(2*DP)
       RRB=(TB-2.5)*25.4/(2*DP)
       DYAR=RBA*WA
       DYMA=0.0
       PO=2*PI*RBA/TA
       YY=SQRT(CD**2-(RBA+RBB)**2)
       YOMN=YY-SQRT(ROB**2-RBB**2)
       PANG=ATAN(YY/(RBA+RBB))
       YOPH=RBA*TAN(PANG)
       YOMX=SQRT(ROA**2-RBA**2)
       IA=PI*FWG*RCA**4*7.759E-6/2
       IB=PI*FWG*RCB**4*7.759E-6/2
       MA=IA/RBA**2
       MB=IB/RBB**2
       M=1.0*TA/TB
       E1=(1-V**2)/E
       EV=1/E1
       L=2.25*25.4/DP
       GNA=PI*25.4/(2*DP) +2*ACA*TAN(PSY)
       GNB=PI*25.4/(2*DP) +2*ACB*TAN(PSY)
       IF(RRA .LT. RBA) THEN
       R=RBA
       ELSE
       R=RRA
       ENDIF
```

```
      CALL THICK(R,RBA,INVPSY,GNA,RCA,HRA,RI)
      IF(RRB .LT. RBB) THEN
      R=RBB
      ELSE
      R=RRB
      ENDIF
      CALL THICK(R,RBB,INVPSY,GNB,RCB,HRB,RI)
      CALL THICK(ROA,RBA,INVPSY,GNA,RCA,HOA,RI)
      CALL THICK(ROB,RBB,INVPSY,GNB,RCB,HOB,RI)
      LA=L/(1-(HOA/HRA)**2)
      LB=L/(1-(HOB/HRB)**2)
C  CONSTANTS FOR SHEAR DEFLN. `A'  AND `B'
      CSA=(2.4*SQRT(LA))/(G*HRA)
      CSB=(2.4*SQRT(LB))/(G*HRB)
C  CONSTANTS FOR DEFLN. DUE TO NORMAL LOAD `A' AND `B'
      CNA=(2*SQRT(LA))/(E*HRA)
      CNB=(2*SQRT(LB))/(E*HRB)
C  CONSTANTS FOR BENDING DEFLN. `A' AND `B'
      CBA=8.0*LA/(E*HRA**3)
      CBB=8.0*LB/(E*HRB**3)
C  CONSTANTS FOR HERTZ DEFLN. `A' AND `B'
      CH=2.0/(PI*EV)
C  CONST. FOR HERTZ CONTACT WIDTH `BT'
      CBT=SQRT(8.0/(PI*EV))
C  CONSTANTS FOR DEFLN. OF BODY
      C11A=9/(PI*EV*HRA**2)
      C11B=9/(PI*EV*HRB**2)
      C12A=(1+V)*(1-2*V)/(2*E*HRA)
      C12B=(1+V)*(1-2*V)/(2*E*HRB)
      C22A=2.4/(PI*EV)
      C22B=2.4/(PI*EV)
      GOTO 200
300   END
C  INVOLUTE FUNCTION
      SUBROUTINE INV(R,RB,INVR)
      REAL INVR
      ALPA=ATAN(SQRT((R**2-RB**2)/RB**2))
      INVR=TAN(ALPA)-ALPA
      RETURN
      END
C  TOOTH THICKNESS
      SUBROUTINE THICK(R,RB,INVPSY,GN,RC,HC,RI)
      REAL INVPSY,INVR
      CALL INV(R,RB,INVR)
      G2R=(GN/(2*RC)) + INVPSY - INVR
      HC=2*R*SIN(G2R)
      RI=R*COS(G2R)
      RETURN
      END
C  SUBROUTINE TO CALCULATE 'YAO1'
      SUBROUTINE SURF1(YAO,YAR,YMA,KA,F)
      REAL*8 YAO,YMA
      REAL KA
      IF(KA .LE. 0.0) THEN
      YAO=YAR+YMA
      ELSE
```

```
      YAO=YAR+YMA-F/KA
      ENDIF
      RETURN
      END
C  TOOTH STIFFNESS - INITIAL
      SUBROUTINE STIF1(YAO,HO,FI,COMP,KO,KA,KB)
      COMMON  /DCNS/RRA,RCA,LA,GNA,CBA,CSA,CNA,C11A,C12A,C22A,CH,V
     1,RRB,RCB,LB,GNB,CBB,CSB,CNB,C11B,C12B,C22B,INVPSY,CBT
      COMMON /ALL/RBA,ROA,RBB,ROB,YY,WA,M,PANG,DT,PI
      REAL*8 EPA,EPB,YAO,YBO,HO,DHO,COMP
      REAL LA,LB,KO,KA,KB,INVPSY,LCA,LCB
      IF (FI .LE. 0.0) THEN
      COMP=0.0
      KO=0.0
      KA=0.0
      KB=0.0
      GOTO 2050
      ENDIF
      YBO=YAO+HO
      YYBO=YY-YBO
2000  R=DSQRT(YAO**2+RBA**2)
      CALL THICK(R,RBA,INVPSY,GNA,RCA,HCA,RI)
      ALPA=DATAN(YAO/RBA)-ATAN(HCA/(2*RI))
      HA=HCA/(2*COS(ALPA))
      YP=RBA/COS(ALPA)-SQRT(RRA**2-(HRA/2)**2)
      LCA=LA-YP
      AK=CBA*(COS(ALPA))**2*(LA**2-6*LCA*LA-3*LCA**2+8*LCA**1.5*LA**.5)
      C2SA=CSA*(COS(ALPA))**2*(SQRT(LA)-SQRT(LCA))
      C2NA=CNA*(SIN(ALPA))**2*(SQRT(LA)-SQRT(LCA))
      CDA=C11A*YP**2+2*C12A*YP+C22A*(1+((TAN(ALPA))**2)/3.1)
      C2DA=2*(COS(ALPA))**2*CDA
      R=SQRT(YYBO**2+RBB**2)
      CALL THICK(R,RBB,INVPSY,GNB,RCB,HCB,RI)
      ALPA=ATAN(YYBO/RBB)-ATAN(HCB/(2*RI))
      HB=HCB/(2*COS(ALPA))
      YP=RBB/COS(ALPA)-SQRT(RRB**2-(HRB/2)**2)
      LCB=LB-YP
      BK=CBB*(COS(ALPA))**2*(LB**2-6*LCB*LB-3*LCB**2+8*LCB**1.5*LB**.5)
      C2SB=CSB*(COS(ALPA))**2*(SQRT(LB)-SQRT(LCB))
      C2NB=CNB*(SIN(ALPA))**2*(SQRT(LB)-SQRT(LCB))
      CDB=C11B*YP**2+2*C12*YP+C22B*(1+((TAN(ALPA))**2/3.1))
      C2DB=2*(COS(ALPA))**2*CDB
2010  BT= CBT*DSQRT((FI*YAO*YYBO)/(YAO+YYBO))
      ZHA=FI*CH*(ALOG(2*HA/BT) - V/((1-V)*2))
      ZHB=FI*CH*(ALOG(2*HB/BT) - V/((1-V)*2))
      ZA=FI*(C2SA+C2NA+C2DA+AK)
      ZB=FI*(C2SB+C2NB+C2DB+BK)
      COMPA=(ZHA+ZA)
      COMPB=(ZHB+ZB)
      COMP=COMPA+COMPB
      KA=FI/COMPA
      KB=FI/COMPB
      KO=FI/COMP
2050  RETURN
      END
C    TO CALCULATE `YA' FOR ANY X
```

```
      SUBROUTINE DISA(RBA,YAO,X,YA,E)
      REAL*8 X,YA,E,E2,FE,DFE,THA,DE,BETA,YAO
      IF (X .EQ. 0.0) THEN
      YA=YAO
      GOTO 1420
      ENDIF
      E=DATAN(X/YAO)
      BETA=YAO/RBA
1400  FE=E-(RBA+X-RBA*DCOS(E))/(RBA*DSIN(E))+BETA
      DFE=1+(((RBA+X)*DCOS(E))/RBA-1.)/(DSIN(E))**2
      E2=E-(FE/DFE)
      DE=DABS(E2-E)
      IF(DE .LE. 0.000001) GOTO 1410
      E=E2
      GOTO 1400
1410  E=E2
      THA=DATAN(BETA+E) - E
      YA=(RBA+X)*DTAN(THA)
1420  RETURN
      END
C   TO CALCULATE `YB' FOR ANY X
      SUBROUTINE DISB(YY,RBB,YBO,X,YB,E)
      REAL*8 X,YB,E,THA,E2,FE,DFE,DE,YBO,BETA
      IF (X .EQ. 0.0) THEN
      YB=YBO
      GOTO 1470
      ENDIF
      E=DATAN(X/(YY-YBO))
      BETA=(YY-YBO)/RBB
1450  FE=E-(RBB-X-RBB*DCOS(E))/(RBB*DSIN(E))-BETA
      DFE=1+(((RBB-X)*DCOS(E))/RBB-1.)/(DSIN(E))**2
      E2=E-(FE/DFE)
      DE=DABS(E2-E)
      IF(DE .LE. 0.000001) GOTO 1460
      E=E2
      GOTO 1450
1460  E=E2
      THA=DATAN(BETA-E) + E
      YB=YY-(RBB-X)*DTAN(THA)
1470  RETURN
      END
C  SUBROUTINE TO CALCULATE `HO' FOR A GIVEN FORCE
      SUBROUTINE OFTH(YAO,HO,FI,DHO,ERAL)
      COMMON /OIL/DYAO,VISCT,RBTA,MRBTA,TO,ALP,TM,BET
      COMMON /ALL/RBA,ROA,RBB,ROB,YY,WA,M,PANG,DT,PI
      COMMON /VCNS/ERFX
      COMMON /VCNS2/DEL
      REAL NA,M,LT,INVPSY,INVR,MRBTA
      REAL*8 X,X1,XMX,XPO,XPON1,XPON2,XPON3,YA,YB,EPA,EPB,C,Q,Q1
     1,YAO,YBO,HO,DHO,XMN,HON1,HOL,HOR,HOH
      FN1=0.0
      ITR4=1
      ITR5=1
      SQFI=SQRT(FI)
1200  FIN1=0.0
      FNL=0.0
```

```
      FNR=0.0
      HOH=0.0
1205  YBO=YAO+HO
      CALL OFLM(YAO,YBO,HO,DHO,FI,XPO,C,XMX,XMN)
1210  CALL FORCE(YAO,YBO,XMX,XPO,C,FIN,DHO)
      WRITE(*,111)HO,FIN
111   FORMAT(2E17.8)
      FN=FI-FIN
      IF(ABS(FN) .LE. ERAL) GOTO 1250
      IF(FNL*FNR .LT. 0.0) GOTO 1240
      IF(FN1*FN .LT. 0.0) GOTO 1235
1220  FIN1=FIN
      HON1=HO
      FN1=FN
      IF(FN1 .GT. 0.0) THEN
      HO=HON1-DEL
      ELSE
      HO=HON1+DEL
      ENDIF
      IF(HO .LT. HOH) HO=(HOH+HON1)/2.0
      GOTO 1205
1226  HO=HO+DEL
      GOTO 1205
1235  FNL=FN1
      FNR=FN
      SQFNL=SQRT(FI-FN1)-SQFI
      SQFNR=SQRT(FIN)-SQFI
      HOL=HON1
      HOR=HO
      GOTO 1245
1240  IF(FNL*FN)1241,1241,1242
1241  HOR=HO
      FNR=FN
      SQFNR=SQRT(FIN)-SQFI
      GOTO 1245
1242  HOL=HO
      FNL=FN
      SQFNL=SQRT(FIN)-SQFI
1245  IF(ITR4 .GT. 3)THEN
      HO=(HOL+HOR)/2.0
      ITR4=1
      ELSE
      HO=HOL-SQFNL*(HOL-HOR)/(SQFNL-SQFNR)
      ITR4=ITR4+1
      ENDIF
      IF(DABS(HOL-HOR) .LE. 0.1E-8)GOTO 1250
      GOTO 1205
1250  RETURN
      END
C  SUBROUTINE TO FIND `XPO'
      SUBROUTINE OFLM(YAO,YBO,HO,DHO,FI,XPO,C,XMX,XMN)
      COMMON /OIL/DYAO,VISCT,RBTA,MRBTA,TO,ALP,TM,BET
      COMMON /ALL/RBA,ROA,RBB,ROB,YY,WA,M,PANG,DT,PI
      COMMON /VCNS/ERFX
      REAL NA,M,LT,INVPSY,INVR,MRBTA
      REAL*8 X,X1,XMX,XPO,XPON1,XPON2,XPON3,YA,YB,EPA,EPB,C,Q,Q1
```

```
1,YAO,YBO,HO,DHO,XMN
 CALL LMTS(RBA,RBB,ROA,RBB,YY,YAO,YBO,XM)
 XMX=XM
 CALL LMTS(RBA,RBB,RBA,ROB,YY,YAO,YBO,XM)
 XMN=XM
 FXN1=0.0
 DX=(XMX-XMN)
 IF((XMX-DX/50) .LE. 0.0) THEN
 XPON1=XMX-DX/500
 ELSE
 XPON1=XMN
 ENDIF
 ITR1=0
       ITR2=0
       ITR3=0
       CALL CONS(YAO,YBO,XPON1,DHO,C,EPA,EPB)
       CALL FUNC1(YAO,YBO,XMX,XPON1,FXN1,C,DHO,EPA,EPB)
       FXN2=0.0
       IF(XMN)1,5,5
1      IF(XMX-DX/50)2,2,3
2      IF(FXN1 .LE. 0.0) GOTO 1337
       DX=-DX/500
       GOTO 6
3      IF(FXN1)4,4,1335
4      DX=DX/50
       XPON2=0.0
       GOTO 1300
5      IF(FXN1)1337,1335,1335
6      XPON2=XPON1+DX
1300   CALL CONS(YAO,YBO,XPON2,DHO,C,EPA,EPB)
       CALL FUNC1(YAO,YBO,XMX,XPON2,FXN2,C,DHO,EPA,EPB)
       IF(FXN1*FXN2)1317,1316,1316
1316   XPON1=XPON2
       FXN1=FXN2
       XPON2=XPON2+DX
       IF(XPON2 .GE. XMX) GOTO 1337
       IF(XPON2 .LE. XMN) GOTO 1335
       GOTO 1300
1317   FSQ1=(ABS(FXN1)/FXN1)*SQRT(ABS(FXN1))
       FSQ2=(ABS(FXN2)/FXN2)*SQRT(ABS(FXN2))
1320   XPON3=XPON1+(FSQ1*(XPON2-XPON1))/(FSQ1-FSQ2)
1321   ITR2=ITR2+1
       IF(ITR2 .GT. 50) GOTO 1340
1322   CALL CONS(YAO,YBO,XPON3,DHO,C,EPA,EPB)
       CALL FUNC1(YAO,YBO,XMX,XPON3,FXN3,C,DHO,EPA,EPB)
       IF(DABS(XPON2-XPON1) .LT. 1.D-5) GOTO 1345
       IF(ABS(FXN3) .LT. ERFX) GOTO 1345
1325   IF(ITR3 .GE. 15) GOTO 1331
       ITR3=ITR3+1
       IF(FXN3*FXN1)1326,1326,1327
1326   XPON2=XPON3
       FXN2=FXN3
       GOTO 1328
1327   XPON1=XPON3
       FXN1=FXN3
       GOTO 1328
```

```
1328  IF(DABS(XPON1-XPON2) .GT. 0.01)GOTO 1317
      XPON3=XPON2-FXN2*(XPON2-XPON1)/(FXN2-FXN1)
      GOTO 1321
1331 . IF(FXN3*FXN1)1332,1332,1333
1332  XPON2=XPON3
      XPON3=(XPON1+XPON2)/2
      GOTO 1322
1333  XPON1=XPON3
      XPON3=(XPON1+XPON2)/2
      GOTO 1322
1335  CALL ALTC(YAO,YBO,XMX,XMN,DHO,C)
      XPO=XMN
      GOTO 1350
1337  XPO=XMX
      GOTO 1350
1340  WRITE(*,1341)'* FXAP CONVERGENCE ERROR * '
1341  FORMAT(A)
1345  FX=FXN3
      XPO=XPON3
1350  RETURN
      END
C   TO FIND THE MAXM. AND MINM. X VALUES
      SUBROUTINE LMTS(RBA,RBB,RA,RB,YY,YAO,YBO,XM)
      REAL*8 YAO,YBO
      BETA=YAO/RBA
      E=ACOS(RBA/RA)
      THA=BETA-TAN(E)+E
      XAM=RA*COS(THA)-RBA
      BETA=(YY-YBO)/RBB
      E=ACOS(RBB/RB)
      THA=BETA-TAN(E)+E
      XBM=RBB-RB*COS(THA)
      DXM=ABS(XAM)-ABS(XBM)
      IF(DXM .LE. 0.0) THEN
      XM=XAM
      ELSE
      XM=XBM
      ENDIF
      RETURN
      END
C   TO CALCULATE THE CONSTANT - C -
      SUBROUTINE CONS(YAO,YBO,X,DHO,CX,EPA,EPB)
      COMMON /OIL/DYAO,VISCT,RBTA,MRBTA,TO,ALP,TM,BET
      COMMON /ALL/RBA,ROA,RBB,ROB,YY,WA,M,PANG,DT,PI
      REAL M,MRBTA
      REAL*8 X,YA,YB,EPA,EPB,CX,FC,YAO,YBO,HO,DHO
      CALL DISA(RBA,YAO,X,YA,EPA)
      CALL DISB(YY,RBB,YBO,X,YB,EPB)
      FC=DHO*(MRBTA*(YA+YB)-M*(YA*YB+X**2)+2*RBA*X)
      CX=DYAO*(M+1)*(X**2+YA*YB-RBTA*(YA+YB))-FC
      RETURN
      END
C  TO CALCULATE 'C' AT THE BEGINNING OF CONTACT
      SUBROUTINE ALTC(YAO,YBO,XMX,XN,DHO,C)
      COMMON /OIL/DYAO,VISCT,RBTA,MRBTA,TO,ALP,TM,BET
      COMMON /ALL/RBA,ROA,RBB,ROB,YY,WA,M,PANG,DT,PI
```

```
      COMMON /VCNS/ERFX
      REAL M,MRBTA
      REAL*8 XMX,X,DX,XN,C,YA,YB,EPA,EPB,F11,F22,F33,SF11,SF22,SF33,XPO
     1,DHO,YAO,YBO
      SF11=0.0
      SF22=0.0
      SF33=0.0
      N=121
      X=XMX
      DX=(XN-X)/(N-1)
      DO 1590 I=1,N
      CALL DISA(RBA,YAO,X,YA,EPA)
      CALL DISB(YY,RBB,YBO,X,YB,EPB)
      F11=DYAO*(M+1)*(RBTA*(YA+YB)-(YA*YB)-X**2)/((YB-YA)**3)
      F22=DHO*(MRBTA*(YA+YB)-M*(YA*YB+X**2)+2.*RBA*X)/((YB-YA)**3)
      F33=1.0/((YB-YA)**3)
      IF(I .EQ. 1) GOTO 1580
      IF(I .EQ. N) GOTO 1580
      DIFF=I/2.0-INT(I/2)
      IF(ABS(DIFF) .LT. 0.1) THEN
      L=4
      ELSE
      L=2
      ENDIF
      F11=F11*L
      F22=F22*L
      F33=F33*L
1580  SF11=SF11+F11
      SF22=SF22+F22
      SF33=SF33+F33
      X=X+DX
1590  CONTINUE
      C=-(SF11+SF22)/SF33
      RETURN
      END
C  PRESSURE FUNCTION
      SUBROUTINE FUNC1(YAO,YBO,XMX,XPO,FX,C,DHO,EPA,EPB)
      COMMON /OIL/DYAO,VISCT,RBTA,MRBTA,TO,ALP,TM,BET
      COMMON /ALL/RBA,ROA,RBB,ROB,YY,WA,M,PANG,DT,PI
      COMMON /VCNS/ERFX
      REAL NA,M,LT,INVPSY,INVR,MRBTA
      REAL*8 X,X1,XMX,XPO,YA,YB,EPA,EPB,C,Q,Q1,XPM,DHO,YAO,YBO
      Q1=0.0
      IF (FX .EQ. 0.0) GOTO 1500
      IF (ABS(FX) .GT. 0.1E7) GOTO 1500
      NITR1=11
      NITR2=21
      NITR3=121
      GOTO 1510
1500  NITR1=11
      NITR2=11
      NITR3=51
1510  IF (DABS(XPO) .LT. 0.005)THEN
      X=0.05
      GOTO 1520
      ENDIF
```

```
      X=5.*DABS(XPO)
1520  IF (X .GT. XMX) THEN
      X=XMX
      GOTO 1550
      ENDIF
      X1=3.*X
      IF (X1 .GT. XMX) THEN
      X1=XMX
      GOTO 1540
      ENDIF
1530  CALL FUNC2(YAO,YBO,XMX,X1,C,DHO,EPA,EPB,NITR1,Q,Q1,XPO)
      Q1=Q
1540  CALL FUNC2(YAO,YBO,X1,X,C,DHO,EPA,EPB,NITR2,Q,Q1,XPO)
      Q1=Q
1550  CALL FUNC2(YAO,YBO,X,XPO,C,DHO,EPA,EPB,NITR3,Q,Q1,XPO)
      FX=Q
      RETURN
      END
C  TO CALCULATE THE REDUCED PRESSURE (Q) AT ANY POINT
      SUBROUTINE FUNC2(YAO,YBO,XMX,XN,C,DHO,EPA,EPB,N,Q,Q1,XPO)
      COMMON /OIL/DYAO,VISCT,RBTA,MRBTA,TO,ALP,TM,BET
      COMMON /ALL/RBA,ROA,RBB,ROB,YY,WA,M,PANG,DT,PI
      COMMON /VCNS/ERFX
      REAL M,MRBTA
      REAL*8 XMX,X,DX,XN,C,YA,YB,EPA,EPB,F11,F22,FF,Q,Q1,EP2,XPO
     1,DHO,YAO,YBO
      FX=0.0
      X=XMX
      DX=(XN-X)/(N-1)
      DO 1590 I=1,N
      CALL DISA(RBA,YAO,X,YA,EPA)
      CALL DISB(YY,RBB,YBO,X,YB,EPB)
      F11=(M+1)*(RBTA*(YA+YB)-(YA*YB)-X**2)
      F22=MRBTA*(YA+YB)-M*(YA*YB+X**2)+2.*RBA*X
      FF=6*VISCT*(DYAO*F11+DHO*F22+C)/(RBA*(YB-YA)**3)
      DQX=FF
      IF(I .EQ. 1) GOTO 1580
      IF(I .EQ. N) GOTO 1580
      DIFF=I/2.0-INT(I/2)
      IF(ABS(DIFF) .LT. 0.1) THEN
      L=4
      ELSE
      L=2
      ENDIF
      FF=FF*L
1580  FX=FX+FF
      X=X+DX
1590  CONTINUE
      Q=FX*DX/3. + Q1
      RETURN
      END
C  TO CALCULATE THE PRESSURE AND SHEAR STRESS AT ANY POINT
      SUBROUTINE FUNC(YAO,YBO,XMX,XN,C,DHO,SS,EPA,EPB,N,Q,Q1,XPO)
      COMMON /OIL/DYAO,VISCT,RBTA,MRBTA,TO,ALP,TM,BET
      COMMON /ALL/RBA,ROA,RBB,ROB,YY,WA,M,PANG,DT,PI
      COMMON /VCNS/ERFX
```

```
      REAL M,MRBTA
      REAL*8 XMX,X,DX,XN,C,YA,YB,EPA,EPB,F11,F22,FF,Q,Q1,EP2,XPO
     1,DHO,YAO,YBO
      FX=0.0
      X=XMX
      DX=(XN-X)/(N-1)
      DO 1590 I=1,N
      CALL DISA(RBA,YAO,X,YA,EPA)
      CALL DISB(YY,RBB,YBO,X,YB,EPB)
      F11=(M+1)*(RBTA*(YA+YB)-(YA*YB)-X**2)
      F22=MRBTA*(YA+YB)-M*(YA*YB+X**2)+2.*RBA*X
      FF=6*VISCT*(DYAO*F11+DHO*F22+C)/(RBA*(YB-YA)**3)
      DQX=FF
      IF(I .EQ. 2) THEN
      L=4
      ELSE
      L=1
      ENDIF
      FF=FF*L
1580  FX=FX+FF
      X=X+DX
1590  CONTINUE
      Q=FX*DX/3. + Q1
      SF1=DQX*(YA-YB)/(2.*VISCT)
      SF2=WA*(YA+MRBTA-M*YB)/(2.*(YB-YA))
      SF3=DHO*(MRBTA-M*YB)/(RBA*(YA-YB))
      EP2=(DCOS(EPA))**2
      SS=VISCT*EP2*(SF1+SF2+SF3)
      RETURN
      END
C  TO CALCULATE THE FORCE
      SUBROUTINE FORCE(YAO,YBO,XMX,XN,C,TLD,DHO)
      COMMON /OIL/DYAO,VISCT,RBTA,MRBTA,TO,ALP,TM,BET
      COMMON /ALL/RBA,ROA,RBB,ROB,YY,WA,M,PANG,DT,PI
      COMMON /VCNS/ERFX
      REAL M,MRBTA
      REAL*8 XMX,X,X1,X2,XR,XN,DX,C,EPA,EPB,Q,Q1,XPO,DHO,YAO,YBO
      TEMP=TM-273.
      IF(XN .GE. (XMX-1.0E-6)) THEN
      TLD=0.0
      GOTO 655
      ENDIF
      XPO=XN
      N1=11
      N2=21
      N3=121
      NITR=3
      THL=0.0
      PR=0.0
      Q1=0.0
      SS=0.0
      XR=XMX
      IF (DABS(XN) .LE. 0.005) THEN
      X2=0.05
      ELSE
      X2=5.*DABS(XN)
```

```
      ENDIF
      IF(X2 .GE. XMX)THEN
      X2=XMX
      GOTO 560
      ENDIF
      X1=3.0*DABS(X2)
      IF(X1 .GE. XMX) THEN
      X1=XMX
      GOTO 460
      ENDIF
      DX=(XMX-X1)/(N1-1)
      X=XR
      DO 451 J=1,N1
      CALL FUNC(YAO,YBO,XR,X,C,DHO,SS0,EPA,EPB,NITR,Q,Q1,XPO)
      Q1=Q
      IF(Q .GE. (1/ALP)) THEN
      PR=-(DLOG(1.0D-100))/ALP
      ELSE
      PR=-(DLOG(1-ALP*Q))/ALP
      ENDIF
      L=1
      IF(J .EQ. 1) GOTO 440
      XR=XR-DX
      IF(J .EQ. N1) GOTO 440
      DIFF=J/2.0-INT(J/2)
      IF(ABS(DIFF) .LT. 0.1) THEN
      L=4
      ELSE
      L=2
      ENDIF
440   SS1=SS0*EXP(ALP*PR)
      SS2=1.0E9/(4*7.5*(2.52+0.25*TEMP))
      SS3=0.3*PR/(2.52+0.024*TEMP) - 0.25E8
      IF(SS3 .LE. SS2) THEN
      SS4=SS2
      ELSE
      SS4=SS3
      ENDIF
      IF(SS4 .GT. ABS(SS1)) THEN
      SS=SS1
      ELSE
      SS=SS4*(SS0/ABS(SS0))
      ENDIF
      PR=(PR+SS*(YAO/RBA+EPA))*L/DCOS(EPA)
      THL=THL+PR
      X=X-DX
451   CONTINUE
      THL1=THL*DX/3.0E6
460   THL=0.0
      PR=0.0
      XR=X1
      X=XR
      DX=(X1-X2)/(N2-1)
      DO 551 J=1,N2
      CALL FUNC(YAO,YBO,XR,X,C,DHO,SS0,EPA,EPB,NITR,Q,Q1,XPO)
      Q1=Q
```

```
      IF(Q .GE. (1/ALP)) THEN
      PR=-(DLOG(1.0D-100))/ALP
      ELSE
      PR=-(DLOG(1-ALP*Q))/ALP
      ENDIF
      L=1
      IF(J .EQ. 1) GOTO 540
      XR=XR-DX
      IF(J .EQ. N2) GOTO 540
      DIFF=J/2.0-INT(J/2)
      IF(ABS(DIFF) .LT. 0.1) THEN
      L=4
      ELSE
      L=2
      ENDIF
540   SS1=SS0*EXP(ALP*PR)
      SS2=1.0E9/(4*7.5*(2.52+0.25*TEMP))
      SS3=0.3*PR/(2.52+0.024*TEMP) - 0.25E8
      IF(SS3 .LE. SS2) THEN
      SS4=SS2
      ELSE
      SS4=SS3
      ENDIF
      IF(SS4 .GT. ABS(SS1)) THEN
      SS=SS1
      ELSE
      SS=SS4*(SS0/ABS(SS0))
      ENDIF
      PR=(PR+SS*(YAO/RBA+EPA))*L/DCOS(EPA)
      THL=THL+PR
      X=X-DX
551   CONTINUE
      THL2=THL*DX/(3.0E6)
560   THL=0.0
      PR=0.0
      XR=X2
      X=XR
      DX=(X2-XN)/(N3-1)
      DO 651 J=1,N3
      CALL FUNC(YAO,YBO,XR,X,C,DHO,SS0,EPA,EPB,NITR,Q,Q1,XPO)
      Q1=Q
      IF(Q .GE. (1/ALP)) THEN
      PR=-(DLOG(1.0D-100))/ALP
      ELSE
      PR=-(DLOG(1-ALP*Q))/ALP
      ENDIF
      L=1
      IF(J .EQ. 1) GOTO 640
      XR=XR-DX
      IF(J .EQ. N3) GOTO 640
      DIFF=J/2.0-INT(J/2)
      IF(ABS(DIFF) .LT. 0.1) THEN
      L=4
      ELSE
      L=2
      ENDIF
```

```
640     SS1=SS0*EXP(ALP*PR)
        SS2=1.0E9/(4*7.5*(2.52+0.25*TEMP))
        SS3=0.3*PR/(2.52+0.024*TEMP) - 0.25E8
        IF(SS3 .LE. SS2) THEN
        SS4=SS2
        ELSE
        SS4=SS3
        ENDIF
        IF(SS4 .GT. ABS(SS1)) THEN
        SS=SS1
        ELSE
        SS=SS4*(SS0/ABS(SS0))
        ENDIF
        PR=(PR+SS*(YAO/RBA+EPA))*L/DCOS(EPA)
        THL=THL+PR
        X=X-DX
651     CONTINUE
        THL3=THL*DX/(3.0E6)
        TLD=THL1+THL2+THL3
        IF(TLD .LT. 0.0) TLD=0.0
655     RETURN
        END
```

APPENDIX IV

```
C     PROGRAM TO ANALYSE THE TRANSIENT BEHAVIOUR OF THE OIL FILM BETWEEN
C     A PAIR OF SPUR GEAR TEETH FOR A STEP CHANGE IN LOAD
      COMMON  /DCNS/RRA,RCA,LA,GNA,CBA,CSA,CNA,C11A,C12A,C22A,CH,V
     1,RRB,RCB,LB,GNB,CBB,CSB,CNB,C11B,C12B,C22B,INVPSY,CBT
      COMMON /ALL/RBA,ROA,RBB,ROB,YY,WA,M,PANG,DT,PI
      COMMON /OIL/DYAO,VISCT,RBTA,MRBTA,TO,ALP,TM,BET
      COMMON /VCNS/ERFX
      COMMON /VCNS2/DELHO
      COMMON /VCNS3/DEL
      CHARACTER*12 RESFN
      REAL IA,IB,INVPSY,INVR,L,LA,LB,LT,KA1,KB1,KO1,KA2,KB2,KO2,M,
     1MA,MB,MAB,MRBTA,NA
      REAL*8 COMP1,DHO1,HO,HO1,HO2,X,X1,XMN,XMX,XPO,YA,YB,YAO,YBO
     1,YAO1,YBO1,YAON,YMA
      INTEGER TA,TB,DP
      DATA SY/20./,FWG/1.0/,FWT/1.0/,E/2.068E5/,GOIL/5000./,G/8.273E4/
      WRITE(*,10) '   NO. OF TEETH - GEAR - A        : '
      READ(*,90) TA
      WRITE(*,10) '   NO. OF TEETH - GEAR - B        : '
      READ(*,90) TB
      WRITE(*,10) '   DIAMETRAL PITCH                : '
      READ(*,90) DP
      WRITE(*,10) '   SPEED OF GEAR  A  (rpm)        : '
      READ(*,30) NA
      WRITE(*,10) '   FO - STEADY STATE  (N/mm)      : '
      READ(*,40) FOSS
      WRITE(*,10) '   VISCOSITY (Ns/m2)              : '
      READ(*,40) VISC
      WRITE(*,10)' NAME OF FILE TO STORE RESULTS  : '
      READ(*,20) RESFN
      OPEN(4,FILE=RESFN,STATUS='NEW')
C     DATA PTS./CYCLE
100   NDAT=70
C     STEP INPUT
      EX=1.1
      FO=FOSS
C  SYSTEM PARAMETERS
      GOTO 295
200   ALP=2.32E-8
      DYAO=DYAR
      YAR=YOPH
      RBTA=RBA*TAN(PANG)
      MRBTA=(M+1)*RBTA
      MAB=(MA+MB)/MB
      RAD=YOMX*(YY-YOMX)/YY
      CERFX=E/(2*PI*RAD*(1-V**2))
      ERFX=10.0*SQRT(FO*CERFX)
      ERAL=FO*1.0E-3
C  VISCOSITY IN Ns/m2
      BET=3890.0
      TM=90.0+273
```

```
      TO=30.0+273
      VISCT=VISC*EXP(BET*(1.0/TM - 1.0/TO))
C  VISCOSITY/PRESSURE COEFFICIENT
      Y=0.8
      PP=200.0
      D=2.15
      ALCON=1.0E-6*Y/PP
      ALP=ALCON*(ALOG(VISCT*1.0E3+0.5)+D)
      DHO1=0.0
      F1=EX*FOSS
      FO=FOSS
      YAO1=YAR
C  OIL FILM THICKNESS `GRUBIN' FORMULA
210   RA=YAO1
      RB=YY-YAO1
      R=RA*RB/(RA+RB)
      UA=RA*WA
      UB=RB*WA*M
      U1=(UA+UB)/2
      U=VISCT*U1/(EV*R*1E6)
      W=F1/(EV*R)
      H=1.95*(GOIL*U)**0.727/(W**0.091)
      HO=H*R
      HO1=HO
      DELHO=HO/5.0
      DEL=(VISC/0.1)**0.4*(NA/3000.)**0.25*(1./FO)
      CALL OFTH(YAO1,HO1,F1,DHO1,ERAL)
C   INITIAL MESH STIFFNESS
215   CALL STIF1(YAO1,HO1,F1,COMP1,KO1,KA1,KB1)
      YMA=(COMP1-HO1)/MAB
      YAON=YAR+YMA-F1/KA1
      IF(DABS(YAO1-YAON) .GT. 1.0E-6) THEN
      YAO1=YAON
      GOTO 215
      ELSE
      YAO1=YAON
      ENDIF
      FREQ=(SQRT(KO1*1E3*MAB/MA))/(2.*PI)
      ICNT=0
      ITME=0
      ILMT=INT(NDAT/35)
      DT=1.0/(NDAT*FREQ)
      T=0.0
      TMAX=5.0/FREQ
      WRITE(4,80)TA,TB,DP,FO,NA,VISCT,R
      WRITE(*,80)TA,TB,DP,FO,NA,VISCT,R
      DYAO=(DYMA*((KA1/KB1)-(MA/MB))-DHO1)*KB1/(KA1+KB1) + DYAR
220   CALL INTGR(MA,MB,YAO1,YMA,DYMA,F1,KO1,DYAO,FO,COMP1,HO1
     1,DHO1)
      HO1=HO1+DT*DHO1
227   COMP1=YMA*MAB+HO1
      CALL  MESH(YAO1,HO1,F1,COMP1,KO1,KA1,KB1)
      CALL SURF1(YAO1,YAR,YMA,KA1,F1)
      YBO1=YAO1+HO1
      IF (F1 .LE. 0.0) THEN
```

```
      DHO1=-DYMA*MAB
      DYAO=DYAR+DYMA
      GOTO 245
      ENDIF
240   DYAO=(DYMA*((KA1/KB1)-(MA/MB))-DHO1)*KB1/(KA1+KB1) + DYAR
      CALL DOFT(YAO1,HO1,F1,DHO1,ERAL)
245   IF(ICNT .LE. ILMT) GOTO 250
      WRITE(*,76)T,YMA,KO1,DHO1,HO1,F1
      WRITE(4,75)T,YMA,KO1,DHO1,HO1,F1
      ICNT=0
250   ICNT=ICNT+1
      IF(ITME .GE. 1) GOTO 260
      IF(HO2 .LE. HO1) GOTO 255
      TMAX=4.07*T
      ITME=1
255   HO2=HO1
260   IF(T .GE. TMAX)GOTO 290
      T=T+DT
      GOTO 220
290   WRITE(*,85)YAR,YAO1,YMA,DYMA,HO1,F1,KO1
      CLOSE(4)
291   GOTO 300
10    FORMAT(A\)
20    FORMAT(A)
30    FORMAT(F9.3)
40    FORMAT(F10.7)
75    FORMAT(F10.7,4E13.5,F9.4\)
76    FORMAT(F10.7,4E13.5,F9.4)
80    FORMAT(3I4,4E15.6)
85    FORMAT(7E17.8)
90    FORMAT(I4)
C  SYSTEM PARAMETERS
295   PI=3.14159
      V=0.3
      WA=2*PI*NA/60
      PSY=SY*PI/180
      INVPSY=TAN(PSY) - PSY
      RCA=TA*25.4/(2*DP)
      RCB=TB*25.4/(2*DP)
      CD=RCA+RCB
      RBA=RCA*COS(PSY)
      RBB=RCB*COS(PSY)
      ROA=((TA+2)*25.4+ACA*TAN(PSY))/(2*DP)
      ROB=((TB+2)*25.4+ACB*TAN(PSY))/(2*DP)
      RRA=(TA-2.5)*25.4/(2*DP)
      RRB=(TB-2.5)*25.4/(2*DP)
      DYAR=RBA*WA
      DYMA=0.0
      PO=2*PI*RBA/TA
      YY=SQRT(CD**2-(RBA+RBB)**2)
      YOMN=YY-SQRT(ROB**2-RBB**2)
      PANG=ATAN(YY/(RBA+RBB))
      YOPH=RBA*TAN(PANG)
      YOMX=SQRT(ROA**2-RBA**2)
      IA=PI*FWG*RCA**4*7.759E-6/2
```

```
      IB=PI*FWG*RCB**4*7.759E-6/2
      MA=IA/RBA**2
      MB=IB/RBB**2
      M=1.0*TA/TB
      E1=(1-V**2)/E
      EV=1/E1
      L=2.25*25.4/DP
      GNA=PI*25.4/(2*DP) +2*ACA*TAN(PSY)
      GNB=PI*25.4/(2*DP) +2*ACB*TAN(PSY)
      IF(RRA .LT. RBA) THEN
      R=RBA
      ELSE
      R=RRA
      ENDIF
      CALL THICK(R,RBA,INVPSY,GNA,RCA,HRA,RI)
      IF(RRB .LT. RBB) THEN
      R=RBB
      ELSE
      R=RRB
      ENDIF
      CALL THICK(R,RBB,INVPSY,GNB,RCB,HRB,RI)
      CALL THICK(ROA,RBA,INVPSY,GNA,RCA,HOA,RI)
      CALL THICK(ROB,RBB,INVPSY,GNB,RCB,HOB,RI)
      LA=L/(1-(HOA/HRA)**2)
      LB=L/(1-(HOB/HRB)**2)
C     CONSTANTS FOR SHEAR DEFLN. `A'  AND `B'
      CSA=(2.4*SQRT(LA))/(G*HRA)
      CSB=(2.4*SQRT(LB))/(G*HRB)
C     CONSTANTS FOR DEFLN. DUE TO NORMAL LOAD `A' AND `B'
      CNA=(2*SQRT(LA))/(E*HRA)
      CNB=(2*SQRT(LB))/(E*HRB)
C     CONSTANTS FOR BENDING DEFLN. `A' AND `B'
      CBA=8.0*LA/(E*HRA**3)
      CBB=8.0*LB/(E*HRB**3)
C     CONSTANTS FOR HERTZ DEFLN. `A' AND `B'
      CH=2.0/(PI*EV)
C     CONST. FOR HERTZ CONTACT WIDTH `BT'
      CBT=SQRT(8.0/(PI*EV))
C     CONSTANTS FOR DEFLN. OF BODY
      C11A=9/(PI*EV*HRA**2)
      C11B=9/(PI*EV*HRB**2)
      C12A=(1+V)*(1-2*V)/(2*E*HRA)
      C12B=(1+V)*(1-2*V)/(2*E*HRB)
      C22A=2.4/(PI*EV)
      C22B=2.4/(PI*EV)
      GOTO 200
300   END
C     INVOLUTE FUNCTION
      SUBROUTINE INV(R,RB,INVR)
      REAL INVR
      ALPA=ATAN(SQRT((R**2-RB**2)/RB**2))
      INVR=TAN(ALPA)-ALPA
      RETURN
      END
C     TOOTH THICKNESS
```

```
      SUBROUTINE THICK(R,RB,INVPSY,GN,RC,HC,RI)
      REAL INVPSY,INVR
      CALL INV(R,RB,INVR)
      G2R=(GN/(2*RC)) + INVPSY - INVR
      HC=2*R*SIN(G2R)
      RI=R*COS(G2R)
      RETURN
      END
C  SUBROUTINE TO CALCULATE 'YAO1'
      SUBROUTINE SURF1(YAO,YAR,YMA,KA,F)
      REAL*8 YAO,YMA
      REAL KA
      IF(KA .LE. 0.0) THEN
      YAO=YAR+YMA
      ELSE
      YAO=YAR+YMA-F/KA
      ENDIF
      RETURN
      END
C  TOOTH STIFFNESS - INITIAL
      SUBROUTINE STIF1(YAO,HO,FI,COMP,KO,KA,KB)
      COMMON  /DCNS/RRA,RCA,LA,GNA,CBA,CSA,CNA,C11A,C12A,C22A,CH,V
     1,RRB,RCB,LB,GNB,CBB,CSB,CNB,C11B,C12B,C22B,INVPSY,CBT
      COMMON /ALL/RBA,ROA,RBB,ROB,YY,WA,M,PANG,DT,PI
      REAL*8 EPA,EPB,YAO,YBO,HO,DHO,COMP
      REAL LA,LB,KO,KA,KB,INVPSY,LCA,LCB
      IF (FI .LE. 0.0) THEN
      COMP=0.0
      KO=0.0
      KA=0.0
      KB=0.0
      GOTO 2050
      ENDIF
      YBO=YAO+HO
      YYBO=YY-YBO
2000  R=DSQRT(YAO**2+RBA**2)
      CALL THICK(R,RBA,INVPSY,GNA,RCA,HCA,RI)
      ALPA=DATAN(YAO/RBA)-ATAN(HCA/(2*RI))
      HA=HCA/(2*COS(ALPA))
      YP=RBA/COS(ALPA)-SQRT(RRA**2-(HRA/2)**2)
      LCA=LA-YP
      AK=CBA*(COS(ALPA))**2*(LA**2-6*LCA*LA-3*LCA**2+8*LCA**1.5*LA**.5)
      C2SA=CSA*(COS(ALPA))**2*(SQRT(LA)-SQRT(LCA))
      C2NA=CNA*(SIN(ALPA))**2*(SQRT(LA)-SQRT(LCA))
      CDA=C11A*YP**2+2*C12A*YP+C22A*(1+((TAN(ALPA))**2)/3.1)
      C2DA=2*(COS(ALPA))**2*CDA
      R=SQRT(YYBO**2+RBB**2)
      CALL THICK(R,RBB,INVPSY,GNB,RCB,HCB,RI)
      ALPA=ATAN(YYBO/RBB)-ATAN(HCB/(2*RI))
      HB=HCB/(2*COS(ALPA))
      YP=RBB/COS(ALPA)-SQRT(RRB**2-(HRB/2)**2)
      LCB=LB-YP
      BK=CBB*(COS(ALPA))**2*(LB**2-6*LCB*LB-3*LCB**2+8*LCB**1.5*LB**.5)
      C2SB=CSB*(COS(ALPA))**2*(SQRT(LB)-SQRT(LCB))
      C2NB=CNB*(SIN(ALPA))**2*(SQRT(LB)-SQRT(LCB))
```

```
      CDB=C11B*YP**2+2*C12*YP+C22B*(1+((TAN(ALPA))**2/3.1))
      C2DB=2*(COS(ALPA))**2*CDB
2010  BT= CBT*DSQRT((FI*YAO*YYBO)/(YAO+YYBO))
      ZHA=FI*CH*(ALOG(2*HA/BT) - V/((1-V)*2))
      ZHB=FI*CH*(ALOG(2*HB/BT) - V/((1-V)*2))
      ZA=FI*(C2SA+C2NA+C2DA+AK)
      ZB=FI*(C2SB+C2NB+C2DB+BK)
      COMPA=(ZHA+ZA)
      COMPB=(ZHB+ZB)
      COMP=COMPA+COMPB
      KA=FI/COMPA
      KB=FI/COMPB
      KO=FI/COMP
2050  RETURN
      END
C  MESH  STIFFNESS AND TOOTH LOAD
      SUBROUTINE MESH(YAO,HO,FI,COMP,KO,KA,KB)
      COMMON  /DCNS/RRA,RCA,LA,GNA,CBA,CSA,CNA,C11A,C12A,C22A,CH,V
     1,RRB,RCB,LB,GNB,CBB,CSB,CNB,C11B,C12B,C22B,INVPSY,CBT
      COMMON /ALL/RBA,ROA,RBB,ROB,YY,WA,M,PANG,DT,PI
      REAL*8 EPA,EPB,YAO,YBO,HO,DHO,COMP
      REAL LA,LB,KO,KA,KB,INVPSY,LCA,LCB
      YBO=YAO+HO
      YYBO=YY-YBO
      IF (COMP .LE. 0.0) THEN
      COMP=0.0
      FI=0.0
      KO=0.0
      KA=0.0
      KB=0.0
      GOTO 2050
      ENDIF
      IF (FI .GT. 0.0) GOTO 2000
      FI=0.001
2000  R=DSQRT(YAO**2+RBA**2)
      CALL THICK(R,RBA,INVPSY,GNA,RCA,HCA,RI)
      ALPA=DATAN(YAO/RBA)-ATAN(HCA/(2*RI))
      HA=HCA/(2*COS(ALPA))
      YP=RBA/COS(ALPA)-SQRT(RRA**2-(HRA/2)**2)
      LCA=LA-YP
      AK=CBA*(COS(ALPA))**2*(LA**2-6*LCA*LA-3*LCA**2+8*LCA**1.5*LA**.5)
      C2SA=CSA*(COS(ALPA))**2*(SQRT(LA)-SQRT(LCA))
      C2NA=CNA*(SIN(ALPA))**2*(SQRT(LA)-SQRT(LCA))
      CDA=C11A*YP**2+2*C12A*YP+C22A*(1+((TAN(ALPA))**2)/3.1)
      C2DA=2*(COS(ALPA))**2*CDA
      R=SQRT(YYBO**2+RBB**2)
      CALL THICK(R,RBB,INVPSY,GNB,RCB,HCB,RI)
      ALPA=ATAN(YYBO/RBB)-ATAN(HCB/(2*RI))
      HB=HCB/(2*COS(ALPA))
      YP=RBB/COS(ALPA)-SQRT(RRB**2-(HRB/2)**2)
      LCB=LB-YP
      BK=CBB*(COS(ALPA))**2*(LB**2-6*LCB*LB-3*LCB**2+8*LCB**1.5*LB**.5)
      C2SB=CSB*(COS(ALPA))**2*(SQRT(LB)-SQRT(LCB))
      C2NB=CNB*(SIN(ALPA))**2*(SQRT(LB)-SQRT(LCB))
      CDB=C11B*YP**2+2*C12*YP+C22B*(1+((TAN(ALPA))**2/3.1))
```

```
      C2DB=2*(COS(ALPA))**2*CDB
      DZB=AK+BK
      DZS=C2SA+C2SB
      DZN=C2NA+C2NB
      DZD=C2DA+C2DB
2010  BT= CBT*DSQRT((FI*YAO*YYBO)/(YAO+YYBO))
      DBT=(BT)/(2*FI)
      ZHA=FI*CH*(ALOG(2*HA/BT) - V/((1-V)*2))
      ZHB=FI*CH*(ALOG(2*HB/BT) - V/((1-V)*2))
      ZSA=FI*C2SA
      ZSB=FI*C2SB
      ZNA=FI*C2NA
      ZNB=FI*C2NB
      ZBA=FI*AK
      ZBB=FI*BK
      ZDA=FI*C2DA
      ZDB=FI*C2DB
      DZHA=ZHA/FI - CH/2
      DZHB=ZHB/FI - CH/2
      FF =ZHA+ZHB+ZSA+ZSB+ZNA+ZNB+ZBA+ZBB+ZDA+ZDB-COMP
      DFF=DZHA+DZHB+DZS+DZN+DZB+DZD
      FI1=FI - FF/DFF
      IF (ABS(FI1-FI) .LE. 0.01) GOTO 2020
      IF (FI1 .LE. 0.0) THEN
      FI=FI/2
      ELSE
      FI=FI1
      ENDIF
      GOTO 2010
2020  FI=FI1
      COMPA=(ZHA+ZBA+ZSA+ZNA+ZDA)
      COMPB=(ZHB+ZBB+ZSB+ZNB+ZDB)
      KA=FI/COMPA
      KB=FI/COMPB
      KO=FI/COMP
2050  RETURN
      END
C     RUNGE-KUTTA (4th. order) INTEGRATION
      SUBROUTINE INTGR(MA,MB,YAO1,YMA,DYMA,F1,KO1,DYAO1,FO,COMP1,HO1
     1,DHO1)
      COMMON /ALL/RBA,ROA,RBB,ROB,YY,WA,M,PANG,DT,PI
      REAL*8 YAO1,YAO1DT,HO1,HO1DT,DHO1,CMP1DT,YMA
      REAL MA,MB,MAB,KO1,KO1DT,KA1DT,KB1DT,KKDT
      MAB=(MA+MB)/MB
C     VALUES OF HO,COMP AND KO AFTER TIME DT/2
      HO1DT=HO1+DHO1*DT/2
      YAO1DT=YAO1+DYAO1*DT/2
      CALL STIF1(YAO1DT,HO1DT,F1,CMP1DT,KO1DT,KA1DT,KB1DT)
      HO2DT=HO2+DHO2*DT/2
      KKDT=KO1DT*MAB
      HKDT=HO1DT*KO1DT-FO
      HK=HO1*KO1-FO
      CY0=DYMA
      CV0=-(1.0E3/MA)*(YMA*KO1*MAB+HK)
      CY1=DYMA+CV0*DT/2
```

```
      CV1=-(1.0E3/MA)*((YMA+CY0*DT/2)*KKDT+HKDT)
      CY2=DYMA+CV1*DT/2
      CV2=-(1.0E3/MA)*((YMA+CY1*DT/2)*KKDT+HKDT)
      CY3=DYMA+CV2*DT/2
      CV3=-(1.0E3/MA)*((YMA+CY2*DT/2)*KKDT+HKDT)
      YMA=YMA+(CY0+2*CY1+2*CY2+CY3)*DT/6
      DYMA=DYMA+(CV0+2*CV1+2*CV2+CV3)*DT/6
      RETURN
      END
C     TO CALCULATE `YA' FOR ANY X
      SUBROUTINE DISA(RBA,YAO,X,YA,E)
      REAL*8 X,YA,E,E2,FE,DFE,THA,DE,BETA,YAO
      IF (X .EQ. 0.0) THEN
      YA=YAO
      GOTO 1420
      ENDIF
      E=DATAN(X/YAO)
      BETA=YAO/RBA
1400  FE=E-(RBA+X-RBA*DCOS(E))/(RBA*DSIN(E))+BETA
      DFE=1+(((RBA+X)*DCOS(E))/RBA-1.)/(DSIN(E))**2
      E2=E-(FE/DFE)
      DE=DABS(E2-E)
      IF(DE .LE. 0.000001) GOTO 1410
      E=E2
      GOTO 1400
1410  E=E2
      THA=DATAN(BETA+E) - E
      YA=(RBA+X)*DTAN(THA)
1420  RETURN
      END
C     TO CALCULATE `YB' FOR ANY X
      SUBROUTINE DISB(YY,RBB,YBO,X,YB,E)
      REAL*8 X,YB,E,THA,E2,FE,DFE,DE,YBO,BETA
      IF (X .EQ. 0.0) THEN
      YB=YBO
      GOTO 1470
      ENDIF
      E=DATAN(X/(YY-YBO))
      BETA=(YY-YBO)/RBB
1450  FE=E-(RBB-X-RBB*DCOS(E))/(RBB*DSIN(E))-BETA
      DFE=1+(((RBB-X)*DCOS(E))/RBB-1.)/(DSIN(E))**2
      E2=E-(FE/DFE)
      DE=DABS(E2-E)
      IF(DE .LE. 0.000001) GOTO 1460
      E=E2
      GOTO 1450
1460  E=E2
      THA=DATAN(BETA-E) + E
      YB=YY-(RBB-X)*DTAN(THA)
1470  RETURN
      END
C  SUBROUTINE TO CALCULATE `HO' FOR A GIVEN FORCE
      SUBROUTINE OFTH(YAO,HO,FI,DHO,ERAL)
      COMMON /OIL/DYAO,VISCT,RBTA,MRBTA,TO,ALP,TM,BET
      COMMON /ALL/RBA,ROA,RBB,ROB,YY,WA,M,PANG,DT,PI
```

```
      COMMON /VCNS/ERFX
      COMMON /VCNS2/DEL
      REAL NA,M,LT,INVPSY,INVR,MRBTA
      REAL*8 X,X1,XMX,XPO,XPON1,XPON2,XPON3,YA,YB,EPA,EPB,C,Q,Q1
     1,YAO,YBO,HO,DHO,XMN,HON1,HOL,HOR,HOH
      FN1=0.0
      ITR4=1
      ITR5=1
      SQFI=SQRT(FI)
1200  FIN1=0.0
      FNL=0.0
      FNR=0.0
      HOH=0.0
1205  YBO=YAO+HO
      CALL OFLM(YAO,YBO,HO,DHO,FI,XPO,C,XMX,XMN)
1210  CALL FORCE(YAO,YBO,XMX,XPO,C,FIN,DHO)
      WRITE(*,111)HO,FIN
111   FORMAT(2E17.8)
      FN=FI-FIN
      IF(ABS(FN) .LE. ERAL) GOTO 1250
      IF(FNL*FNR .LT. 0.0) GOTO 1240
      IF(FN1*FN .LT. 0.0) GOTO 1235
1220  FIN1=FIN
      HON1=HO
      FN1=FN
      IF(FN1 .GT. 0.0) THEN
      HO=HON1-DEL
      ELSE
      HO=HON1+DEL
      ENDIF
      IF(HO .LT. HOH) HO=(HOH+HON1)/2.0
      GOTO 1205
1226  HO=HO+DEL
      GOTO 1205
1235  FNL=FN1
      FNR=FN
      SQFNL=SQRT(FI-FN1)-SQFI
      SQFNR=SQRT(FIN)-SQFI
      HOL=HON1
      HOR=HO
      GOTO 1245
1240  IF(FNL*FN)1241,1241,1242
1241  HOR=HO
      FNR=FN
      SQFNR=SQRT(FIN)-SQFI
      GOTO 1245
1242  HOL=HO
      FNL=FN
      SQFNL=SQRT(FIN)-SQFI
1245  IF(ITR4 .GT. 3)THEN
      HO=(HOL+HOR)/2.0
      ITR4=1
      ELSE
      HO=HOL-SQFNL*(HOL-HOR)/(SQFNL-SQFNR)
      ITR4=ITR4+1
```

```
      ENDIF
      IF(DABS(HOL-HOR) .LE. 0.1E-8)GOTO 1250
      GOTO 1205
1250  RETURN
      END
C  SUBROUTINE TO CALCULATE 'DHO' FOR A GIVEN FORCE
      SUBROUTINE DOFT(YAO,HO,FI,DHO,ERAL)
      COMMON /OIL/DYAO,VISCT,RBTA,MRBTA,TO,ALP,TM,BET
      COMMON /ALL/RBA,ROA,RBB,ROB,YY,WA,M,PANG,DT,PI
      COMMON /VCNS/ERFX
      COMMON /VCNS3/DEL
      REAL NA,M,LT,INVPSY,INVR,MRBTA
      REAL*8 X,X1,XMX,XPO,XPON1,XPON2,XPON3,YA,YB,EPA,EPB,C,Q,Q1
     1,YAO,YBO,HO,DHO,XMN
      DHON1=DHO
      YBO=YAO+HO
      FN1=0.0
      ITR4=1
      ITR5=1
      SQFI=SQRT(FI)
1200  FIN1=0.0
      FNL=0.0
      FNR=0.0
1205  CALL OFLM(YAO,YBO,HO,DHO,FI,XPO,C,XMX,XMN)
1210  CALL FORCE(YAO,YBO,XMX,XPO,C,FIN,DHO)
      FN=FI-FIN
      IF(ABS(FN) .LE. ERAL) GOTO 1250
      IF(FNL*FNR .LT. 0.0) GOTO 1240
      IF(FIN1 .NE. 0.0) GOTO 1220
      FIN1=FIN
      DHON1=DHO
      FN1=FN
      IF(FN1 .GT. 0.0) THEN
      DHO=DHON1-DEL
      ELSE
      DHO=DHON1+DEL
      ENDIF
      GOTO 1205
1220  IF(FN1*FN .LT. 0.0) GOTO 1235
      DHON1=DHO
      FN1=FN
      IF(FN1 .GT. 0.0)THEN
      DHO=DHO-ITR5*DEL
      ELSE
      DHO=DHO+ITR5*DEL
      ENDIF
      ITR5=ITR5+1
      GOTO 1205
1235  FNL=FN1
      FNR=FN
      SQFNL=SQRT(FI-FN1)-SQFI
      SQFNR=SQRT(FIN)-SQFI
      DHOL=DHON1
      DHOR=DHO
      GOTO 1245
```

```
1240   IF(FNL*FN)1241,1241,1242
1241   DHOR=DHO
       FNR=FN
       SQFNR=SQRT(FIN)-SQFI
       GOTO 1245
1242   DHOL=DHO
       FNL=FN
       SQFNL=SQRT(FIN)-SQFI
1245   IF(ITR4 .GT. 3)THEN
       DHO=(DHOL+DHOR)/2.0
       ITR4=1
       ELSE
       DHO=DHOL-SQFNL*(DHOL-DHOR)/(SQFNL-SQFNR)
       ITR4=ITR4+1
       ENDIF
       IF(ABS(DHOL-DHOR) .LE. 0.1E-5)GOTO 1250
       GOTO 1205
1250   RETURN
       END
C  SUBROUTINE TO FIND `XPO'
       SUBROUTINE OFLM(YAO,YBO,HO,DHO,FI,XPO,C,XMX,XMN)
       COMMON /OIL/DYAO,VISCT,RBTA,MRBTA,TO,ALP,TM,BET
       COMMON /ALL/RBA,ROA,RBB,ROB,YY,WA,M,PANG,DT,PI
       COMMON /VCNS/ERFX
       REAL NA,M,LT,INVPSY,INVR,MRBTA
       REAL*8 X,X1,XMX,XPO,XPON1,XPON2,XPON3,YA,YB,EPA,EPB,C,Q,Q1
      1,YAO,YBO,HO,DHO,XMN
       CALL LMTS(RBA,RBB,ROA,RBB,YY,YAO,YBO,XM)
       XMX=XM
       CALL LMTS(RBA,RBB,RBA,ROB,YY,YAO,YBO,XM)
       XMN=XM
       FXN1=0.0
       DX=(XMX-XMN)
       IF((XMX-DX/50) .LE. 0.0) THEN
       XPON1=XMX-DX/500
       ELSE
       XPON1=XMN
       ENDIF
       ITR1=0
       ITR2=0
       ITR3=0
       CALL CONS(YAO,YBO,XPON1,DHO,C,EPA,EPB)
       CALL FUNC1(YAO,YBO,XMX,XPON1,FXN1,C,DHO,EPA,EPB)
       FXN2=0.0
       IF(XMN)1,5,5
1      IF(XMX-DX/50)2,2,3
2      IF(FXN1 .LE. 0.0) GOTO 1337
       DX=-DX/500
       GOTO 6
3      IF(FXN1)4,4,1335
4      DX=DX/50
       XPON2=0.0
       GOTO 1300
5      IF(FXN1)1337,1335,1335
6      XPON2=XPON1+DX
```

```
1300  CALL CONS(YAO,YBO,XPON2,DHO,C,EPA,EPB)
      CALL FUNC1(YAO,YBO,XMX,XPON2,FXN2,C,DHO,EPA,EPB)
      IF(FXN1*FXN2)1317,1316,1316
1316  XPON1=XPON2
      FXN1=FXN2
      XPON2=XPON2+DX
      IF(XPON2 .GE. XMX) GOTO 1337
      IF(XPON2 .LE. XMN) GOTO 1335
      GOTO 1300
1317  FSQ1=(ABS(FXN1)/FXN1)*SQRT(ABS(FXN1))
      FSQ2=(ABS(FXN2)/FXN2)*SQRT(ABS(FXN2))
1320  XPON3=XPON1+(FSQ1*(XPON2-XPON1))/(FSQ1-FSQ2)
1321  ITR2=ITR2+1
      IF(ITR2 .GT. 50) GOTO 1340
1322  CALL CONS(YAO,YBO,XPON3,DHO,C,EPA,EPB)
      CALL FUNC1(YAO,YBO,XMX,XPON3,FXN3,C,DHO,EPA,EPB)
      IF(DABS(XPON2-XPON1) .LT. 1.D-5) GOTO 1345
      IF(ABS(FXN3) .LT. ERFX) GOTO 1345
1325  IF(ITR3 .GE. 15) GOTO 1331
      ITR3=ITR3+1
      IF(FXN3*FXN1)1326,1326,1327
1326  XPON2=XPON3
      FXN2=FXN3
      GOTO 1328
1327  XPON1=XPON3
      FXN1=FXN3
      GOTO 1328
1328  IF(DABS(XPON1-XPON2) .GT. 0.01)GOTO 1317
      XPON3=XPON2-FXN2*(XPON2-XPON1)/(FXN2-FXN1)
      GOTO 1321
1331  IF(FXN3*FXN1)1332,1332,1333
1332  XPON2=XPON3
      XPON3=(XPON1+XPON2)/2
      GOTO 1322
1333  XPON1=XPON3
      XPON3=(XPON1+XPON2)/2
      GOTO 1322
1335  CALL ALTC(YAO,YBO,XMX,XMN,DHO,C)
      XPO=XMN
      GOTO 1350
1337  XPO=XMX
      GOTO 1350
1340  WRITE(*,1341)'* FXAP CONVERGENCE ERROR * '
1341  FORMAT(A)
1345  FX=FXN3
      XPO=XPON3
1350  RETURN
      END
C     TO FIND THE MAXM. AND MINM. X VALUES
      SUBROUTINE LMTS(RBA,RBB,RA,RB,YY,YAO,YBO,XM)
      REAL*8 YAO,YBO
      BETA=YAO/RBA
      E=ACOS(RBA/RA)
      THA=BETA-TAN(E)+E
      XAM=RA*COS(THA)-RBA
```

```
      BETA=(YY-YBO)/RBB
      E=ACOS(RBB/RB)
      THA=BETA-TAN(E)+E
      XBM=RBB-RB*COS(THA)
      DXM=ABS(XAM)-ABS(XBM)
      IF(DXM .LE. 0.0) THEN
      XM=XAM
      ELSE
      XM=XBM
      ENDIF
      RETURN
      END
C     TO CALCULATE THE CONSTANT - C -
      SUBROUTINE CONS(YAO,YBO,X,DHO,CX,EPA,EPB)
      COMMON /OIL/DYAO,VISCT,RBTA,MRBTA,TO,ALP,TM,BET
      COMMON /ALL/RBA,ROA,RBB,ROB,YY,WA,M,PANG,DT,PI
      REAL M,MRBTA
      REAL*8 X,YA,YB,EPA,EPB,CX,FC,YAO,YBO,HO,DHO
      CALL DISA(RBA,YAO,X,YA,EPA)
      CALL DISB(YY,RBB,YBO,X,YB,EPB)
      FC=DHO*(MRBTA*(YA+YB)-M*(YA*YB+X**2)+2*RBA*X)
      CX=DYAO*(M+1)*(X**2+YA*YB-RBTA*(YA+YB))-FC
      RETURN
      END
C  TO CALCULATE 'C' AT THE BEGINNING OF CONTACT
      SUBROUTINE ALTC(YAO,YBO,XMX,XN,DHO,C)
      COMMON /OIL/DYAO,VISCT,RBTA,MRBTA,TO,ALP,TM,BET
      COMMON /ALL/RBA,ROA,RBB,ROB,YY,WA,M,PANG,DT,PI
      COMMON /VCNS/ERFX
      REAL M,MRBTA
      REAL*8 XMX,X,DX,XN,C,YA,YB,EPA,EPB,F11,F22,F33,SF11,SF22,SF33,XPO
     1,DHO,YAO,YBO
      SF11=0.0
      SF22=0.0
      SF33=0.0
      N=121
      X=XMX
      DX=(XN-X)/(N-1)
      DO 1590 I=1,N
      CALL DISA(RBA,YAO,X,YA,EPA)
      CALL DISB(YY,RBB,YBO,X,YB,EPB)
      F11=DYAO*(M+1)*(RBTA*(YA+YB)-(YA*YB)-X**2)/((YB-YA)**3)
      F22=DHO*(MRBTA*(YA+YB)-M*(YA*YB+X**2)+2.*RBA*X)/((YB-YA)**3)
      F33=1.0/((YB-YA)**3)
      IF(I .EQ. 1) GOTO 1580
      IF(I .EQ. N) GOTO 1580
      DIFF=I/2.0-INT(I/2)
      IF(ABS(DIFF) .LT. 0.1) THEN
      L=4
      ELSE
      L=2
      ENDIF
      F11=F11*L
      F22=F22*L
      F33=F33*L
```

```
1580   SF11=SF11+F11
       SF22=SF22+F22
       SF33=SF33+F33
       X=X+DX
1590   CONTINUE
       C=-(SF11+SF22)/SF33
       RETURN
       END
C  PRESSURE FUNCTION
       SUBROUTINE FUNC1(YAO,YBO,XMX,XPO,FX,C,DHO,EPA,EPB)
       COMMON /OIL/DYAO,VISCT,RBTA,MRBTA,TO,ALP,TM,BET
       COMMON /ALL/RBA,ROA,RBB,ROB,YY,WA,M,PANG,DT,PI
       COMMON /VCNS/ERFX
       REAL NA,M,LT,INVPSY,INVR,MRBTA
       REAL*8 X,X1,XMX,XPO,YA,YB,EPA,EPB,C,Q,Q1,XPM,DHO,YAO,YBO
       Q1=0.0
       IF (FX .EQ. 0.0) GOTO 1500
       IF (ABS(FX) .GT. 0.1E7) GOTO 1500
       NITR1=11
       NITR2=21
       NITR3=121
       GOTO 1510
1500   NITR1=11
       NITR2=11
       NITR3=51
1510   IF (DABS(XPO) .LT. 0.005)THEN
       X=0.05
       GOTO 1520
       ENDIF
       X=5.*DABS(XPO)
1520   IF (X .GT. XMX) THEN
       X=XMX
       GOTO 1550
       ENDIF
       X1=3.*X
       IF (X1 .GT. XMX) THEN
       X1=XMX
       GOTO 1540
       ENDIF
1530   CALL FUNC2(YAO,YBO,XMX,X1,C,DHO,EPA,EPB,NITR1,Q,Q1,XPO)
       Q1=Q
1540   CALL FUNC2(YAO,YBO,X1,X,C,DHO,EPA,EPB,NITR2,Q,Q1,XPO)
       Q1=Q
1550   CALL FUNC2(YAO,YBO,X,XPO,C,DHO,EPA,EPB,NITR3,Q,Q1,XPO)
       FX=Q
       RETURN
       END
C  TO CALCULATE THE REDUCED PRESSURE (Q) AT ANY POINT
       SUBROUTINE FUNC2(YAO,YBO,XMX,XN,C,DHO,EPA,EPB,N,Q,Q1,XPO)
       COMMON /OIL/DYAO,VISCT,RBTA,MRBTA,TO,ALP,TM,BET
       COMMON /ALL/RBA,ROA,RBB,ROB,YY,WA,M,PANG,DT,PI
       COMMON /VCNS/ERFX
       REAL M,MRBTA
       REAL*8 XMX,X,DX,XN,C,YA,YB,EPA,EPB,F11,F22,FF,Q,Q1,EP2,XPO
      1,DHO,YAO,YBO
```

```
      FX=0.0
      X=XMX
      DX=(XN-X)/(N-1)
      DO 1590 I=1,N
      CALL DISA(RBA,YAO,X,YA,EPA)
      CALL DISB(YY,RBB,YBO,X,YB,EPB)
      F11=(M+1)*(RBTA*(YA+YB)-(YA*YB)-X**2)
      F22=MRBTA*(YA+YB)-M*(YA*YB+X**2)+2.*RBA*X
      FF=6*VISCT*(DYAO*F11+DHO*F22+C)/(RBA*(YB-YA)**3)
      DQX=FF
      IF(I .EQ. 1) GOTO 1580
      IF(I .EQ. N) GOTO 1580
      DIFF=I/2.0-INT(I/2)
      IF(ABS(DIFF) .LT. 0.1) THEN
      L=4
      ELSE
      L=2
      ENDIF
      FF=FF*L
1580  FX=FX+FF
      X=X+DX
1590  CONTINUE
      Q=FX*DX/3. + Q1
      RETURN
      END
C  TO CALCULATE THE PRESSURE AND SHEAR STRESS AT ANY POINT
      SUBROUTINE FUNC(YAO,YBO,XMX,XN,C,DHO,SS,EPA,EPB,N,Q,Q1,XPO)
      COMMON /OIL/DYAO,VISCT,RBTA,MRBTA,TO,ALP,TM,BET
      COMMON /ALL/RBA,ROA,RBB,ROB,YY,WA,M,PANG,DT,PI
      COMMON /VCNS/ERFX
      REAL M,MRBTA
      REAL*8 XMX,X,DX,XN,C,YA,YB,EPA,EPB,F11,F22,FF,Q,Q1,EP2,XPO
     1,DHO,YAO,YBO
      FX=0.0
      X=XMX
      DX=(XN-X)/(N-1)
      DO 1590 I=1,N
      CALL DISA(RBA,YAO,X,YA,EPA)
      CALL DISB(YY,RBB,YBO,X,YB,EPB)
      F11=(M+1)*(RBTA*(YA+YB)-(YA*YB)-X**2)
      F22=MRBTA*(YA+YB)-M*(YA*YB+X**2)+2.*RBA*X
      FF=6*VISCT*(DYAO*F11+DHO*F22+C)/(RBA*(YB-YA)**3)
      DQX=FF
      IF(I .EQ. 2) THEN
      L=4
      ELSE
      L=1
      ENDIF
      FF=FF*L
1580  FX=FX+FF
      X=X+DX
1590  CONTINUE
      Q=FX*DX/3. + Q1
      SF1=DQX*(YA-YB)/(2.*VISCT)
      SF2=WA*(YA+MRBTA-M*YB)/(2.*(YB-YA))
```

```
      SF3=DHO*(MRBTA-M*YB)/(RBA*(YA-YB))
      EP2=(DCOS(EPA))**2
      SS=VISCT*EP2*(SF1+SF2+SF3)
      RETURN
      END
C  TO CALCULATE THE FORCE
      SUBROUTINE FORCE(YAO,YBO,XMX,XN,C,TLD,DHO)
      COMMON /OIL/DYAO,VISCT,RBTA,MRBTA,TO,ALP,TM,BET
      COMMON /ALL/RBA,ROA,RBB,ROB,YY,WA,M,PANG,DT,PI
      COMMON /VCNS/ERFX
      REAL M,MRBTA
      REAL*8 XMX,X,X1,X2,XR,XN,DX,C,EPA,EPB,Q,Q1,XPO,DHO,YAO,YBO
      TEMP=TM-273.
      IF(XN .GE. (XMX-1.0E-6)) THEN
      TLD=0.0
      GOTO 655
      ENDIF
      XPO=XN
      N1=11
      N2=21
      N3=121
      NITR=3
      THL=0.0
      PR=0.0
      Q1=0.0
      SS=0.0
      XR=XMX
      IF (DABS(XN) .LE. 0.005) THEN
      X2=0.05
      ELSE
      X2=5.*DABS(XN)
      ENDIF
      IF(X2 .GE. XMX)THEN
      X2=XMX
      GOTO 560
      ENDIF
      X1=3.0*DABS(X2)
      IF(X1 .GE. XMX) THEN
      X1=XMX
      GOTO 460
      ENDIF
      DX=(XMX-X1)/(N1-1)
      X=XR
      DO 451 J=1,N1
      CALL FUNC(YAO,YBO,XR,X,C,DHO,SS0,EPA,EPB,NITR,Q,Q1,XPO)
      Q1=Q
      IF(Q .GE. (1/ALP)) THEN
      PR=-(DLOG(1.0D-100))/ALP
      ELSE
      PR=-(DLOG(1-ALP*Q))/ALP
      ENDIF
      L=1
      IF(J .EQ. 1) GOTO 440
      XR=XR-DX
      IF(J .EQ. N1) GOTO 440
```

```
      DIFF=J/2.0-INT(J/2)
      IF(ABS(DIFF) .LT. 0.1) THEN
      L=4
      ELSE
      L=2
      ENDIF
440   SS1=SS0*EXP(ALP*PR)
      SS2=1.0E9/(4*7.5*(2.52+0.25*TEMP))
      SS3=0.3*PR/(2.52+0.024*TEMP) - 0.25E8
      IF(SS3 .LE. SS2) THEN
      SS4=SS2
      ELSE
      SS4=SS3
      ENDIF
      IF(SS4 .GT. ABS(SS1)) THEN
      SS=SS1
      ELSE
      SS=SS4*(SS0/ABS(SS0))
      ENDIF
      PR=(PR+SS*(YAO/RBA+EPA))*L/DCOS(EPA)
      THL=THL+PR
      X=X-DX
451   CONTINUE
      THL1=THL*DX/3.0E6
460   THL=0.0
      PR=0.0
      XR=X1
      X=XR
      DX=(X1-X2)/(N2-1)
      DO 551 J=1,N2
      CALL FUNC(YAO,YBO,XR,X,C,DHO,SS0,EPA,EPB,NITR,Q,Q1,XPO)
      Q1=Q
      IF(Q .GE. (1/ALP)) THEN
      PR=-(DLOG(1.0D-100))/ALP
      ELSE
      PR=-(DLOG(1-ALP*Q))/ALP
      ENDIF
      L=1
      IF(J .EQ. 1) GOTO 540
      XR=XR-DX
      IF(J .EQ. N2) GOTO 540
      DIFF=J/2.0-INT(J/2)
      IF(ABS(DIFF) .LT. 0.1) THEN
      L=4
      ELSE
      L=2
      ENDIF
540   SS1=SS0*EXP(ALP*PR)
      SS2=1.0E9/(4*7.5*(2.52+0.25*TEMP))
      SS3=0.3*PR/(2.52+0.024*TEMP) - 0.25E8
      IF(SS3 .LE. SS2) THEN
      SS4=SS2
      ELSE
      SS4=SS3
      ENDIF
```

```
      IF(SS4 .GT. ABS(SS1)) THEN
      SS=SS1
      ELSE
      SS=SS4*(SS0/ABS(SS0))
      ENDIF
      PR=(PR+SS*(YAO/RBA+EPA))*L/DCOS(EPA)
      THL=THL+PR
      X=X-DX
551   CONTINUE
      THL2=THL*DX/(3.0E6)
560   THL=0.0
      PR=0.0
      XR=X2
      X=XR
      DX=(X2-XN)/(N3-1)
      DO 651 J=1,N3
      CALL FUNC(YAO,YBO,XR,X,C,DHO,SS0,EPA,EPB,NITR,Q,Q1,XPO)
      Q1=Q
      IF(Q .GE. (1/ALP)) THEN
      PR=-(DLOG(1.0D-100))/ALP
      ELSE
      PR=-(DLOG(1-ALP*Q))/ALP
      ENDIF
      L=1
      IF(J .EQ. 1) GOTO 640
      XR=XR-DX
      IF(J .EQ. N3) GOTO 640
      DIFF=J/2.0-INT(J/2)
      IF(ABS(DIFF) .LT. 0.1) THEN
      L=4
      ELSE
      L=2
      ENDIF
640   SS1=SS0*EXP(ALP*PR)
      SS2=1.0E9/(4*7.5*(2.52+0.25*TEMP))
      SS3=0.3*PR/(2.52+0.024*TEMP) - 0.25E8
      IF(SS3 .LE. SS2) THEN
      SS4=SS2
      ELSE
      SS4=SS3
      ENDIF
      IF(SS4 .GT. ABS(SS1)) THEN
      SS=SS1
      ELSE
      SS=SS4*(SS0/ABS(SS0))
      ENDIF
      PR=(PR+SS*(YAO/RBA+EPA))*L/DCOS(EPA)
      THL=THL+PR
      X=X-DX
651   CONTINUE
      THL3=THL*DX/(3.0E6)
      TLD=THL1+THL2+THL3
      IF(TLD .LT. 0.0) TLD=0.0
655   RETURN
      END
```

APPENDIX V

```
C       PROGRAM ** DSIM **
C       TO SIMULATE THE DYNAMIC MOTIONS OF A PAIR OF SPUR GEARS
        COMMON  /DCNS/RRA,RCA,LA,GNA,CBA,CSA,CNA,C11A,C12A,C22A,CH,V
       1,RRB,RCB,LB,GNB,CBB,CSB,CNB,C11B,C12B,C22B,INVPSY,CBT
        COMMON /ALL/RBA,ROA,RBB,ROB,YY,WA,M,PANG,DT,PI
        COMMON /GRU/GOIL,VISCT,EV
        COMMON /CT/YOMN,YOMX,HOSS,PO,MA,MB,MAB
        CHARACTER*18 RESFN
        REAL IA,IB,INVPSY,L,LA,LB,LT,KA1,KB1,KO1,KA2,KB2,KO2,KA3,KB3,KEQ
       1,KO3,M,MA,MB,MAB,MEQ,M1E,M2E,M3E,MRBTA,NA
        REAL*8 COMP1,COMP2,COMP3,HE1,HE2,HE3,HO1,HO2,HO3,HO1E,HO2E,HO12,
       1HO22,HOSS,YAON,YAO1,YAO2,YAO3,YBO1,YBO2,YBO3,YMA
        INTEGER DP,TA,TB
        DATA SY/20./,FWG/1.0/,FWT/1.0/,E/2.068E5/,G/8.273E4/
        WRITE(*,10) '   NO. OF TEETH - GEAR - A        : '
        READ(*,90) TA
        WRITE(*,10) '   NO. OF TEETH - GEAR - B        : '
        READ(*,90) TB
        WRITE(*,10) '   DIAMETRAL PITCH                : '
        READ(*,90) DP
100     WRITE(*,10) '   SPEED OF GEAR  A  (rpm)        : '
        READ(*,30) NA
        WRITE(*,10) '   TL  (Nm/m)                     : '
        READ(*,40) TL
        WRITE(*,10) '   CONT. RATIO                    : '
        READ(*,40) CR
        WRITE(*,10) '   VISC (Ns/m2)                   : '
        READ(*,40) VISC
        WRITE(*,10) '   PITCH ERROR - 2 (mm)           : '
        READ(*,40) PEA
        WRITE(*,'(A\)')'  NAME OF FILE TO STORE RESULTS  :-  '
        READ(*,'(A)') RESFN
        OPEN(4,FILE=RESFN,STATUS='NEW')
        NC=3
C  SYSTEM PARAMETERS
        GOTO 295
200     DT=(YOMX-YOMN)/(250*DYAR)
        RBTA=RBA*TAN(PANG)
        MRBTA=(M+1)*RBTA
        MAB=(MA+MB)/MB
        RAD=YOMX*(YY-YOMX)/YY
        FO=TL/RBA
        CERFX=E/(2*PI*RAD*(1-V**2))
        ERFX=10.0*SQRT(FO*CERFX)
        ERAL=FO*5.0E-3
C  VISCOSITY IN Ns/m2
        BET=3890.0
        TM=90.0+273
        TO=30.0+273
        VISCT=VISC*EXP(BET*(1.0/TM - 1.0/TO))
C  VISCISITY/PRESSURE COEFFICIENT ` ALP '
        Y=0.8
        PP=200.0
```

```
      D=2.15
      ALCON=1.0E-6*Y/PP
      ALP=ALCON*(ALOG(VISCT*1.0E3+0.5)+D)
      ICLE=1
      ISTO=0
      F1=FO
      F2=0.0
      F3=0.0
      KO2=0.0
      KO3=0.0
      ICONT1=1
      ICONT2=0
      ICONT3=0
      IPT1=1
      IPT2=2
      IPT3=3
      SPEA2=PEA1+PEA2
      SPEB2=PEB1+PEB2
      SPEA3=SPEA2+PEA3
      SPEB3=SPEB2+PEB3
      PO2=2.*PO
      YAR=YOPH
      YAO1=YAR
  210 CALL GRBN(YAO1,F1,HO1)
      CALL STIF1(YAO1,HO1,F1,COMP1,KO1,KA1,KB1)
      HOSS=HO1
      YMA=(COMP1-HO1)/MAB
      YAON=YAR+YMA-F1/KA1
      IF(DABS(YAO1-YAON) .GT. 1.0E-6) THEN
      YAO1=YAON
      GOTO 210
      ELSE
      YAO1=YAON
      ENDIF
      DYAO1=(DYMA*((KA1/KB1)-(MA/MB))-DHO1)*KB1/(KA1+KB1) + DYAR
      CALL DAMP(YAO1,HO1,F1,DR1)
      IF (DR1 .LT. 0.0)DR=0.0
      MEQ=MA*MB/(MA+MB)
      WRITE(4,50)TA,TB,DP,NA,VISC,TL,YOMN,YOMX
  220 KEQ=KO1+KO2+KO3
      IF (KEQ .LE. 0.0) THEN
      DC1=0.0
      DC2=0.0
      DC3=0.0
      GOTO 225
      ENDIF
      M1E=MEQ*KO1/KEQ
      M2E=MEQ*KO2/KEQ
      M3E=MEQ*KO3/KEQ
      DCR1=2.0*(M1E*KO1*1.0E-3)**0.5
      DCR2=2.0*(M2E*KO2*1.0E-3)**0.5
      DCR3=2.0*(M3E*KO3*1.0E-3)**0.5
      IF (DCR1 .LE. 0.0) THEN
      DC1=0.0
      ELSE
      DC1=DR1/DCR1
      ENDIF
```

```
222    IF (DCR2 .LE. 0.0) THEN
       DC2=0.0
       ELSE
       DC2=DR2/DCR2
       ENDIF
       IF (DCR3 .LE. 0.0) THEN
       DC3=0.0
       ELSE
       DC3=DR3/DCR3
       ENDIF
225    CALL INTGR(MA,MB,YMA,DYMA,KO1,KO2,KO3,PEA1,PEB1,PEA2,PEB2,FO,HO1,
      1HO2,HO3,DC1,DC2,DC3)
       YAR=YAR+DYAR*DT
       CALL SURF1(YAO1,YAR,YMA,KA1,F1)
       IF(ICONT1 .EQ. 0) GOTO 245
       CALL CONT(YAO1,YMA,YAR,DYAO1,DYMA,DYAR,DR1,HO1,HE1,FO,F1,COMP1,
      1KO1,KA1,KB1,PEA1,PEB1,ICONT1,IPT1)
245    CALL SURF2(YAO2,YAR,YMA,KA2,F2,PO,SPEA2)
       HO2=-YMA*MAB+COMP2-PEA2+PEB2
       CALL CONT(YAO2,YMA,YAR,DYAO2,DYMA,DYAR,DR2,HO2,HE2,FO,F2,COMP2,
      1KO2,KA2,KB2,SPEA2,SPEB2,ICONT2,IPT2)
255    IF(ICONT1 .EQ. 1) GOTO 275
       CALL SURF2(YAO3,YAR,YMA,KA3,F3,PO2,SPEA3)
       HO3=-YMA*MAB+COMP3-PEA3+PEB3
       CALL CONT(YAO3,YMA,YAR,DYAO3,DYMA,DYAR,DR3,HO3,HE3,FO,F3,COMP3,
      1KO3,KA3,KB3,SPEA3,SPEB3,ICONT3,IPT3)
275    IF(ICLE .LT. 3) GOTO 285
       IF(ISTO .LT. 2) GOTO 280
       ISTO=0
       DFL=(F1+F2+F3)/FO
       DF2=F2/FO
       WRITE(*,75)YAO2,DF2,YMA,HE2,KEQ,DFL
       WRITE(4,80)YAO2,DF2,YMA,HE2,KEQ,DFL
       GOTO 285
280    ISTO=ISTO+1
285    IF(YAO2 .LT. YOMX) GOTO 220
       IF(F2 .LE. 0.0) GOTO 290
       GOTO 220
290    ICONT1=1
       ICONT2=0
       ICONT3=0
       F1=F3
       HO1=HO3
       HE1=HE3
       KA1=KA3
       KB1=KB3
       KO1=KO3
       DC1=DC3
       DR1=DR3
       COMP1=COMP3
       YAR=YAR-2.*PO+SPEA3
       YAO1=YAO3
       DYAO1=DYAO3
       F2=0.0
       KO2=0.0
       DR2=0.
       HE2=0.
```

```
      HE3=0.
      F3=0.0
      KO3=0.0
      DR3=0.
      WRITE(*,91)ICLE
91    FORMAT(28H *** COMPLETED CYCLE NO.      I3)
      IF(ICLE .GE. NC) GOTO 291
      IF(ICLE .EQ. 2)THEN
      PEA2=PEA
      SPEA2=PEA1+PEA2
      ENDIF
      ICLE=ICLE+1
      GOTO 220
291   WRITE(*,85)YAR,YAO1,YAO2,YMA,DYMA,HO1,HO2,F1,F2,KO1,KO2
      CLOSE(4)
      GOTO 100
10    FORMAT(A\)
20    FORMAT(A)
30    FORMAT(F9.3)
40    FORMAT(F12.7)
50    FORMAT(3I4,5E15.5)
75    FORMAT(2F9.3,3E15.5,F8.3)
80    FORMAT(6E13.5\)
85    FORMAT(11E17.8)
90    FORMAT(I4)
C  SYSTEM PARAMETERS
295   PI=3.14159
      V=0.3
      GOIL=5000.
      WA=2*PI*NA/60
      PSY=SY*PI/180
      INVPSY=TAN(PSY) - PSY
      RCA=TA*25.4/(2*DP)
      RCB=TB*25.4/(2*DP)
      RBA=RCA*COS(PSY)
      RBB=RCB*COS(PSY)
      ROA=((TA+2)*25.4+ACA*TAN(PSY))/(2*DP)
      ROB=((TB+2)*25.4+ACB*TAN(PSY))/(2*DP)
      RRA=(TA-2.5)*25.4/(2*DP)
      RRB=(TB-2.5)*25.4/(2*DP)
      DYAR=RBA*WA
      DYMA=0.0
      PO=2*PI*RBA/TA
      BC=CR*PO
      AD=(ROA**2-RBA**2)**0.5+(ROB**2-RBB**2)**0.5-BC
      PHY=ATAN(AD/(RBA+RBB))
      CD=(RBA+RBB)/COS(PHY)
      YY=SQRT(CD**2-(RBA+RBB)**2)
      YOMN=YY-SQRT(ROB**2-RBB**2)
      PANG=ATAN(YY/(RBA+RBB))
      YOPH=RBA*TAN(PANG)
      YOMX=SQRT(ROA**2-RBA**2)
      IA=PI*FWG*RCA**4*7.759E-6/2
      IB=PI*FWG*RCB**4*7.759E-6/2
      MA=IA/RBA**2
      MB=IB/RBB**2
      M=1.0*TA/TB
```

```
      E1=(1-V**2)/E
      EV=1/E1
      L=2.25*25.4/DP
      GNA=PI*25.4/(2*DP) +2*ACA*TAN(PSY)
      GNB=PI*25.4/(2*DP) +2*ACB*TAN(PSY)
      IF(RRA .LT. RBA) THEN
      R=RBA
      ELSE
      R=RRA
      ENDIF
      CALL THICK(R,RBA,INVPSY,GNA,RCA,HRA,RI)
      IF(RRB .LT. RBB) THEN
         R=RBB
         ELSE
         R=RRB
         ENDIF
         CALL THICK(R,RBB,INVPSY,GNB,RCB,HRB,RI)
         CALL THICK(ROA,RBA,INVPSY,GNA,RCA,HOA,RI)
         CALL THICK(ROB,RBB,INVPSY,GNB,RCB,HOB,RI)
         LA=L/(1-(HOA/HRA)**2)
         LB=L/(1-(HOB/HRB)**2)
C  CONSTANTS FOR SHEAR DEFLN. `A'  AND `B'
         CSA=(2.4*SQRT(LA))/(G*HRA)
         CSB=(2.4*SQRT(LB))/(G*HRB)
C  CONSTANTS FOR DEFLN. DUE TO NORMAL LOAD `A' AND `B'
         CNA=(2*SQRT(LA))/(E*HRA)
         CNB=(2*SQRT(LB))/(E*HRB)
C  CONSTANTS FOR BENDING DEFLN. `A' AND `B'
         CBA=8.0*LA/(E*HRA**3)
         CBB=8.0*LB/(E*HRB**3)
C  CONSTANTS FOR HERTZ DEFLN. `A' AND `B'
         CH=2.0/(PI*EV)
C  CONST. FOR HERTZ CONTACT WIDTH `BT'
         CBT=SQRT(8.0/(PI*EV))
C  CONSTANTS FOR DEFLN. OF BODY
         C11A=9/(PI*EV*HRA**2)
         C11B=9/(PI*EV*HRB**2)
         C12A=(1+V)*(1-2*V)/(2*E*HRA)
         C12B=(1+V)*(1-2*V)/(2*E*HRB)
         C22A=2.4/(PI*EV)
         C22B=2.4/(PI*EV)
         GOTO 200
300      END
C  INVOLUTE FUNCTION
         SUBROUTINE INV(R,RB,INVR)
         REAL INVR
         ALPA=ATAN(SQRT((R**2-RB**2)/RB**2))
         INVR=TAN(ALPA)-ALPA
         RETURN
         END
C  TOOTH THICKNESS
         SUBROUTINE THICK(R,RB,INVPSY,GN,RC,HC,RI)
         REAL INVPSY,INVR
         CALL INV(R,RB,INVR)
         G2R=(GN/(2*RC)) + INVPSY - INVR
         HC=2*R*SIN(G2R)
         RI=R*COS(G2R)
```

```
      RETURN
      END
C  SUBROUTINE TO CALCULATE 'YAO1'
      SUBROUTINE SURF1(YAO,YAR,YMA,KA,F)
      REAL*8 YAO,YMA
      REAL KA
      IF(KA .LE. 0.0) THEN
      YAO=YAR+YMA
      ELSE
      YAO=YAR+YMA-F/KA
      ENDIF
      RETURN
      END
C  SUBROUTINE TO CALCULATE 'YAO2'
      SUBROUTINE SURF2(YAO,YAR,YMA,KA,F,PO,EA)
      REAL*8 YAO,YMA
      REAL KA
      IF(KA .LE. 0.0) THEN
      YAO=YAR+YMA+EA-PO
      ELSE
      YAO=YAR+YMA+EA-PO-F/KA
      ENDIF
      RETURN
      END
C  DEFLN. AT END OF CONTACT - PAIR 1
      SUBROUTINE END1(YAO,HO,HOE)
      COMMON  /DCNS/RRA,RCA,LA,GNA,CBA,CSA,CNA,C11A,C12A,C22A,CH,V
     1,RRB,RCB,LB,GNB,CBB,CSB,CNB,C11B,C12B,C22B,INVPSY,CBT
      COMMON /ALL/RBA,ROA,RBB,ROB,YY,WA,M,PANG,DT,PI
      REAL*8 XO,EPA,EPB,YAO,YAXO,YBO,YBXO,HO,HOE,BETA
      REAL M,INVPSY,INVR
      BETA=YAO/RBA
      YBO=YAO+HO
      CALL INV(ROA,RBA,ALPA)
      YAXO=ROA*DSIN(BETA-ALPA)
      XO=ROA*DCOS(BETA-ALPA) - RBA
      CALL DISB(YY,RBB,YBO,XO,YBXO,EPB)
      HOE=YBXO-YAXO
      RETURN
      END
C  DEFLN. AT THE START OF CONTACT
      SUBROUTINE ST2(YAO,HO,HOE)
      COMMON  /DCNS/RRA,RCA,LA,GNA,CBA,CSA,CNA,C11A,C12A,C22A,CH,V
     1,RRB,RCB,LB,GNB,CBB,CSB,CNB,C11B,C12B,C22B,INVPSY,CBT
      COMMON /ALL/RBA,ROA,RBB,ROB,YY,WA,M,PANG,DT,PI
      REAL*8 XO,EPA,EPB,YAO,YAXO,YBO,YBXO,HO,COMP,HOE,BETA
      REAL M,INVPSY,INVR
      YBO=YAO+HO
      BETA=(YY-YBO)/RBB
      CALL INV(ROB,RBB,ALPA)
      YBXO=YY-ROB*DSIN(BETA-ALPA)
      XO=RBB-ROB*DCOS(BETA-ALPA)
      CALL DISA(RBA,YAO,XO,YAXO,EPA)
      HOE=YBXO-YAXO
      RETURN
      END
C  TOOTH STIFFNESS - INITIAL
```

```
      SUBROUTINE STIF1(YAO,HO,FI,COMP,KO,KA,KB)
      COMMON  /DCNS/RRA,RCA,LA,GNA,CBA,CSA,CNA,C11A,C12A,C22A,CH,V
     1,RRB,RCB,LB,GNB,CBB,CSB,CNB,C11B,C12B,C22B,INVPSY,CBT
      COMMON /ALL/RBA,ROA,RBB,ROB,YY,WA,M,PANG,DT,PI
      REAL*8 EPA,EPB,YAO,YBO,HO,DHO,COMP
      REAL LA,LB,KO,KA,KB,INVPSY,LCA,LCB
      IF (FI .LE. 0.0) THEN
      COMP=0.0
      KO=0.0
      KA=0.0
      KB=0.0
      GOTO 2050
      ENDIF
      YBO=YAO+HO
      YYBO=YY-YBO
2000  R=DSQRT(YAO**2+RBA**2)
      CALL THICK(R,RBA,INVPSY,GNA,RCA,HCA,RI)
      ALPA=DATAN(YAO/RBA)-ATAN(HCA/(2*RI))
      HA=HCA/(2*COS(ALPA))
      YP=RBA/COS(ALPA)-SQRT(RRA**2-(HRA/2)**2)
      LCA=LA-YP
      AK=CBA*(COS(ALPA))**2*(LA**2-6*LCA*LA-3*LCA**2+8*LCA**1.5*LA**.5)
      C2SA=CSA*(COS(ALPA))**2*(SQRT(LA)-SQRT(LCA))
      C2NA=CNA*(SIN(ALPA))**2*(SQRT(LA)-SQRT(LCA))
      CDA=C11A*YP**2+2*C12A*YP+C22A*(1+((TAN(ALPA))**2)/3.1)
      C2DA=2*(COS(ALPA))**2*CDA
      R=SQRT(YYBO**2+RBB**2)
      CALL THICK(R,RBB,INVPSY,GNB,RCB,HCB,RI)
      ALPA=ATAN(YYBO/RBB)-ATAN(HCB/(2*RI))
      HB=HCB/(2*COS(ALPA))
      YP=RBB/COS(ALPA)-SQRT(RRB**2-(HRB/2)**2)
      LCB=LB-YP
      BK=CBB*(COS(ALPA))**2*(LB**2-6*LCB*LB-3*LCB**2+8*LCB**1.5*LB**.5)
      C2SB=CSB*(COS(ALPA))**2*(SQRT(LB)-SQRT(LCB))
      C2NB=CNB*(SIN(ALPA))**2*(SQRT(LB)-SQRT(LCB))
      CDB=C11B*YP**2+2*C12*YP+C22B*(1+((TAN(ALPA))**2/3.1))
      C2DB=2*(COS(ALPA))**2*CDB
2010  BT= CBT*DSQRT((FI*YAO*YYBO)/(YAO+YYBO))
      ZHA=FI*CH*(ALOG(2*HA/BT) - V/((1-V)*2))
      ZHB=FI*CH*(ALOG(2*HB/BT) - V/((1-V)*2))
      ZA=FI*(C2SA+C2NA+C2DA+AK)
      ZB=FI*(C2SB+C2NB+C2DB+BK)
      IF(ZHA .LT. 0.0) ZHA=0.0
      IF(ZHB .LT. 0.0) ZHB=0.0
      COMPA=(ZHA+ZA)
      COMPB=(ZHB+ZB)
      COMP=COMPA+COMPB
      KA=FI/COMPA
      KB=FI/COMPB
      KO=FI/COMP
2050  RETURN
      END
C  MESH  STIFFNESS AND TOOTH LOAD
      SUBROUTINE MESH(YAO,HO,FI,COMP,KO,KA,KB)
      COMMON  /DCNS/RRA,RCA,LA,GNA,CBA,CSA,CNA,C11A,C12A,C22A,CH,V
     1,RRB,RCB,LB,GNB,CBB,CSB,CNB,C11B,C12B,C22B,INVPSY,CBT
      COMMON /ALL/RBA,ROA,RBB,ROB,YY,WA,M,PANG,DT,PI
```

```
      REAL*8 EPA,EPB,YAO,YBO,HO,DHO,COMP
      REAL LA,LB,KO,KA,KB,INVPSY,LCA,LCB
      YBO=YAO+HO
      YYBO=YY-YBO
      IF (COMP .LE. 0.0) THEN
      COMP=0.0
      FI=0.0
      KO=0.0
      KA=0.0
      KB=0.0
      GOTO 2050
      ENDIF
      IF (FI .GT. 0.0) GOTO 2000
      FI=0.001
2000  R=DSQRT(YAO**2+RBA**2)
      CALL THICK(R,RBA,INVPSY,GNA,RCA,HCA,RI)
      ALPA=DATAN(YAO/RBA)-ATAN(HCA/(2*RI))
      HA=HCA/(2*COS(ALPA))
      YP=RBA/COS(ALPA)-SQRT(RRA**2-(HRA/2)**2)
      LCA=LA-YP
      AK=CBA*(COS(ALPA))**2*(LA**2-6*LCA*LA-3*LCA**2+8*LCA**1.5*LA**.5)
      C2SA=CSA*(COS(ALPA))**2*(SQRT(LA)-SQRT(LCA))
      C2NA=CNA*(SIN(ALPA))**2*(SQRT(LA)-SQRT(LCA))
      CDA=C11A*YP**2+2*C12A*YP+C22A*(1+((TAN(ALPA))**2)/3.1)
      C2DA=2*(COS(ALPA))**2*CDA
      R=SQRT(YYBO**2+RBB**2)
      CALL THICK(R,RBB,INVPSY,GNB,RCB,HCB,RI)
      ALPA=ATAN(YYBO/RBB)-ATAN(HCB/(2*RI))
      HB=HCB/(2*COS(ALPA))
      YP=RBB/COS(ALPA)-SQRT(RRB**2-(HRB/2)**2)
      LCB=LB-YP
      BK=CBB*(COS(ALPA))**2*(LB**2-6*LCB*LB-3*LCB**2+8*LCB**1.5*LB**.5)
      C2SB=CSB*(COS(ALPA))**2*(SQRT(LB)-SQRT(LCB))
      C2NB=CNB*(SIN(ALPA))**2*(SQRT(LB)-SQRT(LCB))
      CDB=C11B*YP**2+2*C12*YP+C22B*(1+((TAN(ALPA))**2/3.1))
      C2DB=2*(COS(ALPA))**2*CDB
      DZB=AK+BK
      DZS=C2SA+C2SB
      DZN=C2NA+C2NB
      DZD=C2DA+C2DB
2010  BT= CBT*DSQRT((FI*YAO*YYBO)/(YAO+YYBO))
      DBT=(BT)/(2*FI)
      ZHA=FI*CH*(ALOG(2*HA/BT) - V/((1-V)*2))
      ZHB=FI*CH*(ALOG(2*HB/BT) - V/((1-V)*2))
      ZSA=FI*C2SA
      ZSB=FI*C2SB
      ZNA=FI*C2NA
      ZNB=FI*C2NB
      ZBA=FI*AK
      ZBB=FI*BK
      ZDA=FI*C2DA
      ZDB=FI*C2DB
      IF(ZHA .LT. 0.0) ZHA=0.0
      IF(ZHB .LT. 0.0) ZHB=0.0
      DZHA=ZHA/FI - CH/2
      DZHB=ZHB/FI - CH/2
      FF =ZHA+ZHB+ZSA+ZSB+ZNA+ZNB+ZBA+ZBB+ZDA+ZDB-COMP
```

```
      DFF=DZHA+DZHB+DZS+DZN+DZB+DZD
      FI1=FI - FF/DFF
      IF (ABS(FI1-FI) .LE. 0.01) GOTO 2020
      IF (FI1 .LE. 0.0) THEN
      FI=FI/2
      ELSE
      FI=FI1
      ENDIF
      GOTO 2010
2020  FI=FI1
      COMPA=(ZHA+ZBA+ZSA+ZNA+ZDA)
      COMPB=(ZHB+ZBB+ZSB+ZNB+ZDB)
      KA=FI/COMPA
      KB=FI/COMPB
      KO=FI/COMP
2050  RETURN
      END
C     RUNGE-KUTTA (4th. order) INTEGRATION
      SUBROUTINE INTGR(MA,MB,YMA,DYMA,KO1,KO2,KO3,PEA2,PEB2,PEA3,PEB3,
     1FO,HO1,HO2,HO3,DC1,DC2,DC3)
      COMMON /ALL/RBA,ROA,RBB,ROB,YY,WA,M,PANG,DT,PI
      REAL*8 HO1,HO2,HO3,YMA
      REAL MA,MB,MAB,KO1,KO2,KO3
      MAB=(MA+MB)/MB
      AA=-1.0E3*(DC1+DC2+DC3)*MAB/MA
      BB=-1.0E3*(KO1+KO2+KO3)*MAB/MA
      CC=1.0E3*(FO-KO1*HO1-KO2*(HO2-PEA2+PEB2)-KO3*(HO3-PEA3+PEB3))/MA
      CY0=DYMA
      CV0=AA*DYMA+BB*YMA+CC
      CY1=DYMA+CV0*DT/2
      CV1=AA*(DYMA+CV0*DT/2)+BB*(YMA+CY0*DT/2)+CC
      CY2=DYMA+CV1*DT/2
      CV2=AA*(DYMA+CV1*DT/2)+BB*(YMA+CY1*DT/2)+CC
      CY3=DYMA+CV2*DT/2
      CV3=AA*(DYMA+CV2*DT/2)+BB*(YMA+CY2*DT/2)+CC
      YMA=YMA+(CY0+2*CY1+2*CY2+CY3)*DT/6
      DYMA=DYMA+(CV0+2*CV1+2*CV2+CV3)*DT/6
      RETURN
      END
C   TO CALCULATE `YA' FOR ANY X
      SUBROUTINE DISA(RBA,YAO,X,YA,E)
      REAL*8 X,YA,E,E2,FE,DFE,THA,DE,BETA,YAO
      IF (X .EQ. 0.0) THEN
      YA=YAO
      GOTO 1420
      ENDIF
      E=DATAN(X/YAO)
      BETA=YAO/RBA
1400  FE=E-(RBA+X-RBA*DCOS(E))/(RBA*DSIN(E))+BETA
      DFE=1+(((RBA+X)*DCOS(E))/RBA-1.)/(DSIN(E))**2
      E2=E-(FE/DFE)
      DE=DABS(E2-E)
      IF(DE .LE. 0.000001) GOTO 1410
      E=E2
      GOTO 1400
1410  E=E2
      THA=DATAN(BETA+E) - E
```

```
      YA=(RBA+X)*DTAN(THA)
1420  RETURN
      END
C   TO CALCULATE `YB' FOR ANY X
      SUBROUTINE DISB(YY,RBB,YBO,X,YB,E)
      REAL*8 X,YB,E,THA,E2,FE,DFE,DE,YBO,BETA
      IF (X .EQ. 0.0) THEN
      YB=YBO
      GOTO 1470
      ENDIF
      E=DATAN(X/(YY-YBO))
      BETA=(YY-YBO)/RBB
1450  FE=E-(RBB-X-RBB*DCOS(E))/(RBB*DSIN(E))-BETA
      DFE=1+(((RBB-X)*DCOS(E))/RBB-1.)/(DSIN(E))**2
      E2=E-(FE/DFE)
      DE=DABS(E2-E)
      IF(DE .LE. 0.000001) GOTO 1460
      E=E2
      GOTO 1450
1460  E=E2
      THA=DATAN(BETA-E) + E
      YB=YY-(RBB-X)*DTAN(THA)
1470  RETURN
      END
C   TO CALCULATE THE FILM THICKNESS ** GRUBIN FORMULA **
      SUBROUTINE GRBN(YAO,F,HO)
      COMMON /ALL/RBA,ROA,RBB,ROB,YY,WA,M,PANG,DT,PI
      COMMON /GRU/GOIL,VISCT,EV
      COMMON /CT/YOMN,YOMX,HOSS,PO,MA,MB,MAB
      REAL M,MA,MB,MAB
      REAL*8 YAO,HO,HOSS
      IF(F .LE. 0.0)THEN
      HO=10.*HOSS
      GOTO 100
      ENDIF
      RA=YAO
      RB=YY-YAO
      R=RA*RB/(RA+RB)
      UA=RA*WA
      UB=RB*WA*M
      U1=(UA+UB)/2
      U=VISCT*U1/(EV*R*1E6)
      W=F/(EV*R)
      H=1.95*(GOIL*U)**0.727/(W**0.091)
      HO=H*R
100   CONTINUE
      RETURN
      END
C   TO CALCULATE THE TOOTH FORCE ** GRUBIN FORMULA **
      SUBROUTINE TRGR(YAO,HO,F)
      COMMON /ALL/RBA,ROA,RBB,ROB,YY,WA,M,PANG,DT,PI
      COMMON /GRU/GOIL,VISCT,EV
      COMMON /CT/YOMN,YOMX,HOSS,PO,MA,MB,MAB
      REAL M,MA,MB,MAB
      REAL*8 YAO,HO,HOSS
      IF(HO .LT. 0.1*HOSS) HO=0.1*HOSS
      RA=YAO
```

```
      RB=YY-YAO
      R=RA*RB/(RA+RB)
      UA=RA*WA
      UB=RB*WA*M
      U1=(UA+UB)/2
      U=VISCT*U1/(EV*R*1E6)
      F=(1.95*R*(GOIL*U)**0.727/ HO)**11.0*EV*R
      RETURN
      END
C     TO CALCULATE THE DAMPING RATIO
      SUBROUTINE DAMP(YAO,HO,F,DR)
      COMMON /ALL/RBA,ROA,RBB,ROB,YY,WA,M,PANG,DT,PI
      COMMON /GRU/GOIL,VISCT,EV
      REAL M
      REAL*8 YAO,HO
      RA=YAO
      RB=YY-YAO
      R=RA*RB/(RA+RB)
      UA=RA*WA
      UB=RB*WA*M
      U1=((UA+UB)*1.0E-3)/2.0
      A=18.24*VISCT/(U1**1.09)+ALOG(1.1193/(U1**0.027))
      B=60.0/(390.8*U1)
      C=39.08*VISCT*U1+57.0*VISCT+1.15
      DR=A*EXP(-1.0*B*((C-F)**2))
      RETURN
      END
C   TO  DETERMINE CONTACT STATUS
      SUBROUTINE CONT(YAO,YMA,YAR,DYAO,DYMA,DYAR,DR,HO,HE,FO,F,COMP,
     1KO,KA,KB,PEA,PEB,ICONT,IPT)
      COMMON /ALL/RBA,ROA,RBB,ROB,YY,WA,M,PANG,DT,PI
      COMMON /CT/YOMN,YOMX,HOSS,PO,MA,MB,MAB
      REAL*8 YAO,YBO,HO,HE,HOE,HO22,HOSS,YMA,COMP
      REAL NA,M,KO,KA,KB,MA,MB,MAB
      YBO=YAO+HO
      BPO=PO*(IPT-1)
      IF (YAO .GT. YOMX) GOTO 400
      IF (YBO .LT. YOMN) GOTO 300
200   COMP=YMA*MAB+HO+PEA-PEB
      CALL MESH(YAO,HO,F,COMP,KO,KA,KB)
      IF(F .LE. 0.0) GOTO 600
      CALL GRBN(YAO,F,HO22)
201   IF(DABS(HO22-HO) .LE. 1.0E-3*HOSS) GOTO 210
      HO=HO22
      GOTO 200
210   HO=HO22
      HE=HO
      GOTO 500
600   ITR=0
610   CALL STIF1(YAO,HO,F,COMP,KO,KA,KB)
      HO=-YMA*MAB-PEA+PEB+COMP
      IF(HO .GT. 10.*HOSS) HO=10.*HOSS
      YBO=YAO+HO
620   CALL TRGR(YAO,HO,F22)
      IF(ABS(F22-F) .LE. 1.0E-3*FO) GOTO 650
      IF(F22 .LT. F)THEN
      FDUM=F22
```

```
F22=F
F=FDUM
ENDIF
IF(ITR .EQ. 0) THEN
FL=F
FR=F22
ITR=1
GOTO 630
ENDIF
IF(F .GT. FL)FL=F
IF(F22 .LT. FR)FR=F22
IF(ITR .GE. 100) GOTO 650
      ITR=ITR+1
630   F=(FL+FR)/2.0
      GOTO 610
650   F=F22
      HE=HOE
      GOTO 500
300   ITR=0
310   CALL STIF1(YAO,HO,F,COMP,KO,KA,KB)
      HO=-YMA*MAB-PEA+PEB+COMP
      IF(HO .GT. 10.*HOSS) HO=10.*HOSS
      YBO=YAO+HO
      CALL ST2(YAO,HO,HOE)
      IF (ICONT .EQ. 1) GOTO 320
      IF (HOE .GT. 10*HOSS) THEN
      ICONT=0
      GOTO 520
      ENDIF
      ICONT=1
320   CALL TRGR(YAO,HOE,F22)
      IF(ABS(F22-F) .LE. 1.0E-3*FO) GOTO 350
      IF(F22 .LT. F)THEN
      FDUM=F22
      F22=F
      F=FDUM
      ENDIF
      IF(ITR .EQ. 0) THEN
      FL=F
      FR=F22
      ITR=1
      GOTO 330
      ENDIF
      IF(F .GT. FL)FL=F
      IF(F22 .LT. FR)FR=F22
      IF(ITR .GE. 100) GOTO 350
      ITR=ITR+1
330   F=(FL+FR)/2.0
      GOTO 310
350   F=F22
      HE=HOE
      GOTO 500
400   ITR=0
410   CALL STIF1(YAO,HO,F,COMP,KO,KA,KB)
      HO=-YMA*MAB+COMP-PEA+PEB
      IF(HO .GT. 10.*HOSS) HO=10.*HOSS
      YBO=YAO+HO
```

```
      CALL END1(YAO,HO,HOE)
420   CALL TRGR(YAO,HOE,F12)
      IF(ABS(F12-F) .LE. 1.0E-3*FO) GOTO 440
      IF(F12 .LT. F)THEN
      FDUM=F12
      F12=F
      F=FDUM
      ENDIF
      IF(ITR .EQ. 0) THEN
      FL=F
      FR=F12
      ITR=1
      GOTO 430
      ENDIF
      IF(F .GT. FL)FL=F
      IF(F12 .LT. FR)FR=F12
      IF(ITR .GE. 100) GOTO 440
      ITR=ITR+1
430   F=(FL+FR)/2.0
      GOTO 410
440   F=F12
      IF(F .LT. 1.0E-3*FO) THEN
      ICONT=0
      KO=0.0
      KA=0.0
      KB=0.0
      COMP=0.0
      F=0.0
      ENDIF
      HE=HOE
500   IF(IPT .EQ. 1)GOTO 505
      CALL SURF2(YAO,YAR,YMA,KA,F,BPO,PEA)
      GOTO 506
505   CALL SURF1(YAO,YAR,YMA,KA,F)
506   YBO=YAO+HO
      IF (F .LE. 0.0) THEN
      DYAO=DYAR+DYMA
      DR=0.0
      GOTO 520
      ENDIF
510   DYAO=(DYMA*((KA/KB)-(MA/MB)))*KB/(KA+KB) + DYAR
      CALL DAMP(YAO,HE,F,DR)
      IF(DR .LT. 0.0 ) DR=0.0
520   CONTINUE
      RETURN
      END
```

APPENDIX VI

Torsional vibration analysis of the total system

For this low frequency analysis gear teeth were considered to be rigid and inertias of couplinigs and other elements which were close to each other and connected by relatively short lengths of shafts were lumped together to form single equivalent inertias. Figure VIa shows a schematic diagram of the complete system and Figure VIb shows the equivalent linear-type lumped-mass system. Since the inertia of the rotor of the electric motor was comparatively very high it was taken as infinite as far as the vibration analysis was concerned.

The inertias and stiffnesses of the elements were:

$$I_a = 5.75 \times 10^{-3} \text{ kg m}^2$$

$$I_b = 9.98 \times 10^{-3} \text{ kg m}^2$$

$$I_c = 0.90 \times 10^{-3} \text{ kg m}^2$$

$$I_d = 1.36 \times 10^{-3} \text{ kg m}^2$$

$$I_e = 9.89 \times 10^{-3} \text{ kg m}^2$$

$$I_f = 10.47 \times 10^{-3} \text{ kg m}^2$$

$$k_1 = 0.98 \times 10^{3} \text{ Nm/rad}$$

$$k_2 = 24.03 \times 10^{3} \text{ Nm/rad}$$

$$k_3 = 16.48 \times 10^{3} \text{ Nm/rad}$$

$$k_4 = 9.18 \times 10^{3} \text{ Nm/rad}$$

For the equivalent linear-type system

$$I_1 = I_a + I_e + r^2 I_c = 18.37 \times 10^{-3} \text{ kg m}^2$$
$$I_2 = I_f = 10.47 \times 10^{-3} \text{ kg m}^2$$
$$I_3 = I_b + r^2 I_d = 10.00 \times 10^{-3} \text{ kg m}^2$$

$$K_1 = k_1 = 0.98 \times 10^3 \text{ Nm/rad}$$
$$K_2 = k_2 = 24.03 \times 10^3 \text{ Nm/rad}$$
$$K_3 = k_3 = 16.48 \times 10^3 \text{ Nm/rad}$$
$$K_4 = r^2 k_4 = 27.74 \times 10^3 \text{ Nm/rad}$$

These resulted in the following natural frequencies:

$$\omega_1 = 388.6 \text{ Hz}$$
$$\omega_2 = 361.9 \text{ Hz}$$
$$\omega_3 = 24.8 \text{ Hz}$$

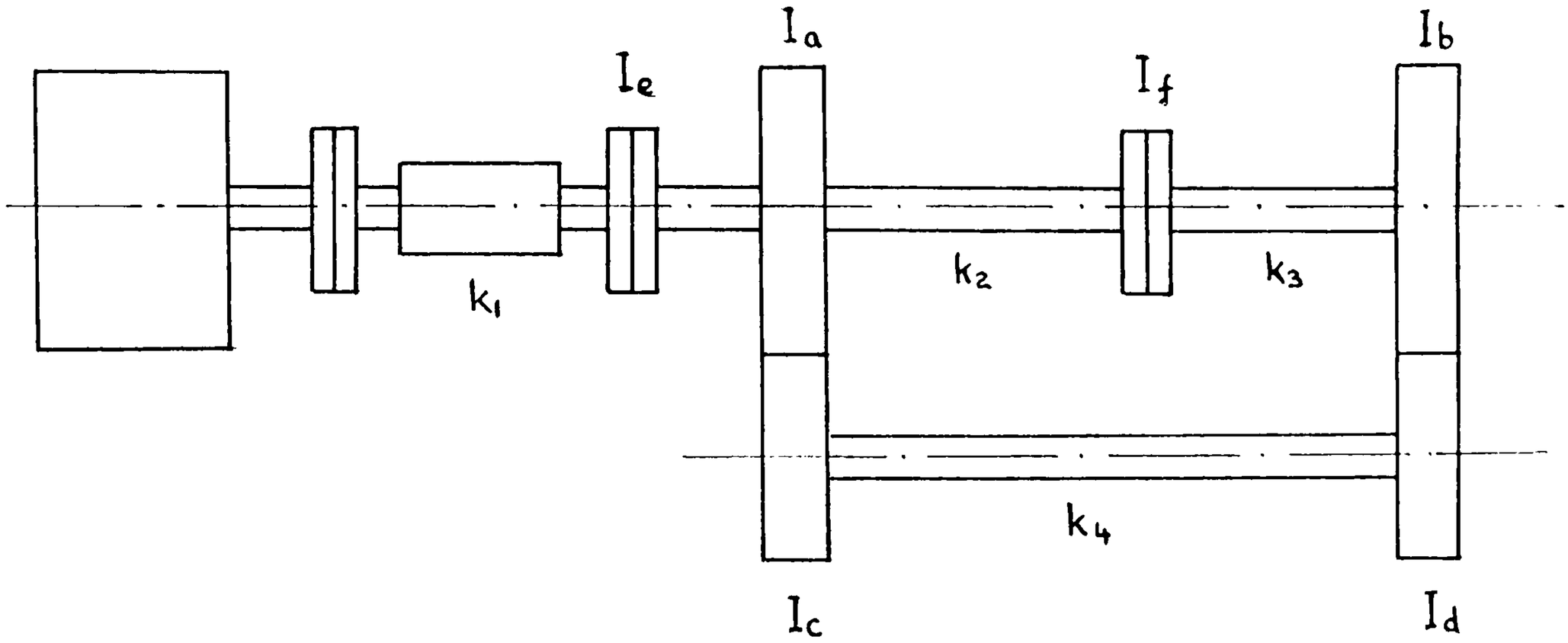

FIGURE VI(a)

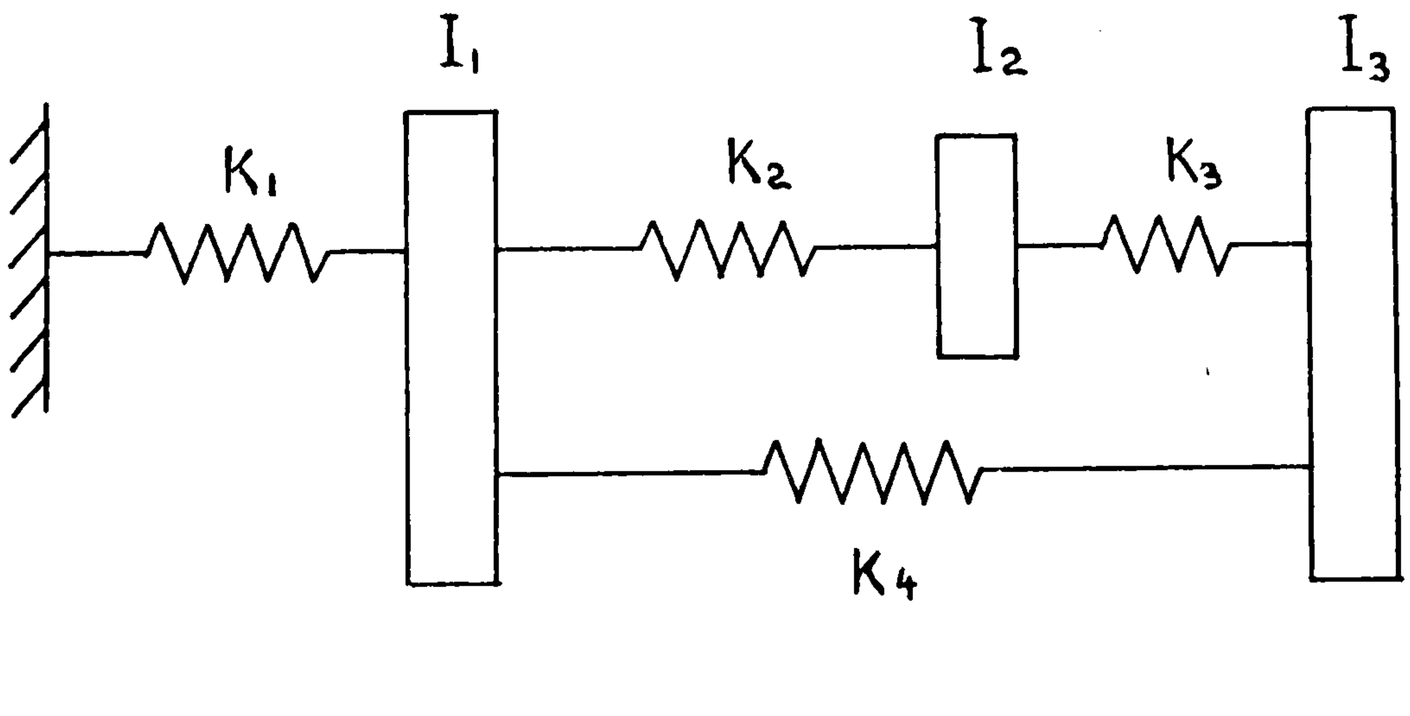

FIGURE VI(b)

APPENDIX VII

Listing of the Assembly Language programme used to record frictional torque:

```
TITLE   GEAR DATA RECORDING PROGRAMME  (GEAR.ASM)
STACK   SEGMENT  PARA STACK  'STACK'
          DB        512 DUP (0)  ;512 BYTES OF STACK SPACE
STACK     ENDS
DATA    SEGMENT  PARA PUBLIC  'DATA'
MSG1      DB  'PRESS <S> TO START SAMPLING OR PRESS <Q> TO QUIT  '
MSG2      DB  'PRESS <Y> TO STORE DATA ON DISC OR <N> TO DISCARD     '
MSG3      DB  'PLEASE TYPE FILE NAME (MAX 8 CHRS)  '
MSG4      DB  '  ERROR  ! ! !  '
FCB       DB  2,'         DAT',25 DUP(?)
DTA       DB  5000 DUP (0)
DEN       DB  10
CNT       DB  0
PLS       DB  54
SPEED     DW  0
MAG       DB  5000 DUP (0)
DATA      ENDS
CODE    SEGMENT  PARA  PUBLIC  'CODE'
MAINPROG  PROC  FAR
;
; STANDARD  PROGRAM PROLOGUE
;
ASSUME  CS:CODE
          PUSH DS
          MOV  AX,0
          PUSH AX
          MOV  AX,DATA
          MOV  DS,AX
ASSUME  DS:DATA
;
;DISPLAY MESSAGE 1
TEST:     MOV  BX,OFFSET MSG1    ;GET ADDRESS OF MESSAGE
          MOV  CX,50             ;NO OF CHARACTERS IN MSG.
          CALL PRINT
;WAIT  FOR  KEY  TO  BE  STRUCK
          MOV  AH,0
KEY:      INT  16H
          CMP  AL,53H            ;IS KEY=`S' ?
          JZ   BEGIN
          CMP  AL,51H            ;IS KEY=`Q' ?
          JNZ  KEY
          RET                    ;RETURN TO DOS
;
;WAIT FOR PULSES FROM OPTO SWITCHES AND START SAMPLING
BEGIN:    MOV  CX,4998           ;NO OF SAMPLES
```

```
        MOV   BX,OFFSET DTA     ;START OF SAMPLE AREA
        ADD   BX,2              ;1ST 2BYTES RESERVED FOR SPEED
CHK_ST: MOV   AL,1              ;AD CHANNEL 0 - OPTO SWITCH 1 O/P
        MOV   DX,816            ;ADC PORT ADDRESS
        OUT   DX,AL             ;START CONVERSION
CHK1:   IN    AL,DX             ;GET ADC STATUS
        CMP   AL,128            ;IS CONVERSION DONE
        JS    CHK1              ;WAIT UNTIL CONVERTED
        ADD   DX,1
        IN    AL,DX             ;READ VALUE
        CMP   AL,135            ;IS IT `LOW'
        JNS   CHK_ST            ;LOOP UNTIL LOW
        MOV   AL,3              ;AD CHANNEL 1 - OPTO SWITCH 2 O/P
        MOV   DX,816            ;ADC PORT ADD.
        OUT   DX,AL             ;START CONVERSION
CHK2:   IN    AL,DX             ;GET ADC STATUS
        CMP   AL,128            ;IS CONVERSION DONE
        JS    CHK2              ;WAIT UNTIL CONVERTED
        ADD   DX,1
        IN    AL,DX             ;READ VALUE
        CMP   AL,135            ;IS IT `LOW'
        JNS   CHK_ST            ;LOOP UNTIL BOTH O/PS ARE LOW
;
START:  MOV   AL,5              ;AD CHANNEL 3 - TORQ O/P
        MOV   DX,816            ;ADC PORT ADD.
        OUT   DX,AL             ;START CONVERSION
WAIT:   IN    AL,DX             ;GET ADC STATUS
        CMP   AL,128            ;IS CONVERSION DONE
        JS    WAIT              ;WAIT UNTIL CONVERTED
        INC   DX
        IN    AL,DX             ;READ VALUE
        MOV   [BX],AL           ;STORE VALUE
        INC   BX                ;NEXT LOCATION
        LOOP  START             ;LOOP UNTIL DONE
;
;SPEED  MEASURING  ROUTINE
        MOV   CX,5000           ;NO OF SAMPLES
        MOV   BX,OFFSET MAG     ;START. ADD. DAT. STORE. AREA
SMR:    MOV   AL,7              ;GH 4 - MAG. PICKUP O/P
        MOV   DX,816            ;ADC PORT ADD.
        OUT   DX,AL             ;START CONVERSION
PULSE1: IN    AL,DX             ;GET AD STATUS
        CMP   AL,128            ;IS CONVERSION DONE ?
        JS    PULSE1            ;STAY UNTIL DONE
        INC   DX
        IN    AL,DX             ;READ VALUE
        MOV   [BX],AL           ;STORE VALUE
        INC   BX
        LOOP  SMR
        JMP   REC
;
FAULT:  JMP   TEST
;
;READ   RECORDED  DATA
REC:    MOV   DX,5000           ;TOTAL NO OF SAMPLE AVAILABLE
        MOV   BX,OFFSET MAG     ;START. ADD. DATA
```

```
UP1:    MOV   AL,[BX]          ;READ SAMPLE
        INC   BX
        DEC   DX
        CMP   DX,0             ;ALL SAMPLES CHECKED ?
        JZ    FAULT            ;RETURN FOR ANOTHER TEST IF YES
        CMP   AL,140           ;IS IT LOW ( <0.5v )
        JNS   UP1              ;READ UNTIL SO
UP2:    MOV   AL,[BX]          ;READ NEXT VALUE
        INC   BX
        DEC   DX
        CMP   DX,0             ;NO MORE SAMPLES ?
        JZ    FAULT            ;IF YES RETURN
        CMP   AL,180           ;IS IT HIGH ( >4.0v )
        JS    UP2              ;REPEAT UNTIL SO
        MOV   CX,0
CNT1:   INC   CX
        MOV   AL,[BX]          ;READ NEXT VALUE
        INC   BX
        DEC   DX
        CMP   DX,0
        JZ    FAULT
        CMP   AL,140           ;IS IT LOW
        JNS   CNT1
CNT2:   INC   CX               ;ADVANCE COUNTER
        MOV   AL,[BX]          ;READ SAMPLE
        INC   BX
        DEC   DX
        CMP   DX,0
        JZ    FAULT
        CMP   AL,180           ;IS IT HIGH
        JS    CNT2             ;REPEAT UNTIL SO
        DEC   PLS              ;ONE MORE PULSE COMPLETE
        CMP   PLS,0            ;54 PULSES COMPLETE ?
        JNZ   CNT1             ;IF NOT LOOP AGAIN
        MOV   PLS,54           ;SET PLS FOR NEXT RECORDING
        MOV   SPEED,CX         ;TRANSFER COUNT TO MEMORY
        MOV   BX,OFFSET DTA    ;START OF DTA
        MOV   [BX],CX          ;STORE VALUE
;
;DATA  DISPLAY  ROUTINE
        MOV   BX,OFFSET DTA    ;SAMPLE AREA ADD.
        MOV   CX,260           ;NO OF SAMPLES TO BE DISPLAYED
DIS:    MOV   AH,0
        MOV   AL,[BX]          ;GET DATA TO DISPLAY
        INC   BX               ;NEXT DATA LOCATION
        DIV   DEN
PUSH AX                        ;SAVE REMAINDER
MOV   AH,0
DIV   DEN
PUSH AX                        ;SAVE REMAINDER
CALL DISPCHAR                  ;DISPLAY 100'S CHAR.
POP   AX                       ;GET 10'S CHAR
MOV   AL,AH                    ;GET REMAINDER INTO AL
CALL DISPCHAR                  ;AND DISPLAY
POP   AX                       ;GET 1'S CHAR.
MOV   AL,AH                    ;GET REMAINDER INTO AL
```

```
            CALL DISPCHAR           ;AND DISPLAY
            MOV  AL,240             ;LOAD SPACE CHAR.
            CALL DISPCHAR
            LOOP DIS
            MOV  AL,13              ;CR
            CALL DISP
            MOV  AL,10              ;LF
            CALL DISP
;
;ASK  IF  DATA  TO  BE  STORED
            MOV  AX,DATA
            MOV  DS,AX
            MOV  BX,OFFSET MSG2     ;ADD. OF MSG2
            MOV  CX,51              ;NO OF CHRS.
            CALL PRINT
;WAIT  FOR  KEY
            MOV  AH,0
KEY2:       INT  16H
            CMP  AL,'Y'             ;IS KEY=Y
            JZ   TRY                ;BRANCH IF YES
            CMP  AL,'N'             ;IS KEY=N
            JNZ  KEY2
            JMP  TEST               ;RETURN FOR ANOTHER TEST
;
;ROUTINE  TO  STORE  DATA  ON  DISC
TRY:        MOV  BX,OFFSET MSG3     ;ADD. OF MSG3
            MOV  CX,35              ;NO OF CHRS. IN MSG.
            CALL PRINT
;
;FILE  NAME  FROM  KEY BOARD
            MOV  BX,OFFSET FCB+1
KEY1:       MOV  AH,0               ;SETUP FOR KEYBOARD INT
            INT  16H
            INC  CNT
            CMP  CNT,9              ;ARE THERE 8 CHRS.
            JZ   LAST               ;JUMP IF YES
            CMP  AL,13              ;IS THIS CARRIAGE RETURN
            JZ   SPACE              ;JUMP IF YES
            MOV  [BX],AL            ;GET CHR INTO FCB
            SUB  AL,0               ;MAINTAIN ASCII ADJUST
            CALL DISP               ;AND DISPLAY
            INC  BX                 ;NEXT FCB LOCATION
            JMP  KEY1
;
LAST:       CMP  AL,13              ;IS 9TH CHR A CARRIAGE RET.
            JZ   FIN                ;JUMP IF YES
            DEC  CNT                ;DISCARD IF NOT
            JMP  KEY1               ;AND GET NEXT CHR.
SPACE:      MOV  AL,20H             ;SPACE CHR.
            MOV  [BX],AL            ;INTO EXTRA POSITIONS
            INC  BX
            INC  CNT
            CMP  CNT,9              ;ARE 8 CHRS FILLED
            JNZ  SPACE              ;NO MORE SPACES
FIN:        MOV  CNT,0              ;RESET COUNTER FOR NEXT FILE
            MOV  AL,13              ;CR
```

```
          CALL DISP
          MOV  AL,10              ;LF
          CALL DISP
          MOV  AX,DATA
          MOV  DS,AX
;SET  DTA  AND  CREATE  FILE
          MOV  DX,OFFSET DTA      ;ADD. OF DTA
          MOV  AH,1AH             ;DOS FUNCTION = `SET DTA'
          INT  21H                ;INVOKE  DOS FUNCTIN
          MOV  DX,OFFSET FCB      ;ADDR. FCB
          MOV  AH,16H             ;DOS FUNCTN. CREATE FILE
          INT  21H                ;INVOKE DOS FUNCTION
          CMP  AL,0               ;DID `FILE CREATE' WORK
          JNZ  ERROR
;INITIALIZE  FCB
          MOV  WORD PTR FCB+0CH,0
          MOV  WORD PTR FCB+0EH,5000
          MOV  FCB+20H,0
;PUT  ALL  SAMPLES  TO  DISC
          MOV  DX,OFFSET FCB      ;ADDR. OF FCB
          MOV  AH,15H             ;DISC WRITE FUNCTION
          INT  21H                ;EXECUTE DISC WRITE
          CMP  AL,0               ;DID WRITE WORK ?
          JNZ  ERROR              ;BRANCH  IF NOT
;CLOSE  FILE
          MOV  DX,OFFSET FCB
          MOV  AH,10H
          INT  21H                ;INVOKE DOS FUNC. `FILE CLOSED'
          JMP  TEST               ;RETURN FOR ANOTHER TEST
;
ERROR:    MOV  AL,0DH             ;CARRIAGE RET.
          CALL DISP
          MOV  AL,0AH             ;LINE FEED
          CALL DISP
          MOV  AX,DATA
          MOV  DS,AX
          MOV  BX,OFFSET MSG4     ;GET ERROR MESSAGE
          MOV  CX,13
          CALL PRINT
          JMP  TRY
;
;SCREEN  PRINT  ROUTINE
PRINT  PROC  NEAR
CHAR:     MOV  AL,[BX]            ;GET NEXT CHAR.
          CALL DISP               ;DISPLAY IT
          INC  BX                 ;NEXT CHAR.
          LOOP CHAR
          MOV  AL,0DH             ;CR
          CALL DISP
          MOV  AL,0AH             ;LF
          CALL DISP
          RET
PRINT     ENDP
;
;BIOS  CALL  FOR  DISPLAY  DRIVER
DISP  PROC  NEAR
```

```
            PUSH BX                 ;SAVE BX REG.
            MOV  BX,0               ;SELECT DISPLAY PAGE 0
            MOV  AH,14              ;WRITE
            INT  10H                ;CALL VIDEO DRIVER IN BIOS
            POP  BX                 ;RESTORE REG.
            RET                     ;RETURN TO CALLER
DISP        ENDP
;
DISPCHAR  PROC  NEAR
            PUSH BX                 ;SAVE BX REG
            MOV  BX,0               ;SELECT DISPLAY PAGE 0
            ADD  AL,'0'             ;CONVERT TO ASCII
            MOV  AH,14              ;WRITE
            INT  10H                ;CALL VIDEO DRIVER IN BIOS
            POP  BX                 ;RESTORE REG.
            RET                     ;RETURN TO CALLER
DISPCHAR  ENDP
MAINPROG  ENDP
CODE        ENDS
            END
```

APPENDIX VIII

(a) Details of the torque transducer used to measure the frictional torque:

British Hovercraft Corporation Ltd., Torque transducer type TT2/4/BA

Load range:	0 - 33.9 Nm (torque)
Speed range:	0 - 8000 rpm
Sensitivity:	2.174 mv/v
Maximum total error due to linearity and hysterisis:	± 0.1% f.s.d.

(b) Specifications of the microcomputer used:

Columbia Data Products Multi-Personal Computer

16 Bit 8088 processor

128K RAM

Data transfer rate to and from memory 250 kilobits per second

5 1/4 inch dual floppy disk drives

(c) Features of the Analog to Digital converter:

Lab Tender 8 bit A/D and D/A

Input range ± 5v

50 kHz conversion rate

32 single-ended or 16 differential channels.

REFERENCES

1. Adkins, R. W. and Radzimovsky, E. I. (1965):

   'Lubrication phenomena in spur gears: capacity, film thickness variation, and efficiency',
   Trans. ASME J. of Basic Eng., v. 87.

2. Attia, A. Y.:

   (a) (1959) 'Dynamic loading on spur gear teeth',
   Trans. ASME J. of Eng. for Ind., v. 81.

   (b) (1963) 'Deflection of spur gear teeth cut in thin rims',
   ASME paper 63-WA-14.

   (c) (1969) 'Noise of involute helical gears',
   Trans. ASME J. of Eng. for Ind., v. 91.

3. Azar, R. C. and Crossley, F. R. E. (1977):

   'Digital simulation of impact phenomenon in spur gear systems',
   J. of Eng. for Ind., v. 99.

4. Barwell, F. T. (1956):

   'Lubrication of bearings',
   Butterworths Scientific Publications, London.

5. Benton, M. and Seireg, A. (1981):

   'Factors influencing instability and resonances in geared systems',
   Trans. ASME J. of Mech. Des., v. 103.

6. Buckingham, E. (1949):
   'Analytical mechanics of gears',
   McGraw-Hill Book Company Inc., New York.

7. Cameron, A.:

(a) (1952) 'Hydrodynamic theory in gear lubrication',
J. Inst. Petroleum, v. 38.

(b) (1954) 'Surface failure in gears',
J. Inst. Petroleum, v. 40.

8. Cheng, H. S. (1973):

'Isothermal elastohydrodynamic theory for the full range of pressure-viscosity coefficient',
Trans. ASME J. of Lub. Tech., v. 95.

9. Cheng, H. S. and Sternlicht, B. (1964):

'A numerical solution for the pressure, temperature and film thickness between two infinitely long, lubricated rolling and sliding cylinders, under heavy loads',
ASME paper 64-Lub-11.

10. Conry, T. F. and Seireg, A. (1973):

'A mathematical programming technique for the evaluation of load distribution and optimal modifications for gear systems',
Trans. ASME J. of Eng. for Ind., v. 95.

11. Cornell, R. W. (1981):

'Compliance and stress sensitivity of spur gear teeth',
Trans. ASME J. of Mech. Des., v. 103.

12. Crook, A. W.:

(a) (1957) 'Simulated gear tooth contact: some experiments upon their lubrication and sub-surface deformations',
Proc. I.Mech.E., London, v. 171.

(b) (1958) 'Lubrication of rollers (I)',
Phil. Trans., v. A250.

(c) (1961) 'Lubrication of rollers (II)',
Phil. Trans., v. A254.

(d) (1961) 'Lubrication of rollers (III)',
Phil. Trans., v. A254.

(e) (1963) 'Lubrication of rollers (IV)',
Phil. Trans., v. A255.

13. Davenport, T. C. (1973):

'The rheology of lubricants',
Applied Science Publishers Ltd.

14. Dowson, D. and Higginson, G. R. (1977):

'Elasto-hydrodynamic lubrication',
Pergamon Press Ltd., UK.

15. Dudley, D. W. (1962):

'Gear Handbook',
McGraw-Hill Book Company Inc., New York.

16. Franklin, L. J. and Smith, C. H. (1924):

'The effect of inaccuracy of spacing on the strength of gear teeth',
Trans. ASME, v. 46.

17. Gatcombe, E. K.:

(a) (1945) 'Lubrication characteristics of involute spur gears - a theoretical investigation',
Trans. ASME, v. 67.

(b) (1951) 'The non-steady-state, load-supporting capacity of fluid wedge-shaped films',
Trans. ASME, v. 73.

18. Gregory, R. W.; Harris, S. L. and Munro, R. G. (1963):

'Dynamic behaviour of spur gears',
Proc. I.Mech.E., v. 178.

19. Grubin, A. N. and Vinogradova, I. E. (1949):

Central Scientific Research Institute for Technology and Mechanical Engineering, Book No. 30.
Moscow (D.S.I.R., Translation No. 337).

20. Gu, A. (1973):

'Elastohydrodynamic lubrication of involute gears',
Trans. ASME J. of Eng. for Ind., v. 95.

21. Harris, S. L. (1958):

'Dynamic load on the teeth of spur gears',
Proc. I.Mech.E., v. 172.

22. Hersey, M. D. and Lowdenslager, D. B. (1950):

'Film thickness between gear teeth',
Trans. ASME, v. 72.

23. Houser, D. R. and Seireg, A. (1970):

'An experimental investigation of dynamic factors in spur and helical gears',
Trans. ASME J. of Eng. for Ind., v. 92.

24. Ichimaru, K. and Hirano, F. (1974):

'Dynamic behaviour of heavily loaded spur gears',
Trans. ASME, J. of Eng. for Ind., v. 96.

25. Ishikawa, J.; Hayashi, K. and Yokoyama, M. (1974):

'Surface temperature and scoring resistance of heavy-duty gears',
Trans. ASME, J. of Eng. for Ind., v. 96.

26. Johnson, D. C. (1958):

'The excitation of resonant vibration by gear tooth meshing effects',
Proc. of the International Conference on Gearing, I.Mech.E.

27. Kasuba, R. (1971):

'Dynamic loads on spur gear teeth by analog computation',
ASME paper 71-DE-26.

28. Kasuba, R. and Evans, J. W. (1981):

'An extended model for determining dynamic loads in spur gearing',
Trans. ASME J. of Mech. Des., v. 103.

29. Kohler, H. K.; Pratt, A. and Thompson, A. M. (1970):

'Dynamics and noise of parallel axis gearing',
Gearing in 1970, I.Mech.E. Conference.

30. MacConochie, I. O. and Cameron, A. (1960):

'The measurement of oil film thickness in gear teeth',
Trans. ASME J. of Basic Eng., v. 82.

31. Mahalingam, S. and Bishop, R. E. D. (1974):

'Dynamic loading of gear teeth',
J. of Sound and Vibration, v. 36, n. 2.

32. Martin, H. H. (1916):

'Lubrication of gear teeth',
Engineering, London, v. 102.

33. Martin, K. F. (1981):

'The efficiency of involute spur gears',
Trans. ASME J. of Mech. Des., v. 103.

34. McEwen, E.

(a) (1948) 'Load carrying capacity of the oil film between gear teeth',
Engineer, London, v. 186.

(b) (1952) 'The effect of variation of viscosity with pressure on the load carrying capacity of oil films between gear teeth',
J. Inst. of Petroleum, v. 38.

35. Moore, D. F. (1975):

'Principles and applications of tribology',
Pergamon Press Ltd., UK.

36. Munro, R. G. (1970):

'Effect of geometrical errors on the transmission of motion between gears',
Gearing in 1970, I.Mech.E. Conference.

37. Nagaya, K. and Uematsu, S. (1981):

'Effects of moving speeds of dynamic loads on the deflection of gear teeth',
Trans. ASME J. of Mech. Des., v. 103.

38. Niemann, G. and Rettig, H. (1958):

'Error induced dynamic tooth loads',
Proceedings of the International Conference on Gearing, I.Mech.E.

39. Niemann, G. and Lechner, G. (1965):

'The measurement of surface temperatures on gear teeth',
Trans. ASME J. of Basic Eng., v. 87.

40. Radzimovsky, E. I. and Vathayanon, B. (1966):

'Influence of the tooth surface deformation upon the capacity of hydrodynamically lubricated spur gears',
ASME paper no. 66-Lubs-12.

41. Remmers, E. P. (1971):

'Dynamics of gear pair systems',
ASME paper 71-DE-23.

42. Reswick, J. B. (1955):

'Dynamic loads on spur and helical gear teeth',
Trans. ASME, v. 77.

43. Saada, A. S. (1974):

'Elasticity: theory and applications',
Pergamon Press Ltd., UK.

44. Seireg, A. and Houser, D. R. (1970):

'Evaluation of dynamic factors for spur and helical gears',
Trans. ASME, J. of Eng. for Ind., v. 92, n. 2.

45. Smith, J. D. (1983):

'Gears and their vibration',
McMillan Press Ltd., London.

46. Sternlicht, B.; Lewis, P. and Flynn, P. (1961):

'Theory of lubrication and failure of rolling contacts',
Trans. ASME, J. of Basic Eng., v. 83, n. 2.

47. Terauchi, Y. and Nagamura, K. (1981):

'Study on deflection of spur gear teeth - 2, Calculation of tooth deflection for spur gears with various tooth profiles',
Bull. J.S.M.E., v. 24, n. 188.

48. Timoshenko, S. P. and Goodier, J. N. (1970):

'Theory of elasticity',
McGraw-Hill Kogakusha Ltd., Japan.

49. Timoshenko, S.; Young, D. H. and Weaver, W. Jr. (1974):

'Vibration problems in engineering',
John Wiley & Sons Inc.

50. Tobe, T.; Sato, K. and Takatsu, K.:

(a) (1976) 'Statistical analysis of dynamic loads on spur gear teeth (effects on shaft stiffness)',
Bull. J.S.M.E., v. 19, n. 133.

(b) (1977) 'Statistical analysis of dynamic loads on spur gear teeth (experimental study)',
Bull. J.S.M.E., v. 20, n. 148.

51. Tobe, T. and Takatsu, K. (1973):

'Dynamic load on spur gear teeth caused by teeth impact',
Bull. J.S.M.E., v. 16, n. 96.

52. Tourret, R. and Wright, E. P. (1980):

'Performance and testing of gear oils and transmission fluids',
Mansell (Bookbinders) Ltd., Essex, UK.

53. Tuplin, W. A.:

(a) (1950) 'Gear tooth stresses at high speed',
Proc. I.Mech.E., London, v. 163.

(b) (1953) 'Dynamic loads on gear teeth',
Machine Design, v. 25.

(c) (1958) 'Dynamic loads on gear teeth',
Proceedings of the International Conference on Gearing,
I.Mech.E.

54. Wallace, D. B. and Seireg, A. (1973):

'Computer simulation of dynamic stress, deformation and fracture of gear teeth',
Trans. ASME, J. of Eng. for Ind., v. 95.

55. Wang, C. C. (1981):

'Calculating natural frequencies with extended Tuplin's method',
Trans. ASME, J. of Mech. Des., v. 103.

56. Wang, K. L. and Cheng, H. S. (1981):

'A numerical solution to the dynamic load, film thickness, and surface temperatures in spur gears (a) Part I - Analysis; (b) Part II - Results',
Trans. ASME, J. of Mech. Des., v. 103.

57. Wang, S. M. and Morse, I. E. (1971):

'Torsional response of a gear train system',
ASME paper 71-Vibr-77.

58. Waterworth, N. (1958):

'Effects of deflection of gears and their supports',
Proceedings of the International Conference on Gearing,
I.Mech.E.

59. Weber, C. (1949):

'The deformation of loaded gears and the effect on their load-carrying capacity', Part I.
Department of Scientific and Industrial Research, sponsored research (Germany), no. 3.